

QUANTIFICATION OF AQUIFER RECHARGE DISTRIBUTION
USING ENVIRONMENTAL ISOTOPES
AND REGIONAL HYDROCHEMISTRY

by
Eilon Adar

A Dissertation Submitted to the Faculty of the
DEPARTMENT OF HYDROLOGY AND WATER RESOURCES
In Partial Fulfillment of the Requirements
For the Degree of
DOCTOR OF PHILOSOPHY
WITH A MAJOR IN HYDROLOGY
In the Graduate College
THE UNIVERSITY OF ARIZONA

1 9 8 4

THE UNIVERSITY OF ARIZONA
GRADUATE COLLEGE

As members of the Final Examination Committee, we certify that we have read
the dissertation prepared by Eilon Adar

entitled Quantification of Aquifer Recharge Distribution using
Environmental Isotopes and Regional Hydrochemistry

and recommend that it be accepted as fulfilling the dissertation requirement
for the Degree of Doctor or Philosophy.

A. H. Harvie

Date

Dec. 27, 1984

David A. Woolhiser

Date

Dec 27, 1984

W. G. Mottack

Date

27 DEC 84

Garth King

Date

Jugare S. Sempson

Date

27 Dec 84

Final approval and acceptance of this dissertation is contingent upon the
candidate's submission of the final copy of the dissertation to the Graduate
College.

I hereby certify that I have read this dissertation prepared under my
direction and recommend that it be accepted as fulfilling the dissertation
requirement.

Glenn R. [Signature]

Dissertation Director

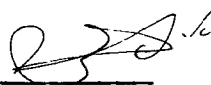
Date

12/27/84

STATEMENT BY AUTHOR

This dissertation has been submitted in partial fulfillment of requirements for an advanced degree at The University of Arizona and is deposited in the University Library to be made available to borrowers under rules of the Library.

Brief quotations from this dissertation are allowable without special permission, provided that accurate acknowledgment of source is made. Requests for permission for extended quotation from or reproduction of this manuscript in whole or in part may be granted by the head of the major department or the Dean of the Graduate College when in his or her judgment the proposed use of the material is in the interests of scholarship. In all other instances, however, permission must be obtained from the author.

SIGNED: Cilon Adar 

This dissertation is dedicated to
The Defenders of Wildlife Trust
for the George Whittell Wildlife Preserve
at Aravaipa Canyon

ACKNOWLEDGMENTS

This dissertation would not have been possible without the generous help and support of certain individuals and organizations.

I wish to express my sincere appreciation to Dr. Shlomo P. Neuman, dissertation director and academic advisor, for his guidance and encouragement throughout the course of this research. His close supervision and invaluable comments and guidance during the construction of the model and his assistance during the writing of the dissertation were extremely helpful, and he is gratefully acknowledged for this.

I also would like to thank Professor Sol D. Resnick for his confidence in and support of this research program. The useful discussions with Dr. David A. Woolhiser, Dr. Emanuel Mazor, and Dr. Austin Long are gratefully remembered. I wish also to express my appreciation to other members of the dissertation committee: Dr. Eugene S. Simpson, Dr. Arthur W. Warrick, and Dr. W.G. Matlock for their guidance and encouragement. James Cullen, my office partner, is gratefully acknowledged for his continuous support during the course of this program.

I wish to express my gratitude and respect to Dr. Arie Issar and Dr. Jiftah Ben-Asher of the Blaustien Institute for Desert Research (Ben Gurion University of the Negev, Israel) for providing me with the opportunity to obtain an advanced degree at the University of Arizona.

The cooperation of the Defenders of Wildlife Trust for the George Whittell Wildlife Preserve at Aravaipa Canyon made this study possible. Special thanks are due to Mr. William Roe, Mr. J. Luepke, and Dr. J. Schnell and his wife, Jean, of the Whittell Wildlife Preserve for their invaluable assistance. The work upon which this dissertation is based was also supported in part by funds provided by the Office of Water Research and Technology, U.S. Department of the Interior, Washington, D.C., under Contract No. A-099-ARIZ.

TABLE OF CONTENTS

	Page
LIST OF ILLUSTRATIONS.	viii
LIST OF TABLES	xiv
ABSTRACT	xvi
1. INTRODUCTION	1
2. PHYSICAL DESCRIPTION AND GEOLOGY OF ARAVAIPA BASIN	8
Physiography and Climate	8
Geology of Aravaipa Basin.	13
3. HYDROLOGY.	19
Aquifer Tests.	25
Spatial Groundwater Level Variations	27
4. AQUIFER RECHARGE AND DISCHARGE MECHANISMS.	40
5. IDENTIFICATION OF AQUIFER FLOW COMPONENTS THROUGH THE USE OF AQUEOUS CHEMICAL AND ENVIRONMENTAL ISOTOPE DATA	51
Effect of Altitude on Stable Isotope Distribution in Aravaipa Watershed.	52
Distribution of Oxygen-18 and Deuterium in Groundwaters	57
Identification of Flow Components in the Upper Eureka Section	61
Lateral Contribution into the Upper Aquifer through the Alluvial Fans.	71
Chemistry and Stable Isotopes in the Deep Aquifer.	81
Hydraulic Connection Between the Two Major Aquifers.	86
Stable Isotopes in Floods and Runoff	90
6. MODEL OF QUANTITATIVE RECHARGE ESTIMATION.	97
Theory	97
Model Testing with Synthetic Data.	103
Effect of Errors	104

TABLE OF CONTENTS--continued

	Page
7. APPLICATION OF MODEL TO LOWER ARAVAIPA VALLEY.	129
Sensitivity of Computed Inflow Rates to Weights, Pumping Rates and Source Distribution.	143
8. CONCLUSIONS.	155
APPENDIX A: ARAVAIPA WELL LOGS.	164
APPENDIX B: PUMPING TEST RESULTS FOR KLONDYKE SECTION	182
APPENDIX C: LOCATION, CHEMICAL AND ISOTOPE SAMPLING RESULTS FOR WELLS AND SPRINGS IN ARAVAIPA WATERSHED	192
C.1 Collection and Analyses of Water Samples.	192
C.2 Tables of Chemical and Isotopic Data.	195
APPENDIX D: RAIN SAMPLER FOR STABLE ISOTOPES.	236
APPENDIX E: SYNTHETIC DATA USED FOR TESTING THE MULTICELL MATHEMATICAL ALGORITHM.	239
LIST OF REFERENCES	243

LIST OF ILLUSTRATIONS

Figure		Page
1	Location of study area	9
2	Location of sections, piezometric profiles across valley, isotope rain samplers, and other sites mentioned in text	10
3	Average distribution of precipitation and temperature in Klondyke	12
4	Geological map of Aravaipa Basin	14
5	Schematic geologic cross-section and piezo- metric profile across Klondyke section.	17
6	Location of well and spring sample sites in Aravaipa Watershed.	20
7	Schematic configuration of water table aquifer in upper Klondyke section	22
8	Longitudinal hydrogeological cross-section along Aravaipa Valley and Stowe Gulch	26
9	Map of piezometric surface in confined aquifer	29
10	Spatial distribution of piezometric head in confined aquifer.	30
11	Map of water table in phreatic aquifer	31
12	Spatial distribution of water table in phreatic aquifer.	32
13	Water level profiles along Aravaipa Valley	33
14	Hydraulic head distribution in Aravaipa Valley	34
15	Water level profiles across Aravaipa Valley.	36
16	Head distribution in Stowe Gulch section	37
17	Flow pattern in Stowe Gulch section.	38

LIST OF ILLUSTRATIONS--continued

Figure	Page
18	Water level profile in Stowe Gulch basin 39
19	Schematic diagram of flow in Aravaipa Basin (division into cells is for modeling purposes) 41
20	Water level fluctuations in four wells 45
21	Average monthly discharge in Aravaipa Canyon 48
22	Schematic geologic section and piezometric profile across Aravaipa Canyon along B-B' in Figure 4. 50
23	Stable isotope distribution in precipitations in Aravaipa Valley. 53
24	Distribution of $\delta O-18$ (o/oo) in precipitation across Aravaipa Valley. 54
25	Oxygen-18 versus deuterium in seven rain storms sampled in Aravaipa Valley. 56
26	Oxygen-18 versus deuterium in wells, springs, floods, and base-flows in Aravaipa Watershed. 59
27	Oxygen-18 versus deuterium in waters obtained from:
	(A) Floods, deep and upper aquifers 60
	(B) Base-flows, deep and upper aquifers and Aravaipa Spring 60
	(C) Deep wells in the valley and along the margins 60
28	Schoeller diagram for wells along the boundaries of upper Eureka section
	(A) Group (a); wells along the southeastern boundary. 62
	(B) Group (b); wells along the southwestern boundary. 63

LIST OF ILLUSTRATIONS--continued

Figure		Page
29	Groundwater chemistry in the upper Eureka section.	65
30	Schoeller diagram for shallow wells in upper Eureka section (group c).	66
31	Oxygen-18 across the upper Eureka section.	68
32	Oxygen-18 versus deuterium in groundwaters in Eureka section.	69
33	Groundwater chemistry and oxygen-18 for Eureka section	70
34	Hydraulic head distribution and flow components near Haby Spring.	72
35	Groundwater chemistry and oxygen-18 near Haby Spring	74
36	Schoeller diagram for wells near Haby Spring	75
37	Schoeller diagram for wells upstream and down- stream of Haby Spring and the confluence with Rattlesnake.	76
38	Groundwater chemistry upstream and downstream of Haby Spring.	77
39	Groundwater chemistry near Klondyke at the confluence of Fourmile Canyon with Aravaipa Creek.	78
40	Schoeller diagram for wells near the confluence with Fourmile Canyon.	79
41	Correlation between chemical and isotopic constituents in shallow groundwaters around Aravaipa Spring	80
42	Schoeller diagram for deep wells in the confined aquifer	82

LIST OF ILLUSTRATIONS--continued

Figure	Page
43	Schoeller diagram showing the similarity between wells in the deep aquifer
	(A) Karakula Old Adobe House and Whiting Deep 83
	(B) Klondyke Deep #2 and Cobra New Irrigation 84
44	Carbon-14 and tritium versus discharge in Whiting Deep well 87
45	Tritium versus carbon-14
	(A) Key wells in Aravaipa Valley. 88
	(B) Wells in upper Klondyke section. 88
	(C) Wells near Aravaipa and Haby Springs. 88
46	Oxygen-18 versus deuterium in runoff and floods. 92
47	Amount effect of rainfall on oxygen-18 in floods. 94
48	Schematic flow pattern with cell configuration 100
49	Schematic compartmental aquifer used for testing the mathematical algorithm in a multi-cell scheme 105
50	Variation of mean computed Q with number of realizations with constant β
	(A) $\beta = 0.20$ 109
	(B) $\beta = 0.10$ 110
	(C) $\beta = 0.05$ 111
51	Average solutions and standard deviations from Monte Carlo simulations with a constant weight $\beta = 0.01$ 112
52	Standard deviations of computed Q values versus β 115

LIST OF ILLUSTRATIONS--continued

Figure	Page
53	Results of Monte Carlo simulations with β values equal to coefficients of variation from laboratory standards
	(A) Average Q versus number of realizations 119
	(B) Standard deviations of Q versus number of realizations. 119
	(C) Frequency distribution of computed Q values 120
	(D) Cumulative frequencies of Q estimation errors 120
54	Results of Monte Carlo simulations with perturbed concentrations restricted to ionic balance of 10 percents, electric conductivity to TDI ratios between 30 and 60, and D to O-18 ratios between 5 and 11
	(A) Average Q versus number of realizations 122
	(B) Standard deviations of Q versus number of realizations. 122
	(C) Frequency distribution of computed Q values 123
	(D) Cumulative frequencies of Q estimation errors. . . . 123
55	Results of Monte Carlo simulations with perturbed concentrations with noisy concentrations restricted to ionic balance of 5 percents, electric conductivity to TDI ratios between 35 and 60, and D to O-18 ratios between 6.5 and 9.5
	(A) Average Q versus number of realizations 124
	(B) Standard deviations of Q versus number of realizations. 124
	(C) Frequency distribution of computed Q values 125
	(D) Cumulative frequencies of Q estimation errors 125

LIST OF ILLUSTRATIONS--continued

Figure	Page
56	Results of Monte Carlo simulations with per- turbed concentrations restricted to ionic balance of 2 percents, electric conductivity to TDI ratios between 35 and 55, and D to O-18 ratios between 6.5 and 8.5
	(A) Average Q versus number of realizations 126
	(B) Standard deviations of Q versus number of realizations. 126
	(C) Frequency distribution of computed Q values 127
	(D) Cumulative frequencies of Q estimation errors 127
57	Outline of the modeled portion of the water table aquifer 130
58	Activity diagrams for waters in the mixing cell. 138
59	Activity diagrams for waters among selected inflows. 139
A-1	U.S.G.S. method of well location 166
A-2	Location of sampling wells and springs 167
B-1	Drawdown test in Whiting's Deep well 184
B-2	Recovery test in Whiting's Deep well 187
B-3	Interference test: drawdown in the observation well. 190
B-4	Recovery test in Whiting's IR-1. 191
D-1	Rain sampler for oxygen-18 and deuterium 238

LIST OF TABLES

Table	Page
1. Estimated discharge by means of pumpage for each section in Aravaipa Valley.	44
2. δO --18 and δD in flood waters before and after the peak discharge.	95
3. Comparison between assigned and calculated inflows obtained by testing the optimization scheme for a multicell aquifer:	
A: Test 1 (four cells and eight unknowns).	106
B: Test 2 (four cells and 19 unknowns)	106
4. Comparison between the observed and calculated mass transport for each constituent obtained from the test analysis	
A: Test 1.	107
B: Test 2.	107
5. Average inflows and statistics from 100 realizations of noisy C data with four constant β values.	114
6. Average inflows and statistics from 100 realizations of noisy C data with different β_k values assigned to each species	117
7. Average inflows and statistics from 250 realizations with chemical and isotopic constraints	128
8. Type of inflow and the representative water sample associated with each cell in the modeled area	132
9. Average concentrations for each cell and inflow whose dissolved constituents were obtained from several water samples	134
10. Examples of weight vectors used in the model.	142
11. Computed inflows, water balance, and salt balance for β_2 with W_1 , W_2 , and W_3	144

LIST OF TABLES--continued

Table	Page
12. Computed inflows, water balance, and salt balance for \underline{W}_2 with $\underline{\beta}_1$ and $\underline{\beta}_2$	146
13. Computed inflows, water balance, and salt balance for $\underline{\beta}_2$ and \underline{W}_2 with variable pumping rates	147
14. Computed inflow rates into the water table aquifer for different source distributions.	149

ABSTRACT

A mathematical model is proposed to estimate annual recharge rates from various sources into an aquifer, based on chemical and isotopic data. The aquifer is divided into mixing cells. For each mixing cell, annual mass balance equations are written which express the conservation of water, dissolved chemicals, and stable environmental isotopes. These equations are solved simultaneously for unknown recharge rates by quadratic programming. A similar approach was used earlier to estimate inflows into a river reach which acts as a single mixing cell. The sensitivity of the model to input errors is analyzed by applying it to synthetic data corrupted by artificial noise. The ability of the model to deal with real data is illustrated by applying it to the semi-arid Aravaipa basin in southern Arizona.

CHAPTER 1

INTRODUCTION

Groundwater is a major source of water in many arid and semiarid regions. In order to properly manage this valuable resource, there is a need for accurate information about the inputs (recharge) and outputs (pumpage and natural discharge) within each groundwater basin. Experience has shown that evaluating pumpage and natural discharge is often technically easier than estimating recharge. In fact, the largest uncertainty in calculating the water budget of a groundwater basin generally stems from the hydrologist's inability to reliably estimate the spatial and temporal distribution of recharge rates. In arid and semiarid regions, the difficulty is compounded by the intermittent nature of recharge which often occurs in pulses of a relatively short duration, lasting from several hours to several days (cf., Zimmerman et al., 1966, 1967).

In this work, the term "recharge" designates waters that replenish the saturated region of a given groundwater basin from all sources and all directions. Sources of recharge may include stream infiltration; surface infiltration due to rainfall, irrigation, or artificial recharge from ponds; lateral inflow from nearby basins or due to mountain-front recharge; and artificial recharge due to water injection.

In many studies, surface infiltration and stream losses are equated with recharge. It is important to recognize, however, that in

arid and semiarid regions, the fate of waters which have infiltrated underground is determined by the saturated/unsaturated flow regime prevailing above the regional water table. Following stream infiltration, part of the water may flow laterally away from the channel as has been demonstrated by Wilson and DeCook (1969). After following such a lateral course for a certain distance, part of the water may be taken up by the roots of phreatophytes and transpire into the atmosphere; part may rise to the soil surface due to capillary forces and evaporate from the bare soil, whereas the rest may either stay in the unsaturated zone to replenish existing deficits in storage or, if the field capacity of the soil is exceeded, percolate slowly down toward the water table. Only that water which actually reaches the water table and, in this way, becomes part of the saturated zone, should be considered recharge.

Since not all the water that infiltrates into the soil, or into a stream bed, reaches the water table, the volume and rate of water table recharge are generally less than those of infiltration. In addition to these numerical differences between water table recharge and infiltration, the former lags in time behind the latter due to travel through the vadose zone. This time lag may be short (hours, days, weeks) if the water table is situated at relatively shallow depths, or long (months or years) if the water table is deep or overlain by low-permeability strata.

Models that compute recharge by equating it to infiltration at the soil surface, including stream beds, in response to rainfall, irrigation, and stream flow, abound in the literature. Examples can be found in the works of Eakin (1966), Feth et al. (1966), Briggs and Werho

(1966), Burkham (1970), Rantz and Eakin (1971), Belan (1972), Mazor et al. (1974), Shick (1977), Ben Asher (1978), Kafri and Ben Asher (1978), Durbin et al. (1978), Howard and Lloyd (1979), and others. Of particular interest for recharge from ephemeral stream losses in the arid southwestern United States are the studies of Matlock (1965), Marsh (1968), and Keith (1981). Matlock compared measured stream losses in the Tucson basin with field and laboratory data on infiltration. Marsh conducted infiltration experiments on riverbed materials from the same basin. He found that stream losses are controlled primarily by sediment loads in the flood water and, to a lesser extent, by flow velocity. Both authors found that high-velocity, sediment-laden summer floods may result in significant stream losses due to scouring of the riverbed. While winter floods are characterized by lower velocities, stream losses are greater in winter than in summer due to longer flow duration and reduced sediment load. Keith showed that ephemeral stream losses in the Tucson basin increase with streamflow up to a certain threshold value of the latter, beyond which flow duration becomes the parameter controlling stream infiltration.

Surface and stream infiltration represent gross input of water into the subsurface, initiating the water table recharge process. For the computation of net input, one needs to transform the infiltration into volumes or rates of deep percolation beneath the root zone, including the root zone of phreatophytes near streams and washes. Methods to effect such a transformation have been described by numerous authors including Thornthwaite and Mather (1957), Mero (1963, 1978), Walker

(1970), Degallier (1972), Olmstead et al. (1973), Advisory Committee on Irrigation Efficiency (1974), Bos and Nugteren (1974), Heerman and Kincaid (1974), Wind and Van Doorne (1975), King and Lambert (1976), Hillel (1977), Tanji (1977), Willmott (1977), Karmeli et al. (1978), and Mero (1978). While some of these methods may work well in humid regions, their applicability to arid and semiarid conditions is in question.

Deep percolation may be regarded as net input of water into the vadose zone; most or all of this water will ultimately reach the water table in the form of groundwater recharge. When the time delay involved in flow through the vadose zone is significant, its effect on the computation of recharge must be considered. A rigorous approach to the problem of routing water through the vadose zone, starting directly beneath the root zone and ending at the groundwater table, would require the solution of highly nonlinear partial differential equations describing unsaturated flow in soils (e.g., Richards' equation). Such an approach, however, is not feasible for basin-wide recharge studies. Simplified models tailored specifically for such studies have been proposed by Mero (1963), Degallier (1972), King and Lambert (1976), Besbes et al. (1978), and Mero (1978).

Among the most readily available hydrologic data that could be used to estimate groundwater recharge in arid and semiarid regions are stream flow records and hydrographs of nearby wells. Very often, the fluctuation of water levels in wells situated close to streams reflects fluctuations in the rate of recharge as well as the rate of deep percolation beneath the stream. The idea of using groundwater level fluctuations as an indicator of recharge dates back to the early works of

Leggette (1936) and Jacob (1943, 1944). Various methods based on this idea have been discussed by Matlock (1965, 1972), Moench and Kisiel (1970), Venetis (1971), Gelhar (1974), Besbes (1978), Preller (1978), Gelhar and Duffy (1979), and Flug et al. (1980). When streamflow infiltration is the main source of recharge, some of these methods may yield acceptable results. However, none of the techniques mentioned thus far are able to deal with situations where the relative importance of various potential recharge sources is unknown.

In this work, we are interested in developing a methodology for the identification and quantification of multiple recharge sources. In other words, we are interested in identifying the major mechanisms of recharge in a given basin, the spatial distribution of the recharge sources, and the relative as well as absolute strength of each such source. Under certain conditions, this can be accomplished by solving the so-called "inverse problem" of aquifer hydrology, i.e., by treating recharge as an unknown parameter in a numerical aquifer flow model (Carrera, 1984). However, as pointed out by Neuman (1975, 1980), this method often is prone to difficulties. A more promising approach is one that utilizes not only information about the groundwater flow system, but also information about the groundwater chemistry including isotopic data.

In the past, hydrogeologists have used chemical and isotopic data for recharge studies primarily in a qualitative sense. Environmental isotopes played a dominant role in such studies, as exemplified by the works of Verhagen et al. (1970, 1978), Gat and Dansgaard (1972), Blake (1973), Breckenkamp et al. (1974), Mazor (1974, 1982), Yurtsever

and Payne (1978), Sampine et al. (1979), Levin et al. (1980), Issar and Gat (1981), Issar and Gilad (1982) and Issar (1983). In some important studies, tritium was used to obtain quantitative estimates of recharge (Zimmermann, 1966, 1967; Dincer et al., 1974; Bredenkamp et al., 1974; and Vogel et al., 1974). More recent attempts to extract quantitative information about recharge from hydrochemical data often rely on statistical analyses. As an example, Lawrence and Upchurch (1982) used factor analysis to identify recharge sources for certain groups of dissolved chemical species in an aquifer. For all of these works, the authors either evaluate the magnitude of a given recharge source, or evaluate potential sources of recharge without providing quantitative estimates of recharge rates.

We are aware of only one attempt to incorporate hydrological and hydrochemical information into a mathematical groundwater model for the purpose of source identification and quantification. This attempt by Gorelick et al. (1983) deals with the question of identifying the location and magnitude of pollution sources that might have contributed to the contamination of an aquifer. For this, they utilize a two-dimensional numerical model of solute transport in the aquifer, coupled with various optimization techniques. The method could, in principle, be used for recharge estimation.

The purpose of the present study is to examine the feasibility of incorporating hydrogeological and hydrochemical information jointly into a mathematical model of a southwestern basin to identify sources of recharge, their location, and their magnitude. For this, we have chosen

an area of 540 square miles within the upper Aravaipa Watershed in southern Arizona. Our investigation has been divided into two stages. Stage 1 consisted of a thorough field investigation of the study area coupled with laboratory analyses of water samples. Environmental isotopes and dissolved ions were used to identify the flow pattern and potential flow components of recharge. These data were also used to isolate relatively homogeneous cells that may be assigned with an average value for each of the dissolved constituents. As we shall see, this study has led us to the postulation of a combined hydrological-hydrochemical model for the basin. Stage 2 involves the application of this model to Aravaipa Valley. Mathematically, the proposed model is similar to that developed by Woolhiser et al. (1982) for a surface drainage system. This model is based on hydrological and hydrochemical balances applied to a system of discrete "mixing cells" representing the basin, and requires a solution by quadratic programming. The model is tested with synthetic data for a schematic aquifer configuration. It is followed by a sensitivity analysis and solution for the recharge components into the alluvial aquifer of Aravaipa Valley.

CHAPTER 2

PHYSICAL DESCRIPTION OF ARAVAIPA BASIN

Physiography and Climate

The Aravaipa Watershed is located about sixty miles northeast of Tucson, Arizona (Figure 1). Aravaipa Valley within the watershed is surrounded by the Galiuro Mountains (7,540 feet above m.s.l. at Kennedy Peak) on the west and southwest, and by the Santa Teresa and Pinaleno mountains (7,489 feet above m.s.l. at Cottonwood Peak) on the east. On the south, the watershed has a common boundary with the internally drained basin of Willcox. On the north, the subbasin of Stowe Gulch is blocked by the Horse Mountain complex (6,174 feet above m.s.l.).

The main watercourse in the watershed is Aravaipa Creek. The creek is ephemeral in its upper reaches but becomes perennial at Aravaipa Spring, at the head of Aravaipa Canyon. Aravaipa Creek flows into the San Pedro River through Aravaipa Canyon. In the valley, the creek is located close to the feet of the Santa Teresa and Pinaleno Mountains. As a result, eastern tributaries are shorter and steeper than western tributaries. Among the most important tributaries are Sheep Wash, Buford Wash, Klondyke Wash, and Laurel Canyon in the east, and Deer Creek, Oak Creek, Rattlesnake Canyon, Squaw Creek, and Fourmile Canyon in the west. Stowe Gulch, whose confluence with Aravaipa Creek is located at the seepage zone of Aravaipa Spring, drains the Horse Mountain complex (Figure 2).

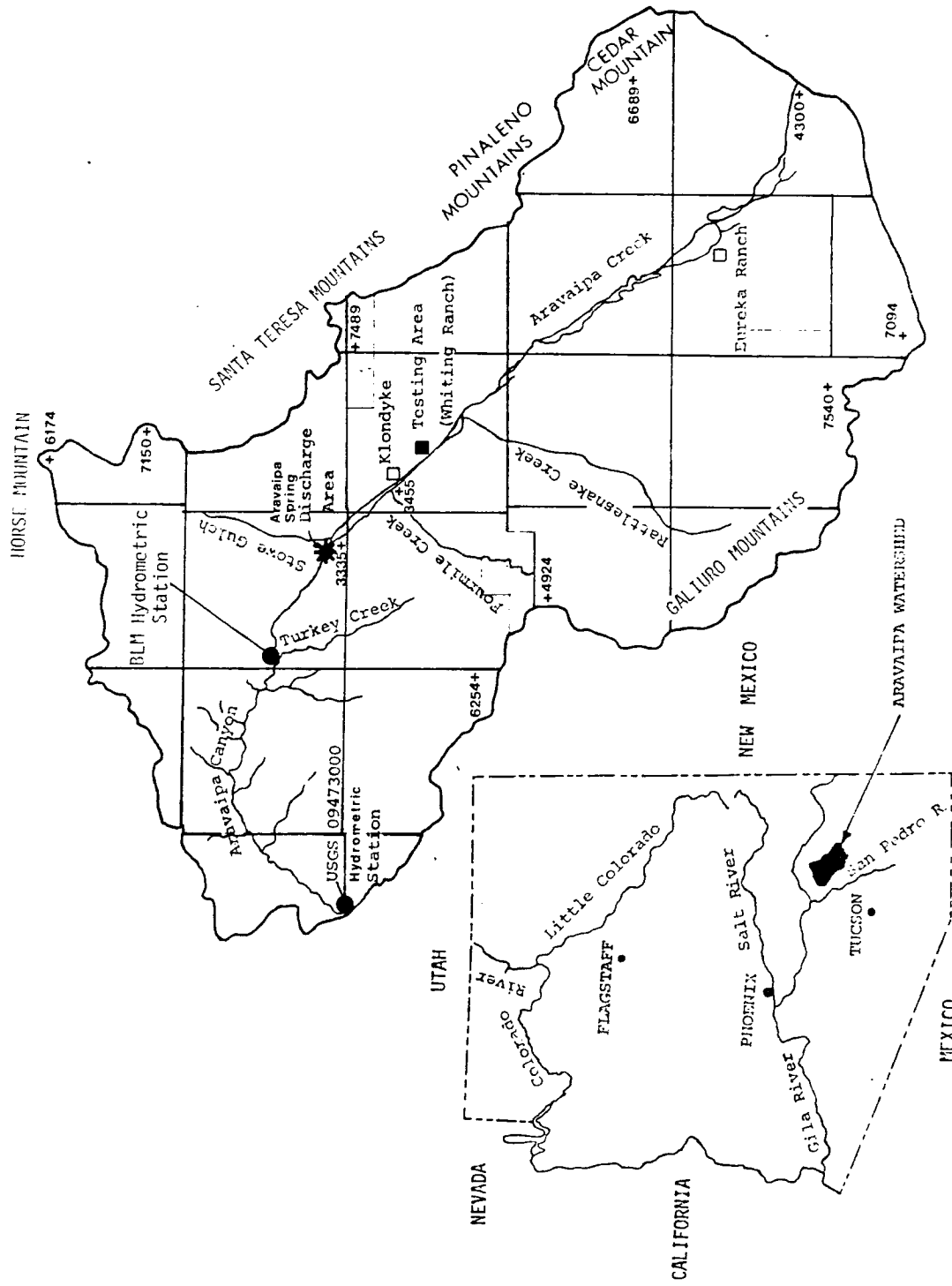


Figure 1. Location of study area

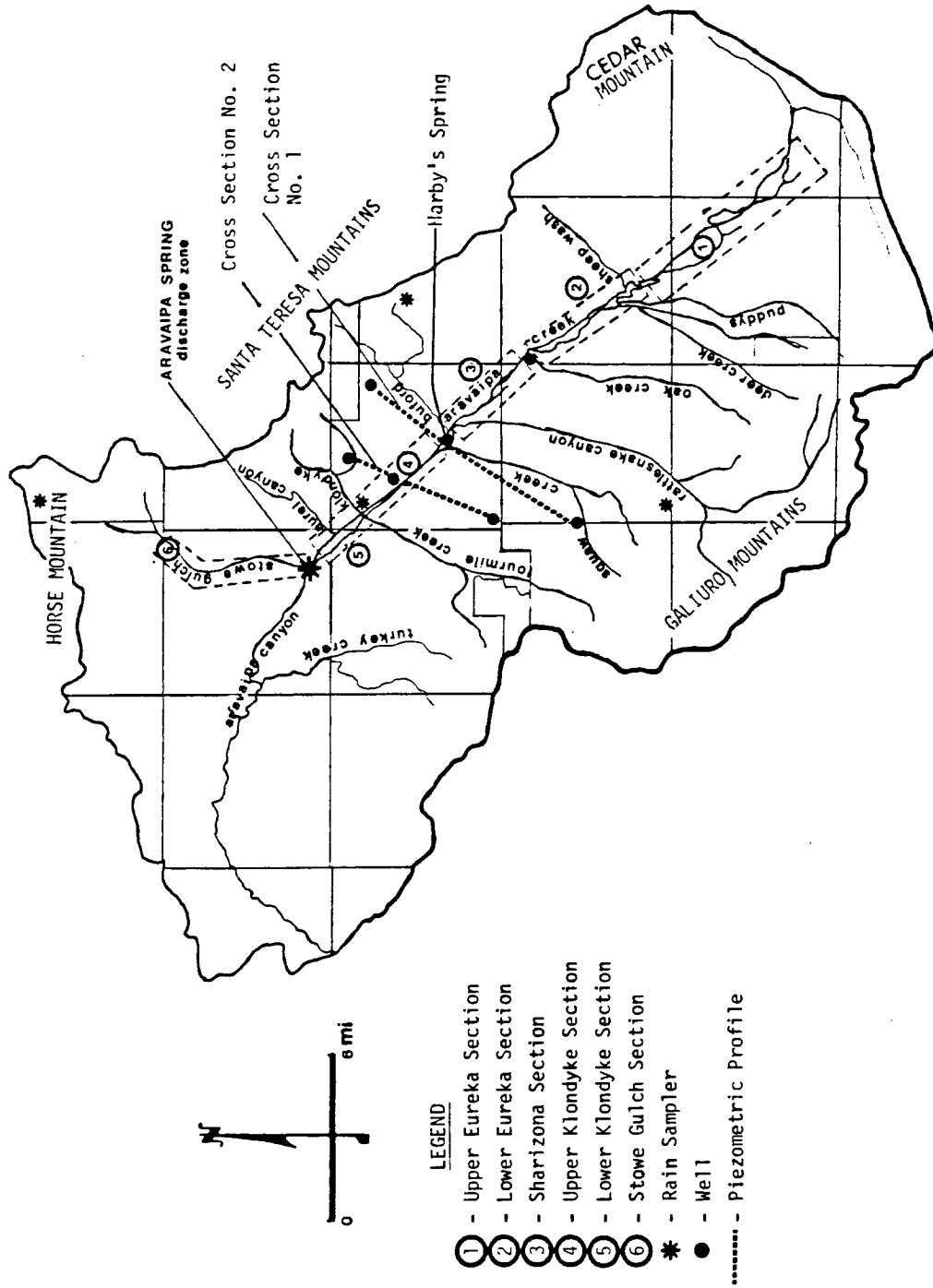


Figure 2. Location of sections, piezometric profiles across valley, isotope rain samplers and other sites mentioned in text

Annual precipitation ranges from 355 mm (14 inches) in the lower valley at Klondyke, through 430 mm (17 inches) in the upper valley near Eureka, to 510 mm (20.8 inches) in the surrounding mountains (NOAA Atlas).

Winter storms usually approach the valley from west to southwest and summer storms from southwest to southeast. Summer storms are shorter in duration and have higher intensities than winter rains. Figure 3 shows the seasonal variation of average monthly precipitation (and temperature) at Klondyke. Deviations from these monthly averages can exceed 100 per cent.

In winter, snow is found at elevations exceeding 5500 feet along the foreside of the Santa Teresa and Horse Mountains, and above 6000 feet along the leese side of the Galiuro Mountains.

Aravaipa Valley is situated at the northeastern edge of the Sonora Desert in an area of transition from arid desert scrub to more mesic (humid) vegetation. Desert scrub is found along the valley bottom and pediments. In the deeper canyon where water is available perennially, the vegetation is dominated by riparian deciduous trees such as sycamore, walnut, willow, and cottonwood. A much lower density of similar trees is found at higher elevations near Haby Spring and Stowe Gulch Spring. Mesquite and palo verde appear in meadows at intermediate elevations. At higher elevations, the vegetation includes conifers, oak, aspen, and mountain mahogany.

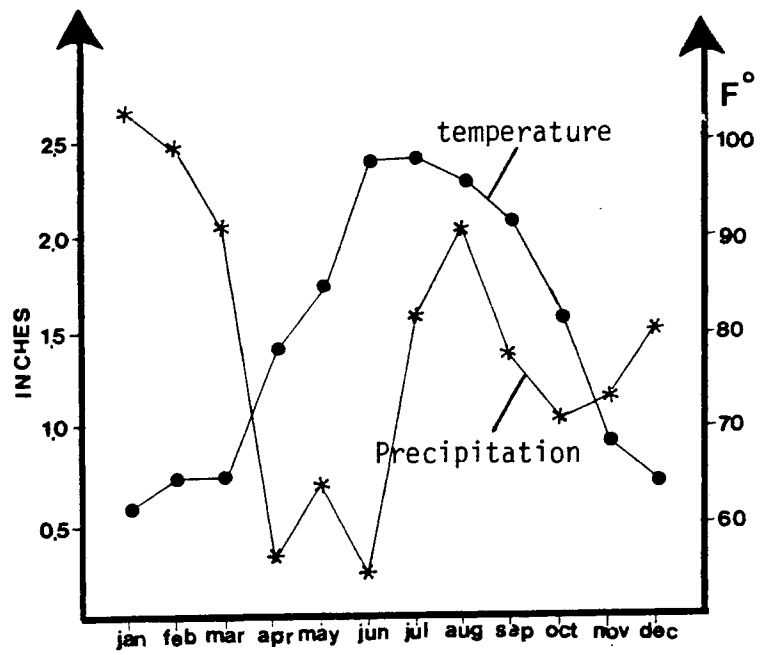


Figure 3. Average distribution of precipitation and temperature in Klondyke

Geology of Aravaipa Basin

The local geology has been studied by Rose (1925) and Simon (1964), and geological cross sections were published by Moor (1962) and Simon (1964), accompanied by the geological map of the Klondyke quadrangle. Robinson (1976) published detailed residual gravity data on the Aravaipa basin. It is his data that most clearly indicate the graben structure with normal faults bounding both sides of the valley. Magnetic and seismic surveys were conducted by Ellingson (1980) to provide more information on the accurate location of the western fault and on the vertical distribution of the young and the old alluvium at the entrance to Aravaipa Canyon.

During late cretaceous and early tertiary times, the site of the Aravaipa Watershed was part of a huge erosional surface of considerable relief on a granodioritic pluton. The ancestral Santa Teresa granitic pluton formed the eastern boundary of the ancient Aravaipa watershed. The late cretaceous Horse Mountain volcanics consisting of lava, tuff, and agglomerate formed the high relief in the northeast around Stowe Gulch basin (Figure 4).

Later in mid tertiary, the Galiuro volcanics (a sequence of andesitic to rhyolitic tuffs and lavas) formed the Galiuro mountains in its present location. The establishment of the present Aravaipa valley started in late tertiary due to a relative uplift of the adjacent mountains blocks. This uplift took place along normal faults and was part of a regional tectonic phenomenon characterized by block faulting (Simon, 1964). Some of the Galiuro volcanics, deposited on the lower

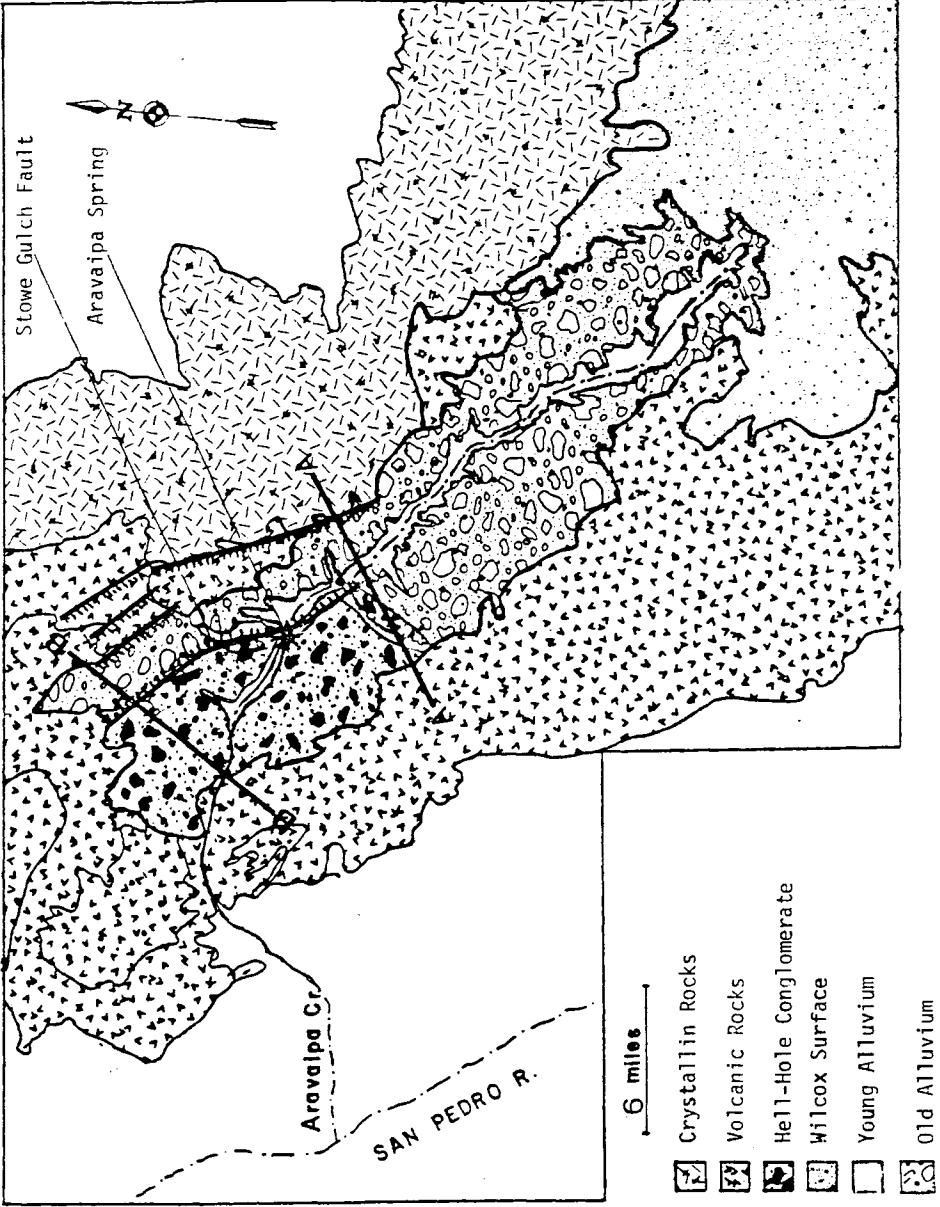


Figure 4. Geological map of Aravaipa Basin

side of the western fault, are buried deep in the basin and are overlain by a sequence of quaternary alluvial deposits.

Aravaipa Valley is a narrow graben filled with fluvial sediments interbedded with lake deposits (Ross, 1925; Simon, 1964). Based on gravity surveys, Robinson (1976) concluded that the near vertical normal offset of the graben is between 6,000 and 10,000 feet, and the bedrock consists primarily of Galiuro volcanics. A geological map of Aravaipa Basin is presented in Figure 4. The map shows major geological units and the location of major faults. Figure 5 is a schematic geological cross-section along line A-A in Figure 4. The cross-section is based on similar sections prepared by Moor (1962) and Simon (1964).

The Aravaipa Watershed consists of two major rock categories: (1) a belt of hard volcanic, metamorphic, and granitic rocks, and (2) an elongated pediment of valley fill. The basin fill consists of three major lithostratigraphic units having some common characteristics.

The lowermost unit is the indurated Hell Hole conglomerate of late Tertiary which consists mainly of volcanic rock fragments of variable size and shape. Most, if not all, of the fragments seem to have originated in the Galiuro Volcanics. The rock matrix is dominated by coarse sand with some fine grained material, held together by calcite. The Hell Hole conglomerate rests unconformably on the Galiuro Volcanics and, to some extent, on Horse Mountain volcanics along the lower portion of the valley. The conglomerate is probably conformably overlain by the Old Alluvium of late Pliocene or Pleistocene age. The coarse fragments of the conglomerate show a well developed bedding. Sandy layers and partially cemented pebbles are uniformly oriented along the plunge of

the valley axis. On a smaller scale, there is considerable interfingering of coarse and fine grained materials. The eastern edge of the Hell Hole conglomerate block is heavily affected by the western faults of the valley.

The Quarternary Old Alluvium lies unconformably on mountain slope rocks such as the Galiuro and Horse Mountain volcanics and the Pinal Schists (Figure 5). Its stratigraphic relation to the Hell Hole conglomerate is not everywhere clear, but in areas of contact, there seems to be a conformity between the two.

The Old Alluvium is poorly bedded and poorly sorted. Its fragments consist of igneous, metamorphic and sedimentary rocks which form a loosely to moderately cemented conglomerate. The alluvium forms conspicuous pediments on both sides of Aravaipa Valley where they are in lateral contact with the country rock. In contrast with the Hell Hole conglomerate, the upper part of the Old Alluvium appears to be unaffected by what must be earlier faulting and tilting. Its fragments derived from both sides of the valley range from sand to boulders and are poorly sorted.

Few patches of lake beds are exposed within the Old Alluvium, mainly along the northeastern part of the valley. The lake beds consist of fine sand and silt, rich in clay minerals. Data from wells near Klondyke (Appendix A) suggest that lacustrine beds of clay and silt, interbedded with sand and coarse material, are continuous across the valley, at least from Lower Eureka section down to Lower Klondyke and Stowe Gulch sections (the division of the valley into sections is shown in Figure 2).

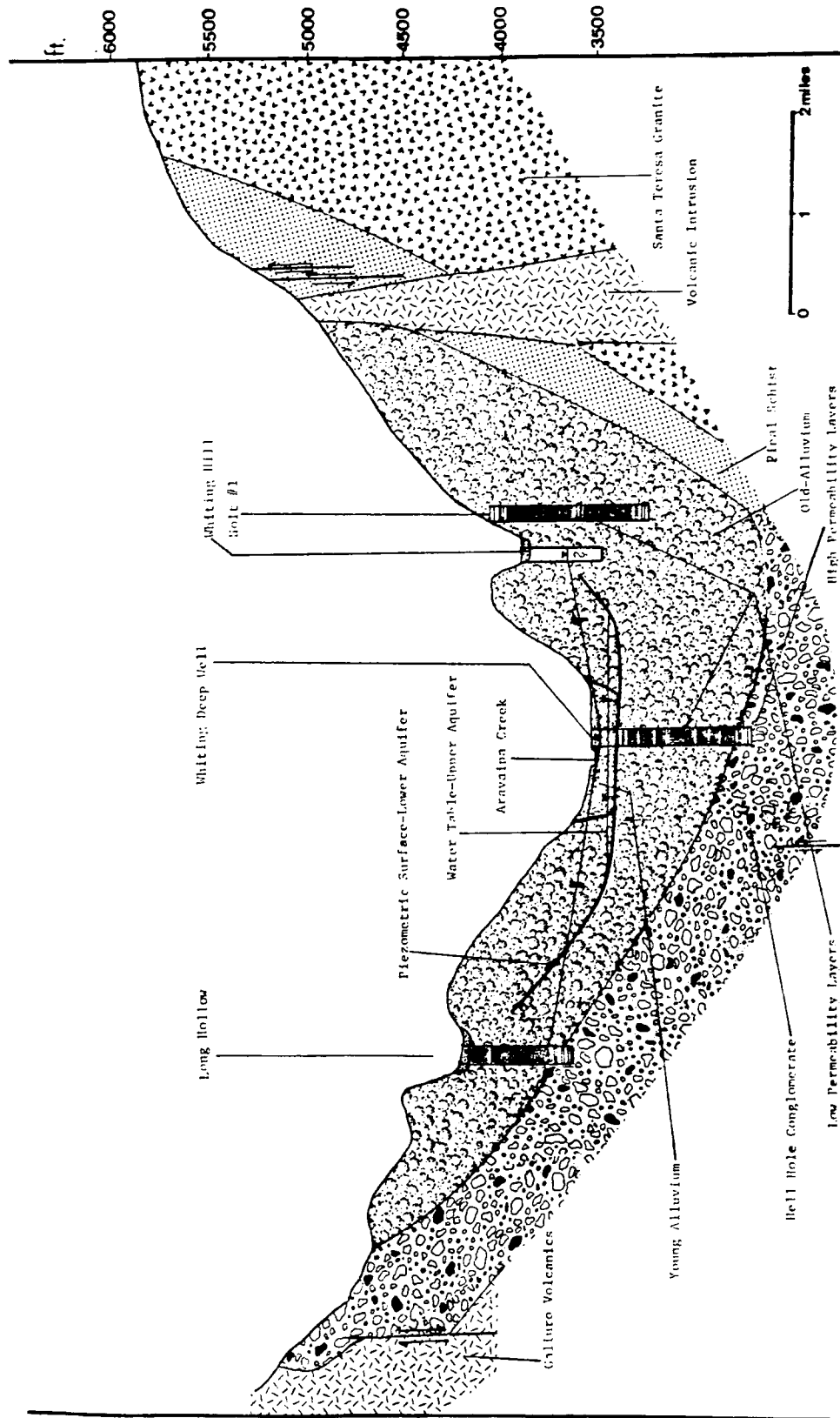


Figure 5. Schematic geologic cross section and piezometric profile across Klondyke section [along A'A', in Figure 4; after Moore (1962), Simon (1964) and Robinson (1976)]

The uppermost unit is the post Holocene Young Alluvium which is confined mostly to the modern channels of the existing drainage system. From the lateral stratigraphic relation between the Young and the Old Alluvium, Simon (1964) concluded that Aravaipa Creek cut a deep valley through the Old Alluvium sometime before or during the Holocene period. Later the valley has been filled with unsorted clastics ranging from fine to coarse gravel through varying boulder sizes. The Young Alluvium is confined to the flood plain of Aravaipa Creek and reaches its maximum width of almost one mile at the confluence with the major tributaries below Haby's Spring in Klondyke sections.

CHAPTER 3

HYDROLOGY

The hard rocks surrounding the valley appear to have a very low primary permeability. Groundwater flow through these rocks occurs mainly in joints and fractures. Due to the topographic prominence of these hard rocks, they are able to maintain groundwater levels above those found in the valley sediments. The resultant regional hydraulic gradient towards the valley is responsible for part of the mountain front recharge to the alluvial sediments.

Most mountain springs in the area have low discharge rates with the exception of Stowe Gulch, Fourmile Canyon, and Deer Creek (Figure 6). The latter three springs issue from the contact between the Old Alluvium and igneous rocks and maintain perennially high discharge rates. It has been found that mountain springs drain small local aquifers within highly fractured zones in the hard rock.

The two major aquifers in Aravaipa Watershed lie in the valley alluvial sediments. The lower aquifer is formed mainly by the older alluvium. It is confined from above by low permeability layers of silt and lacustrine clay belonging to the uppermost part of the Old Alluvium. The confined aquifer consists of several permeable layers of gravel and sand interbedded with thin semipermeable layers of silt and clay. Well logs from the lower and upper Klondyke sections (Long Hollow, Whiting Deep, and Holt #1; see Appendix A), suggest that the most permeable

layers of the Old Alluvium are only 10 to 35 feet thick. These layers are separated by cemented low-permeability sediments ranging from 35 to 100 feet in thickness. This is supported by a downhole camera survey of the Whiting Deep well (Arad and Adar, 1981). The uppermost confining layer is continuous across the width of the valley. This suggests that the aquifer in these sections may be recharged directly from the mountain rocks as well as from its own upstream sections, but not from above.

Along the eastern margins of these sections, the Old Alluvium is in direct lateral contact with schists, volcanic and granitic rocks. Two shallow wells (Buford Hill and Lamb Camp) along with several small springs (such as Dog-Water-Mine) in the Santa Teresa Mountains (Figure 6) indicate the existence of small perched aquifers in these mountains which are far above the piezometric surface of the Lower Aquifer. Since direct contact exists between the mountain rocks and the Old Alluvium, this implies the possibility of mountain front recharge from the Santa Teresa mountains. In the west, the Old Alluvium is in contact with the Hell Hole conglomerate.

Several clay and/or silt layers have been identified in the Old Alluvium eastern pediments (Simon, 1964). Not enough information is available about their lateral extent normal to the stream. However, many seasonal springs emerge from the Old Alluvium pediments along the mountain front of Santa Teresa. This fact implies the existence of small seasonal perched water table aquifers in the Old Alluvium as shown in Figure 7. In sections such as lower and upper Klondyke, where continuous confining layers prevent deep percolation from taking place,

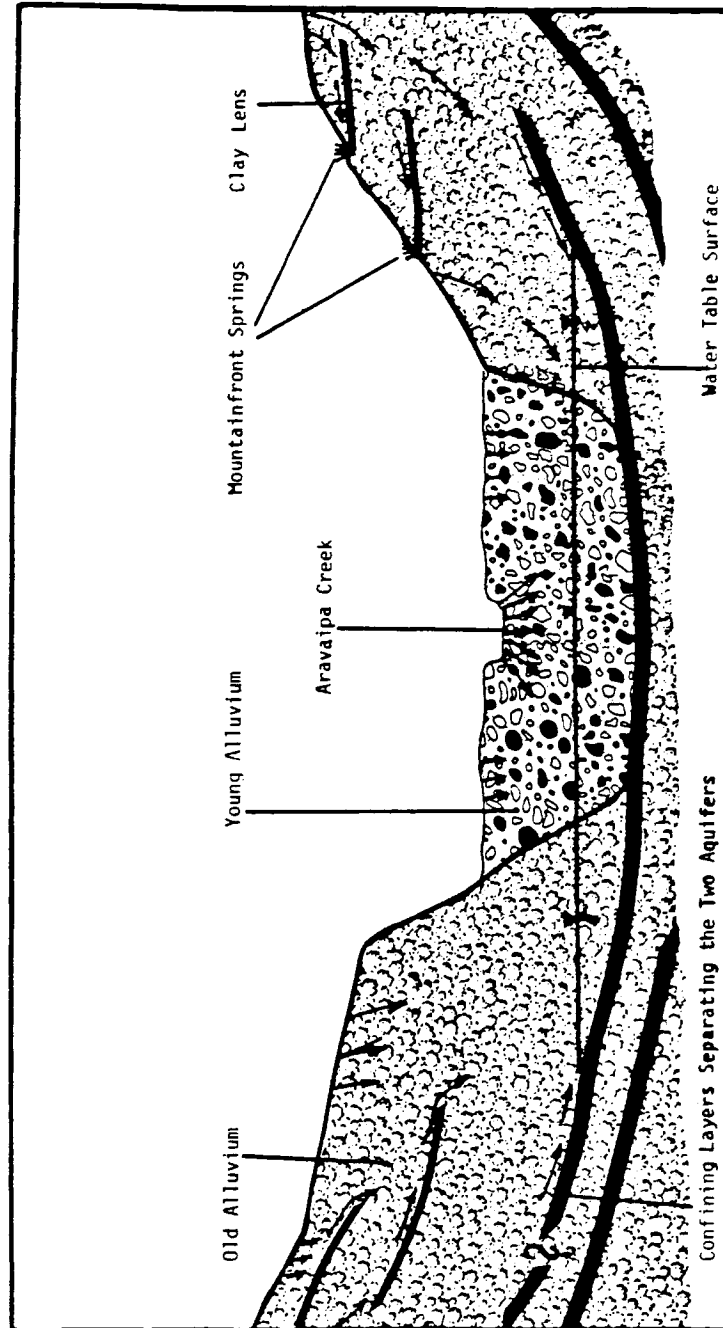


Figure 7. Schematic configuration of water table aquifer in upper Klondyke section

water from local perched aquifers may flow laterally toward the valley into the upper aquifer unit. Information obtained from environmental stable isotope analyses from the eastern margin of the deep aquifer (Whiting Hill) indicates that the water in the Old Alluvium originates from higher elevations in the Santa Teresa Mountains (refer to Chapter 5). Similar analyses from the western margin of this deep aquifer (Long Hollow and Squaw deep wells) suggest that significant recharge takes place via infiltration and deep percolation through the western pediments of the Old Alluvium. This was found to be true for Upper Klondyke, the Sharizona and lower Eureka sections; thus implying that the deep aquifer in these sections is only partially confined. The confining layers are probably continuous only along the eastern and lower portions of the valley. The lack of deep wells in the Sharizona and lower Eureka sections precludes us from elaborating more on the deep aquifer in these sections.

Most wells in the upper and lower Eureka sections draw water from the deep aquifer. Drillers' logs from several wells (Bird Cage, Eureka #4, Eureka Ranch, and Sheep Corral) suggest that the main water bearing layers consist of sand ranging in thickness from 5 to 30 feet. The bottom of the uppermost confining layer is found at depths from 230 to 350 feet below the surface. Logs from two deeper wells (Eureka #11, 1206 feet; Eureka Ranch #6, 1500 feet) show the presence of two thin water bearing layers confined between cemented lava flows at a depth below 1000 feet.

The main source of water in the valley is the upper water table aquifer. This aquifer is limited to the course of Aravaipa Creek and to

alluvial fans at the confluence of this creek with its major tributaries. The aquifer is approximately 20 miles long and is generally narrow (500-1000 yards) except near major alluvial fans where its width may exceed one mile. However, because of a steep topographic relief on the east side of the river, and a relatively moderate relief on the west side, the upper aquifer increases dramatically in width at the confluences with western tributaries such as the Rattlesnake and Fourmile canyons.

The upper aquifer was considered earlier to lie entirely within the Young Alluvium (Ellingson, 1980, and Arad and Adar, 1981). However, we are unable to see any evidence for the existence of a lateral hydrological barrier that would separate the Young Alluvium from the Old Alluvium. A layer of red clay was found at the bottom of most wells penetrating the upper aquifer. The relations between this layer and the Young and Old Alluvium is illustrated in Figure 7. The clay is seen to extend beyond the lateral contact between the Young and the Old Alluvium. This suggests that the upper aquifer extends into the Old Alluvium, which may cause its permeability to decrease toward the margins. Indeed most existing irrigation wells were drilled into the Young Alluvium along Aravaipa Creek.

Existence of the upper aquifer in the lower Eureka section is in question (this aquifer has not been identified in the upper Eureka section). Drillers' logs from both Eureka sections indicate the existence of a very thin water bearing layer on top of the confining layer. However, most of the water derives from the deep confined aquifer (Bird Cage, Sheep Corral, Eureka #4, and Eureka #6; see Table 3 in Appendix C). This implies that the thickness of the upper aquifer decreases to

the south and the aquifer apparently vanishes in the lower Eureka section. The southern boundary of the upper aquifer is probably near Peyote Church (Figure 6); the southernmost well to extract water from it appears to be Little W.M. in the lower Eureka section. South of this well, only a temporary water table is formed during the rainy seasons.

The relationship between the confined and unconfined aquifers in Aravaipa Valley is shown in Figure 8.

Aquifer Tests

Hydraulic parameters for the two major aquifers are known only from two pumping tests in the upper Klondyke section. A pumping test of the lower aquifer was performed in the Whiting deep well, and a test of the upper aquifer was conducted in Whiting #1 (see Figure 1). One hundred and twenty feet of low-permeability conglomerate, silt, and clay separate the two aquifers in this particular section. Complete descriptions of the tests can be found in Appendix B and in Arad and Adar (1981).

A 7-hour step-drawdown test and a 12-hour recovery test were performed in the deep aquifer. No observation wells were available for these tests in the lower aquifer. A piezometer in the upper aquifer, located at a distance of 230 yards from the pumping well, was monitored for a possible response but did not react.

From an analysis of the first drawdown step that lasted 80 minutes, one obtains a specific capacity of 7-9 gpm/foot and a transmissivity, T , of 1,482 ft²/day. If the effective radius of the well is assumed to be 0.5 feet, this T value yields a storativity, S , equal to

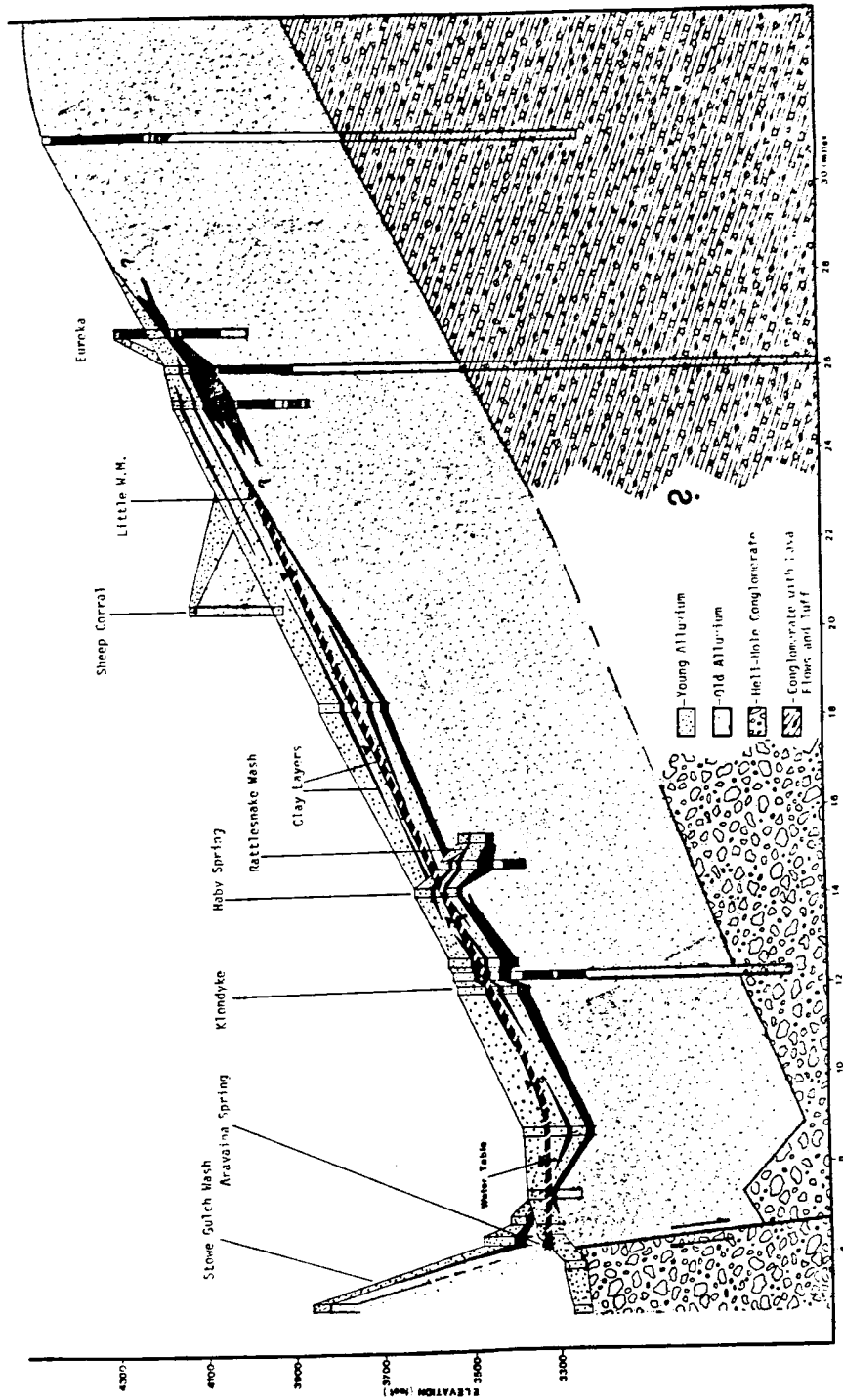


Figure 8. Longitudinal hydrogeological cross-section along Aravaipa Creek and Stowe Gulch

2.62×10^{-2} . This value is unusually high for a confined aquifer and its validity is therefore in question. An analysis of the recovery phase yields a transmissivity of $937.9 \text{ ft}^2/\text{day}$ and a storativity of 1.66×10^{-2} .

A piezometer located at a distance of 50 yards from the pumping well was monitored during an interference test in the phreatic aquifer. Lasting 5 hours, the test yielded a transmissivity of $83,000 \text{ ft}^2/\text{day}$, and a storativity of 4.51×10^{-3} . This low storativity (for an unconfined aquifer) may be due to the presence of thin silt and clay lenses in the predominantly sandy aquifer material (see Bolton, 1964 and Neuman, 1975). A longer test might have given a higher storativity value, closer to the specific yield of the aquifer.

Although the hydraulic tests did not provide any indication that leakage might have been taking place across the confining layer, analyses of carbon-14 (C-14) and tritium (H-3) imply that there is a hydraulic connection between the lower and the upper aquifers. More will be said about this in Chapter 5.

Spatial Groundwater Level Variations

To obtain a consistent picture of hydraulic head distribution in the aquifers, water levels in 73 wells were measured within a short period of three days between July 20 and 22 in 1983. To minimize the effect of pumpage on the measured water levels, the measurement started after six days without any irrigation in the valley. Measurement errors may stem from uncertainties about the elevations of some well heads. The data may be taken to represent a near steady state situation.

Figure 9 shows a contour map of piezometric levels in the confined aquifer within a rectangular segment of the lower valley. The contours were obtained by means of a computer package called Surface II (Sampson, 1978). A three-dimensional view of the piezometric surface is given in Figure 10. As expected, the main component of flow is longitudinal, from Eureka toward Aravaipa Spring. Lateral flow components in the upstream part of the segment may indicate the existence of lateral recharge. Evident in the downstream part is a strong component of lateral inflow from Stowe Gulch, and the convergence of flow toward Aravaipa Spring.

The flow pattern in the water table aquifer is pictured in Figures 11 and 12. Since most wells are clustered within a narrow strip in the center of the valley, not much can be said about lateral flow; however, the predominant direction of flow appears to be longitudinal.

Longitudinal water level profiles for the two aquifers are shown in Figure 13. Both profiles show a decrease in slope downstream near Haby Spring where the Rattlesnake wash joins Aravaipa Creek. A juxtaposition of the two profiles in Figure 14 demonstrates that the piezometric level in the confined aquifer is above the water table in the unconfined aquifer. This is a clear indication that water may leak upward from the confined aquifer to the water table aquifer above, along the entire valley length. While both profiles are higher in winter than in summer, the head difference between the two aquifers is greatest in summer when recharge into the upper aquifer is smallest, and pumpage from this aquifer is greatest.

LEGEND

- Directions of Flows
- Equipotential Piezometric Head in Feet.
- Aravaipa Spring
- Location of Sampled Wells

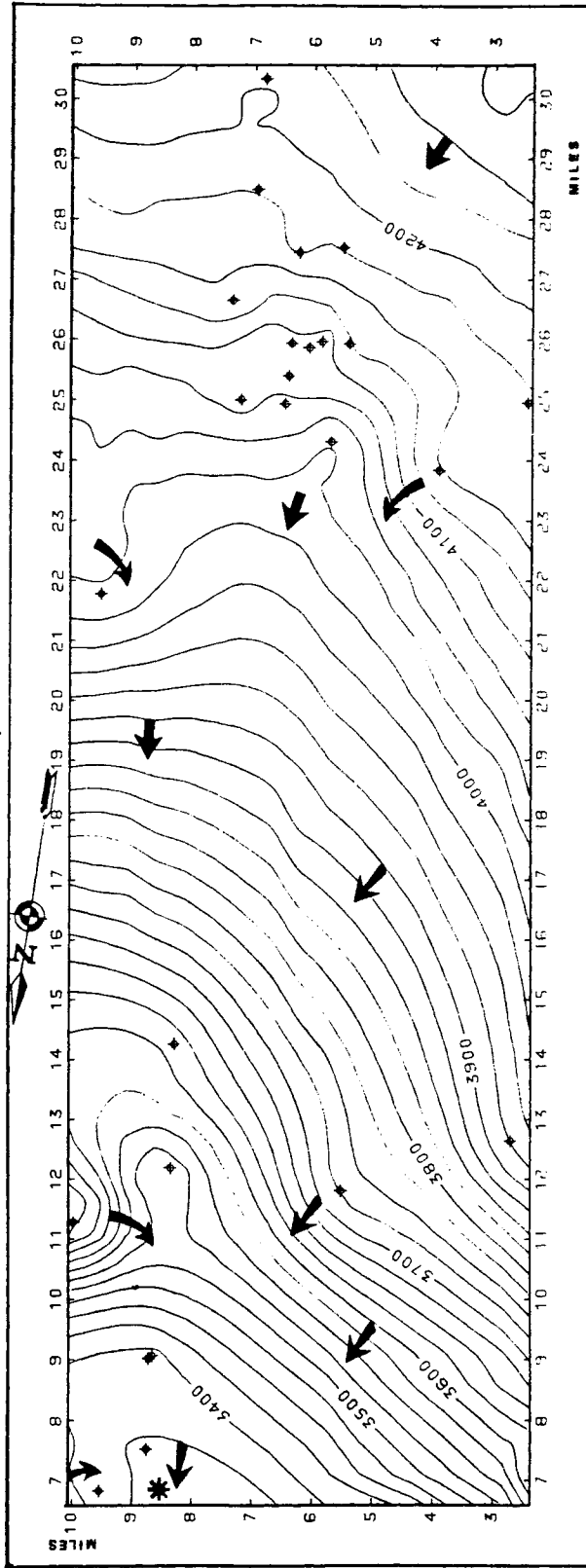


Figure 9. Map of piezometric surface in confined aquifer

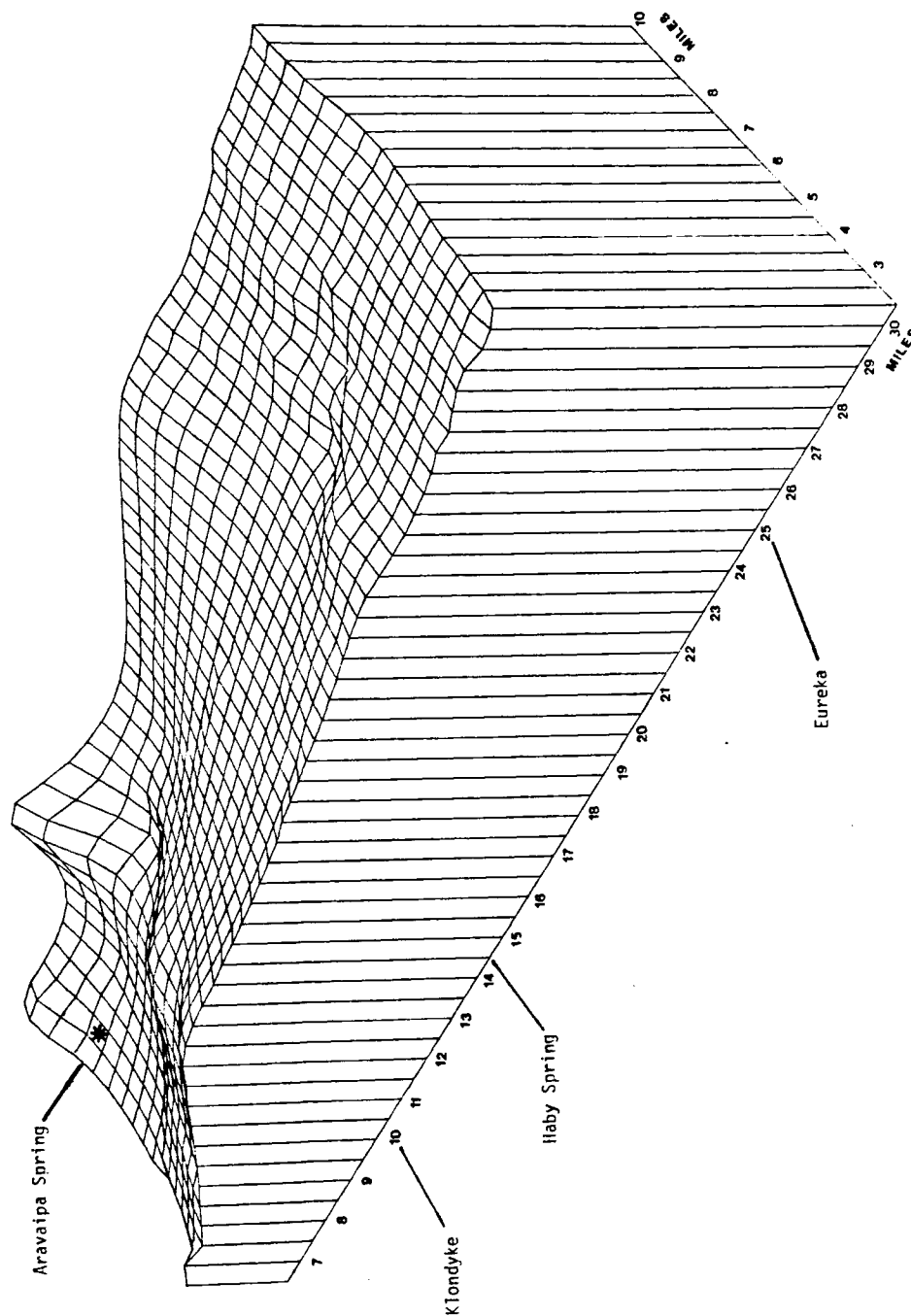


Figure 10. Spatial distribution of piezometric head in confined aquifer

- LEGEND**
- ◆ - Location of Sampled Wells
 - ➔ - Flow Direction
 - 3400 — - Equipotential Head in Feet
 - * - Aravaipa Spring

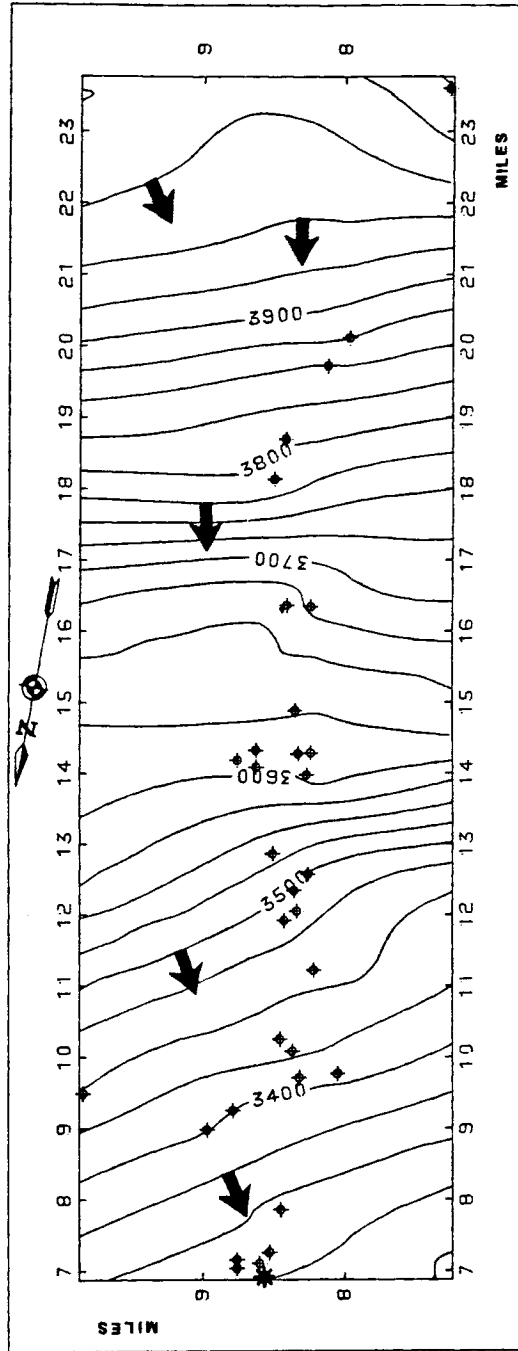


Figure 11. Map of water table in phreatic aquifer

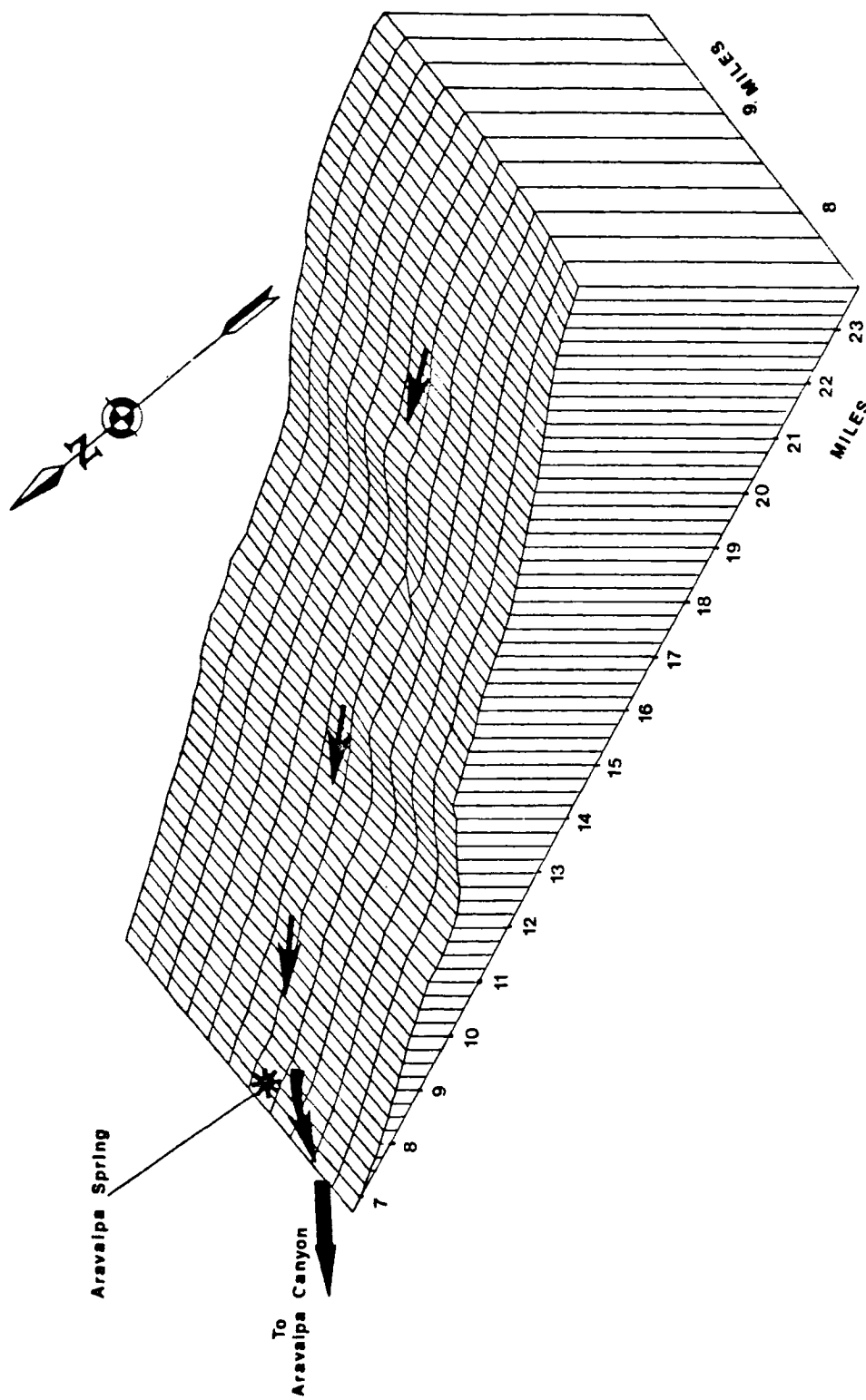


Figure 12. Spatial distribution of water table in phreatic aquifer

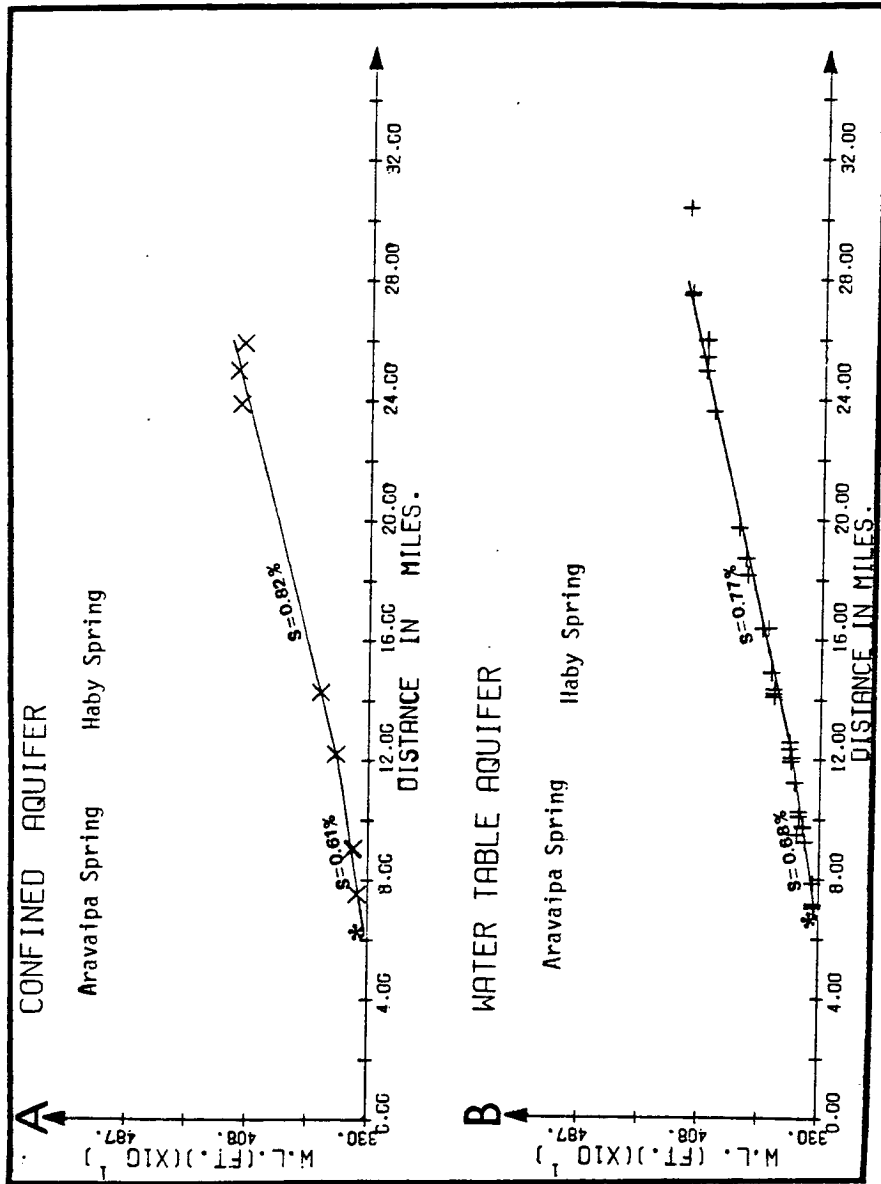


Figure 13. Water level profiles across Aravaipa Valley

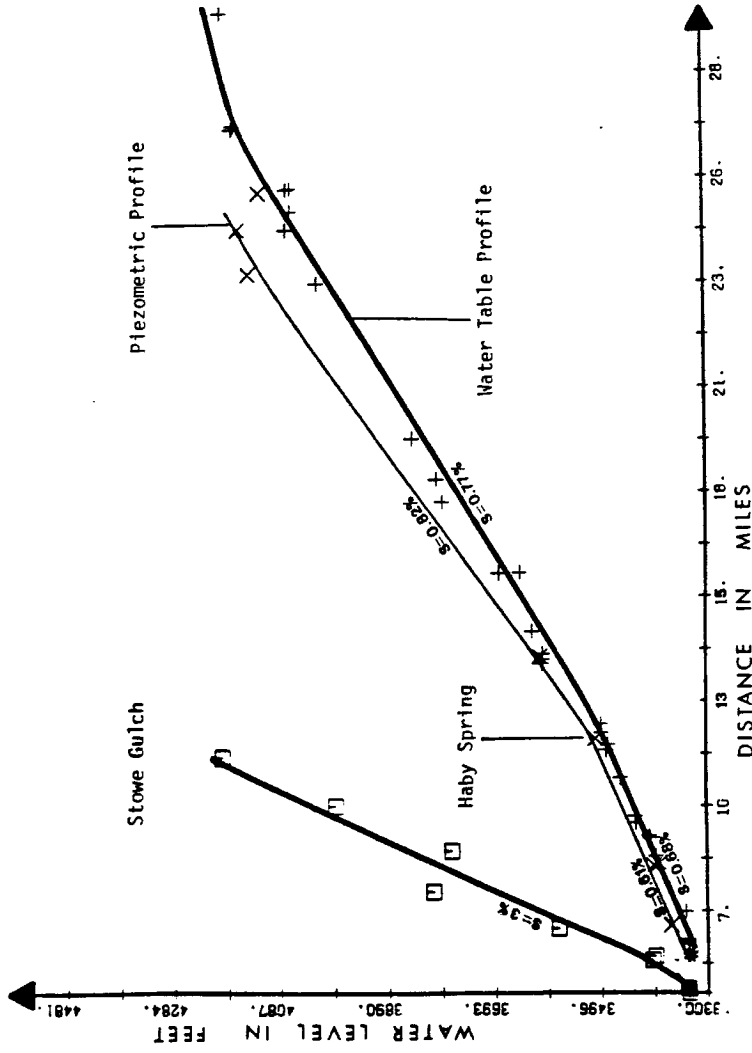


Figure 14. Hydraulic head distribution in Aravaipa Valley

Figure 15 shows lateral water level profiles in the confined aquifer along two cross-sections indicated in Figure 2. The well at Lamb Camp is located on the pediment of the Santa Teresa Mountains and we cannot be sure that its water level is representative of the confined aquifer.

Figures 16 and 17 show water level contours and flow patterns in Stowe Gulch. The hydraulic gradient is seen to be relatively steep and directed south-southwest toward the confluence with Aravaipa Creek. The extent to which this flow pattern may be influenced by Stowe Gulch fault is not clear. Projected longitudinal water level profile is shown in Figure 18.

A comparison between the longitudinal groundwater level profiles of the two Aravaipa Valley aquifers and a projected profile down the main axis of the Stowe Gulch is given in Figure 14. The hydraulic gradient in the Stowe Gulch alluvium is seen to be considerably steeper than in the valley. This is clearly related to the steeper topography of Stowe Gulch.

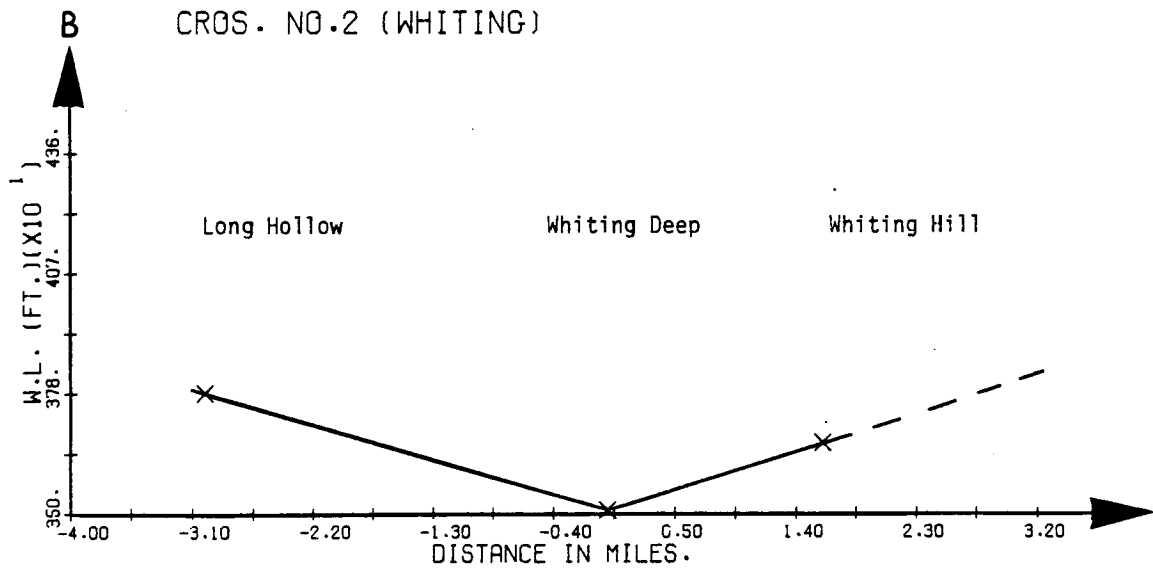
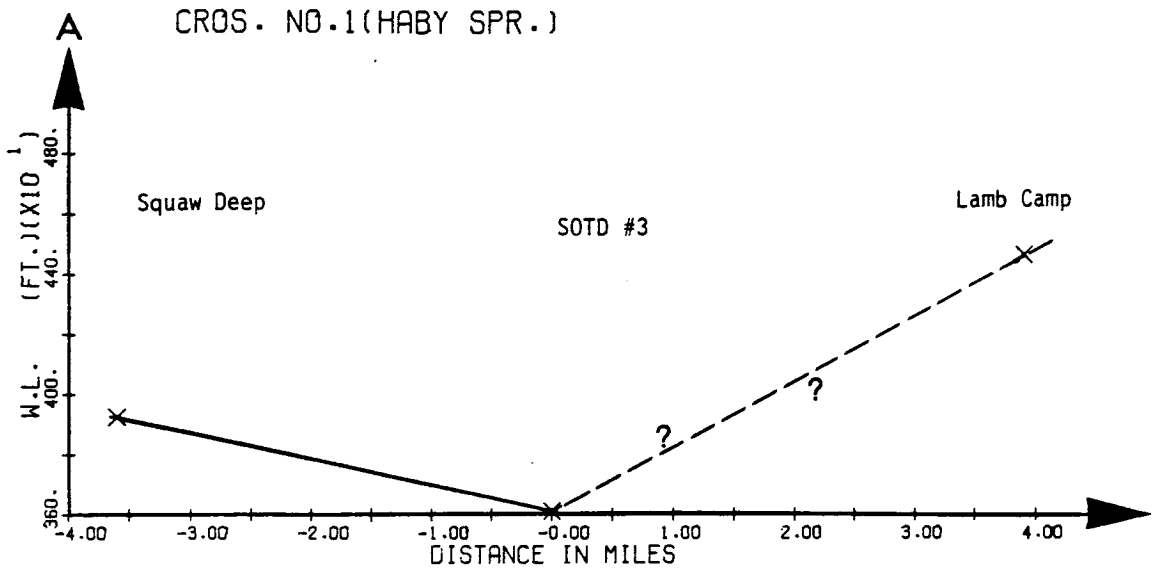


Figure 15. Water level profiles across Aravaipa Valley

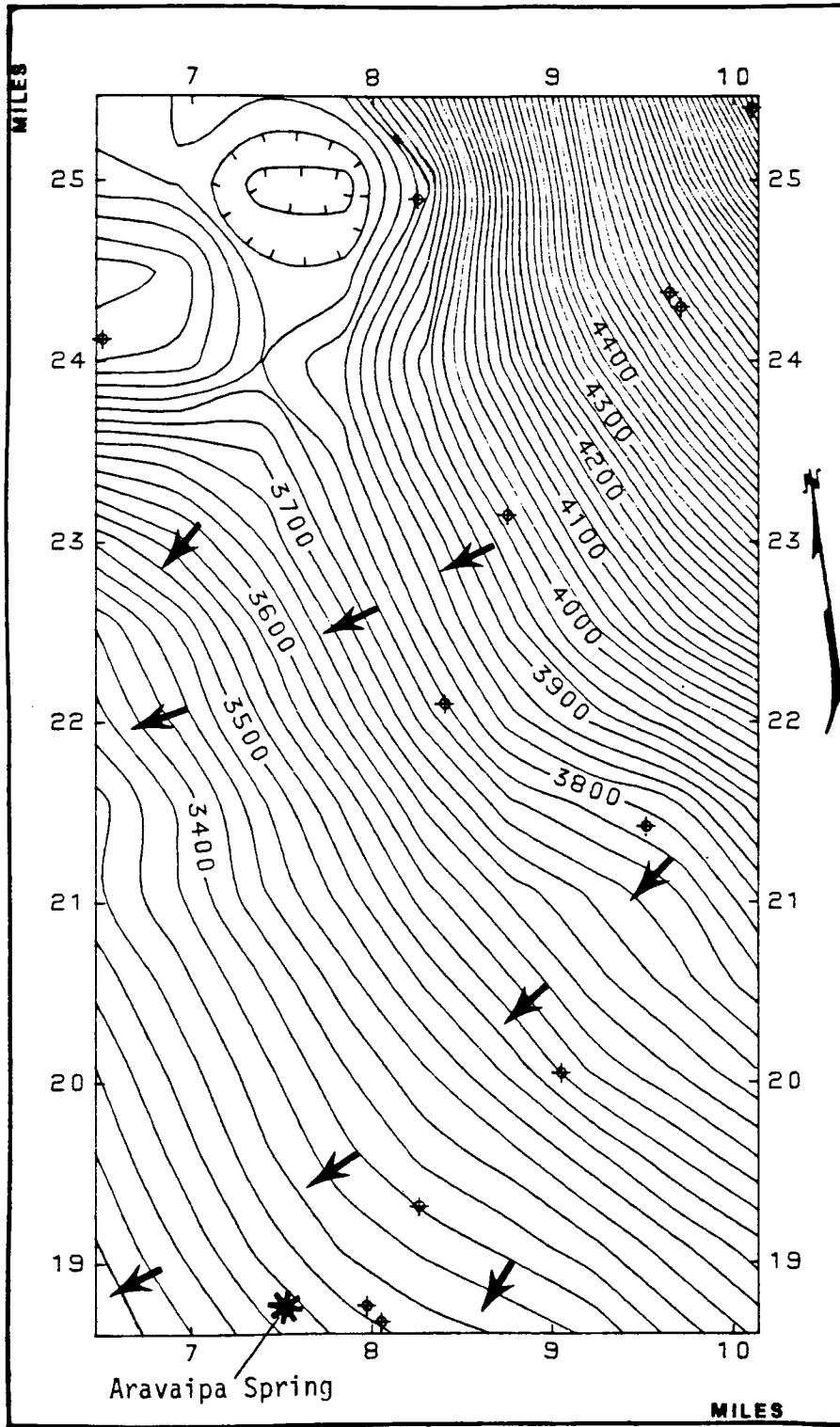


Figure 16. Head distribution in Stowe Gulch section

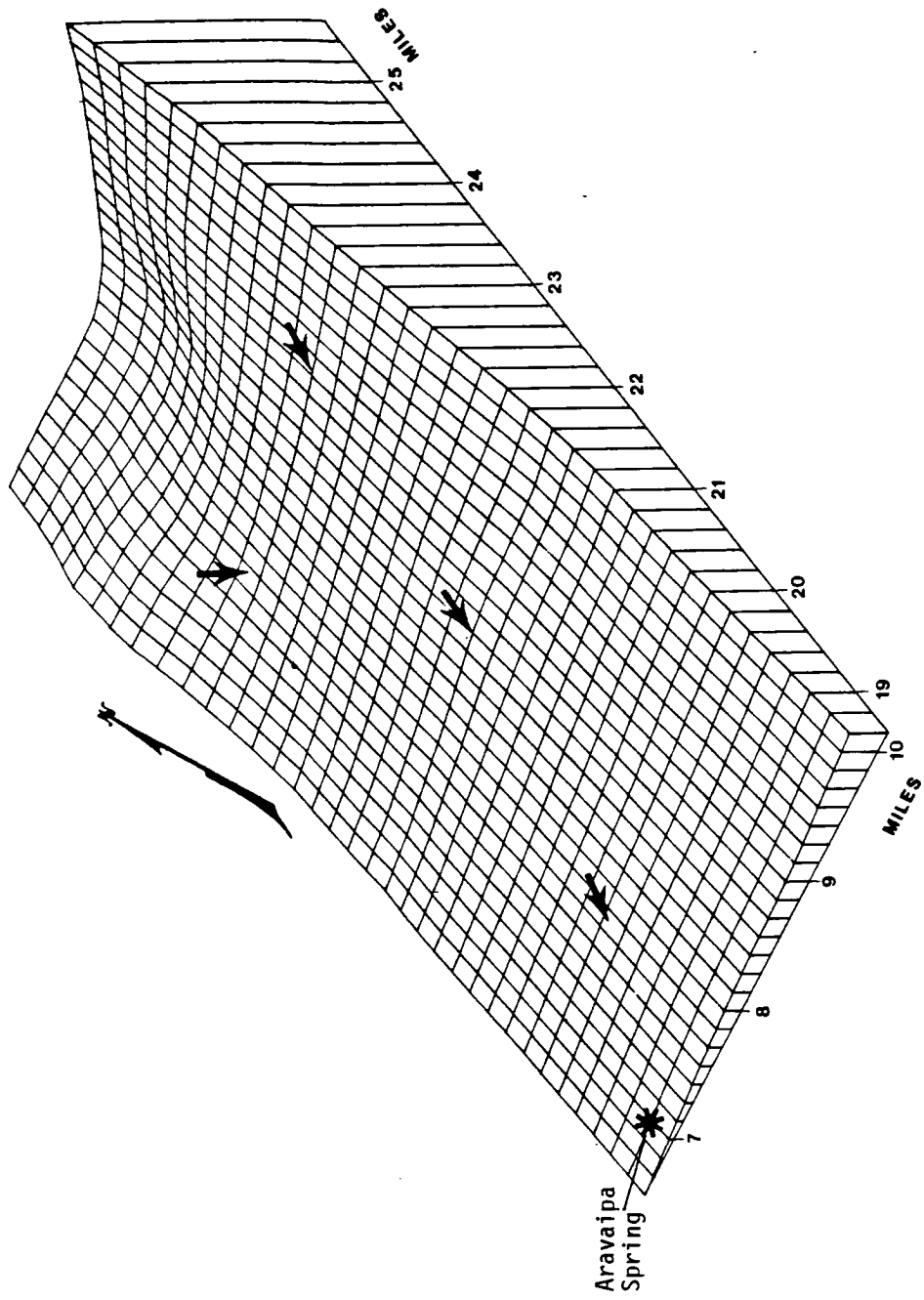


Figure 17. Flow pattern in Stowe-Gulch section

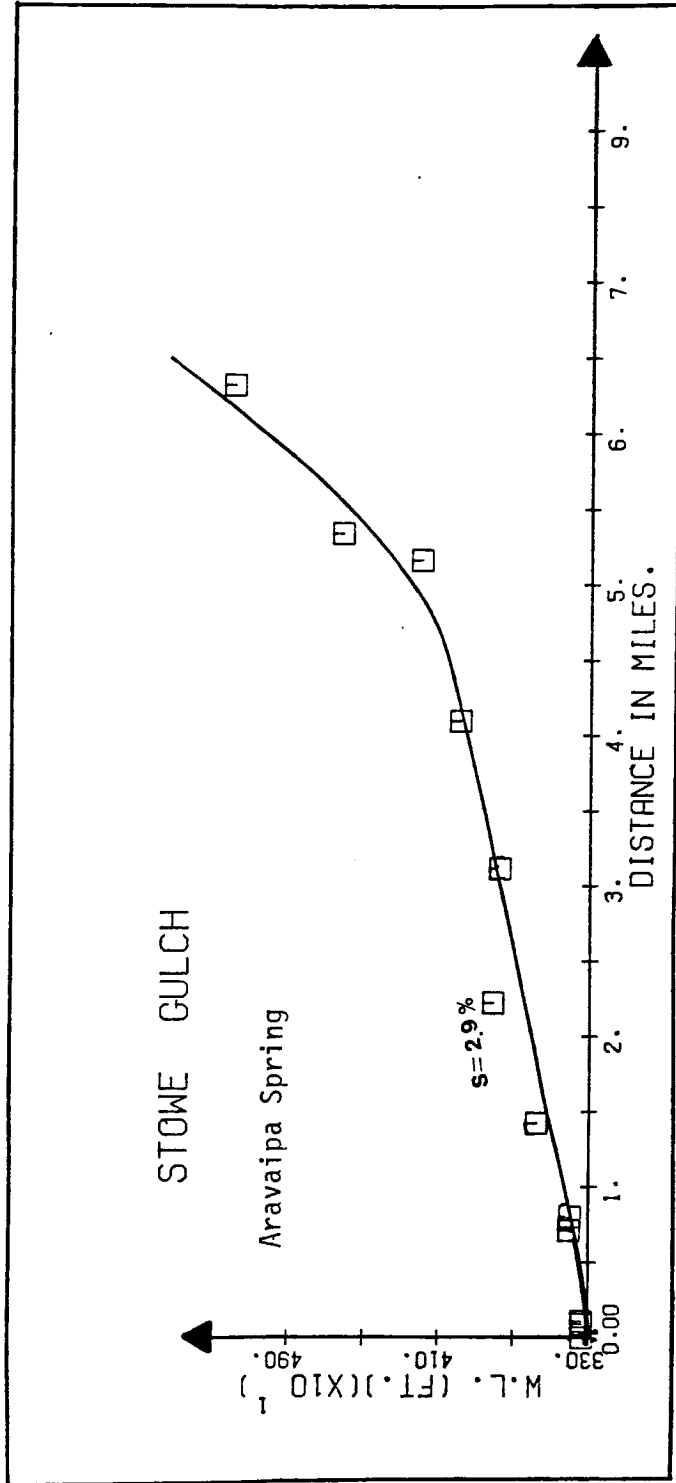


Figure 18. Water level profile in Stowe Gulch basin

CHAPTER 4

AQUIFER RECHARGE AND DISCHARGE MECHANISMS

In this chapter we will use the geological and hydrological information described thus far to postulate a conceptual model of recharge and discharge mechanisms in the Aravaipa watershed. Further support for our model, based on chemical and isotopic data, will be provided in the next chapter. A mathematical framework for the quantitative evaluation of recharge and discharge rates will be described in Chapter 6. Our conceptual model is illustrated in Figure 19.

The major components of recharge into the water table aquifer are:

- a. Direct infiltration from precipitation on the outcrops of the Young Alluvium.
- b. Intermittent stream recharge along Aravaipa Creek during and after winter and summer floods.
- c. Inflows through the alluvial fans at confluences with major mountain washes.
- d. Lateral inflow through the upper layers of the Old Alluvium.
- e. Upward leakage from the deep confined aquifer.

The amount of recharge by direct infiltration from precipitation is related to the outcrop area of the Young Alluvium. Since such outcrops are limited in the lower Eureka and Sharizona sections, this component of recharge there is negligible. This component is expected to be small if any in the upper and lower Klondyke sections.

The amount of recharge caused by stream infiltration is related to the length of streambed at each of the sections and to flood duration

Figure 19. Schematic diagram of flow in Aravaipa Basin

LEGEND

- (1) Mountain front recharge
- (2) Upward leakage into the water table aquifer
- (3) Deep percolation into the confined aquifer
- (4) Side input into the water table aquifer through the old alluvium
- (5) Discharge into the Hell-Hole conglomerate
- (6) Recharge in alluvial fans at the confluences with major tributaries
- (7) Flow in the water table aquifer
- (8) Flow in the confined aquifer
- (9) Stream losses recharge
- (10) Confining layers
- (11) Water table aquifer
- (12) Young alluvium
- (13) Hell-Hole conglomerate
- (14) Old alluvium

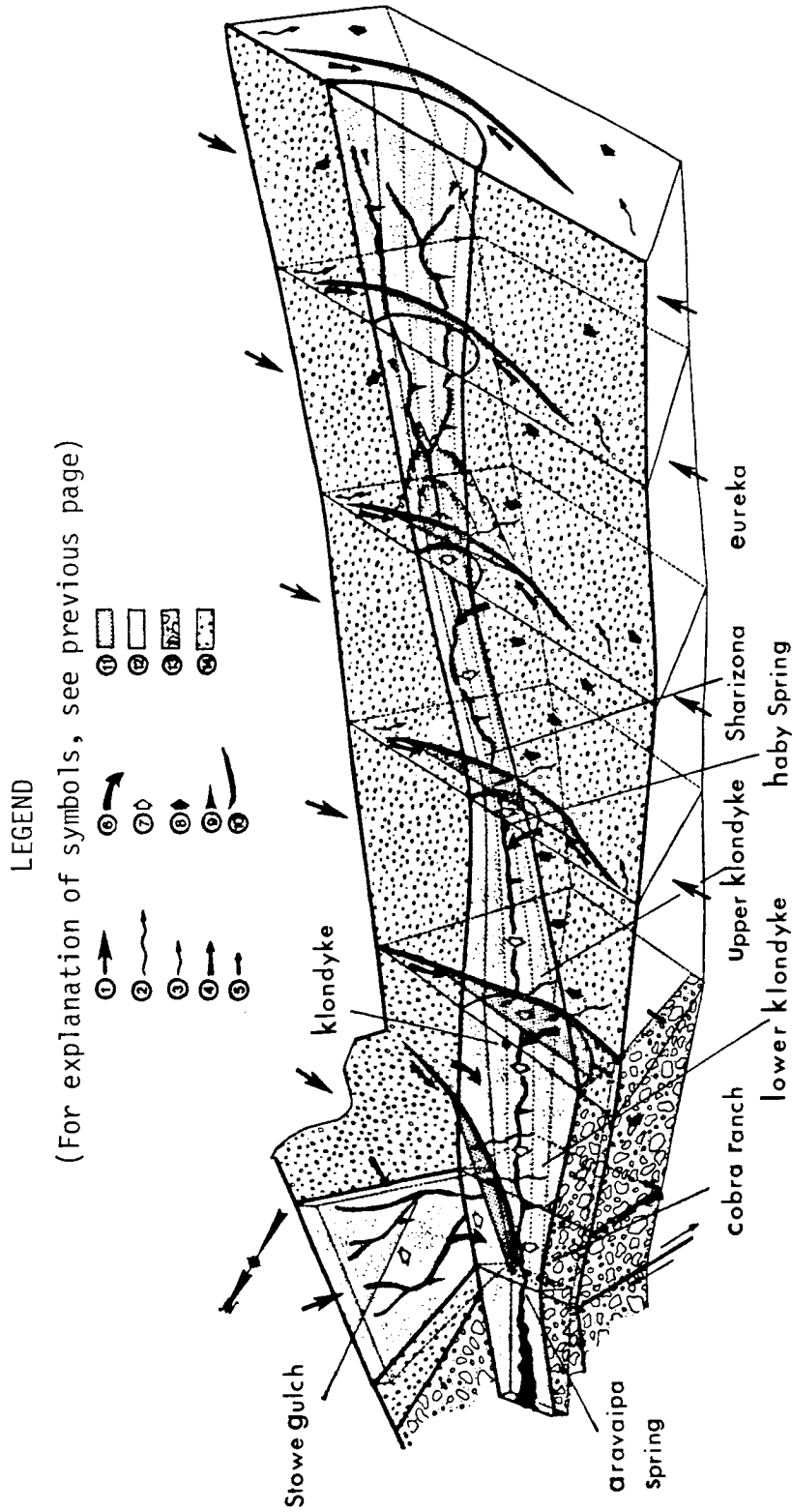


Figure 19. Schematic diagram of flow in Aravaipa Basin (division into cells is for modeling purposes)

and frequency. This component of recharge is significant in the lower Eureka and Sharizona sections. Since most of the floods in Aravaipa Creek are transmitted through Oak Creek, Rattlesnake and Fourmile Canyons, recharge due to stream losses is extremely important in the upper and lower Klondyke sections.

Alluvial fans are recharged by snow melt and floods. Due to steep topographic and hydraulic gradients from these fans to the valley, water flows underground to the upper aquifer at the confluences with Aravaipa Creek. This component of recharge is found to be significant from the Oak Creek alluvial fan at the Sharizona section, from the Rattlesnake fan at the upper Klondyke section, and from the Fourmile, Klondyke, and Laurel canyons at the lower Klondyke section.

Lateral inflows into the Young Alluvium from the Old Alluvium take place along all sections. This component of recharge is expected to be significant. Upward leakage into the upper aquifer from the deep aquifer occurs along the entire length of the valley, as demonstrated earlier in connection with Figure 14.

Recharge into the deep (confined) aquifer consists of direct infiltration from precipitation on the outcrops of the Old Alluvium, intermittent stream recharge along the major tributaries crossing the Old Alluvium, and direct mountain front recharge.

Referring again to Figure 19, recharge in the upper and lower Eureka sections takes place by deep percolation through the Old Alluvium pediment at the valley margins, and through stream infiltration along Aravaipa Creek and its tributaries. Stable isotopes indicate (Chapter 5) that the lower portion of the deep aquifer is recharged from higher

altitudes than the upper portions, possibly by deep inflows from the Pinaleno and Galiuro Mountains.

In the Sharizona section, data regarding the deep aquifer are not available. However hydrogeology indicates (see Chapter 3) that deep percolation along the Old Alluvium pediments is a major source of recharge.

Hydrogeology (Chapter 3) and stable isotopes (Chapter 5) indicate that the confined aquifer in the upper Klondyke section derives its water from lateral inflow originating in the Santa Teresa mountains, and from deep percolation through the western Old Alluvium pediment.

In the lower Klondyke section, the eastern component of mountain-front recharge is similar in nature to that in the upper Klondyke section. The western component (if such exists) comes from deep percolation through the Hell Hole conglomerate.

We now turn to the examination of aquifer discharge. The perennial stream originating at the downstream end of Aravaipa Valley has been assumed by Ellingson (1980) and Arad and Adar (1981) to be the major and perhaps sole natural outlet of water from the basin. Analyses of chemistry and environmental isotopes (Chapter 5) show similarities between the water in the upper aquifer in the lower Klondyke section and the water that emerges at Aravaipa Spring. The question whether the deep aquifer contributes directly to the perennial flow in Aravaipa Canyon remains open. However, indirect discharge from the deep aquifer via upward leakage to the unconfined aquifer is known to exist in the upper Klondyke section.

Estimation of discharge by means of pumpage is given in Table 1 in acre-feet/year for each aquifer and every section:

Table 1. Estimated discharge by means of pumpage for every section in Aravaipa Valley

Section	Upper Aquifer (ac-ft/year)	Lower Aquifer (ac-ft/year)
Upper Eureka	-	650
Lower Eureka	100	40
Sharizona	600	-
Upper Klondyke	900	10
Lower Klondyke	<u>800</u>	<u>-</u>
	2400	700
TOTAL	3,100 acre feet/year	

Pumping from the aquifers in the valley has remained essentially constant since 1957 when mining activities had ceased. The nature of the local agriculture and the size of the irrigated area have also stayed unchanged during the last thirty years. This suggest that with the exception of seasonal and annual fluctuations, the groundwater system in the basin may be considered at steady state.

To further corroborate the last statement, we shall look at the hydrographs of four wells in the Aravaipa Watershed monitored by the U.S.G.S. once every winter: Bull Pasture--near Eureka, since 1953; Bird Cage--also near Eureka, since 1949; Peyote Church--in lower Eureka section, since 1955; Whiting #2--in upper Klondyke section, since 1953; (Gould and Wilson, 1975) as shown in Figure 20.

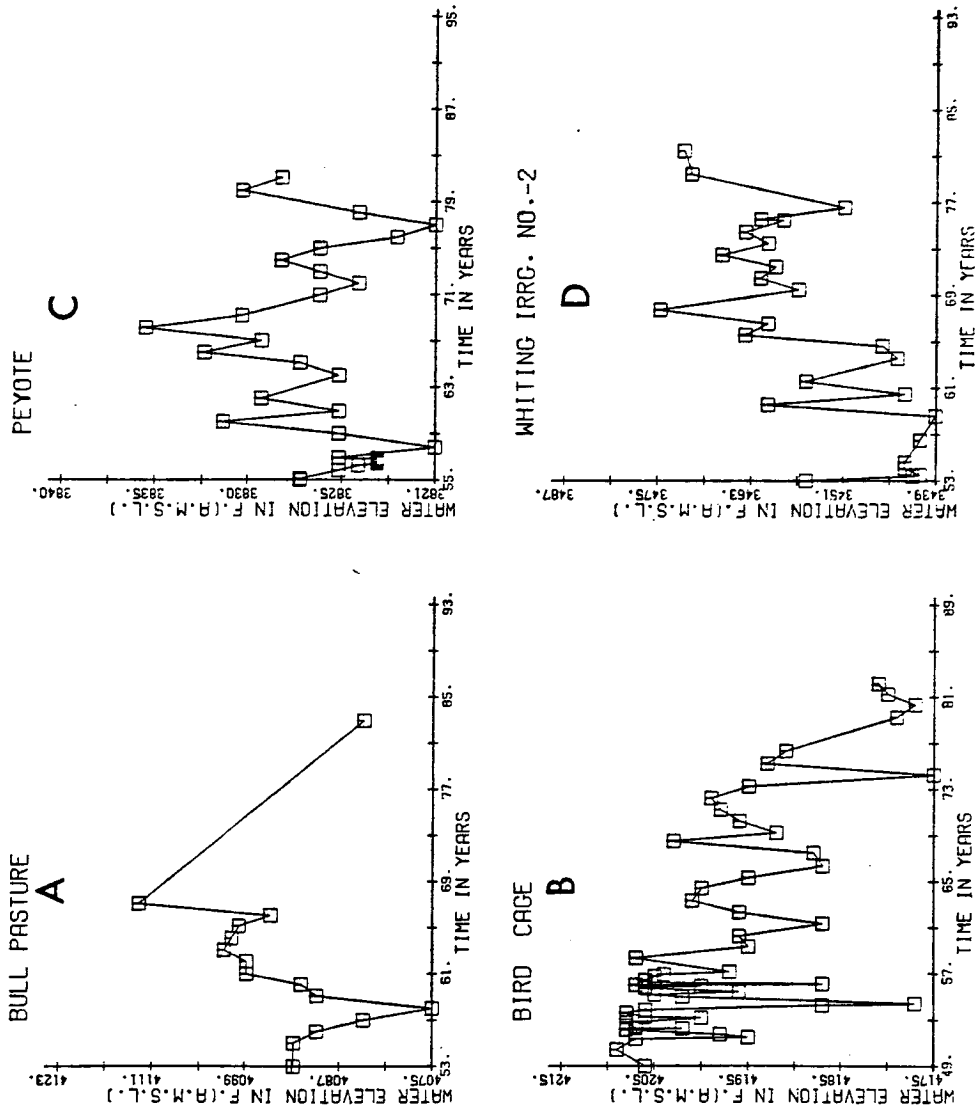


Figure 20. Water level fluctuations in four wells

It appears that the Bull Pasture and Bird Cage wells derive their water from the confined aquifer, whereas the Peyote Church and Whiting #2 wells extract water from the upper aquifer. In the Bull Pasture well, the water level fluctuates ± 20 feet, and the current depth to water is almost the same as in 1953/54. However, since 14 years of data are missing, it is difficult to tell whether a trend exists. At Bird Cage, the water level fluctuates ± 15 feet and shows a discernible downward trend (Figure 20-B). In the Peyote Church well, the water level fluctuates not more than ± 6 feet (Figure 20-C) and there is no apparent trend. During the last 30 years, the water level in the Whiting #2 well has fluctuated at most ± 15 feet and there is some indication of a long term recovery (Figure 20-D). Overall, the water level fluctuations are relatively small and can be attributed to temporary flood effects, annual variations in precipitation, and temporary effects of nearby irrigation.

Depths to water in the Whiting Deep well (upper Klondyke section, Figure 6) were 29 feet in 1959 (U.S.G.S.), 27 feet in 1979 (Ellingson, 1979), 29 feet in summer 1980, 23 feet in winter 1980/1981, 13 feet in winter 1982, 25 feet in summer 1983 and 15 feet in October 1983. This indicates that depth to water in the confined aquifer in the lower portion of the valley has fluctuated ± 10 feet about a constant value. Thus, the hydrological regime in the valley is, for all practical purposes, at steady state. This means that on a long-term basis, total recharge into the valley aquifers equals total discharge.

Some preliminary quantitative statements regarding discharge rates can be made. A hydrometric station located six miles downstream

from the head of the canyon (Figure 1) has been operating since October 1980 (U.S. Department of the Interior, Bureau of Land Management, Safford, Arizona). The base flow, which we assume comes entirely from the valley aquifers and not from the canyon walls, was 13,000 acre feet/year in 1981 and 9,900 acre-feet/year in 1982. Ellingson (1979) estimated the annual natural discharge from the valley aquifers to be 7400 acre feet/year. His estimation was based on 22 years of flow records obtained at the outlet from Aravaipa Canyon (U.S.G.S. No. 9473000, in Figure 1) and on calculated evapotranspiration from the canyon. A summary of his calculations is given below:

- | | |
|--|-----------------------|
| 1. Average annual outflow from western Aravaipa Canyon (22 years of records) | 20,300 acre feet/year |
| 2. Average annual volume of floods, as separated from representative stream hydrographs for four years during which the precipitation was close to the long-term mean annual value | 15,073 acre feet/year |
| 3. Base flow at outlet from Aravaipa Canyon (item 1 minus item 2) | 5,227 acre feet/year |
| 4. Annual evapotranspiration from Aravaipa Canyon (2,440 acres) | 2,172 acre feet/year |
| 5. Mean annual discharge from Aravaipa Basin (item 3 plus item 4) | 7,399 acre feet/year |

Ellingson's was only a rough estimate of the annual natural discharge. His calculations disregard potential contribution to base flow in the canyon from the surrounding hard rocks.

A comparison between stream hydrographs at the inlet to, and outlet from, the canyon for the years 1980-1982 (Figure 21) shows that discharge at the outlet is always higher than that at the inlet. The same is true in months during which no floods have been recorded,

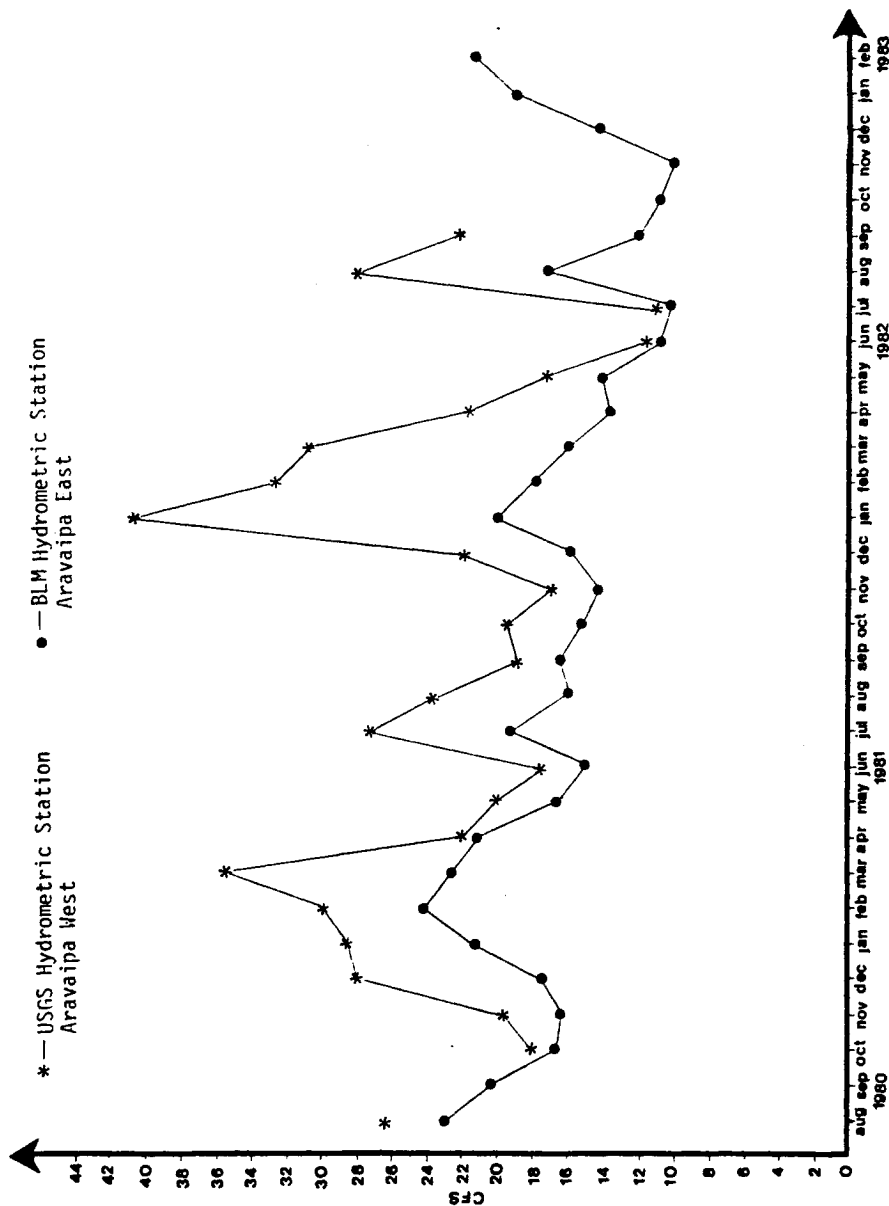


Figure 21. Average monthly discharge in Aravaipa Canyon

suggesting that there must be some contribution to baseflow from the surrounding hard rocks. That there is a hydraulic gradient in these rocks toward the canyon is clearly visible in Figure 22.

If we accept our own measurement of discharge in the amount of 9,900 acre feet/year, and our estimate of pumpage in the amount of 3,100 acre feet/year, we arrive at an approximate figure for total recharge into the the basin of 13,000 acre feet/year.

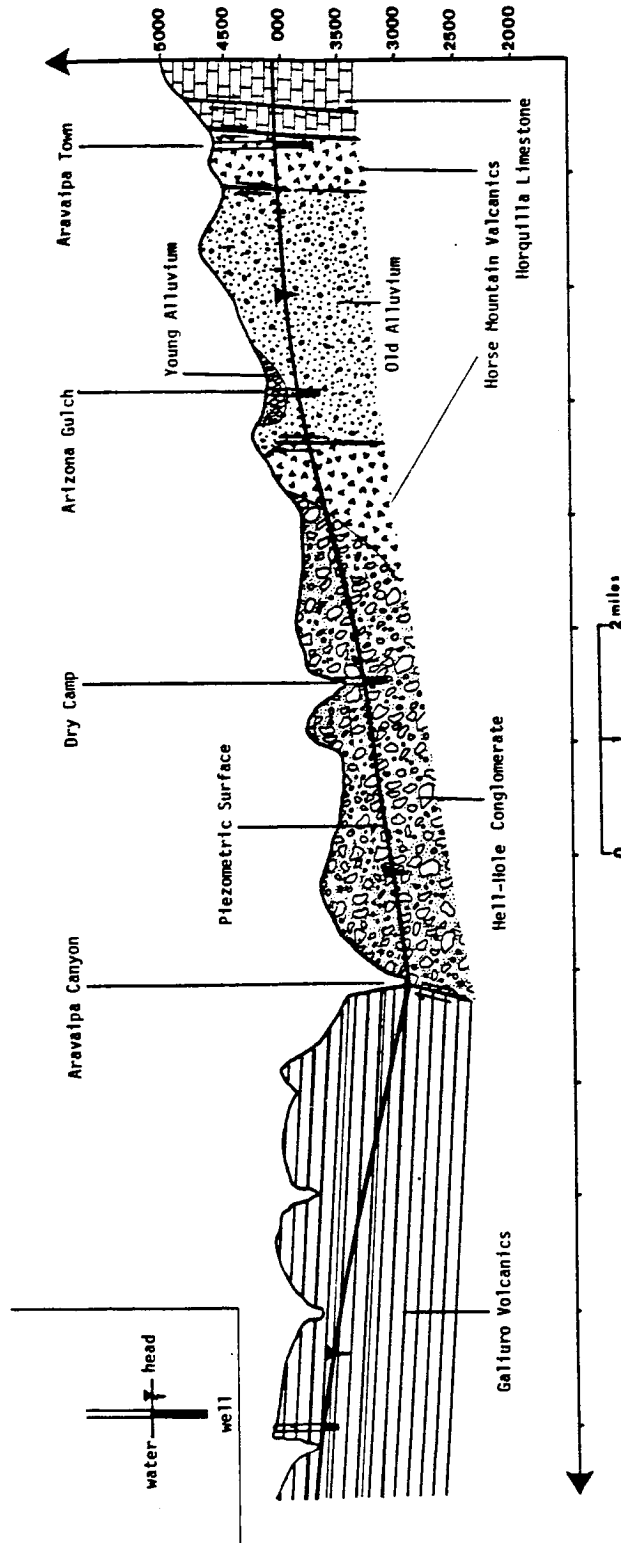


Figure 22. Schematic geologic section and piezometric profile across Aravaipa Canyon along B-B' in Figure 4

CHAPTER 5

IDENTIFICATION OF AQUIFER FLOW
COMPONENTS THROUGH THE USE OF
AQUEOUS CHEMICAL AND ENVIRONMENTAL ISOTOPE DATA

Variations in water chemistry and naturally-occurring isotopes have been used as a means of refining the Aravaipa Watershed flow model. Later, these data will be used to suggest an alternative flow model for the Aravaipa, and to establish the sources of recharge to each aquifer. Only data relevant to the model are discussed.

The upper and lower aquifers exhibited different ranges of temperature, water level, and concentration of environmental isotopes: higher temperatures and hydraulic heads, heavier stable isotopes and lower values of radioactive isotopes are found throughout the entire areal extent of the lower aquifer (data are given in Appendix C, tables 1 and 2). These differences in temperatures and hydraulic heads will help us decide whether various wells are open to the upper, lower, or both aquifers. Chemistry and environmental isotopes will be used to identify potential sources of recharge, possible mixing and dilution of waters from these sources, and to obtain a clearer picture of the sub-surface flow pattern. As we shall see later in this chapter, the initial values of stable isotopes in precipitation are essential to identify locations of potential recharge. The stable isotope distribution in precipitation over Aravaipa Watershed is discussed in the following section.

Effect of Altitude on Stable Isotope
Distribution in Aravaipa Watershed

The composition of stable isotopes in rainfall, as it is sampled at the surface, is controlled by fractionation due to differences in (1) type of storm; (2) elevation of the cloud system; (3) temperature of condensation; (4) moisture content and its origin; (5) distance between the base of the cloud and the surface; (6) ambient air temperature; and (7) the rate of evaporation (Craig, 1961; Dansgard, 1964; Hoefs, 1980; Gat, 1980). A further fractionation causing enrichment in O-18 and D occurs due to evaporation from overland flow and near-surface soil moisture (Gat and Tzur, 1967; Zimmerman et al., (1967). Water that infiltrates underground to a depth at which evaporation ceases usually maintains constant O-18 and D ratios unless oxygen exchange with rocks and retardation of deuterium by soil clay minerals takes place. Any further changes in the concentration of O-18 and D along the flow path within the aquifer must be due to mixing with waters having different isotopic compositions.

The spatial distribution of stable isotopes in precipitation over Aravaipa Basin was evaluated from the four sampling stations shown in Figure 23. A special rain sampler for stable isotopes was designed so as to prevent evaporation of the accumulated water sample. A detailed description of this sampler is given in Appendix D.

Figure 24 shows schematically the distribution of $\delta\text{O-18}$ in precipitation for six sampling periods versus topography and altitude across Aravaipa Valley near Klondyke. It is seen that (a) summer storms are significantly heavier than winter storms; (b) the heaviest water is

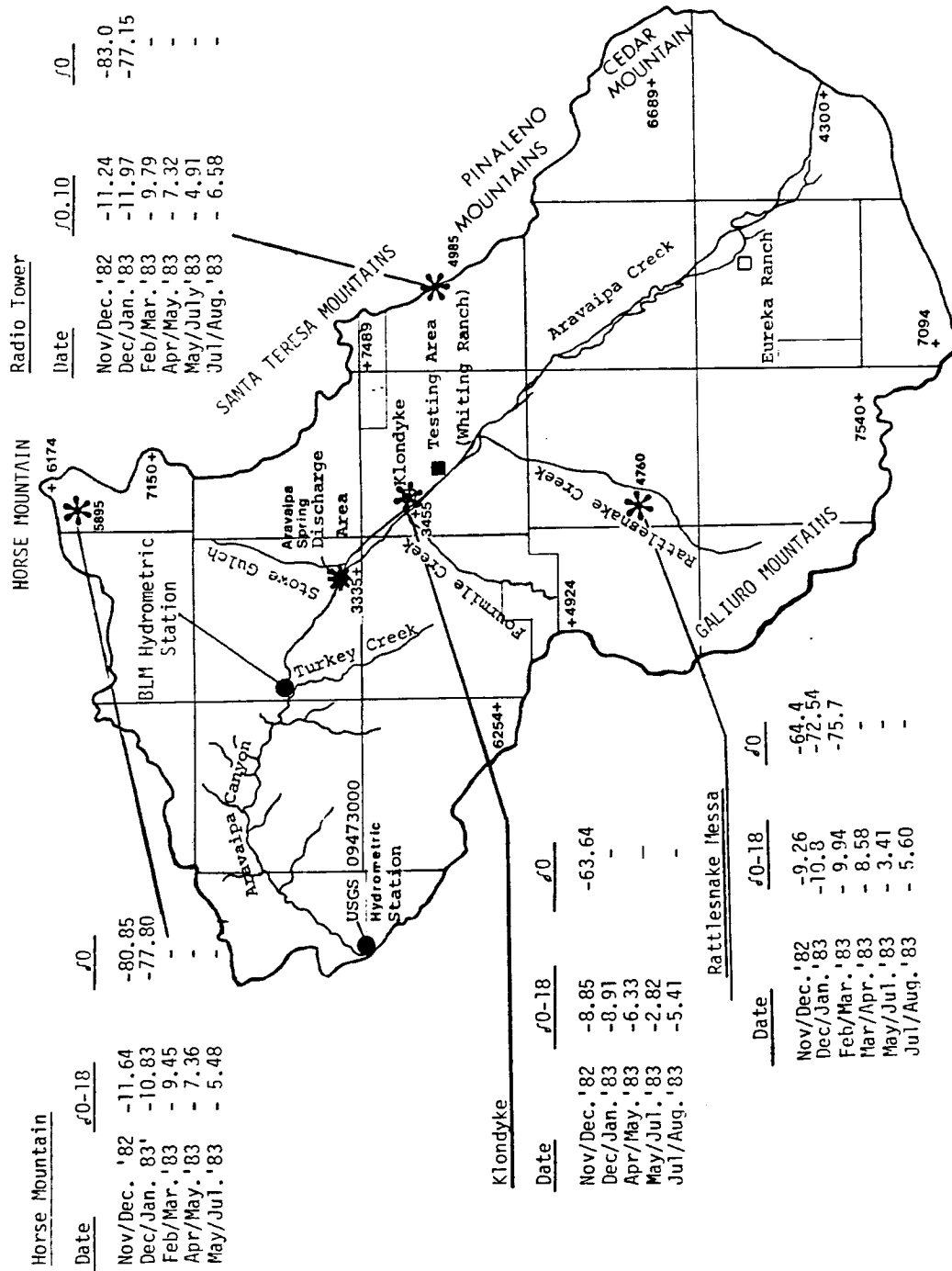


Figure 23. Stable isotope distribution in precipitation in Aravaipa Valley

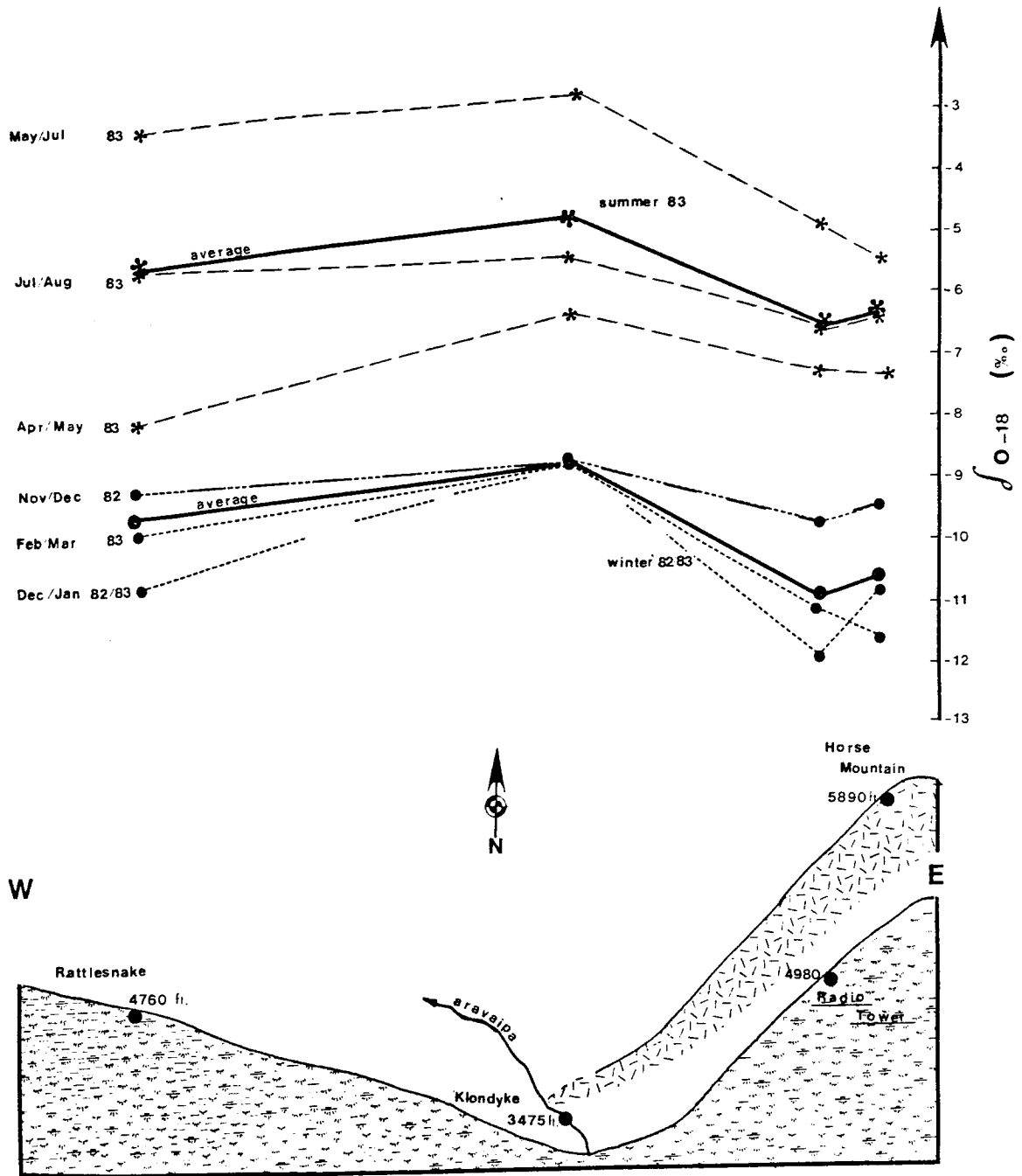


Figure 24. Distribution of $\delta O-18$ (‰) in precipitation across Aravaipa Valley

always found at the bottom of the valley (at Klondyke); and (c) rainfall on the eastern pediments is depleted in O-18 relative to that on the western pediments.

Summer storms are enriched in O-18 in comparison to winter storms due to the fact that they originate over warm bodies of water (such as the Gulf of Mexico; Craig et al., 1963) and due to higher ambient air temperature where enrichment is caused by evaporation. When the storm reaches the valley, the rates of evaporation from rain drop and isotope enrichment are enhanced by the relatively high summer temperatures and low humidity of the air. The heaviest water is found at the bottom of the valley because here the vertical distance traveled by the raindrops is the greatest, allowing more time for evaporation to take place both in summer and in winter. This is known as the "altitude effect." The fact that water in the east is depleted in δ O-18 in comparison to water in the west at a given altitude can be attributed to the relation between the path of the storm and the topography. Thus, the rain sampler at Rattlesnake Mesa is located on the lee side of the Galiuro Mountains, and the sampler near the Radio Tower and Horse Mountain is located on the foreside of the Santa Teresa Mountains. On the lee side, the vertical distance traveled by the raindrops is greater than on the foreside, causing the lee side to be relatively enriched in δ O-18. The storm of April, 1983 is the only one among those shown in Figure 24 that approached the valley from the southeast instead of the southwest; its isotopic pattern is therefore the reverse of the other storms.

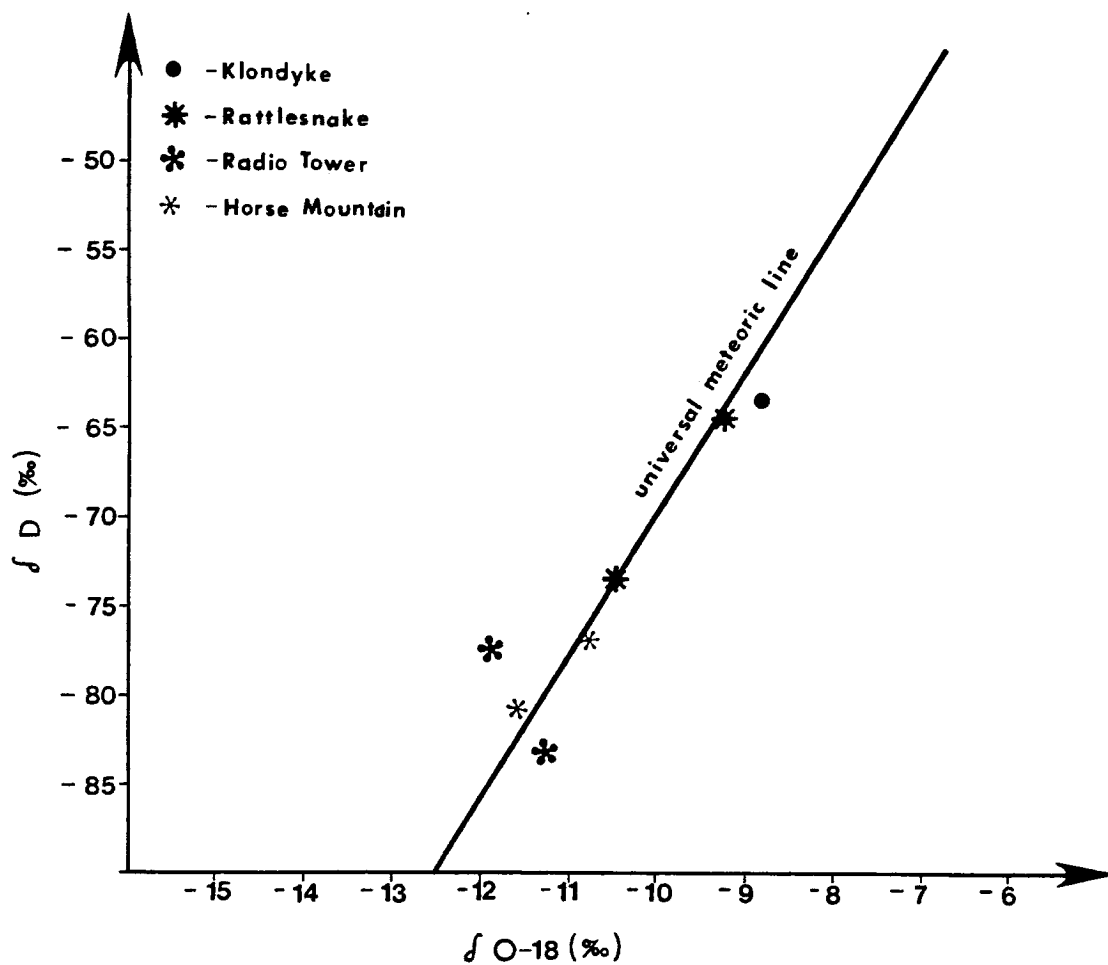


Figure 25. Oxygen-18 versus deuterium in seven rain storms sampled in Aravaipa Valley

The effect of altitude and topography on the distribution of stable isotopes in rainfall is also shown by the binary diagram of $\delta^{18}\text{O}$ versus δD in Figure 25. This diagram shows the same pattern as in Figure 24. The rain sample from Klondyke is located at the heaviest position along the universal meteoric line (Craig, 1961). The samples from the eastern pediments (Radio Tower and Horse Mountain) are located at the most depleted position, and those from the western pediments (Rattlesnake) are placed midway between them. The pattern of isotopic distribution found in rainwater is closely reflected in the groundwaters of the deep aquifer as will be discussed in the following section.

Distribution of Oxygen-18 and Deuterium in Groundwaters

Due to their conservative nature, variations in $\delta^{18}\text{O}$ and δD in groundwater are related primarily to differences in the origin of recharge. On the other hand, variations in the stable isotope ratios of different recharge sources are due mainly to variations in altitude and the nature of local storms. Additional factors include the characteristics of the hydrographic system and soil cover that affect the evaporation of overland flow and near-surface soil moisture. Evaporation from stream channels causes additional fractionation of oxygen and hydrogen isotopes in a manner which results in the enrichment of the stream water in $\delta^{18}\text{O}$ and δD .

The isotopic ratios of subsurface waters in the Aravaipa Valley vary with location and depth. Similar variations were observed by Newman and Dansberg (1977) in the Hula Valley of Israel. The latter

authors were able to relate spatial variations in the isotopic and chemical composition of the Hula Valley waters to the three-dimensional flow pattern in the basin. In particular, they used O-18, tritium, and water chemistry data to obtain a better understanding of this flow pattern than would have been possible with head data alone, and to suggest that the local groundwater is derived from two distinct sources of recharge. We will show that the data from Aravaipa Valley permit an even more detailed identification of recharge sources than was possible in Hula Valley.

Figure 26 presents $\delta^{18}\text{O}$ and δD data for 47 water samples from wells, springs and floods. This figure, together with more detailed diagrams in Figures 27A, 27B, and 27C, shows that:

- (a) the heaviest isotopic composition occurs in the Long Hollow mountain-front well on the western margin of the deep aquifer, springs issuing from old alluvium western pediments and floods in Aravaipa Creek;
- (b) the isotopic composition of the deep aquifer along the valley is heavier than that of the upper aquifer and lighter than that of flood water (Figure 27A);
- (c) four out of five water samples from Aravaipa Spring (Figure 27B) have similar compositions to samples from the upper aquifer and show lack of apparent mixing between the upper and the lower aquifers;
- (d) samples from the Whiting Hill mountain-front deep well on the eastern margin (near Klondyke) are the most depleted in the watershed;
- (e) all five flood samples analyzed to date for both $\delta^{18}\text{O}$ and δD (three from winter floods and two from summer floods) are heavier than water from the upper aquifer.

Based on (a), (b), (d), and Figure 27C, one can postulate that water recharging the deep aquifer could originate partly from stream

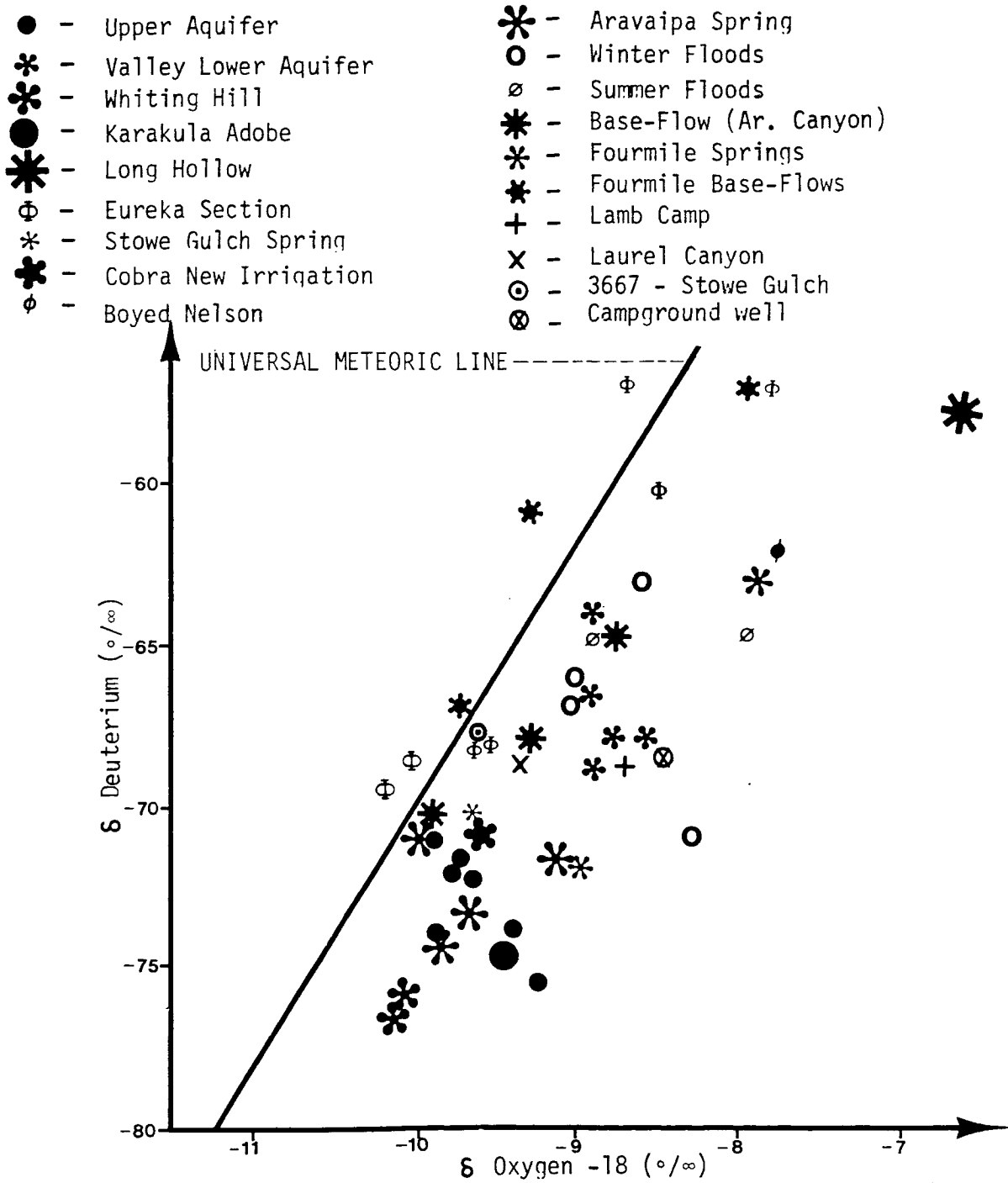


Figure 26. Oxygen-18 versus deuterium in wells, springs, floods, and base-flows in Aravaipa Watershed

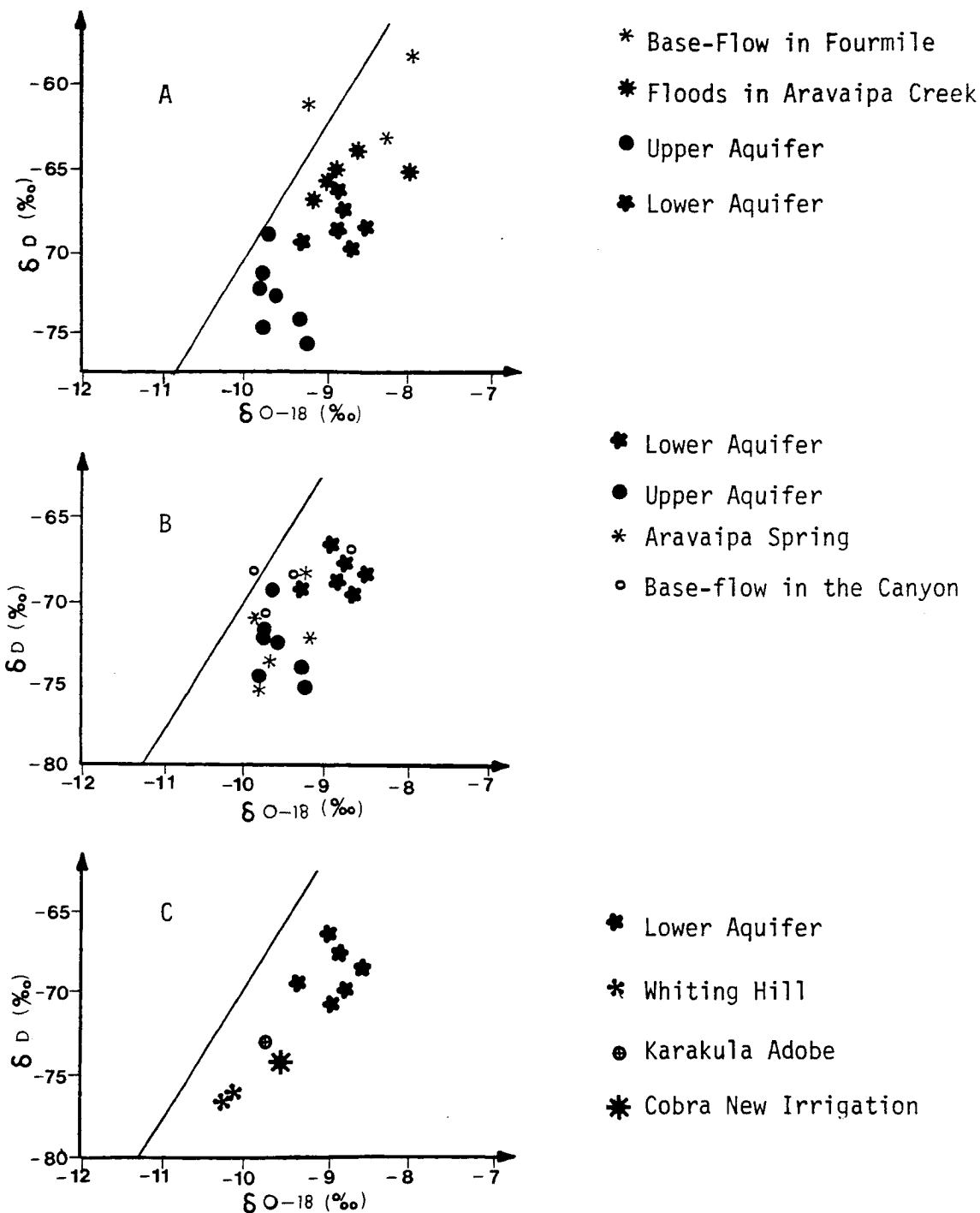


Figure 27. Oxygen - 18 versus deuterium in waters obtained from:
 A) Floods, Deep Aquifer and Upper Aquifer
 B) Base-Flows, Deep Aquifer, Upper Aquifer and Aravaipa Spring
 C) Deep wells in the valley and deep wells along the Margins.

loss and deep percolation through the old alluvial pediments and partly from mountain-front recharge sources as represented by the Long Hollow and Whiting Hill wells.

From (b) and (c), one sees that Aravaipa Spring is fed solely by the upper aquifer; however, base flow three to five miles down the canyon presents heavier $\delta O-18$ than water in the upper aquifer yet similar to water in the deep aquifer. This could be, in part, due to base flow contributed by the lower aquifer and, in part, due to evaporation along the canyon.

Based on (d) and (e) it is clear that since the upper aquifer is recharged partially by floods in Aravaipa Creek, there must be another source of recharge with much lighter $\delta O-18$ and δD ratios. Our data suggest two possible sources: (1) the Whiting Hill well area along the elevated eastern pediments, and (2) floods from intense but short winter storms. The first possibility was already suggested earlier in Chapter 3 and illustrated in Figure 7. A further discussion of the possibility of recharge from floods will be presented later in this chapter.

Identification of Flow Components in the Upper Eureka Section

As mentioned earlier, well logs and hydrogeologic data suggest that the upper aquifer, as it exists near Klondyke, is absent at Upper Eureka section. Figures 28A and B indicate that waters derived from 13 wells in the Eureka section do not all originate from a single source: the "fingerprint" (Schoeller) diagrams in Figure 28A are similar to each other but differ from those in Figure 28B. We will refer to the water

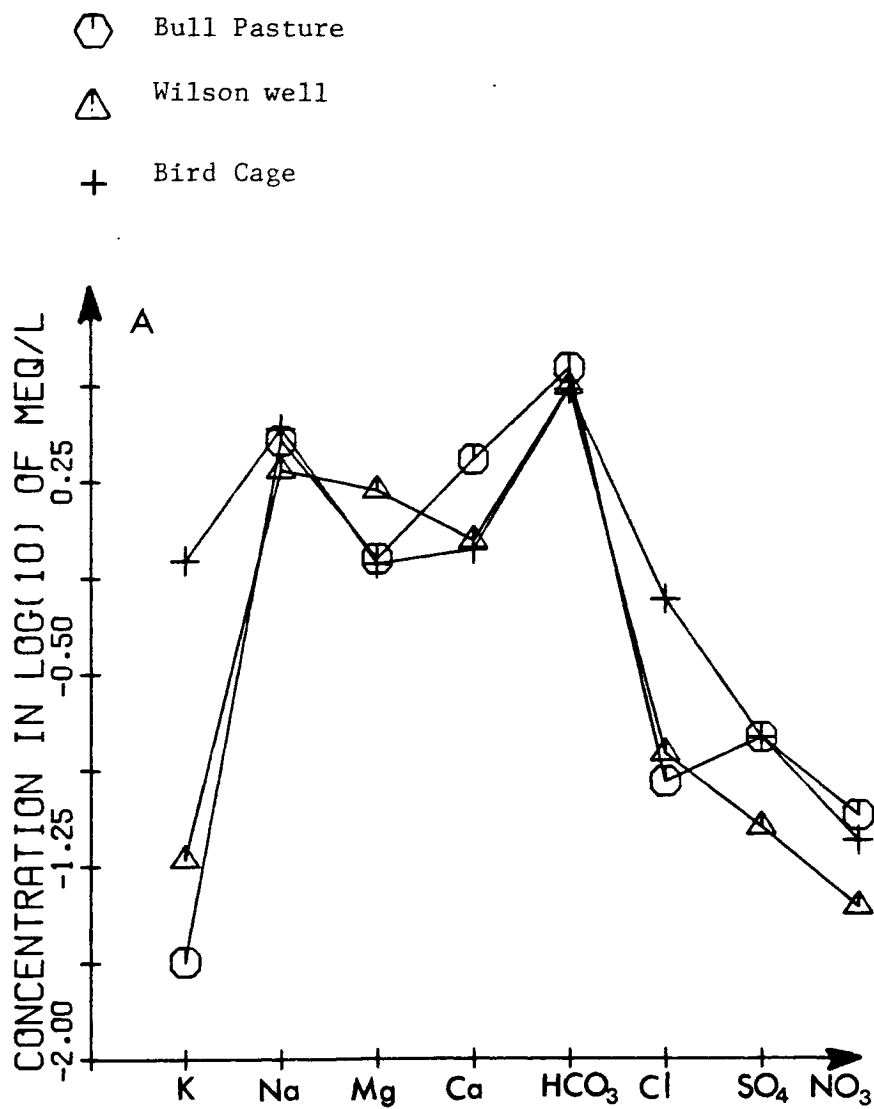


Figure 28. Schoeller diagram for wells along the boundaries of upper Eureka section.
 A) Group (a); wells along the southeastern boundary.

Eureka Dom.
 X Apple Tree.
 Eureka # 6
 Eureka # 1

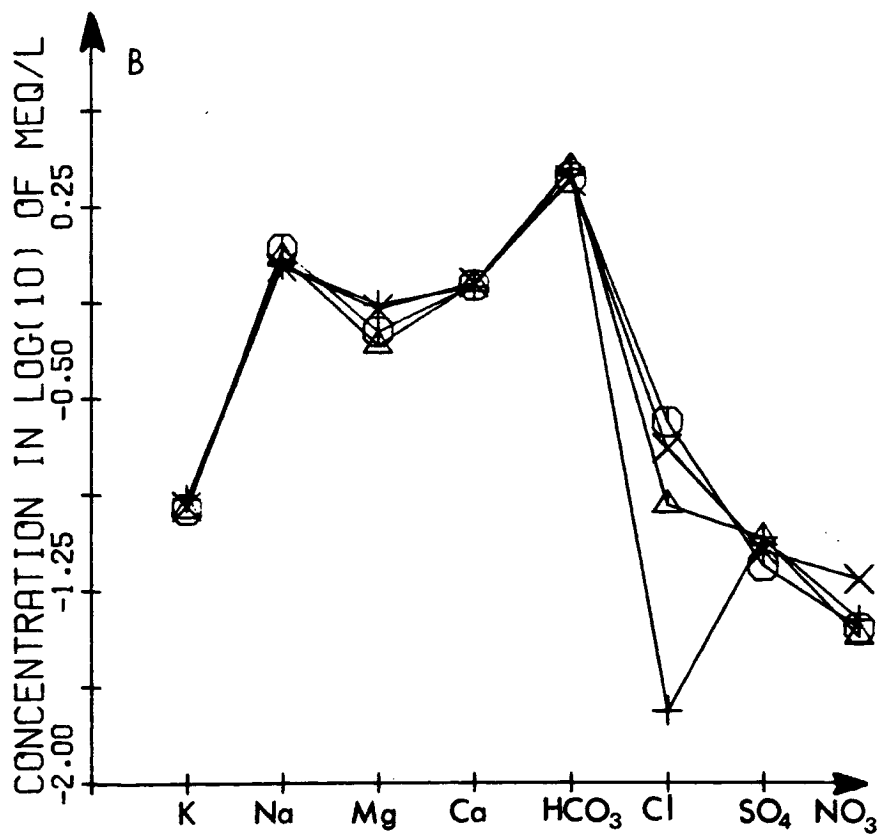


Figure 28 --Continued
 B) Group (b); wells along the southwestern boundary

in the Bull Pasture, Wilson, and Bird Cage wells (Figure 28A) as group a, and to that in the Eureka Dam, Eureka #6, Apple Tree, and Eureka #11 wells (Figure 28B) as group b.

Waters of group a are found in shallow wells located along the southeastern margin of Upper Eureka section. These waters are rich in Ca, Mg-HCO₃, and Ca-SO₄. Waters of group b are found in deep wells located at the bottom of the valley and along the southwestern margin. These waters are significantly depleted in dissolved ions but show higher contents of K and Na than the waters of group a. Further support for the distinction between these two groups is provided by some of the binary diagrams in Figure 29, particularly diagrams, E, F, G, and H.

All of the samples in Figure 29 which do not belong to group a and b (Black Canyon, Big Tank, Eureka #1, Puddy Lynch, and Little Windmill) are derived from shallow wells located along the main wash; we will designate them as group c. As indicated by the arrows in diagrams C-F and I, the chemistry of these samples changes according to a distinct pattern downgradient (samples at the head of each arrow are derived from wells further downstream than those at the tail). The gradual increase in the concentration of Ca⁺⁺, HCO₃⁻, Na, and TDI (diagrams C-F) and decrease in the concentration of NO₃⁻ (diagram I) downstream are most probably due to mixing with recharge water from stream losses along the tributaries; these diagrams clearly show that group a, representing shallow waters on the margin of the basin, is enriched in Ca⁺⁺, HCO₃⁻, Na⁺, and TDI but is depleted in NO₃⁻. Further support for this theory of mixing will be provided below by stable isotope data.

- - Group (a): 1) Bull Pasture, 2) Wilson, 3) Bird Caye.
- - Group (b): 4) Eureka D., 5) Eureka #6, 6) Eureka #11, 7) Eureka A. T.
- ▣ - Group (c): 8) Black Canyon, 9) McGee, 10) Big Tank, 11) Eureka #1, 12) Puddy Lynch, 13) Little Windmill

→ - General flow direction in the upper aquifer

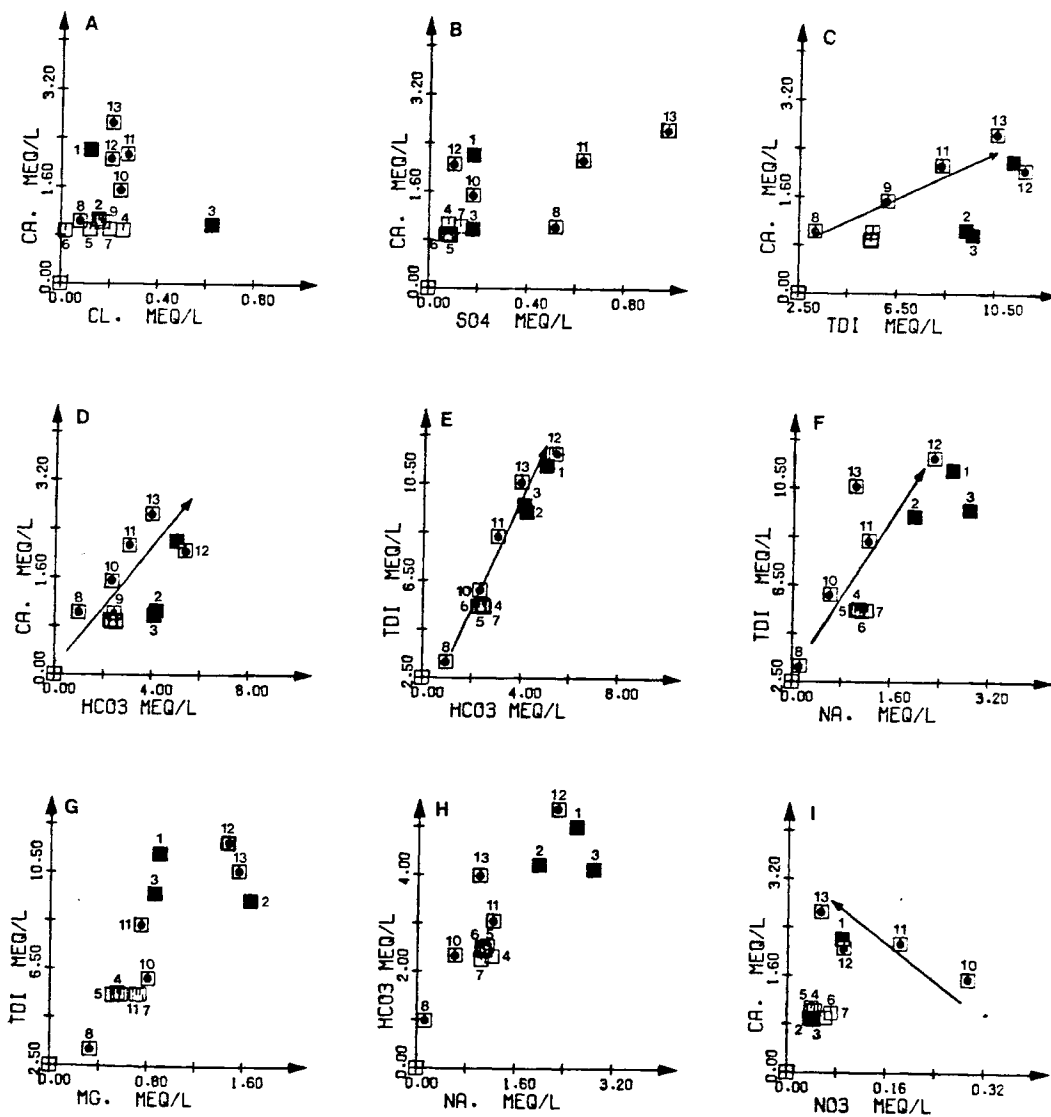


Figure 29. Groundwater chemistry in the upper Eureka section

- | | |
|----------------|---------------|
| ○ Black Canyon | X Eureka # 1 |
| △ Mc Gee | ◇ Puddy Lynch |
| + Big Tank | ⋈ Little Wm. |

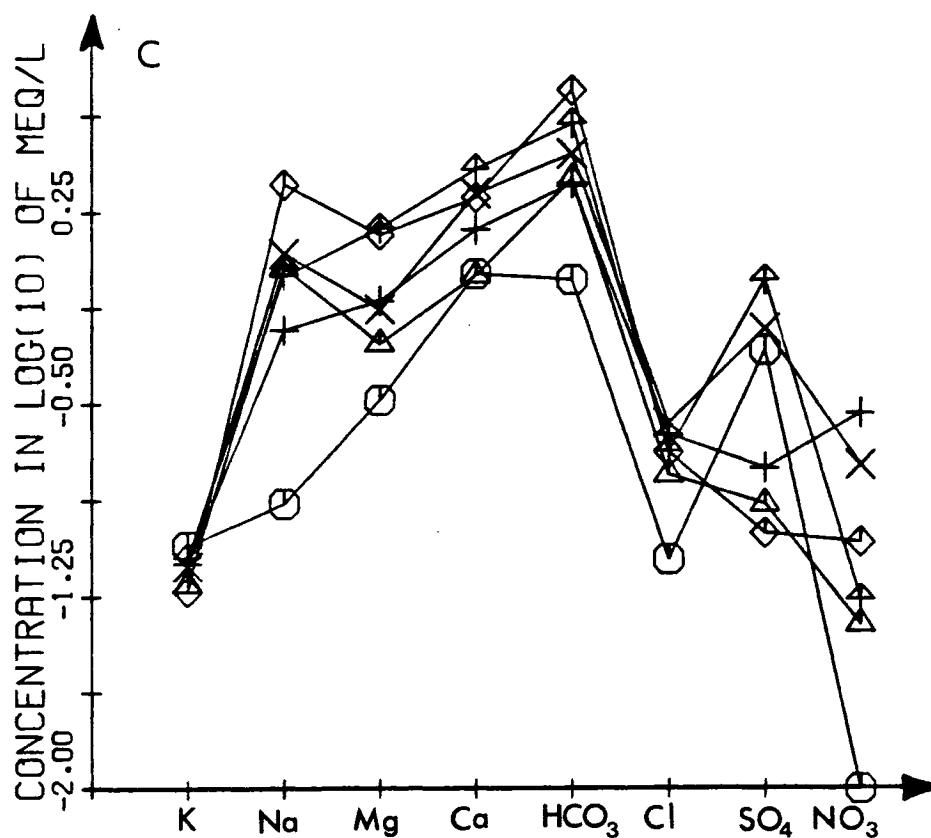


Figure 30. Schoeller diagram for shallow wells in upper Eureka section (group c)

A fingerprint diagram for the waters of group c is shown in Figure 30, illustrating the aforementioned downstream trends from a different perspective.

Figure 31 shows a cross-section across the upper Eureka section with $\delta O-18$ values for several wells. The water in the uppermost aquifer, as sampled in two wells along the eastern margin of the valley, is seen to be relatively light in $\delta O-18$ ($-10.1^0/00$ to $-11.02^0/00$). Wells of intermediate depth in the center of the valley are significantly heavier in $\delta O-18$ ($-8.5^0/00$ to $-10.2^0/00$). These wells obtain their water from confined segments of the lower aquifer. The deepest wells, located on the west margin, penetrate deeper layers of conglomerate, tuff and lava and are heavily depleted in $\delta O-18$ ($-11.9^0/00$ to $-12.1^0/00$). Figure 32 presents $\delta O-18$ versus δD for wells in the Eureka section. It clearly shows that waters of group c are in a heavier state than those of groups a and b. This is due to the evaporation of runoff which is the main source of recharge to the shallow zone tapped by wells of group c.

Figure 33 shows binary diagrams of $\delta O-18$ versus different chemical indicators. The arrows in these diagrams have the same meaning as in Figure 29. We see that the concentration of O-18 in the shallow wells of group c diminishes downstream, and that the waters of group a are generally depleted in O-18. The depleted level of O-18 in the waters of group a can be attributed to their source high on the Cedar and Galiuro Mountains (see Figure 2).

It thus appears that the shallow wells are recharged by direct infiltration of precipitation which has a relatively light composition

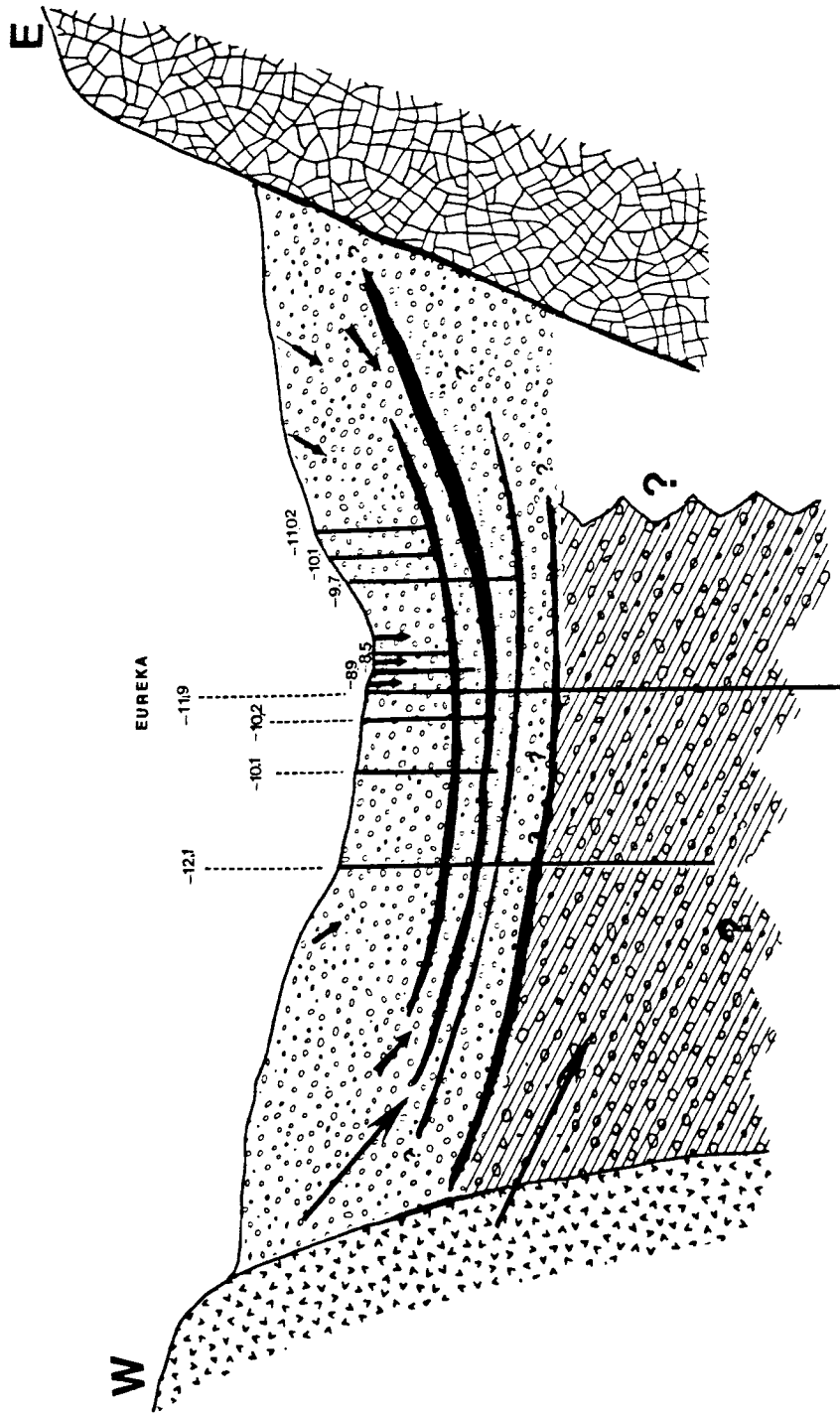


Figure 31. Oxygen-18 across the upper Eureka section

- | | |
|--------------------|--------------------|
| 1- Eureka #1 | 7- Eureka A. T. |
| 2- Black Canyon | 8- Eureka Domestic |
| 3- Puddy Lynch | 9- Eureka #6 |
| 4- Big Tank | 10- Eureka #11 |
| 5- Little Windmill | 11- Bull Pasture |
| 6- Bird Cage | |

*- in group a * - in group b ● - in group c

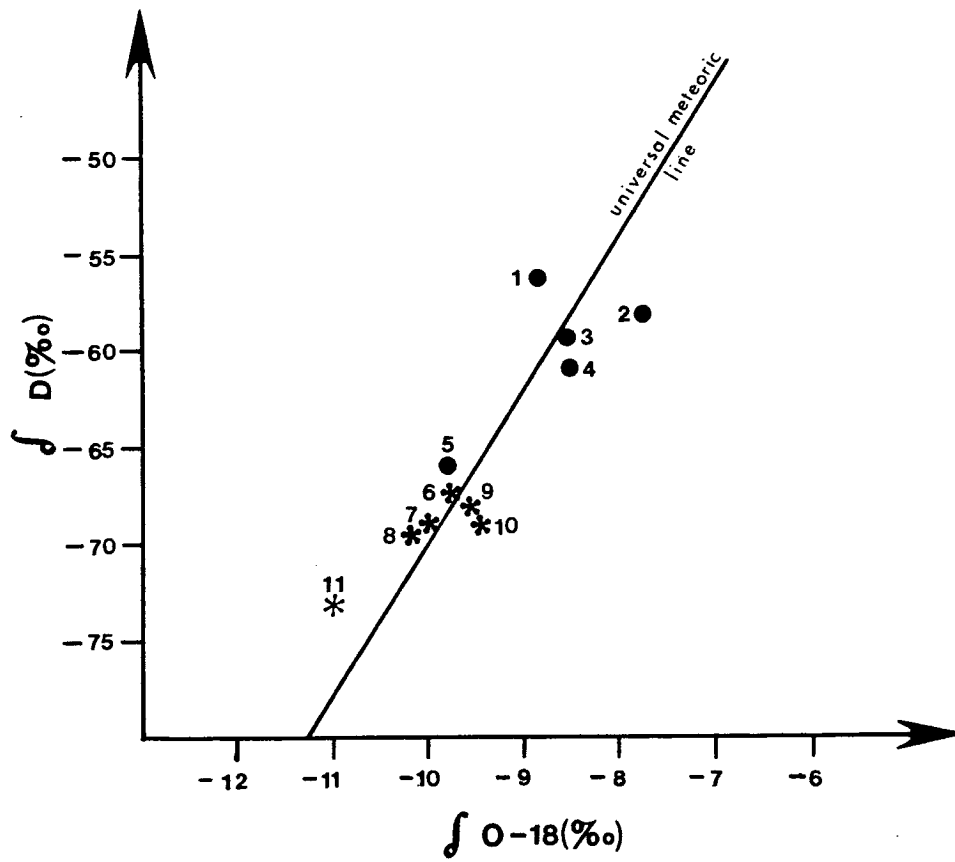


Figure 32. Oxygen-18 versus deuterium in groundwaters in Eureka section

- - Group (a): 1) Bull Pasture, 2) Wilson, 3) Bird Cage.
- - Group (b): 4) Eureka D., 5) Eureka #6, 6) Eureka #11, 7) Eureka A. T.
- ▣ - Group (c): 8) Black Canyon, 9) McGee, 10) Big Tank, 11) Eureka #1, 12) Puddy Lynch, 13) Little Windmill.

→ - General flow direction in the upper aquifer.

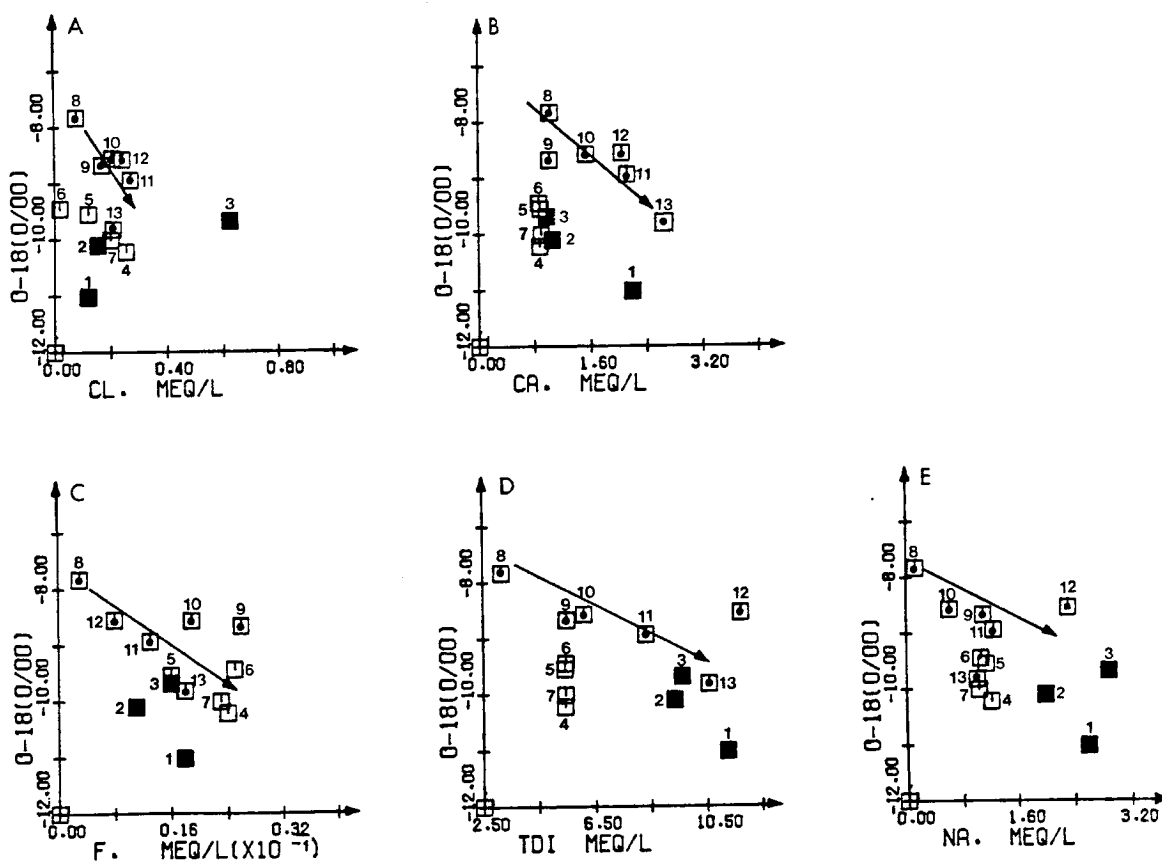


Figure 33. Groundwater chemistry and oxygen-18 for Eureka section

due to the altitude effect. $\delta O-18$ values in the intermediate wells are similar to those measured in flood waters of the upper valley (Appendix C, Table 2). This may indicate that recharge of the middle segments of the aquifer occurs primarily from infiltration of these floods along the washes and lateral flow toward the center (see arrows in Figure 31). The deepest wells are not only depleted in $\delta O-18$ but also exhibit high hydraulic head values (Eureka #6 is, from time to time, a flowing well). This suggests their source of recharge is at still higher elevations, most likely the Galiuro Mountains.

Lateral Contribution Into the Upper Aquifer Through the Alluvial Fans

In Aravaipa Watershed, as was already mentioned before (Chapter 3, Figure 6), most of the wells are clustered within a narrow strip along the center of the valley. In this case, it is hard to define lateral inflows based on spatial distribution of hydraulic heads. Therefore, we must rely entirely on chemistry and environmental isotopes in studying the question of lateral recharge.

The chemical compositions of water in the upper parts of alluvial fans feeding Aravaipa Creek, differ markedly from that of water in the upper aquifer under Aravaipa Creek. We shall use this fact to study the effect of lateral inputs from Rattlesnake Creek and Fourmile Canyon (where enough wells are available) on the chemical composition of the upper aquifer. We shall examine, in particular, the chemistry of wells at the confluence with each tributary as well as upstream and downstream.

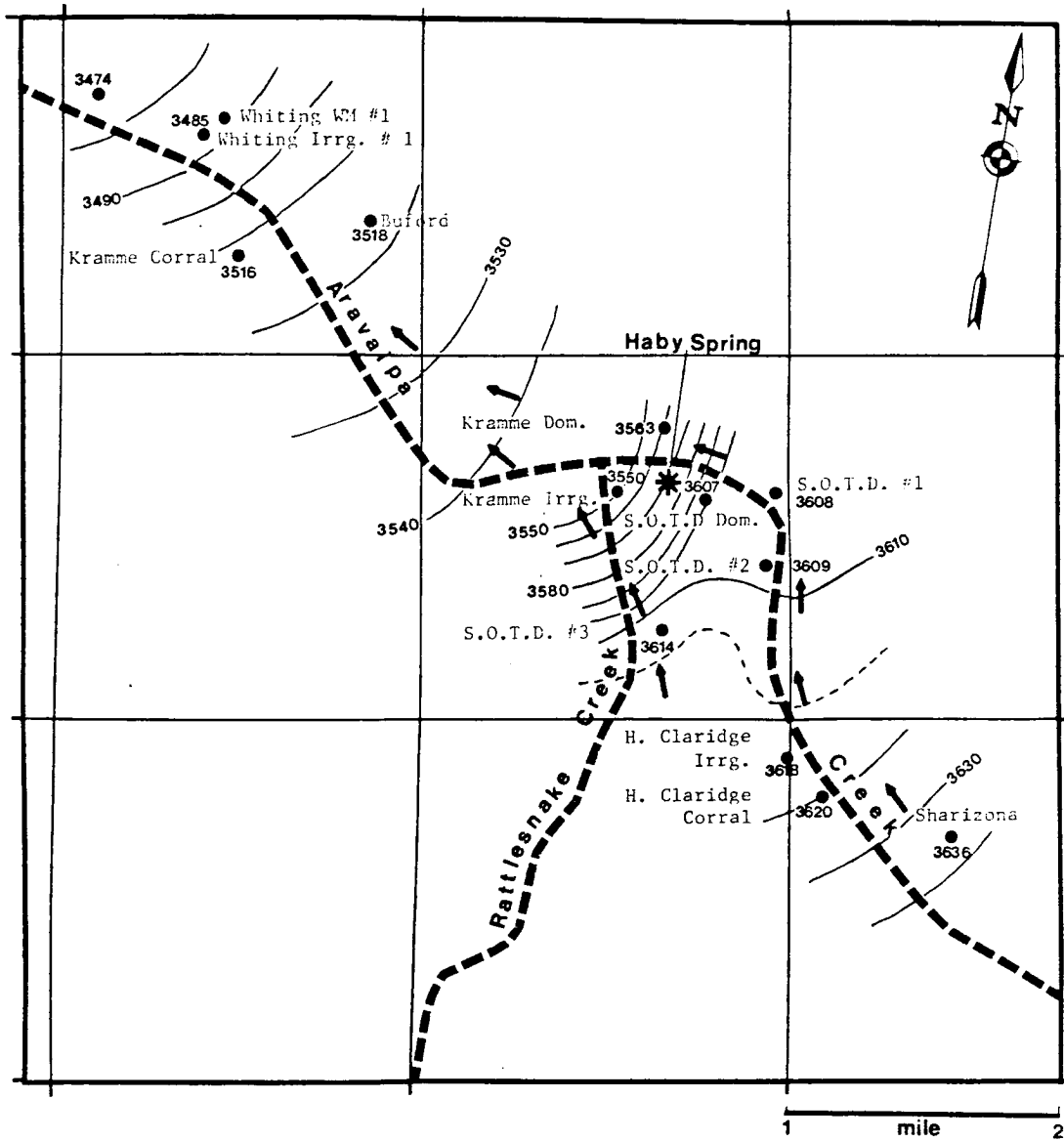


Figure 34. Hydraulic head distribution and flow components near Haby Spring

Figure 34 shows the location of wells, hydraulic head distribution and subsurface flow pattern at the confluence of Rattlesnake Canyon with Aravaipa Creek near Haby Spring. Based on the flow pattern, one should expect some mixing of water coming from the Sharizona section in the southeast with water coming from the alluvial fan of the Rattlesnake. This is supported by the binary diagrams in Figure 35 and the fingerprint diagram in Figure 36. These figures show the chemical and isotopic composition of water samples from wells within one mile downstream of Haby Spring. The lowest chemical concentrations and $\delta^{18}O$ values are exhibited by SOTD #3 which penetrates the Rattlesnake alluvial aquifer. The highest chemical concentrations are exhibited by Kramme Corral which is opened to the upper Aravaipa aquifer. The chemical characteristic curves of all other wells lie between these two lines on what appears to be a well-defined mixing (as indicated in Figure 35). Figures 37 and 38 include data from additional wells upstream of Haby Spring (within Sharizona section). Wells located considerable distances upstream and downstream of Haby Spring are seen to have nearly identical chemical compositions. Only wells close to Haby Spring seem to be affected by input from the Rattlesnake alluvial aquifer.

The effect of Fourmile Creek on the chemical composition of waters near Klondyke (Figure 2) can be seen in Figures 39 and 40. Waters at the confluence of Fourmile Creek with Aravaipa Creek and downstream seem to be a mixture between waters in the campground well (at Fourmile Creek, Figure 6) and in the Haby Domestic well (Upper Klondyke section).

- S.O.T.D. # 1
 - S.O.T.D. # 2
 - Whiting # 1
 - Whiting Wm # 1

 - Kramme Irrig.
 - Kramme Corral
 - S.O.T.D. # 3
 - S.O.T.D. Dom.

 (For location see Figure 6)

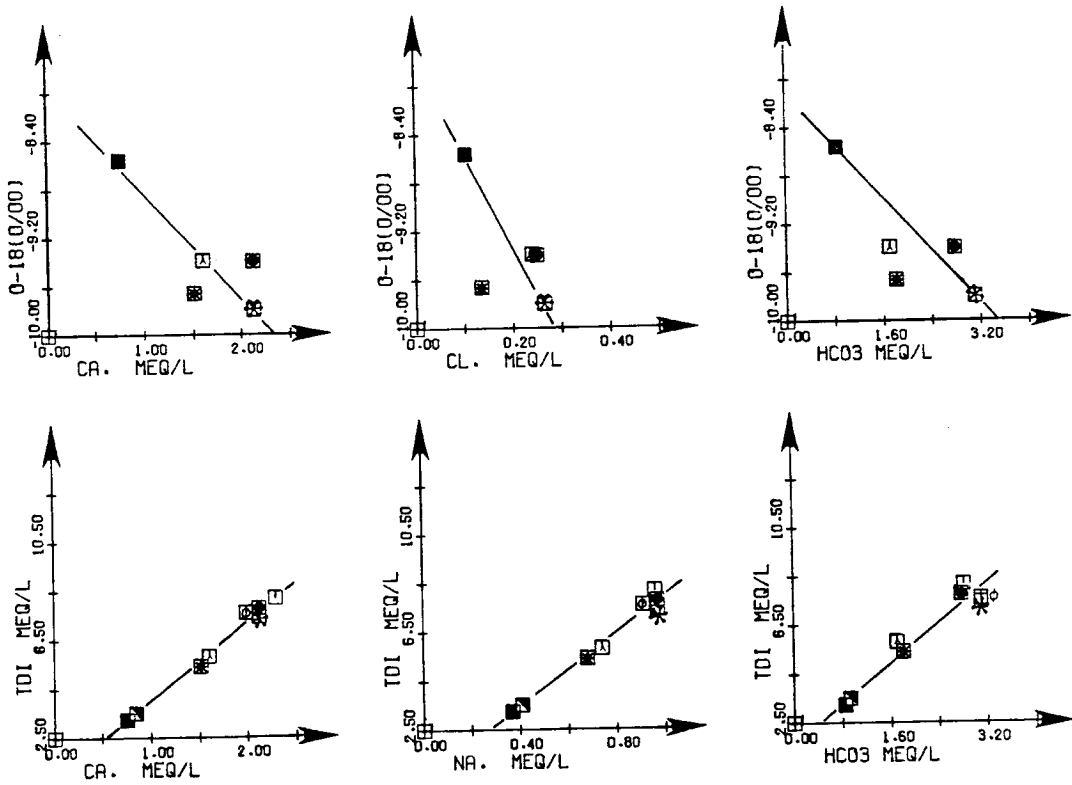


Figure 35. Groundwater chemistry and oxygen-18 near Haby Spring

⊕ Whiting # 1 △ Whiting Wm #1 + Kramme Co. × Kramme Irrig.
 ◇ S.O.T.D. # 3 ⊕ S.O.T.D. Dom.

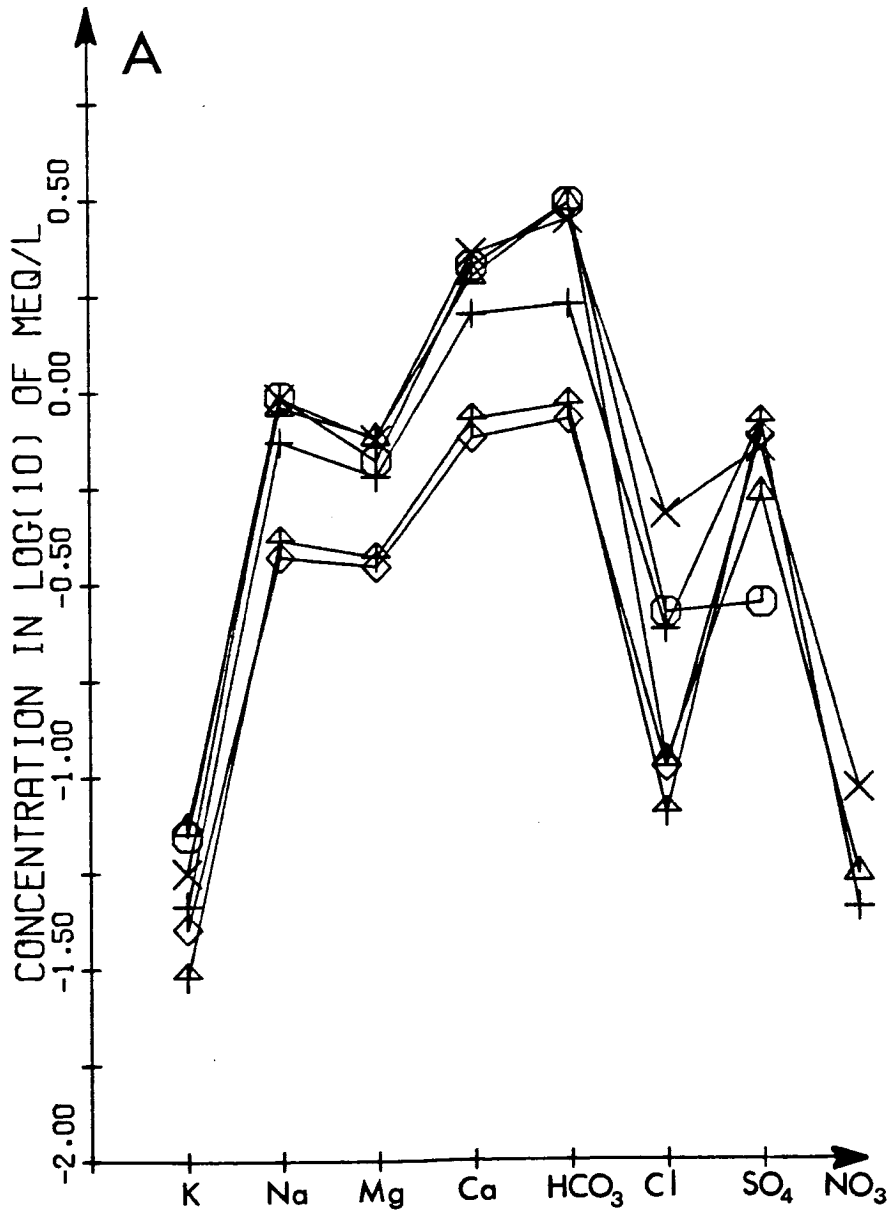


Figure 36. Schoeller diagram for wells near Haby Spring

○ Sharizona △ H. Cl. Cor. + H. Cl. Irrig. × S.O.T.D. # 1
 ◇ S.O.T.D. # 2 ▴ S.O.T.D. # 3 ⋈ S.O.T.D. Dom. ⚡ Kramme Dom.
 ♣ Kramme Irrig. □ Kramme Cor. * Whiting # 1 ⋈ Whiting Wm. # 1

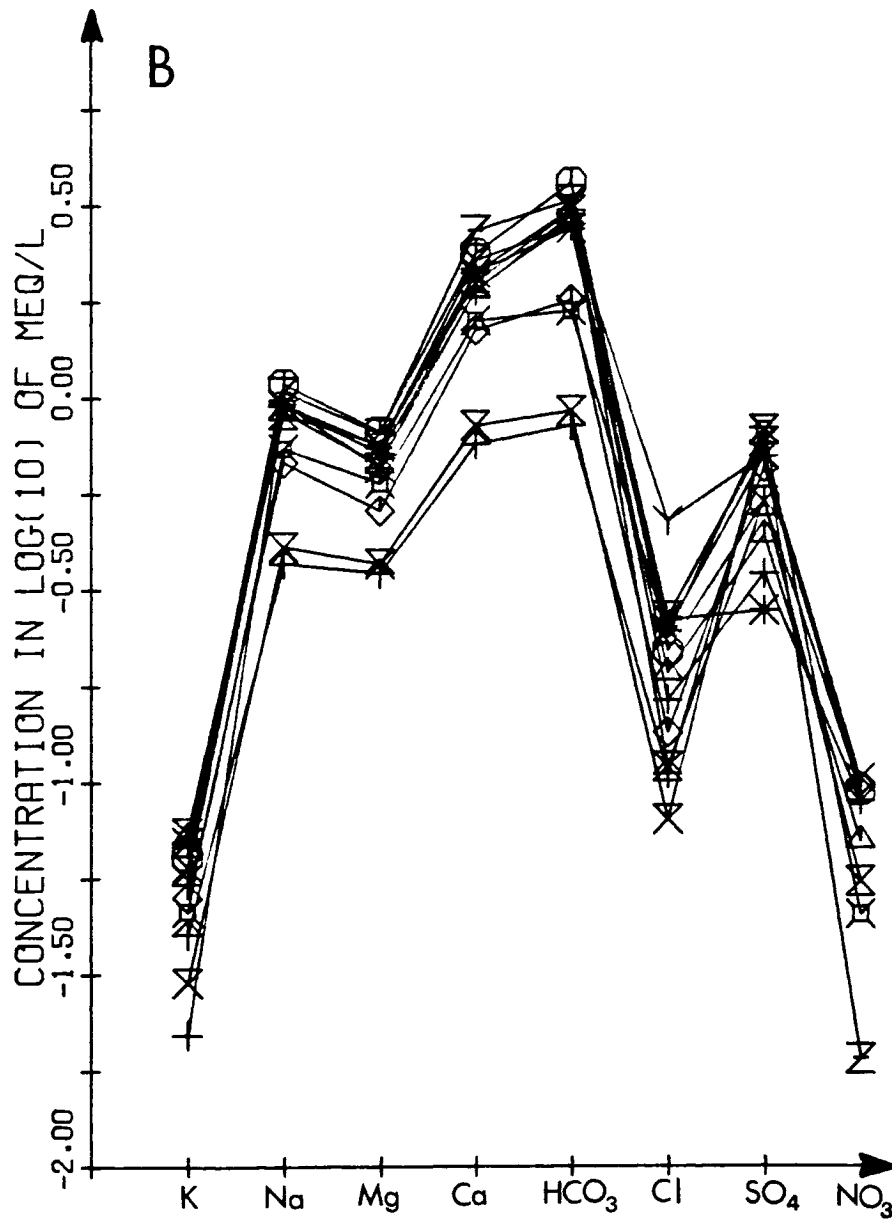


Figure 37. Schoeller diagram for wells upstream and downstream of Haby Spring and the confluence with Rattlesnake

- ☒ - Wells for above Haby Spring
 1- Kramme D. 2- H. Cl. Irrig. 3- H. Cl. Corral 4- Sharizana
- ☒ - Wells far below Haby Spring
 5- Whiting # 1 6- Whiting Wm # 1
- - Wells in Rattlesnake alluvial fan
 7- S.O.T.D. # 3 8- S.O.T.D. Dom.
- - Wells affected by water coming through the alluvial fan
 9-S.O.T.D. # 1 10-S.O.T.D. # 2 11- Kramme Irrig 12- Kramme Corral

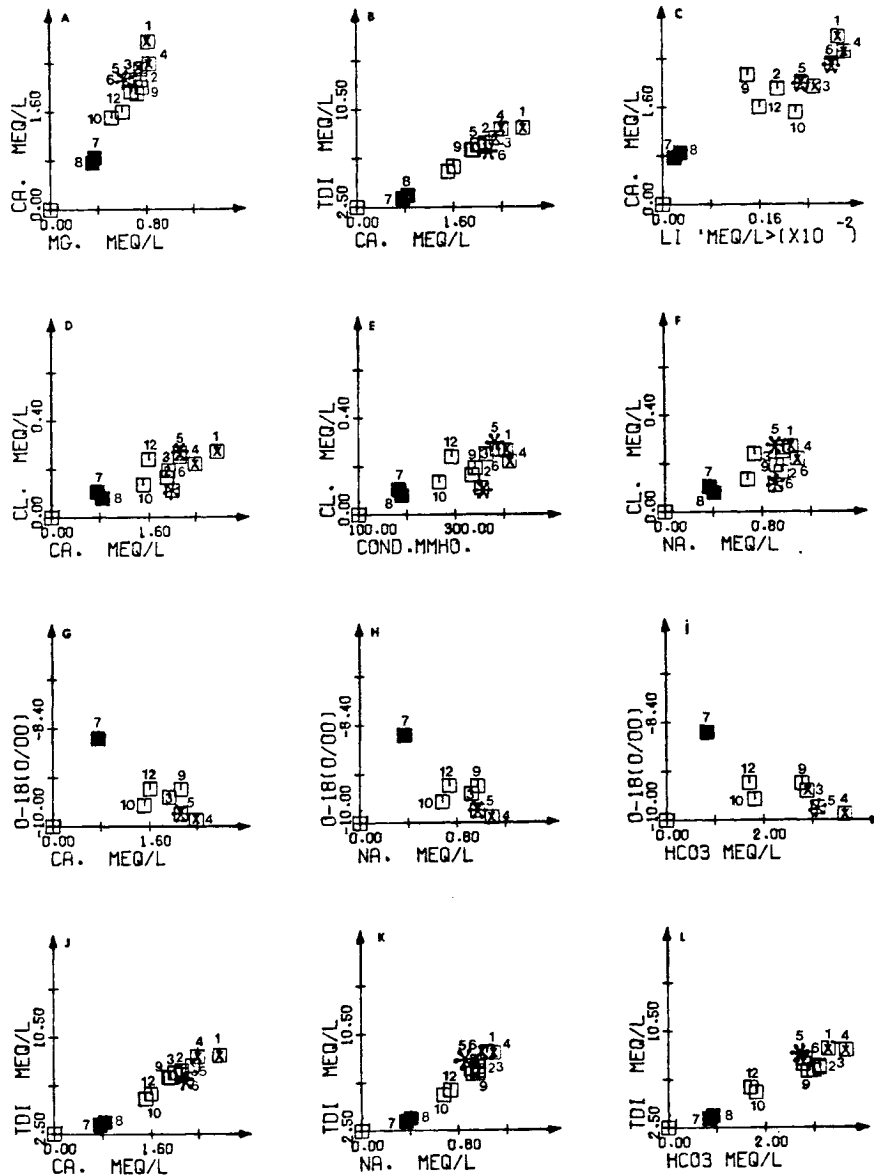


Figure 38. Groundwater chemistry upstream and downstream of Haby Spring

- ☒ - Klondyke School ☒ - Haby Dom ☐ - Haby Old House
- ☐ - Hoby Wm. ☑ - Campground (BLM) (For location see figure 6)

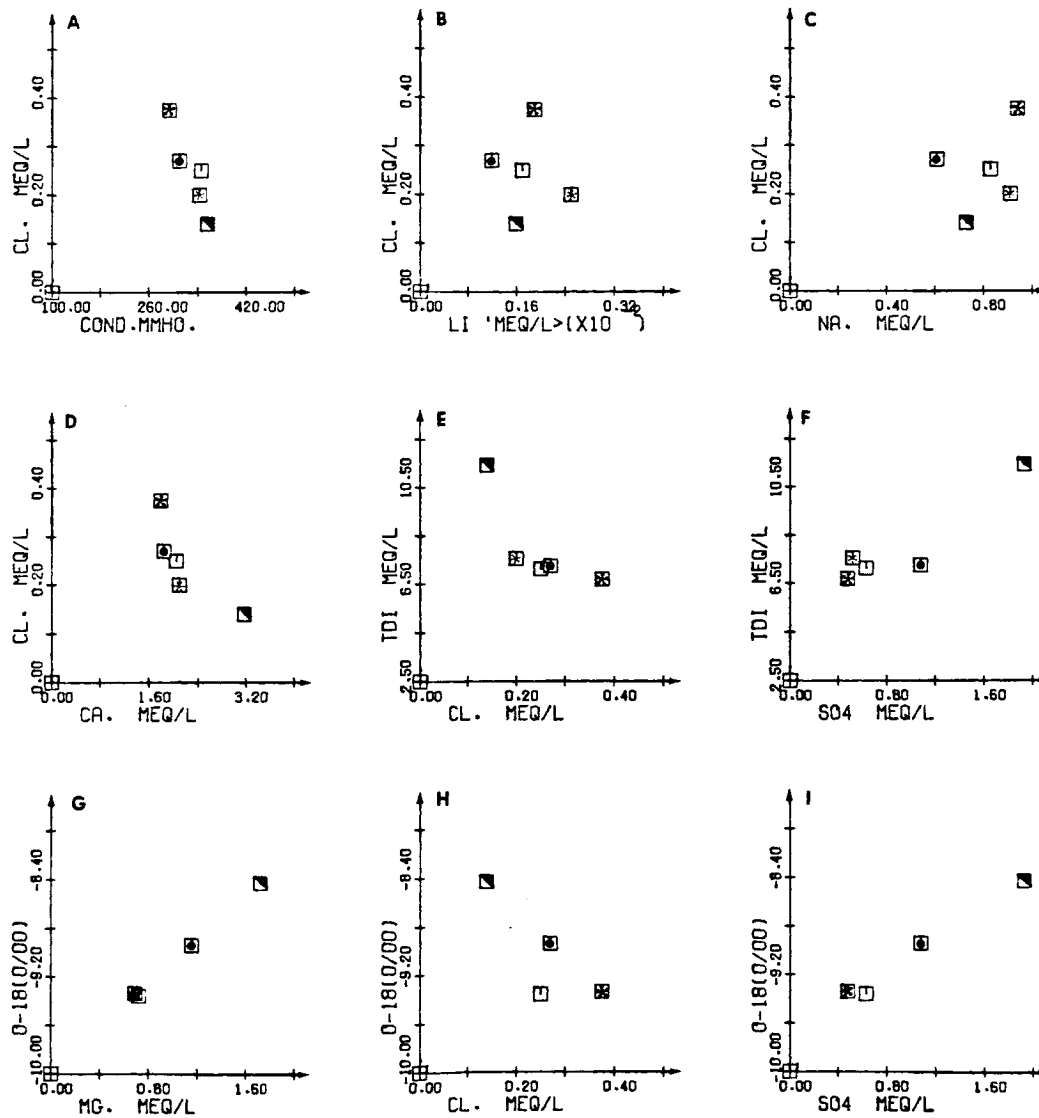


Figure 39. Groundwater chemistry near Klondyke at the confluence of Fourmile Canyon with Aravaipa Creek

○ Hoby Dom
 △ Hoby Old H.
 + Campground
× Hoby Wm.
 ◇ Klondyke School

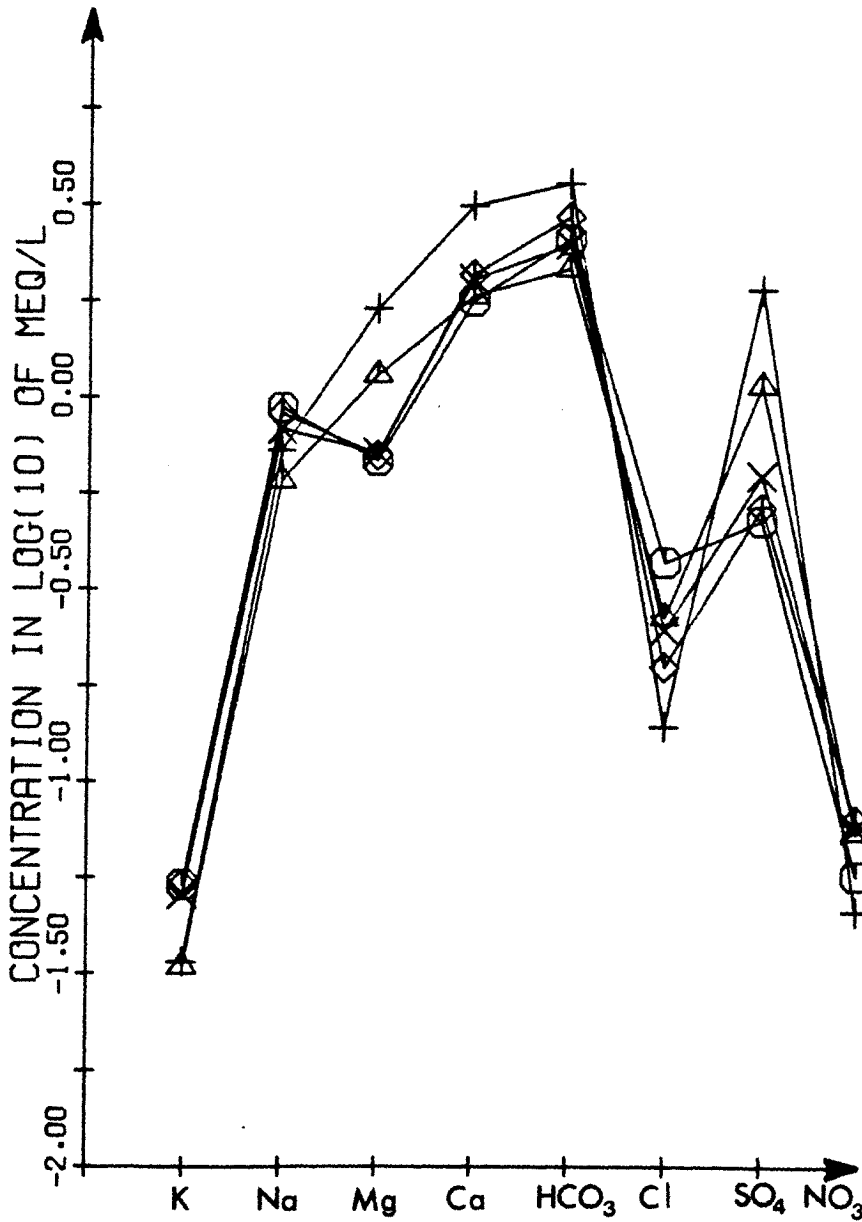


Figure 40. Schoeller diagram for wells near the confluence with Fourmile Canyon

- 1 - Karakula (New)
- 2 - Cobra Dom.
- 3 - Valenzuela
- 4 - Aravaipa Spring
- 5 - Cobra (Old) Irrig.
- 6 - Cobra (New) Irrig.

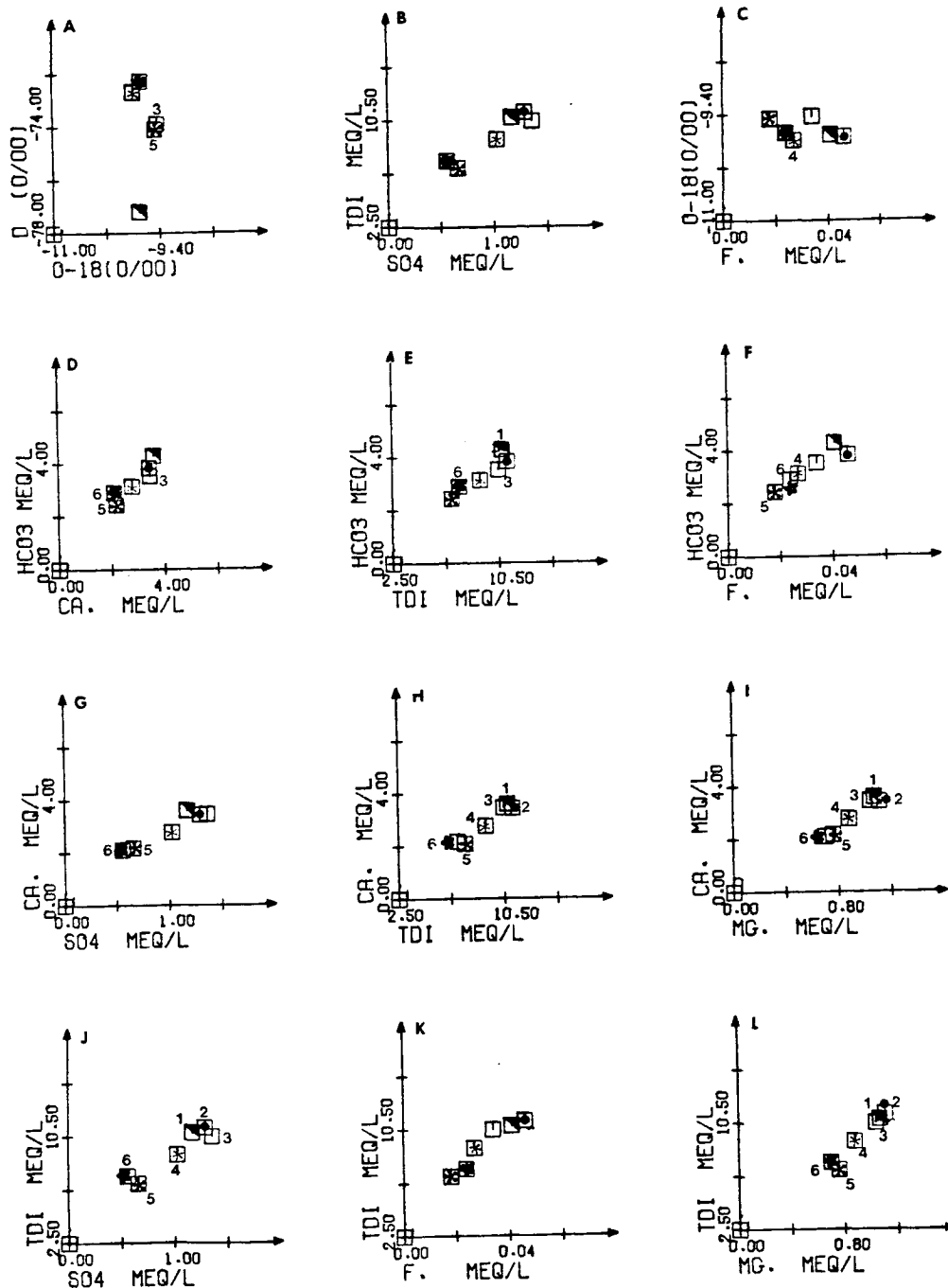


Figure 41. Correlation between chemical and isotopic constituents in shallow groundwaters around Aravaipa Spring

As Aravaipa Spring is located near the confluence of Stowe Gulch with Aravaipa Creek (Figure 2), one should expect Aravaipa Spring to be partly fed by the Stowe Gulch aquifer. This is indeed supported by the binary diagrams in Figure 41. The chemical concentrations and isotopic ratios of all wells surrounding the Aravaipa Spring seepage zone, including the spring itself, fall between those of Cobra New Irrigation Well (in the lower Klondyke section) and Karakula New House (in the Stowe Gulch section).

Chemistry and Stable Isotopes in the Deep Aquifer

Until now, we have discussed only the chemical composition of the upper aquifer. Figure 42 shows Schoeller diagrams for five deep wells in the vicinity of Klondyke which derive their waters solely from the lower confined aquifer. Two of these wells (Whiting Deep and SOTD #3) have chemistries distinctly different than the other three wells. These two wells are located in the valley proper, whereas the other three are located along the eastern and western margins. A comparison of Schoeller diagrams for the Whiting Deep Well and Karakula Adobe that derives its water from the lower aquifer in Stowe Gulch shows a surprising similarity between the two (Figure 43A). On the other hand, $\delta O-18$ in the first well ranges from $-8.7^0/00$ to $-8.9^0/00$, whereas in the second well $\delta O-18$ is $-9.7^0/00$. This means that the deep aquifer regions surrounding the two wells derive their waters from distinctly separate sources. Their chemical similarity may be explained by the creation of chemical equilibrium with lower aquifer materials after prolonged residence in this aquifer (SOTD #3 is upstream of Whiting Deep and its water

⊕ Whiting Deep
 △ Long Hollow
 + Squaw
 X Whiting Hill
 ◇ S.O.T.D. # 3

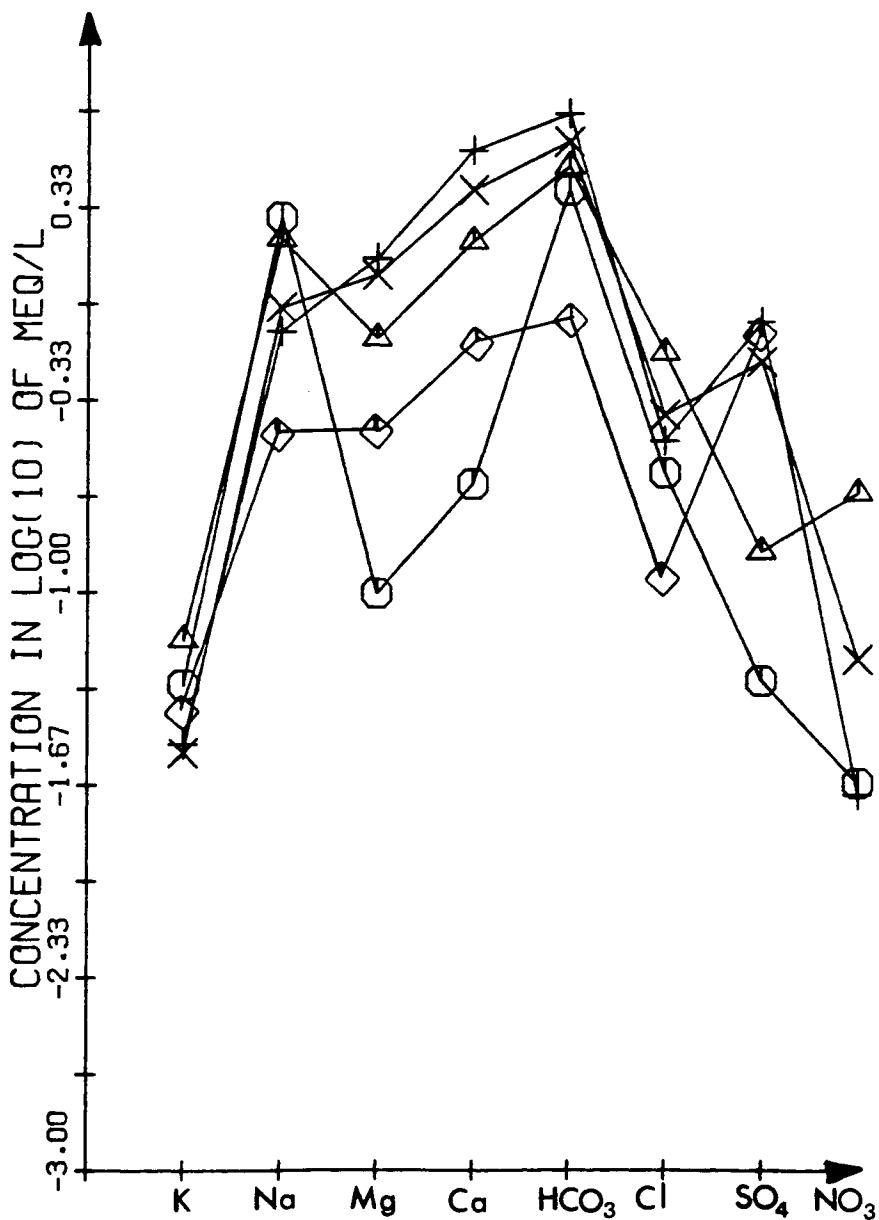


Figure 42. Schoeller diagram for deep wells in the confined aquifer

○ Karakula Old Adobe △ Whiting Deep

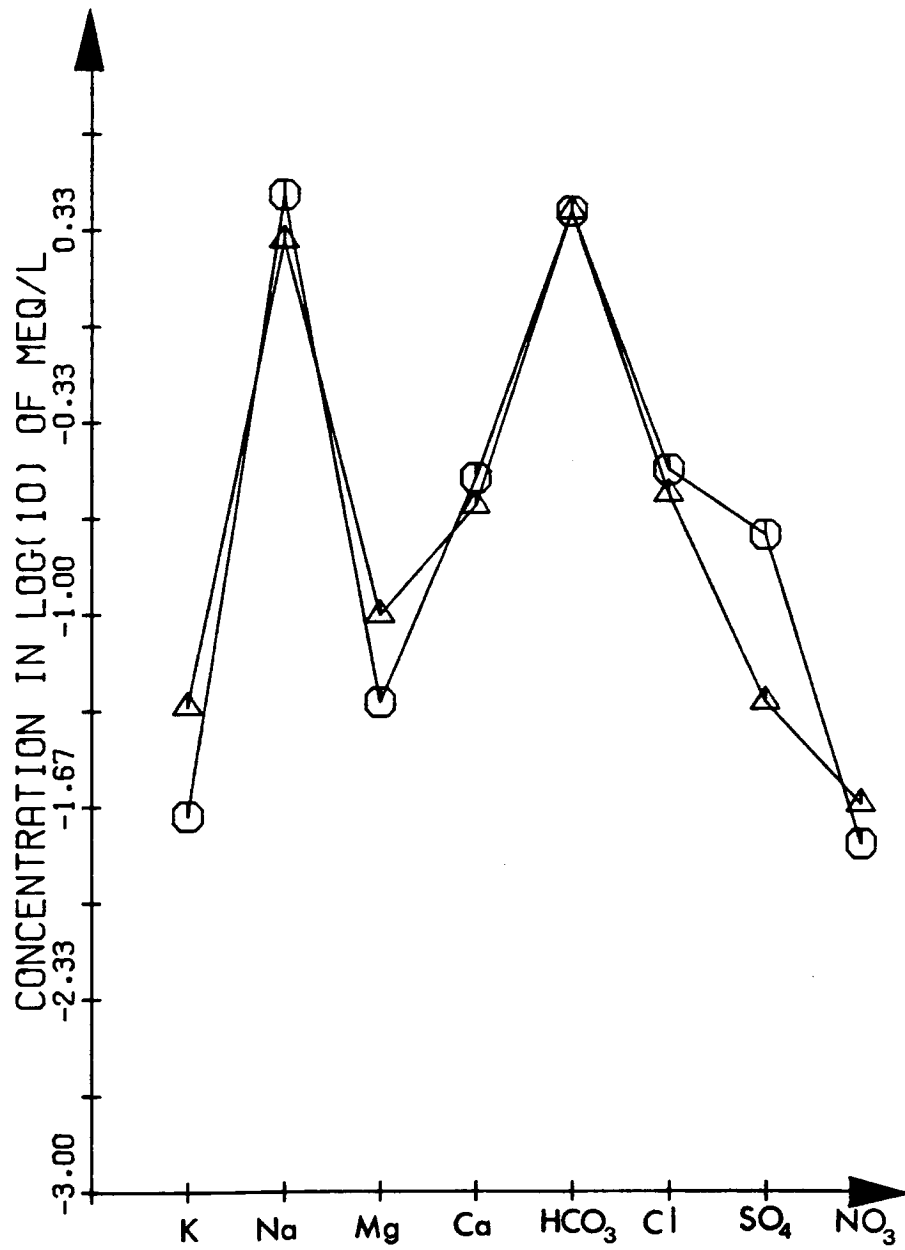


Figure 43. Schoeller diagram showing the similarity between wells in the deep aquifer

(A) Karakula Old Adobe House and Whiting Deep

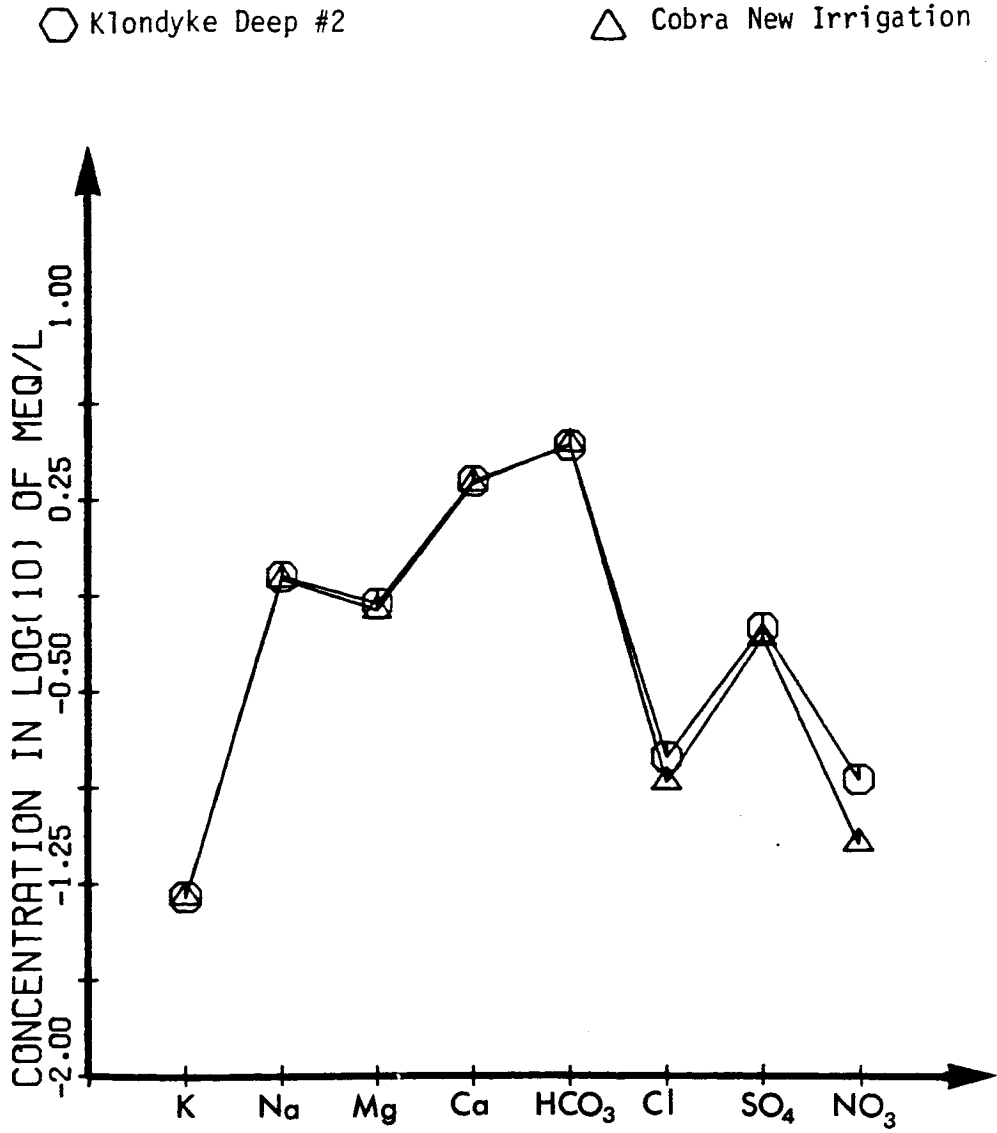


Figure 43 --Continued
(B) Klondyke Deep #2 and Cobra New Irrigation

has most likely not yet reached such equilibrium). Progress toward chemical equilibrium in the lower aquifer seems to entail either precipitation of Ca^{++} and Mg^{++} or cation exchange from Ca^{++} and Mg^{++} to Na^+ and K^+ . Stowe Gulch thus appears to contribute recharge also to Aravaipa lower aquifer.

Two other wells: Cobra New Irrigation (Cobra N. Irr.) and Klondyke Deep #2 (Kl. Deep #2) tap the confined aquifer. These wells are located 1/8 and 1.0 miles upstream from Aravaipa Spring and are only 116 and 160 feet deep, respectively. The hydraulic heads in both wells are between 40 and 15 feet above the water table aquifer (Table 2 of Appendix C). The water chemistry of Cobra N. Irr. is very similar to that of Kl. Deep #2, although it is significantly different from waters sampled either in the deep (Whiting Deep) or in the shallow water table aquifers (Figure 43B). The driller log obtained for Cobra N. Irr. (Appendix A) indicates 35 to 40 feet of confining layers starting about 55 feet below the surface. This suggests that these wells derive the water from an intermediate semi-confined aquifer located between a set of confining layers. Since Whiting deep well has a blank casing along the first 260 feet (about 170 feet below the top confining layer, Arad and Adar, 1981), no information is available about the existence of such an aquifer in the upstream section of Klondyke. The difference in chemical composition can be explained by different lithology or by different sources of recharge. Such possible sources are deep percolation along the nearby pediments (Figure 7) or in the western block of the Hell-Hole conglomerate (Figure 4). Whatever the source, the difference in heads

and the thin confining layer suggests the possibility of upward leakage into the water table aquifer.

Hydraulic Connection Between the Two Major Aquifers

Leakage from the lower to the upper aquifer in Aravaipa Valley has been implied on the basis of hydraulic head measurements (Figure 14 in Chapter 3). Borehole logs of electrical conductivity and temperature did not indicate the presence of leakage. However, such leakage is evidenced by variations in tritium and C-14 during a pumping test conducted by Arad and Adar (1981) on the Whiting Deep well (Appendix B). Prior to the test, tritium concentration was 13.3 TU in the upper aquifer, and 0.7 TU in the lower aquifer; C-14 was at 87.0 pmc in the upper aquifer and 32.4 pmc in the lower aquifer. During the test, the lower aquifer was pumped at up to 900 gpm for 12 hours, causing the head to drop by 191 feet from its initial value of 18 feet above the water table. While there were no discernible changes in overall chemical composition of the pumped water with time, tritium and C-14 showed an increase as illustrated in Figure 44. This suggests that water has leaked from the upper aquifer to the lower one, implying that under normal conditions, leakage is taking place in the reverse direction.

Additional evidence for upward leakage from the confined aquifer is provided by the relationship between tritium (H-3) and carbon-14 (C-14) ratios. Figure 45A shows this relationship for several wells and springs in the Aravaipa Watershed. The dashed curves in the figure are so-called "nonmixing lines" representing constant decay rates of both isotopes in an isolated body of water. The curve which fits Aravaipa

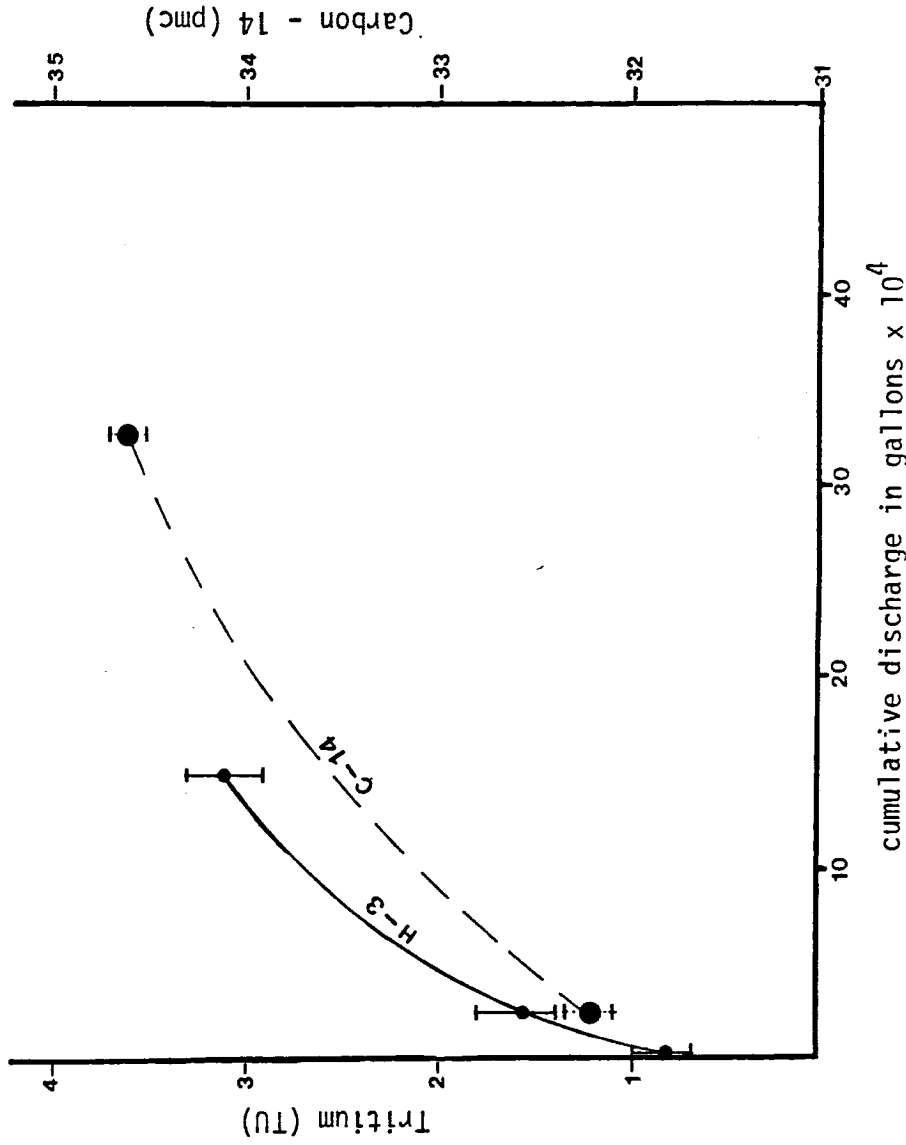


Figure 44. Carbon-14 and tritium versus discharge in Whiting Deep well

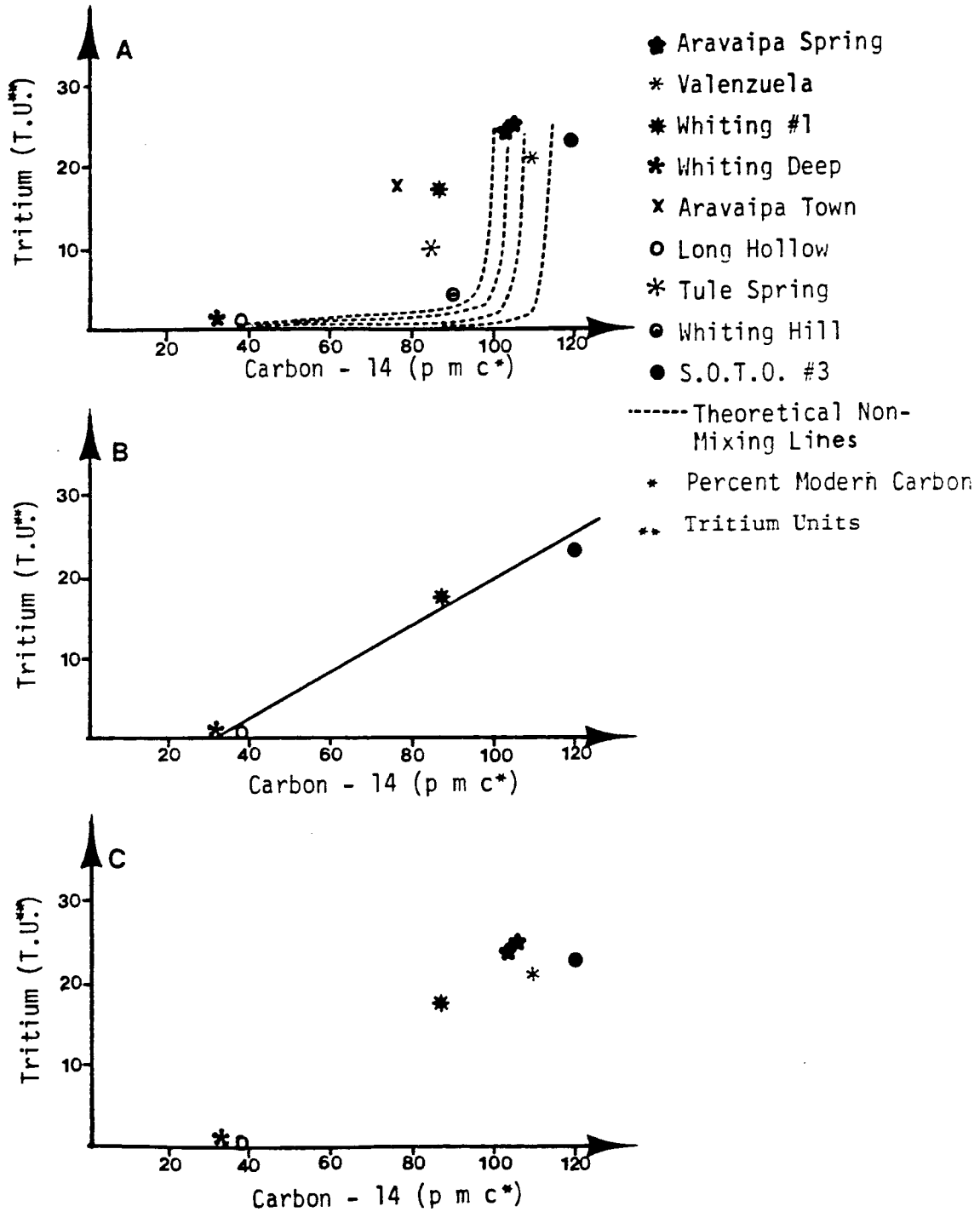


Figure 45. Tritium versus carbon-14
 (A) Key wells in Aravaipa Valley
 (B) Wells in Upper Klondyke section
 (C) Wells near Aravaipa Spring and near Haby Spring

Watershed cannot be accurately obtained as long as the initial activity of C-14 in the recharged water is not known. The average natural activity of atmospheric C-14 is assumed to be constant (13.56 dpm/g = 100 pmc; Faure, 1977) due to a steady state between cosmic production and radioactive decay (Fontes and Garnier, 1979). During the last century, the combustion of fossil fuel, containing no C-14, reduced the C-14 activity of the atmospheric carbon by about 10%. However, this effect is masked by the injection of C-14 into the atmosphere as a result of nuclear tests performed since 1952. The C-14 activity in the atmosphere was temporarily increased by a factor of 2 above normal. Since 1963, it gradually decreased mainly due to an exchange with oceanic carbon (Mook, 1980); even so, the atmospheric C-14 ratio in the post-bomb era has never declined below 130 pmc (Nydal and Lovseth, 1983). When water labeled with an atmospheric ratio of C-14 infiltrates into the soil, its C-14 content decreases due to additional "dead carbon" (C-12) and isotope exchange with gaseous CO₂ in the unsaturated zone. According to Vogel (1970) and Mook (1980), the average decrease due to these causes is on the order of 15±5 pmc in the C-14 content of recent groundwaters. Therefore, it is quite inconceivable that any sample representing recharge from a recent surface source would be to the left of the non-mixing lines in Figure 45A. We conclude that the three points in this figure that do lie to the left of these lines (Whiting #1, Aravaipa Town, and Tule Spring) must represent a mixture of recent recharge with older water.

Let us consider in particular the sample from Whiting #1, taken from the upper aquifer. Figure 45B suggests that this sample lies on a

mixing line with end members which are shallow waters in the Rattlesnake alluvial fan (SOTD #3) and waters of the deep aquifer (Whiting Deep and Long Hollow). The existence of such mixing is most easily explained on the basis of upward leakage from the confined to the overlying unconfined aquifer.

In addition to samples that were presented in Figure 45B, Figure 45C shows the data from Aravaipa Spring and a nearby well, Valenzuela, both located at the outlet of the valley near the confluence with Stowe Gulch. This figure suggests that Aravaipa Spring is not affected by the deep aquifer and that it is recharged with a very recent water. That might confirm what had already been suggested earlier in this chapter, that the Stowe Gulch aquifer contributes significant amounts of water to the discharge of Aravaipa Spring.

Stable Isotopes in Floods and Runoff

Streambed infiltration from runoff and floods along Aravaipa Creek and its tributaries is considered as one of the potential sources of recharge into the upper aquifer. Three types of ephemeral flows have been noticed in the watershed: (1) winter floods; (2) summer floods; and (3) temporary runoff due to snowmelt. After heavy rains and during snowmelt, runoff in the major tributaries seeps into the alluvial fans at the confluence of each tributary with Aravaipa Creek. From time to time, the runoff of the tributaries may reach Aravaipa Creek and infiltrate into its riverbed. The volumes of most winter floods exceed those of most summer floods. However, the intensity of summer floods is

generally greater and they are more heavily loaded with sediments than winter floods.

In order to assess the amount of recharge from floods into the unconfined aquifer, five summer floods (in May, August, and September), four winter floods (from November to March), and four runoff events due to snowmelt were sampled and analyzed for ionic and stable isotopes content. Their ionic concentrations and isotope ratios are listed in Table 3 of Appendix C.

A binary diagram of $\delta^{18}\text{O}$ versus δD is shown in Figure 46. The winter floods are more depleted in heavy isotopes than runoff from snowmelt even though the latter were sampled after heavy rains as well as during snowmelt. The summer floods are scattered along the universal meteoric line. At least two of these have isotopic compositions lighter than some of the winter floods. This is interesting enough to warrant further discussion.

The major parameters which affect the isotopic ratio in runoff are: (1) the original isotopic ratio in precipitation; (2) flow duration; and (3) air and water temperature. It had been shown earlier in connection with Figures 24 and 25 that monthly rain samples of winter precipitation are distinctly lighter than summer rain. Since all floods originate from rainfall, the source of the winter floods is depleted in heavy isotopes compared with the source of the summer floods. Based solely on a consideration of flood duration, winter floods should be enriched in stable isotopes because they often last several days or even

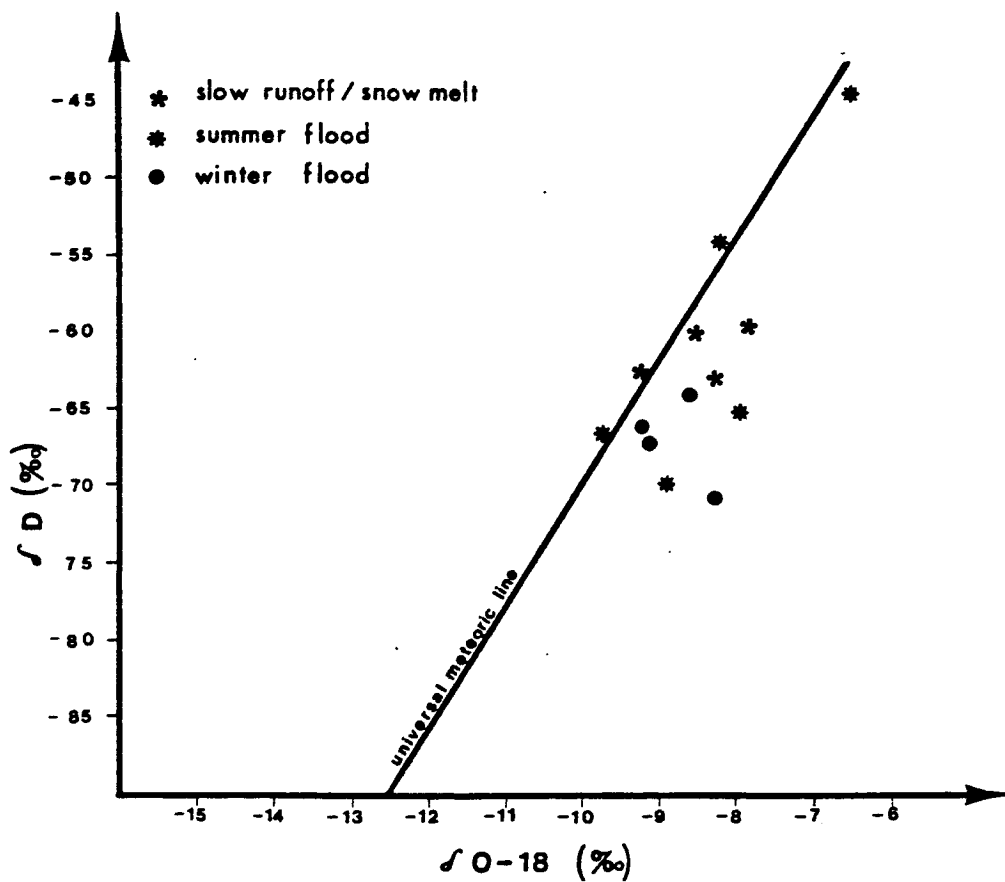


Figure 46. Oxygen-18 versus deuterium in runoff and floods

weeks. However, when only air temperature is considered, hot air during the summer floods enriches the runoff with stable isotopes.

As mentioned earlier, two of the summer floods are lighter than the rain believed to produce them (Table 2 of Appendix C). A similar phenomenon was observed in some floods during 1976-1978 in the Santa Cruz and Rillito rivers of the Tucson basin in Arizona (E.S. Simpson, personal communication, 1984). The reason is that high rainfall intensities are produced by a tall cumulonimbus cloud system with fast condensation at low temperatures. It is reasonable to postulate that summer floods are produced by the most intensive part of the storm, and their isotopic content is controlled by the same part. Adar et al. (1980) found a negative correlation between rainfall intensities and $\delta^{18}\text{O}$ in local storms in the Negev Desert in Israel. This, together with the well-known "amount effect" of rainfall (i.e., the higher the rain volume, the more depleted is the rain in stable isotopes), is probably responsible for the depleted summer floods, even though the ambient air temperature is twice as much as in the winter. The amount effect of precipitation on $\delta^{18}\text{O}$ ratios in floods is shown in Figure 47. $\delta^{18}\text{O}$ in flood water is shown versus the total amount of rain (as was measured in Klondyke) in the storm producing the flood. It is obvious that $\delta^{18}\text{O}$ is negatively correlated with the amount of rainfall. One also sees that heavy summer storms produce depleted floods even though the air temperature may be high. However, small local summer storms are, as expected, relatively enriched in stable isotopes.

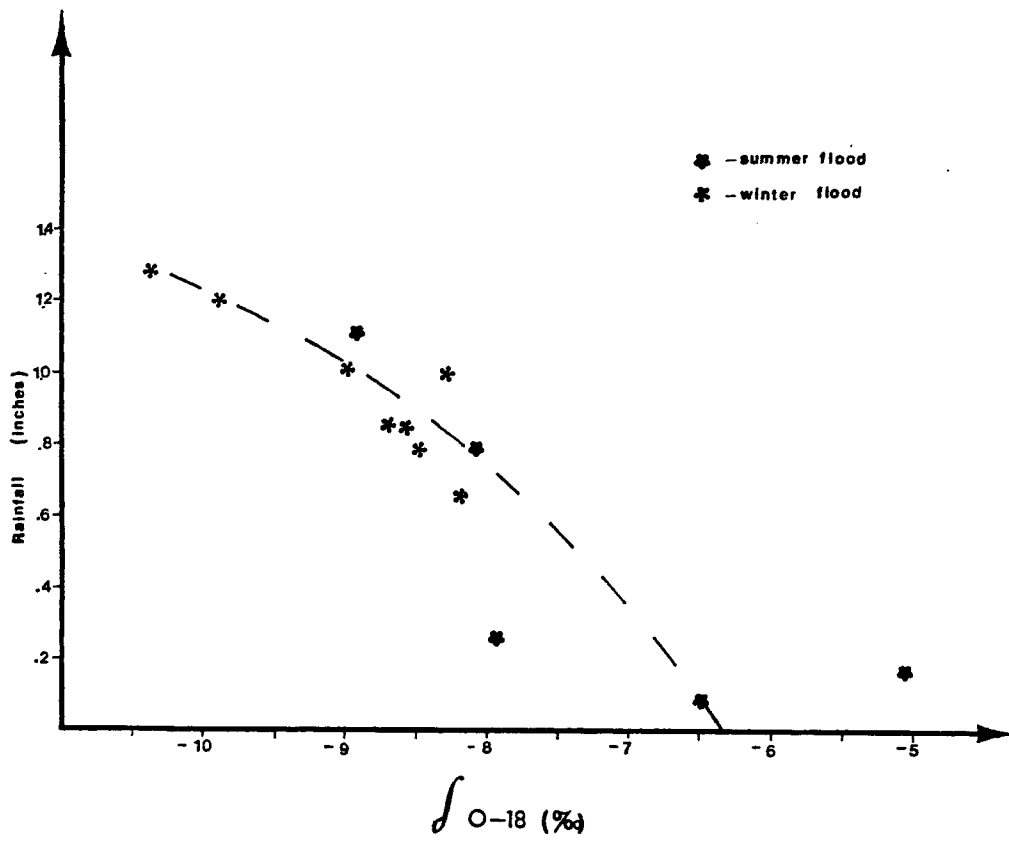


Figure 47. Amount effect of rainfall on oxygen-18 in floods

Three floods were sampled twice, before and after the flow peak. The $\delta O-18$ and δD ratios for each pair of samples are given in Table 2. This table clearly shows that the initial stage of the flood is always lighter than the post-peak flow. This is probably in response to the duration the waters are exposed to evaporation. Usually the tail of the flood carries runoff from remote areas and overland flows originated from longer hillslopes. This increases the chances for evaporation and hence enriches the flood waters with the heavy isotopes.

In spite of the wide range of $\delta O-18$ in summer floods, the average ratio of the stable isotopes in the winter floods is significantly lower than in the summer floods: $-8.98^{\circ}/\text{oo}$ versus $-7.41^{\circ}/\text{oo}$ of $\delta O-18$ and $-67.10^{\circ}/\text{oo}$ versus $-58.7^{\circ}/\text{oo}$ of δD . The differences in the

Table 2. $\delta O-18$ ($^{\circ}/\text{oo}$) and δD ($^{\circ}/\text{oo}$) in flood waters before and after the peak discharge

Date	Water Temp. $^{\circ}\text{C}$	$\delta O-18$	δD	Comments
9/11/82	17.8	-8.93	-70.0	1 hour after flood arrival
9/11/82	16.4	-7.96	-65.5	
3/5/83	6.5	-10.39	--	Pre Peak - 8 hours after flood arrival
3/5/83	12.0	-9.93	--	Post Peak
8/8/83	21.0	-6.50	-44.3	Pre Peak
8/8/83	20.0	-5.04	--	Post Peak

isotopic ratios and in the ionic concentrations, as given in Table 2 of Appendix C, will be used later to assess the relative amount of recharge from winter versus summer floods.

The chemical and isotope analyses described in this chapter helped to determine all possible inflows into the young alluvial aquifer. In the following chapters an attempt will be made to verify and quantify each of these possible components of recharge.

CHAPTER 6

MODEL OF QUANTITATIVE RECHARGE ESTIMATION

The ultimate objective of this research is to develop a mathematical model capable of quantifying recharge into an alluvial aquifer. Since information about hydraulic parameters and flow rates is limited, the model relies primarily on chemical and isotopic information. In this chapter, we outline the theory behind the model and show how it works with synthetically-generated data. Application of the model to actual data from the Aravaipa Watershed is reported in Chapter 7.

Theory

Our approach combines an idea developed by Woolhiser et al. (1982) for a segment of a river channel, and the concept of a mixing cell model as described by Simpson (1982). According to Woolhiser et al., if Q_i ($i = 1, 2, \dots, I$) represents volumetric rates of inflow into a river reach over a certain time interval, Δt , and Q_0 represents the outflow rate, mass balance requires that

$$Q_0 = \sum_{i=1}^I Q_i \quad (1)$$

where changes in storage are taken to be zero. Assume that each Q_i ($i = 1, \dots, I$) is associated with K conservative chemicals having the

concentrations C_{ki} ($k = 1, 2, \dots, K$). If each chemical undergoes a complete mixing in the river reach, it must obey the mass balance expression

$$C_{ko} Q_0 = \sum_{i=1}^I C_{ki} Q_i \quad (2)$$

When Q_0 , C_{ko} , and C_{ki} are known for all k and i , one can evaluate Q_i for all $i > 0$ by quadratic programming on the basis of (1) and (2), provided that $K + 1 > I$ and a sufficient number of the mass balance equations are linearly independent.

In the case of Aravaipa Valley, concentrations in the upper aquifer vary down gradient and the assumption of complete mixing is invalid. For this reason, we subdivide the aquifer into N cells, having sizes small enough for the assumption of complete mixing to be less erroneous. In reality, the chemicals are transported through the aquifer by advection and hydrodynamic dispersion. Had we had sufficient data to describe these transport processes, we might have opted for a more complex but accurate mathematical model of the kind recently proposed by Gorelik et al. (1983). Since such data are not available, we adopt the idea of interconnected mixing cells as used in the simulation model of Simpson (1975, 1982).

The assumption that each chemical species is conservative will also not hold true under most subsurface flow conditions. We will return to the question of how to handle this dilemma later.

We write our model in terms of mean annual mass balance expressions. Let Q_{ni} represent the i^{th} component of the mean annual flow rate into the n^{th} mixing cell, and let Q_{nj} be the j^{th} component of the mean annual

outflow rate. If the mean annual change in storage is negligible (an assumption that could, in principle, be relaxed), mass balance requires

$$\sum_{i=1}^{I_n} Q_{ni} = \sum_{j=1}^{J_n} Q_{nj} \quad (3)$$

for every n (where I_n is the number of inflows and J_n is the number of outflows). Similarly, the mixing cell concept implies that

$$\sum_{i=1}^{I_n} C_{nik} Q_{ni} = C_{nk} \sum_{j=1}^{J_n} Q_{nj} \quad (4)$$

for every n and k where C_{nik} is the concentration of the k^{th} dissolved species (chemical or isotope) identified in the water flowing into the cell at rate Q_{ni} , and C_{nk} is the mixed concentration of the k^{th} species flowing out of cell n . If water is flowing from cell n at the rate Q_{nj} into cell m at the rate Q_{mi} , then

$$Q_{mi} = Q_{nj}; C_{mik} = C_{nk} \quad (5)$$

Figure 48 shows a hypothetical example of how a two-dimensional flow region could be divided into a number (in this case 7) of mixing cells. We see that outflow from one cell (say 3) may become the inflow into two cells (say 4 and 5) or more, and two cells (say 3 and 4) or more may contribute inflows into a single cell (say 5).

When one works with real data, one should not expect the mass balance equations 3-4 to be closed, as both the model and the data are subject to various errors. The annual water balance expressions (3) may not close due to the inadequacy of the assumption that the annual change in storage within each cell is zero, and errors in the measurements of Q_{nj} , C_{nik} , and C_{nk} . The chemical balance equations (4) may not close

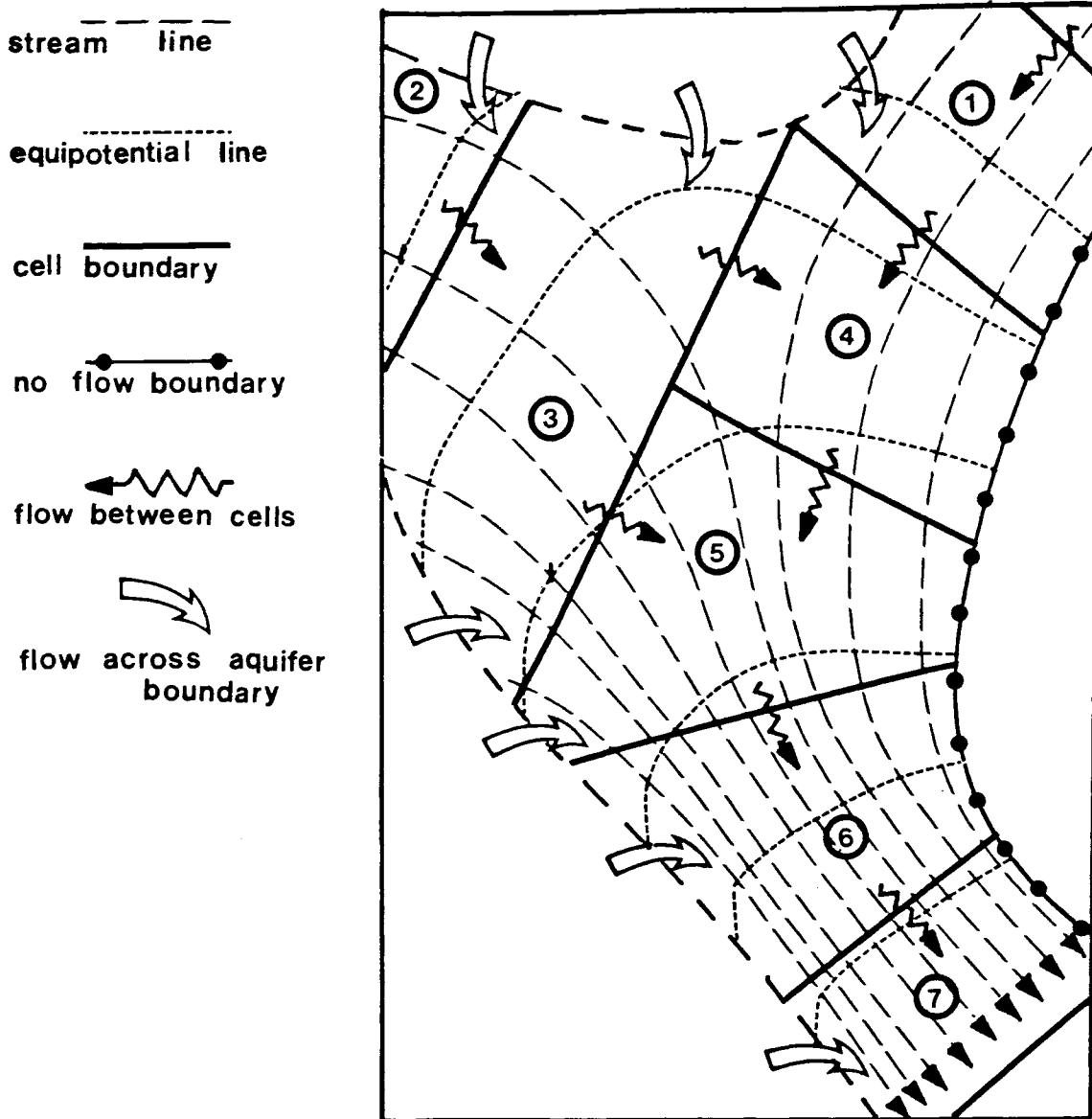


Figure 48. Schematic flow pattern with cell configuration

due to sampling and analytical errors and due to the high probability that at least some of the assumptions behind the model may not hold for several of the species. These assumptions, we recall, include the conservation of each species and complete mixing within each cell.

To account for these errors, we replace (3) and (4) by

$$\sum_{i=1}^{I_n} Q_{ni} - \sum_{j=1}^{J_n} Q_{nj} = \epsilon_n \quad (6)$$

and

$$\sum_{i=1}^{I_n} C_{nik} Q_{ni} - C_{nk} \sum_{j=1}^{J_n} Q_{nj} = \epsilon_{nk} \quad (7)$$

for every n and k , where ϵ represents the mass balance errors.

In matrix form, (6) and (7) can be written as

$$\underline{C}_n \underline{Q}_n - \underline{D}_n = \underline{E}_n; \quad n = 1, 2, \dots, N \quad (8)$$

where \underline{C} is a matrix of order $(K+1) \times I_n$ given by

$$\underline{C} = \begin{pmatrix} 1 & 1 & \dots & 1 \\ C_{11} & C_{12} & \dots & C_{1I_n} \\ C_{21} & C_{22} & \dots & C_{2I_n} \\ \vdots & \vdots & \dots & \vdots \\ C_{k_1} & C_{k_2} & \dots & C_{kI_n} \end{pmatrix} \quad (9)$$

\underline{Q}_n is the I_n -dimensional vector of the Q_{ni} terms, \underline{D}_n is the $(K+1)$ -dimensional vector of known terms defined by

$$D_{n1} = \sum_{j=1}^{J_n} Q_{nj}; \quad D_{n\ell} = C_{n\ell} \sum_{j=1}^{J_n} Q_{nj} \quad (10)$$

$\ell = k+1; \quad k = 1, 2, \dots, K$

and \underline{E}_{nk} is the corresponding error vector defined by

$$E_{n1} = \epsilon_n; E_{n\ell} = \epsilon_{nk}; \ell = k + 1; k = 1, 2, \dots, K$$

Given \underline{C}_n and \underline{D}_n for each n , we estimate \underline{Q}_n by minimizing the weighted least squares criterion

$$J = \sum_{m=1}^N \underline{E}_m^T \underline{W} \underline{E}_m \quad (11)$$

subject to the cell interface constraints (5), and to the positivity constraints

$$Q_{ni,j} > 0 \quad \text{for all } n, i, j \quad (12)$$

\underline{W} is a $(k+1) \times (k+1)$ weight matrix introduced to account for whatever prior knowledge there is about the relative magnitudes of the errors, ϵ . Since information about the correlation of such errors is usually unavailable, we take \underline{W} to be diagonal. The manner in which the nonzero elements of \underline{W} are assigned will be discussed later in this chapter as well as in Chapter 7.

Substitution of (8) into (11) allows us to rewrite the minimization criterion as

$$J = \sum_{m=1}^N (\underline{C}_m \underline{Q}_m - \underline{D}_m)^T \underline{W} (\underline{C}_m \underline{Q}_m - \underline{D}_m) \quad (13)$$

The minimization of (13), subject to (5) and (12), is performed by means of Wolfe's algorithm (1959, see also Hadley, 1970). Results from synthetically-generated data and from sensitivity analyses are shown in the following sections. Results from field data obtained in Aravaipa Valley are given in Chapter 7.

Model Testing with Synthetic Data

Synthetically-generated data have been used to test the validity of the proposed mathematical algorithm. Two tests with eight and 19 unknowns, respectively, were performed on a schematic aquifer with four cells and five outflows (Figure 49). Each of the inflows and outflows were assigned arbitrary values as shown in the figure. Concentrations of 14 chemical and isotopic species were assigned on the basis of actual water samples from the Aravaipa Basin (see Table 1 of Appendix E). In each cell, the concentrations of the mixed waters were calculated as a weighted average of the assigned inflows (the weights being the flow rates). Hence, the error terms in the mass balance equations (6) and (7) should be equal to zero.

In minimizing (13), the outflow rates P_1 - P_4 and Q_{out} (see Figure 49) are treated as known quantities, whereas the inflow rates, Q , as well as the flow rates from one cell to another, are considered to be unknown. Since the errors are zero, the algorithm should yield the exact values of these unknown quantities.

To improve convergence, \underline{W} is taken to be a diagonal matrix with nonzero terms assigned in the following manner:

$$W_{11} = Q_{out}^{-2}; W_{\ell\ell} = C_{ok}^{-2} \quad (14)$$

$$\ell = k + 1; k = 1,2,3,\dots,K$$

where C_{ok} is the concentration of the k -th species at the outlet (i.e., associated with Q_{out}).

The effect of this weighting is to normalize the balance equations so they are all expressed on a scale relative to the downstream outflow equations.

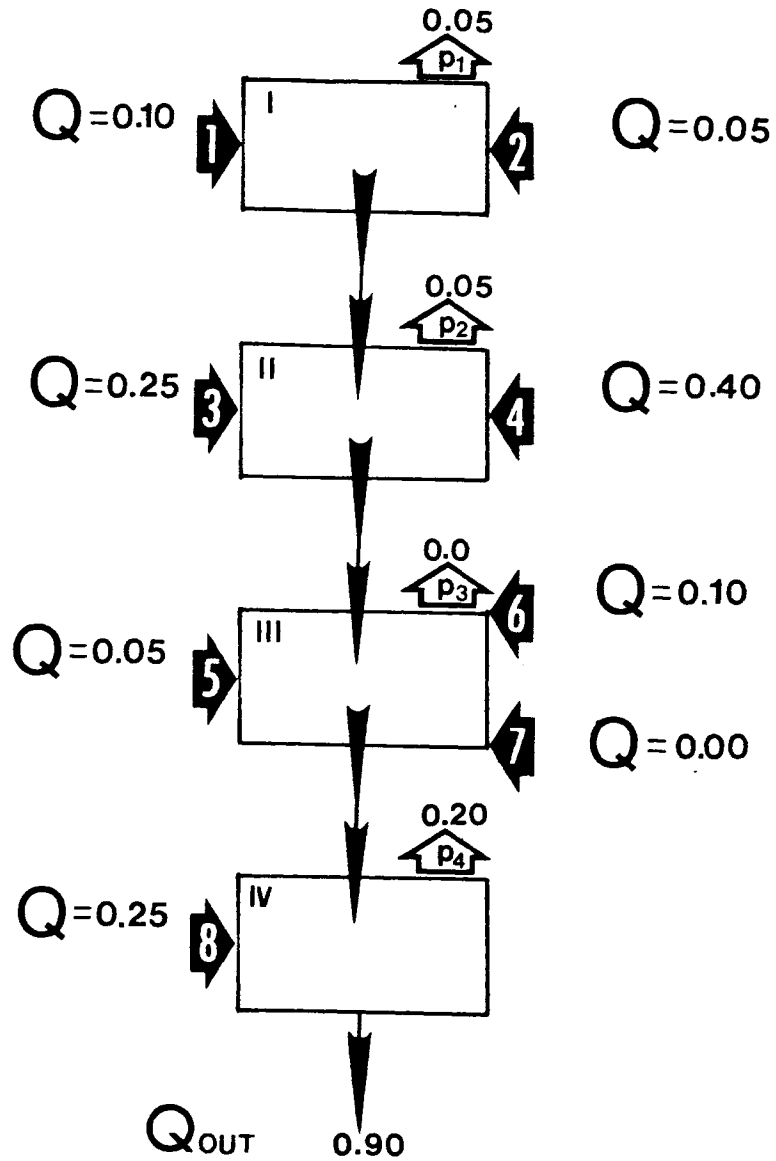
The results are listed in Tables 3A and 4A. As seen in the last column of Table 3A, the total water balance error is -0.0095%. All individual inflow rates were computed with a high precision, including Q_7 which was assigned a value of zero. Table 4A shows that the total chemical balance error is 0.17%. These tiny errors are due to roundoff and an incomplete convergence of the Wolfe algorithm.

Another test was performed with a number of unknown flow rates exceeding the number of chemical species. The model for this second test is similar to that shown in Figure 49, except that there are four inflow sources into cell I and five into cells II-IV. The data relevant to this test are given in Table 2 of Appendix E. Inflows Q_3 , Q_8 , Q_{13} , and Q_{17} represent recharge from winter floods, and Q_4 , Q_9 , Q_{14} , and Q_{18} represent streambed infiltration due to summer floods.

The results of test 2 are listed in Tables 3B and 4B. The water balance error is 0.0078%, and the chemical balance error is 0.06%. The algorithm is seen to work well for error-free data.

Effect of Errors

The purpose of this section is to analyze the performance of the model when the input data are corrupted by random noise. The data of test 1, listed in Table 1 of Appendix E, represent the "true" system. These true data are corrupted by Gaussian noise generated in the following manner. First, a normal error of zero mean and unit variance is



Q - rate of inflow (cfs); P - rate of discharge (cfs)

Figure 49. Schematic compartmental aquifer used for testing the mathematical algorithm in a multi-cell scheme

Table 3. Comparison between assigned and calculated inflows obtained by testing the optimization scheme for a multi-cell aquifer:
 (A) - Test 1 (four cells and eight unknowns);
 (B) - Test 2 (four cells and 19 unknowns).

(A)	Q1	Q2	Q3	Q4	Q5	Q6	Q7	Q8	Total
Inflow									
Assigned Inflows (cfs)	0.100	0.050	0.250	0.40	0.050	0.100	0.000	0.250	1.200
Calculated Inflows (cfs)	0.0988	0.0492	0.2537	0.4001	0.053	0.0977	0.000	0.2470	1.199

(B)	Q1	Q2	Q3	Q4	Q5	Q6	Q7	Q8	Q9	Total
Inflow										
Assigned Inflows (cfs)	45.00	7.50	2.50	1.50	4.00	1.50	4.00	6.00	2.00	7.50
Calculated Inflows (cfs)	44.30	7.40	2.36	1.44	4.17	1.36	4.37	6.30	2.14	7.58

	Q11	Q12	Q13	Q14	Q15	Q16	Q17	Q18	Q19	Total
Inflow										
Assigned Inflows (cfs)	4.00	4.00	6.00	2.00	2.60	8.00	2.00	1.50	2.00	113.6
Calculated Inflows (cfs)	3.97	3.76	6.04	2.01	2.68	8.07	2.08	1.54	2.01	113.59

Table 4. Comparison between the observed and calculated mass transport for each constituent obtained from the test analyses:
 (A) - Test 1 (four cells and eight unknowns);
 (B) - Test 2 (four cells and 19 unknowns).

Ionic and Isotopic Species	(A)			(B)		
	True Mass Inflow	Estimated Mass Inflow	Percentage Error	True Mass Inflow	Estimated Mass Inflow	Percentage Error
E. con.	352.654	352.020	0.180	36,815.94	36,788.62	0.074
Mg	12.260	12.339	- 0.640	1,019.42	1,019.21	0.021
Ca	40.279	40.251	0.071	4,289.66	4,285.13	0.106
Na	27.165	27.161	0.017	2,211.36	2,211.69	- 0.015
K	6.543	6.512	0.477	260.52	260.18	0.130
HCO ₃	182.869	182.276	0.325	17,984.83	17,987.77	- 0.016
Cl	7.240	7.215	0.342	756.67	756.13	0.074
NO ₃	2.082	2.068	0.693	406.21	408.85	- 0.651
SO ₄	58.938	59.174	- 0.400	3,570.12	3,562.35	0.218
F	0.601	6.608	- 1.184	60.55	60.41	0.228
Li	0.017	0.017	1.246	1.61	1.58	1.749
Si	18.525	18.530	- 0.025	1,894.77	1,894.87	- 0.005
H-2	- 81.292	- 81.310	- 0.022	- 7,942.92	- 7,943.85	- 0.012
0-18	- 10.563	- 10.568	- 0.052	- 1,049.62	- 1,049.53	0.009
TOTAL lbs/day	3,326.1	3,331.7	+ 0.17	325,133.7	325,326.6	0.06

generated by means of the following formula (Box and Muller, 1958, as cited in Bard, 1974)

$$N(0,1) = (-2 \log_{10} u_1)^{1/2} \cos (2\pi u_2) \quad (15)$$

where u_1 and u_2 are independent random variables drawn from a uniform distribution. Next, each "true" C_k value entering into the model is transformed into a noisy concentration, C_k^* , computed according to

$$C_k^* = C_k [1 + \beta_k N(0,1)] \quad (16)$$

where β_k is a weighting parameter. This causes the errors to increase linearly with concentration in a manner similar to that of Woolhiser et al. (1982). This is true at least for errors arising from laboratory analyses. When the noise is made independent of C , the Wolfe algorithm at times fails to converge. These authors found that errors in C are more important than errors in Q ; for this reason, we have not superimposed noise on the true Q values.

A total of 100 noisy C data sets was generated for each of the following four β values: 0.01, 0.05, 0.1, and 0.2 (same β for every k). For each of these 400 realizations, the quadratic programming algorithm was used to obtain a corresponding estimate of the unknown Q values. The matrix W used here was the same used earlier with the noise-free data.

Figures 50A-50C show how the mean of the computed Q values varies with the number of realizations for $\beta = 0.2$, 0.1, and 0.05, respectively. Figure 51 shows the same for $\beta = 0.01$, together with the

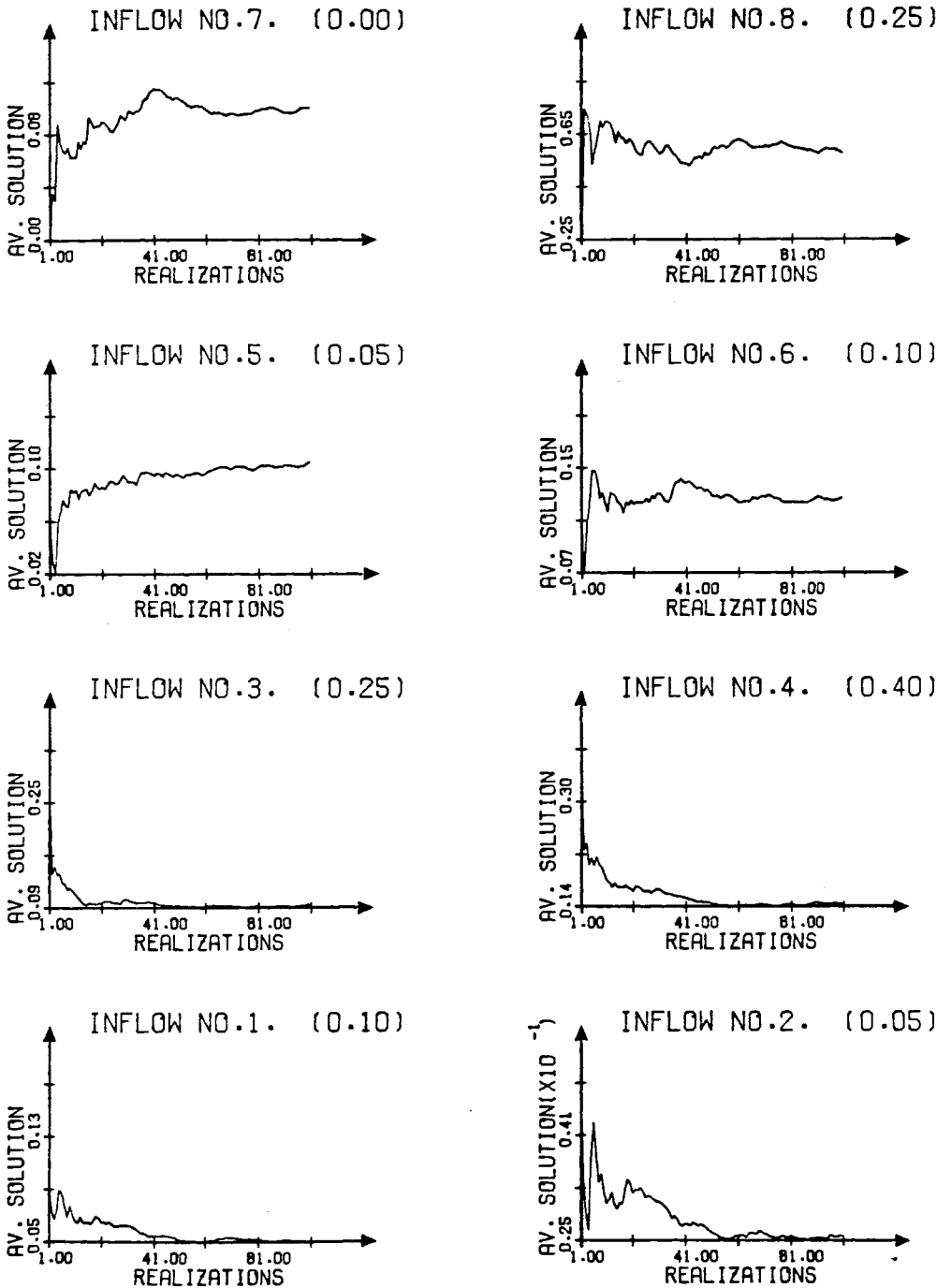


Figure 50. Variation of mean computed Q with number of realizations with constant β :

(A) $\beta = 0.2$

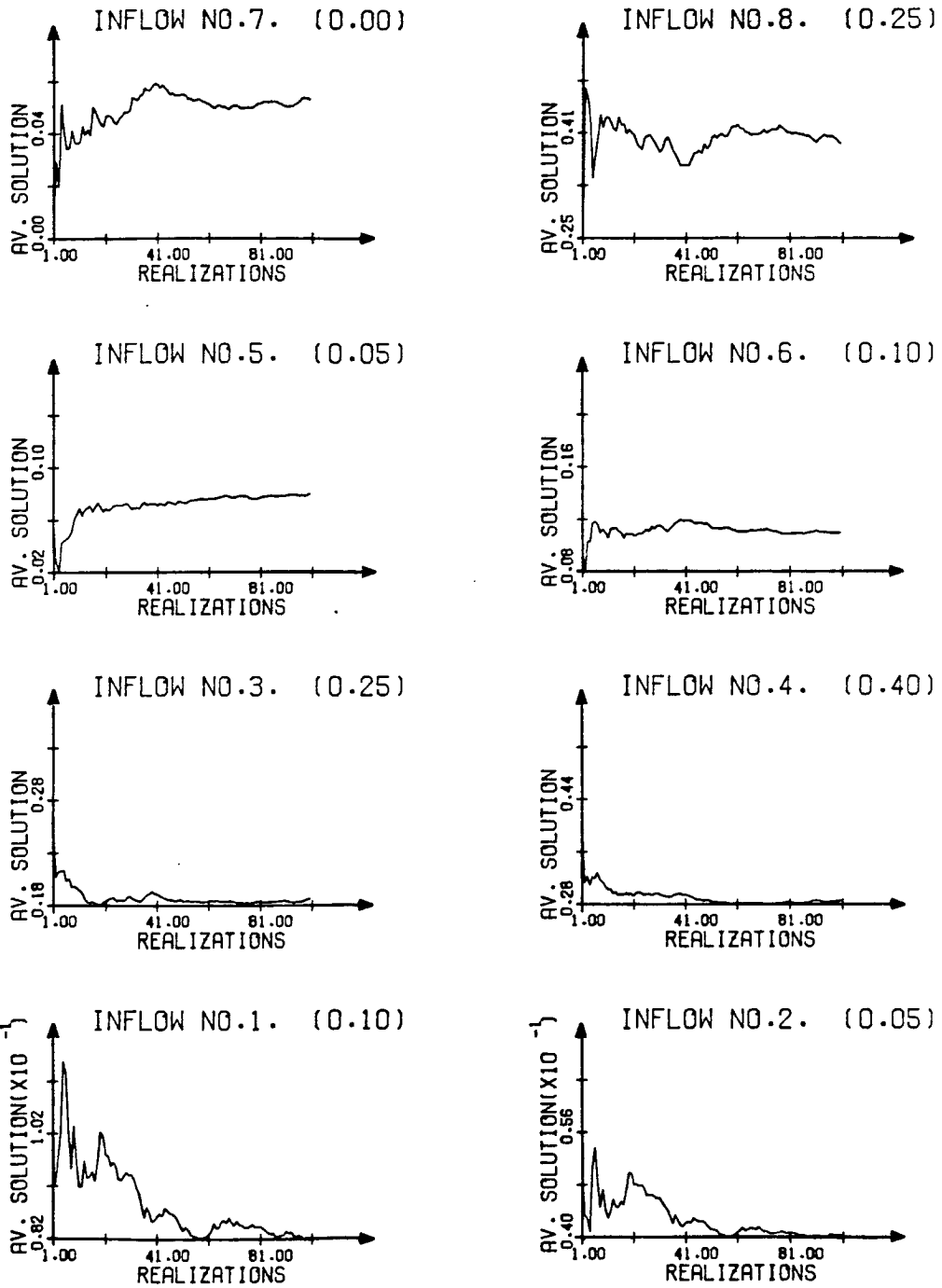


Figure 50.--Continued

(B) $\beta = 0.1$

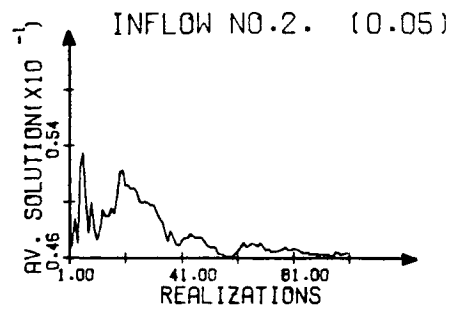
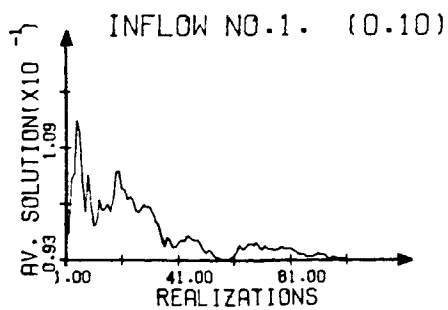
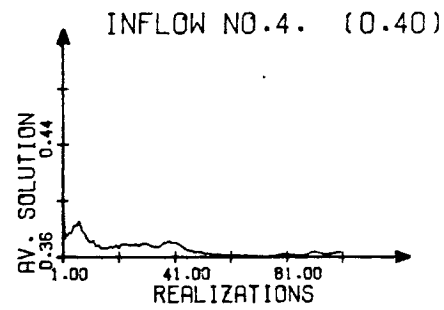
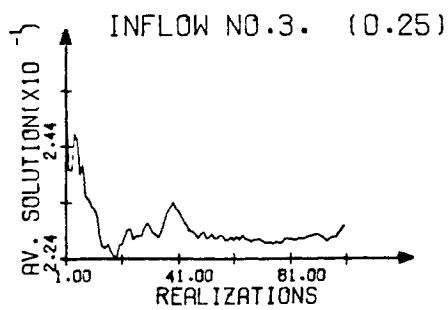
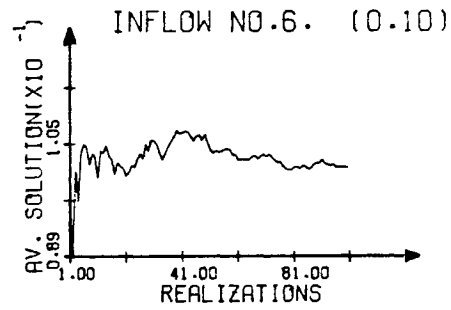
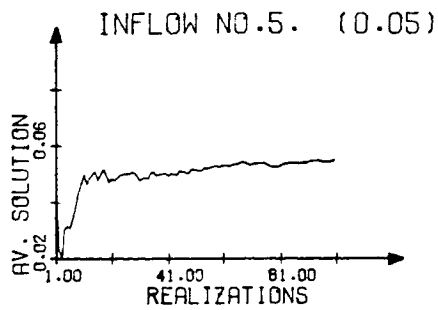
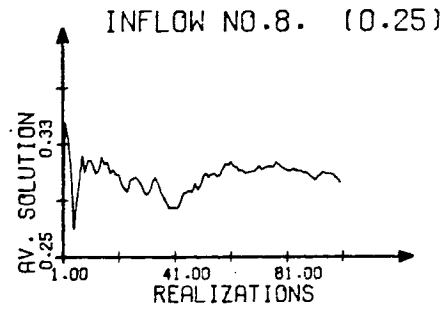
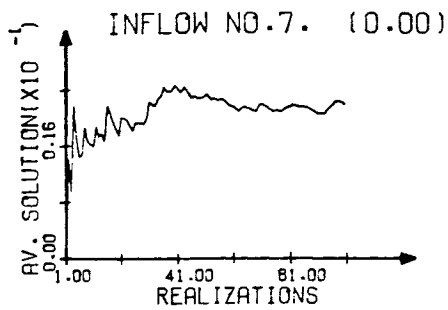


Figure 50.--Continued

(C) $\beta = 0.05$

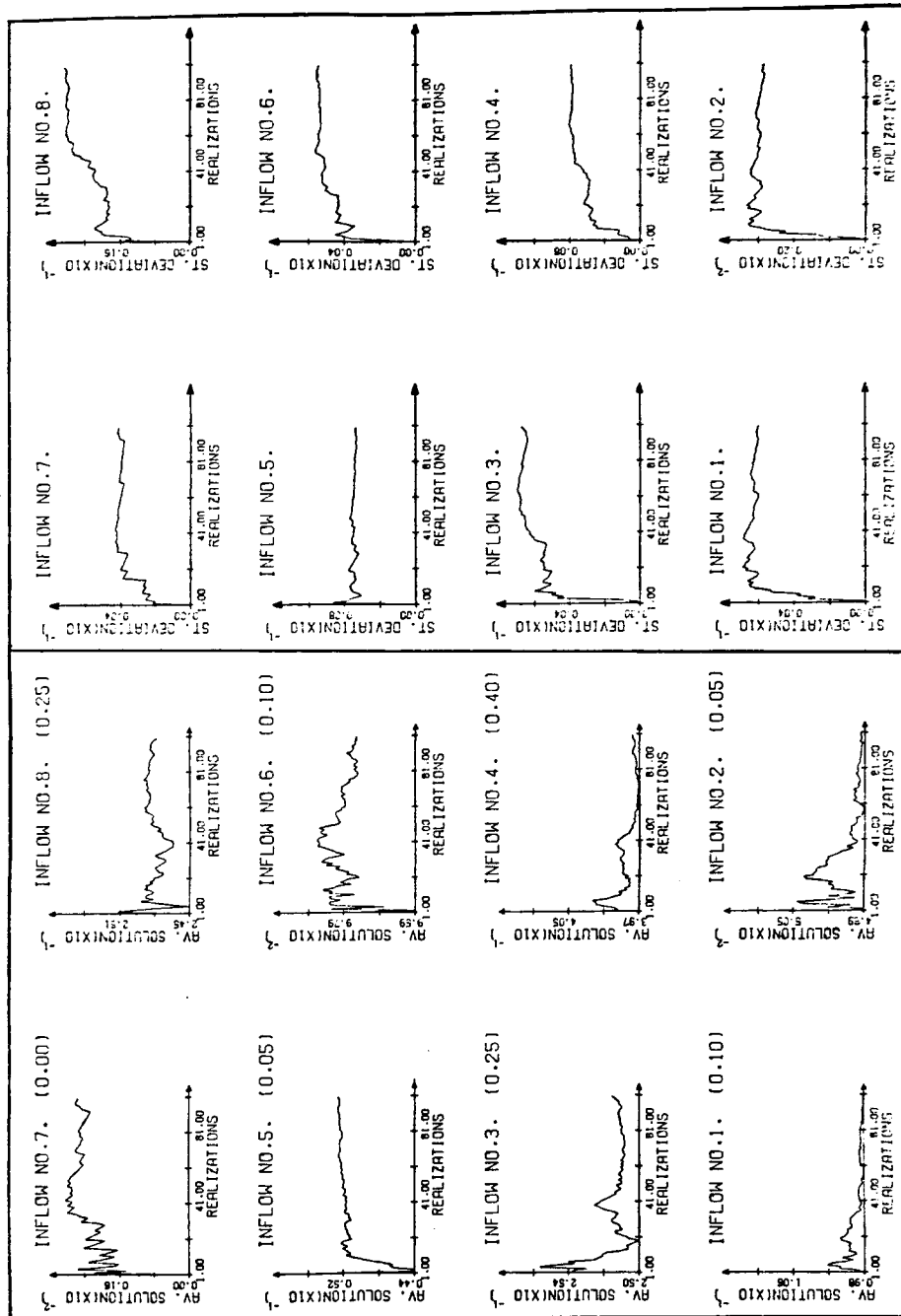


Figure 51. Average solutions and standard deviations from Monte Carlo simulations with a constant weight $\beta = 0.01$

standard deviations of the computed Q values. The final results for all the realizations are summarized in Table 5.

It is seen that, regardless of β , the mean Q values converge to a stable value after 40-50 realizations. However, the magnitudes of these asymptotic limits depend heavily on the magnitude of β . Table 5 shows that, when $\beta = 0.2$, the means of the computed Q values (with the exception of Q_7 which is zero) differs by 30-140% from the true values. When $\beta = 0.1$, the difference ranges from 10 to 56% and, when $\beta = 0.01$, it reduces to 0.2-4%.

As seen in Figure 51, the standard deviations of the computed Q values stabilize (for $\beta = 0.01$) after 20 (for Q_1) to 55 (for Q_8) realizations. The manner in which these standard deviations vary with β is illustrated in Figure 52. Clearly, the larger is β , the greater is the error of estimation. On the other hand, the estimation error generally increases at a slower rate than the magnitude of the noise in the data. We found that, due to incomplete convergence of the Wolfe algorithm, the estimation error is also affected by the order in which the unknowns are numbered (and thus, enter into the equations). Often, the estimation error increases as the ordering number goes up. A similar phenomenon was observed by others (N. Buras, and D.A. Woolhiser, personal communication, 1984).

Another test was performed in which a different β_k value had been assigned to each chemical species, k, according to

$$\beta_k = \frac{\sigma_k}{\mu_k} \quad (18)$$

Table 5. Average inflows and statistics from 100 realizations of noisy C data with four constant β values

	β^*	Q_1	Q_2	Q_3	Q_4	Q_5	Q_6	Q_7	Q_8
Expected Inflow m ³ /sec.	0.1	0.05	0.25	0.40	0.05	0.10	0.00	0.25	
Average inflows for different CV values	0.20 0.10 0.05 0.01	0.062 0.082 0.093 0.0998	0.025 0.041 0.047 0.049	0.10 0.18 0.23 0.252	0.14 0.29 0.37 0.398	0.110 0.076 0.055 0.052	0.130 0.110 0.103 0.0975	0.100 0.050 0.029 0.022	0.60 0.39 0.31 0.253
Deviation in Percents From the Expected Inflows	0.20 0.10 0.05 0.01	38.0 18.0 7.0 0.2	50.0 18.0 6.0 2.0	60.0 28.0 8.0 0.8	65.0 27.5 7.5 0.5	120.0 52.0 10.0 4.0	30.0 10.0 3.0 2.5		140. 56. 24. 1.2
Standard Deviation	0.20 0.10 0.05 0.01	0.0340 0.0395 0.0275 0.0058	0.0175 0.0194 0.0125 0.0029	0.056 0.048 0.029 0.007	0.076 0.065 0.028 0.0075	0.070 0.050 0.025 0.007	0.081 0.060 0.026 0.0055	0.086 0.048 0.025 0.004	0.430 0.260 0.113 0.027
Coefficient of Variations	0.20 0.10 0.05 0.01	0.55 0.48 0.30 0.06	0.70 0.47 0.27 0.06	0.56 0.27 0.13 0.03	0.54 0.22 0.08 0.02	0.64 0.66 0.45 0.13	0.62 0.55 0.25 0.11	0.86 0.96 0.86 0.18	0.72 0.67 0.36 0.11

* Weighting Parameter

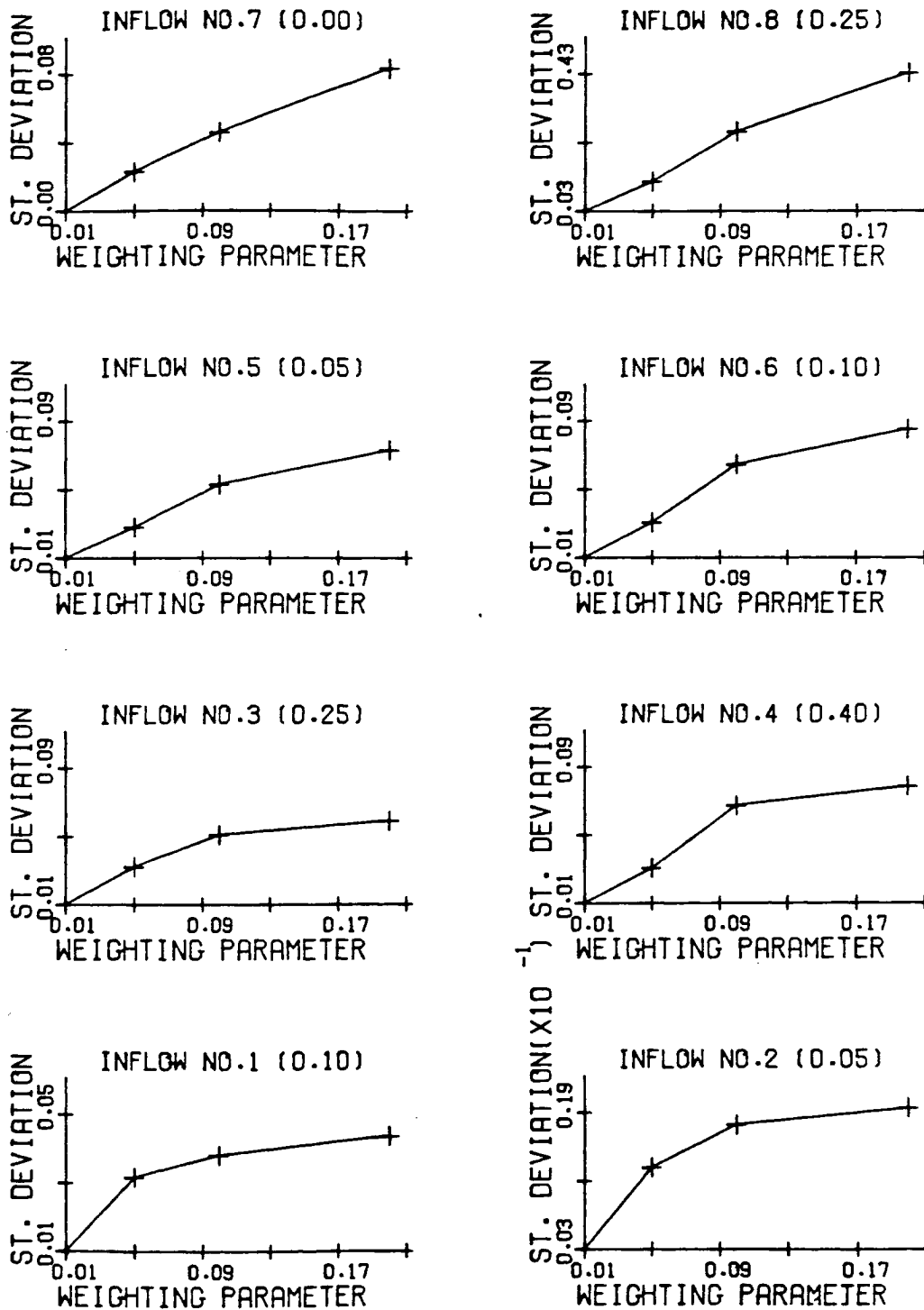


Figure 52. Standard deviations of computed Q values versus β

Here, μ_k is the mean of a large number of concentrations determined for laboratory standards of the k^{th} species, and σ_k is the associated standard deviation (for details, see Table 5 and introduction in Appendix C). In this manner, β_k becomes the coefficient of variation of errors in determining the laboratory standards.

The results of this test are summarized in Table 6. Figures 53A-B show how the mean computed Q values and the standard deviations of these values vary with the number of realizations. Figures 53 C-D show the frequency distributions of the computed Q values and the cumulative frequencies of the errors of estimation, respectively. From Table 6 and Figure 53A, we see that Monte Carlo simulation leads to stable mean Q values which differ by 22-100% from the true values. Figures 53B-D show that the estimation errors have a wide spread (have a large standard deviation) and are generally far from Gaussian (even though the noise in the data is such). In part, deviations from normality are due to the non-negativity constraints imposed on the computed Q values; these affect primarily the smaller values of Q. However, most of the difficulty stems from neglecting to maintain ionic balance between the chemical species and fixed ratios between D and O-18 in generating the noisy data. Laboratory data usually will be rejected unless the concentration of all cations (in meq/lit) matches that of all anions; electrical conductivity varies linearly with TDI; and D varies linearly with O-18.

To test this, we repeated the simulations while imposing constraints on the generated errors (in reality, by rejecting noisy data that did not satisfy specific requirements). Figure 54 shows results

Table 6. Average inflows and statistics from 100 realizations of noisy C data with different β_k values assigned to each species

Inflow	Q1	Q2	Q3	Q4	Q5	Q6	Q7	Q8
Expected Inflow m ³ /sec	0.1	0.05	0.25	0.4	0.05	0.10	0.00	0.25
Average Calculated Inflow	0.845	0.041	0.210	0.315	0.084	0.112	0.055	0.360
Percentage Deviation from the Expected Inflows	15.5	18.0	16.0	21.3	68.0	12.0		44.0
Standard Deviation	0.041	0.0188	0.058	0.069	0.05	0.054	0.055	0.260
Coefficient of Variations	0.485	0.459	0.276	0.219	0.595	0.446	1.00	0.722

Table 6--continued

Inflow	Q1	Q2	Q3	Q4	Q5	Q6	Q7	Q8
Expected Inflow m ³ /sec	0.1	0.05	0.25	0.4	0.05	0.10	0.00	0.25
Average Calculated Inflow	0.845	0.041	0.210	0.315	0.084	0.112	0.055	0.360
Percentage Deviation from the Expected Inflows	15.5	18.0	16.0	21.3	68.0	12.0		44.0
Standard Deviation	0.041	0.0188	0.058	0.069	0.05	0.054	0.055	0.260
Coefficient of Variations	0.485	0.459	0.276	0.219	0.595	0.446	1.00	0.722

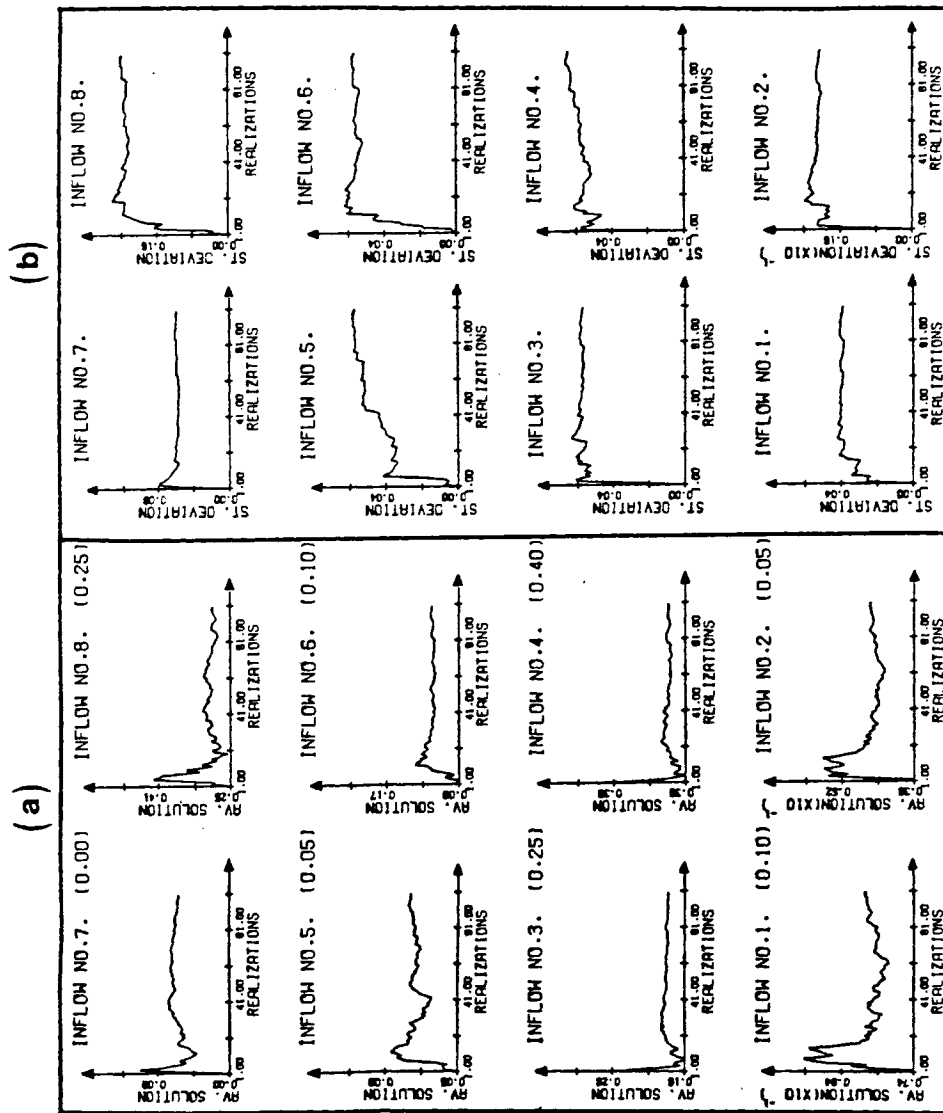


Figure 53. Results of Monte Carlo simulations with β values equal to coefficients of variation from laboratory standards:
 (A) average Q versus number of realizations
 (B) standard deviations of Q versus number of realizations

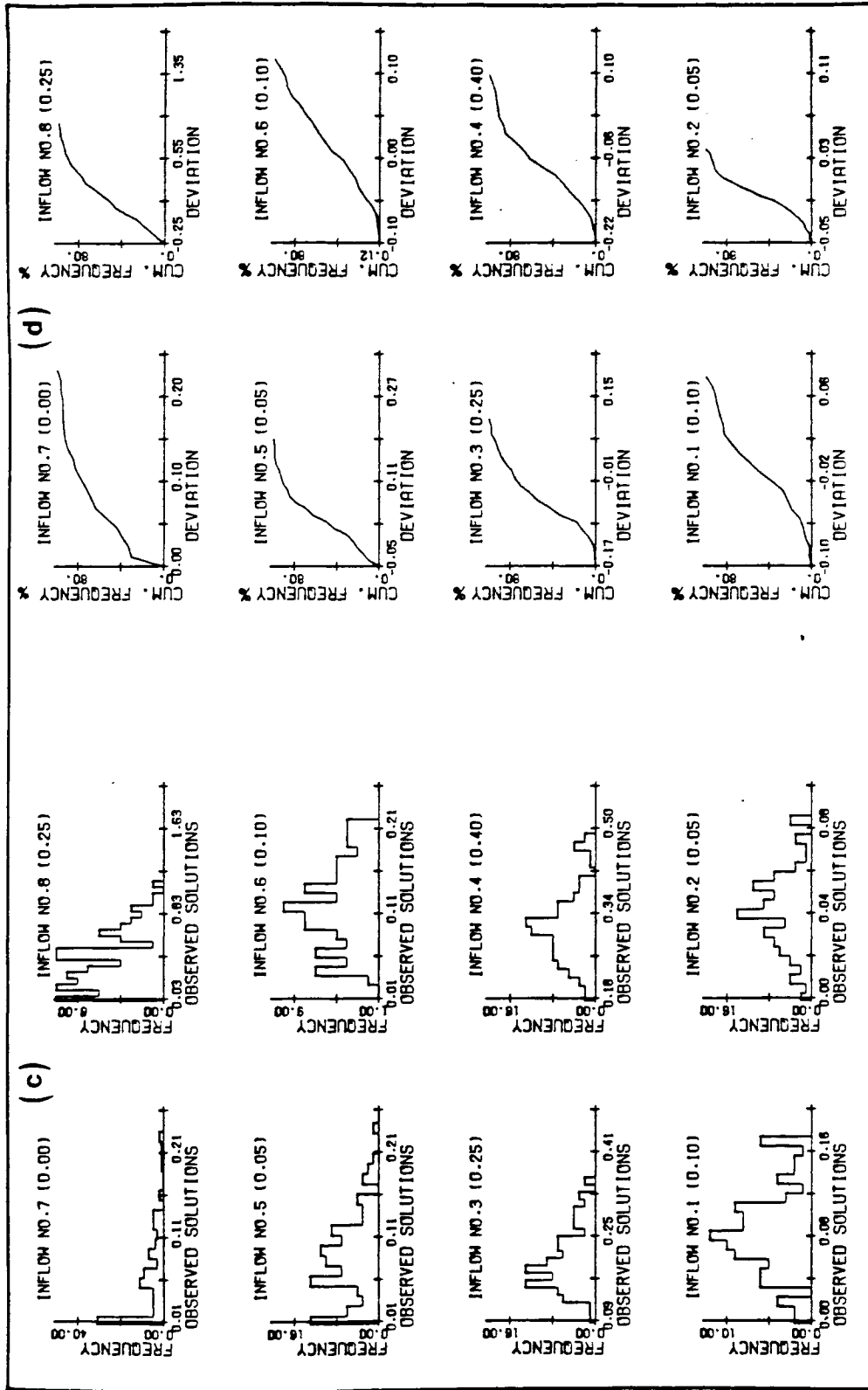


Figure 53--continued

(c) frequency distribution of computed Q values
 (d) cumulative frequencies of Q estimation errors

for the case where the generated data were required to maintain ionic balance to within 10%, a ratio between electrical conductivity and TDI ranging from 30 to 60, and a ratio between D and O-18 ranging from 5 to 11. These ratios represent the minimum and maximum actually obtained for data from the Aravaipa Valley. The results in Figure 54 have a smaller estimation error than those in Figure 53 and their distributions are less skewed (especially those of the larger Q values). Figures 55 and 56 show what happens as the chemical constraints are gradually tightened. The standard deviation of the estimation errors is seen to go down, and the distribution of the results is seen to come closer and closer to normal. The results from all the constrained simulations are summarized in Table 7.

The true value of Q_7 is zero, and its estimates are therefore heavily skewed toward this number (due to the non-negativity requirement). Nevertheless, in Figure 56D, we see that 42% of the time Q_7 is correctly estimated to be zero, and 95% of the time its estimate deviates from zero by not more than 0.07.

Our results show that, when the data are constrained to realistic relationships between the chemical species, the model yields acceptable results. This suggests that the model should be applicable to real data from the Aravaipa Valley.

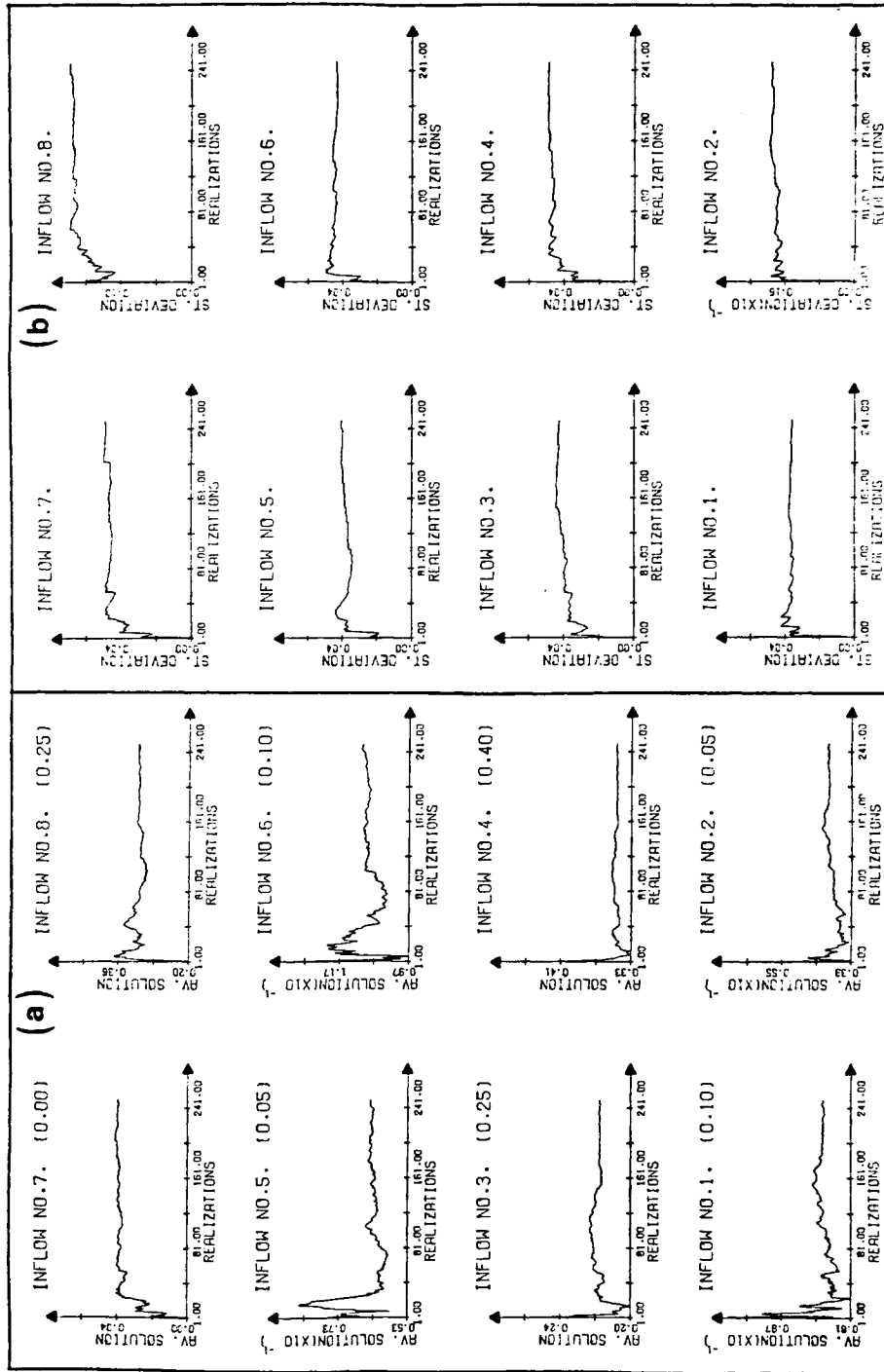


Figure 54. Results of Monte Carlo simulations with noisy concentrations restricted to ionic balance of 10 percents, Electrical Conductivity ratio between 30 and 60, and D to 0-18 ratio Q versus number of realizations
 (A) Average Q versus number of realizations
 (B) Standard deviations of Q versus number of realizations

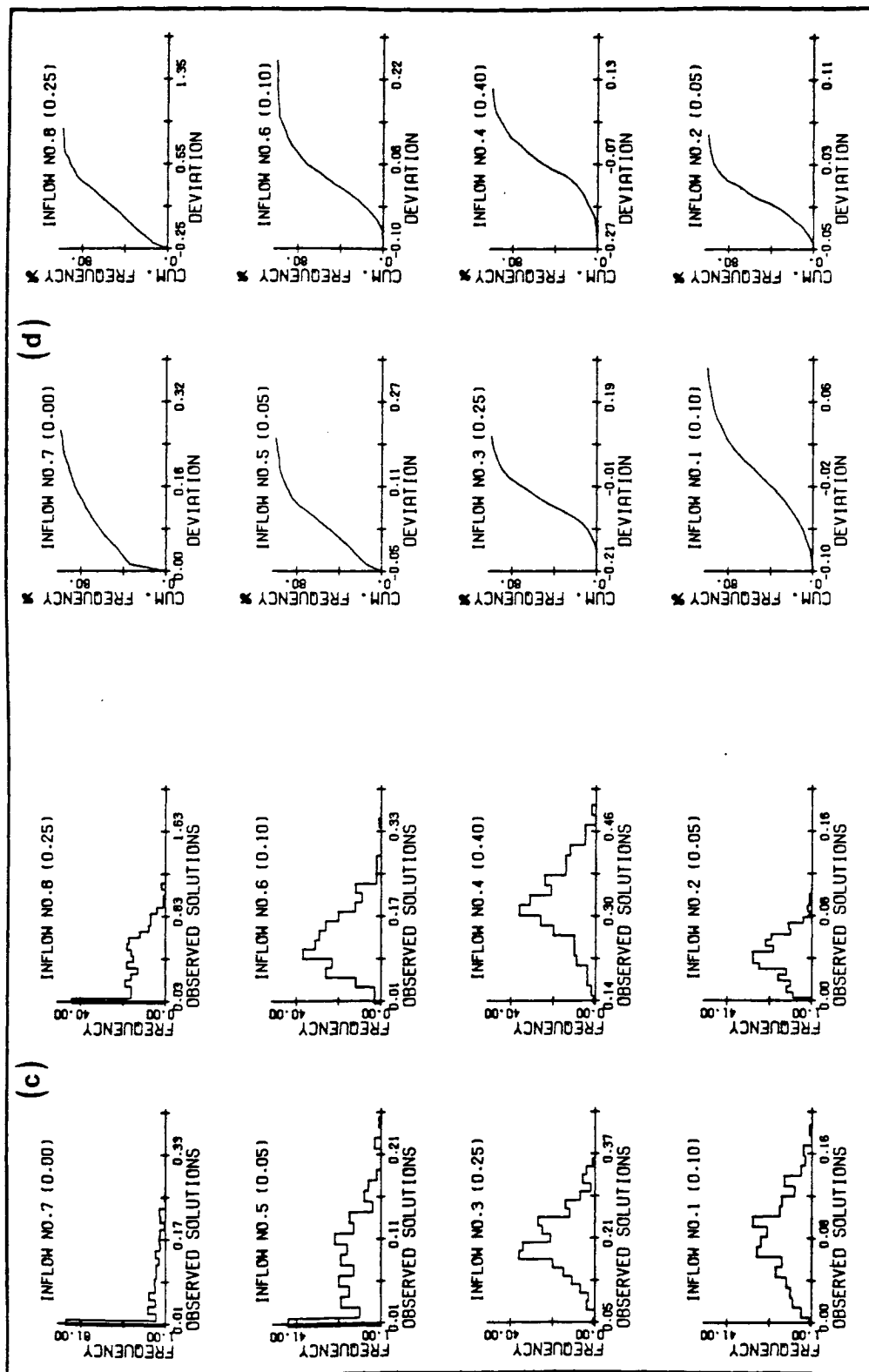


Figure 54--continued
 (C) frequency distribution of computed Q values
 (D) cumulative frequencies of Q estimation errors

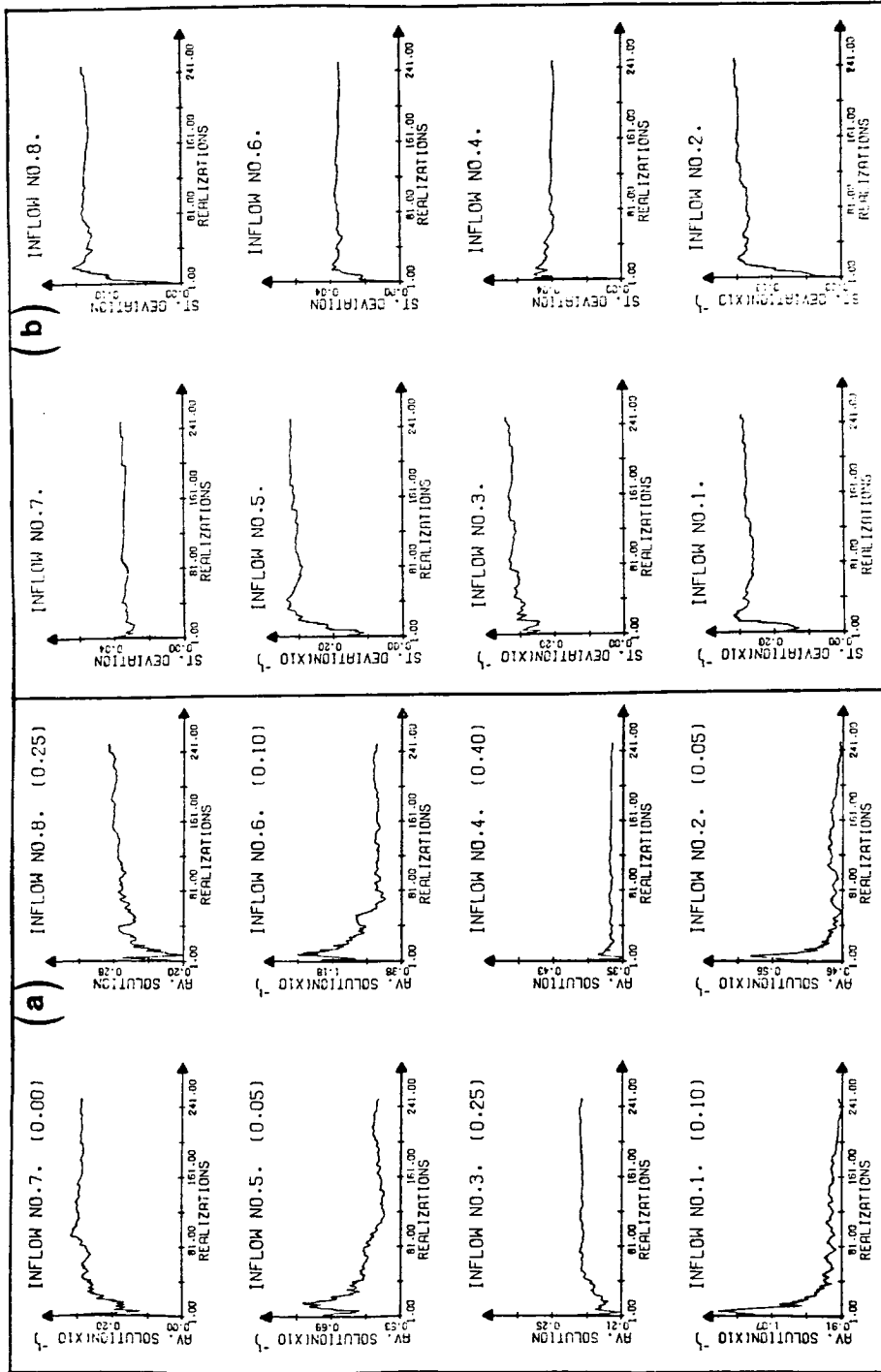


Figure 55. Results of Monte Carlo simulations with noisy concentrations restricted to ionic balance of 5 percents, Electrical Conductivity to TDI ratio between 35 and 60, and D to 0-18 ratio between 6.5 and 9.5
 (A) Average Q versus number of realizations
 (B) standard deviations of Q versus number of realizations

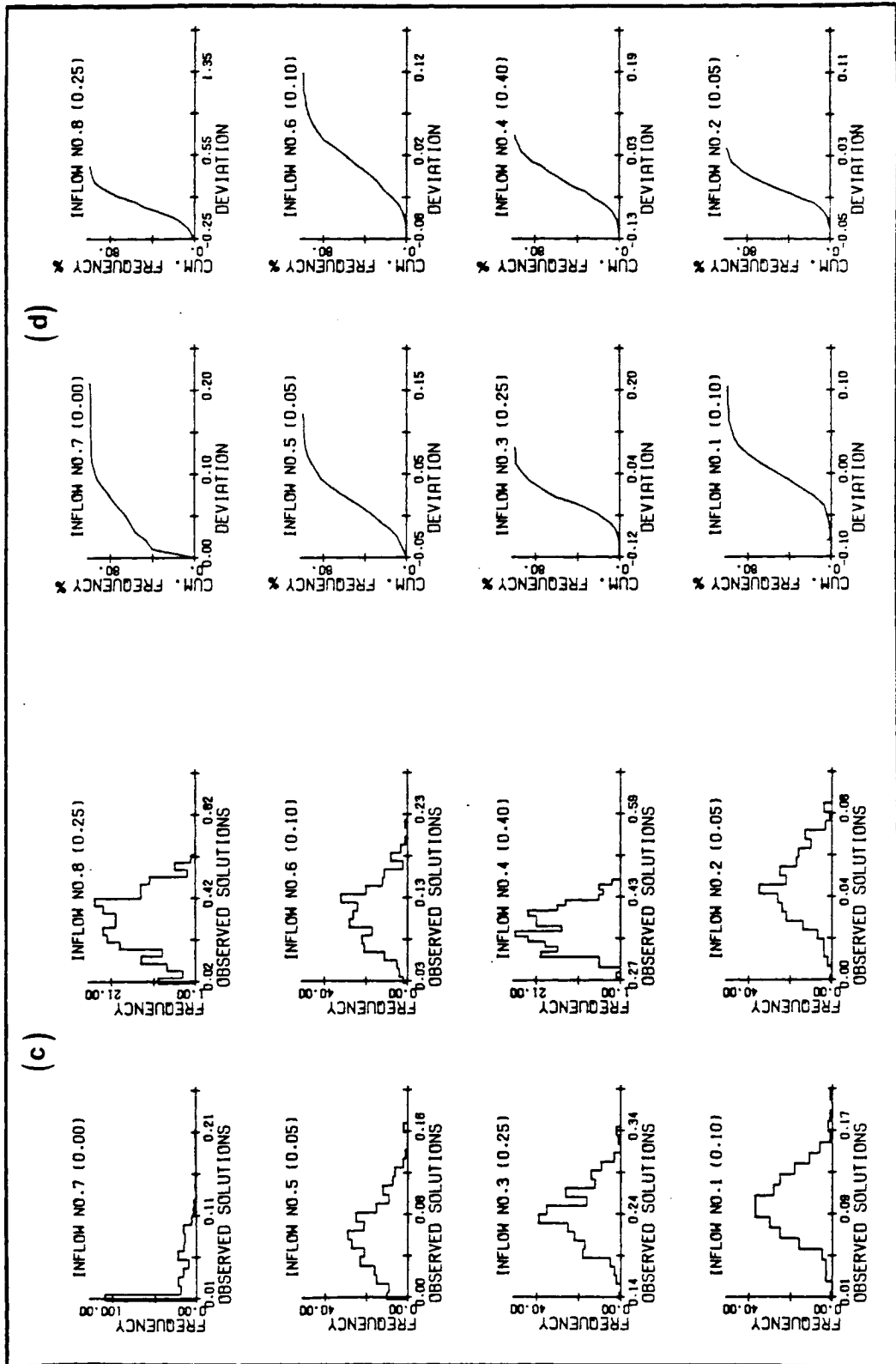


Figure 55-continued

(c) frequency distribution of computed Q values

(d) cumulative frequencies of Q estimation errors

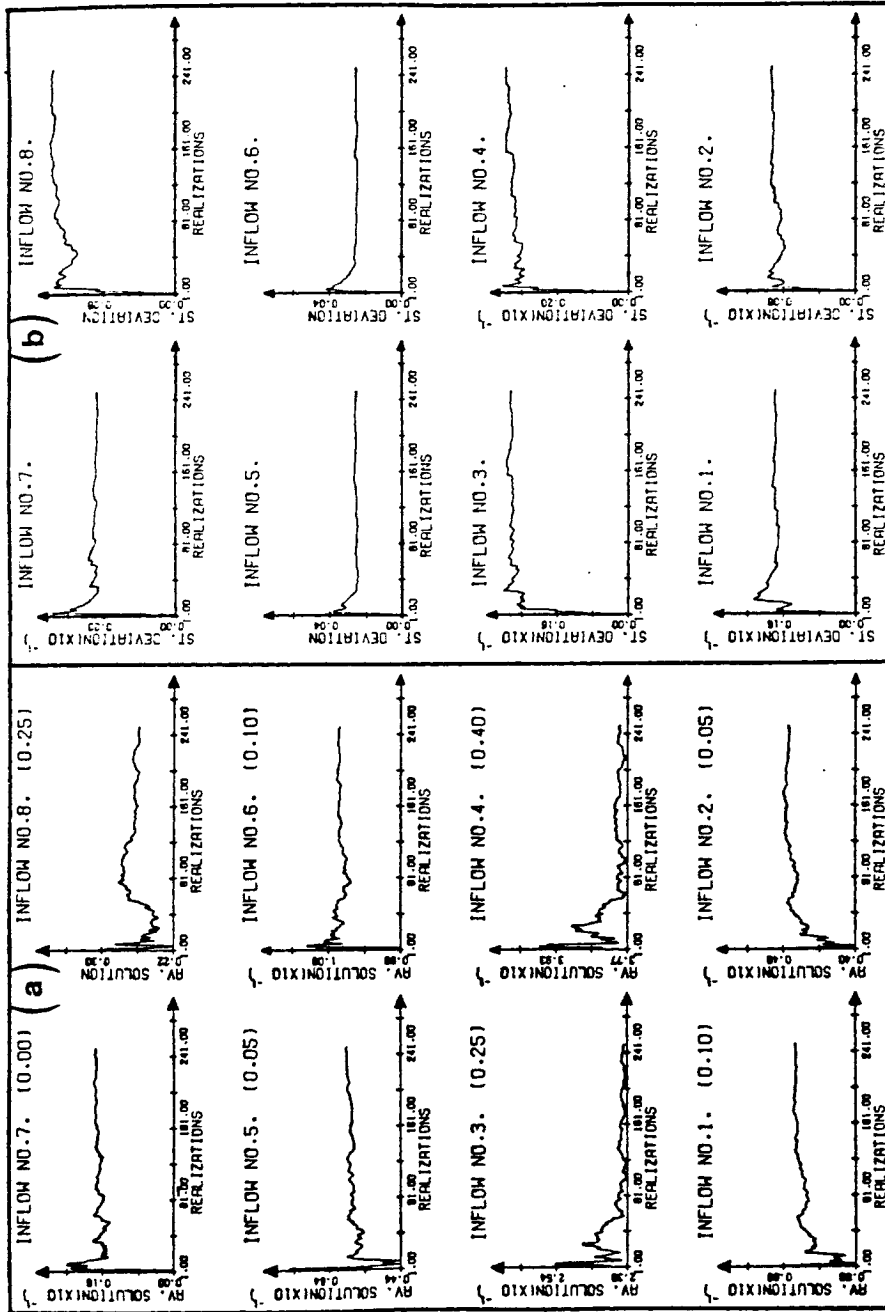


Figure 56. Results of Monte Carlo simulations with perturbed concentrations restricted to ionic balance of 2 percent, Electrical Conductivity to TDI ratios between 35 and 55, and D to 0-18 ratios between 6.5 and 8.5
 (A) Average Q versus number of realizations
 (B) Standard deviations of Q versus number of realizations

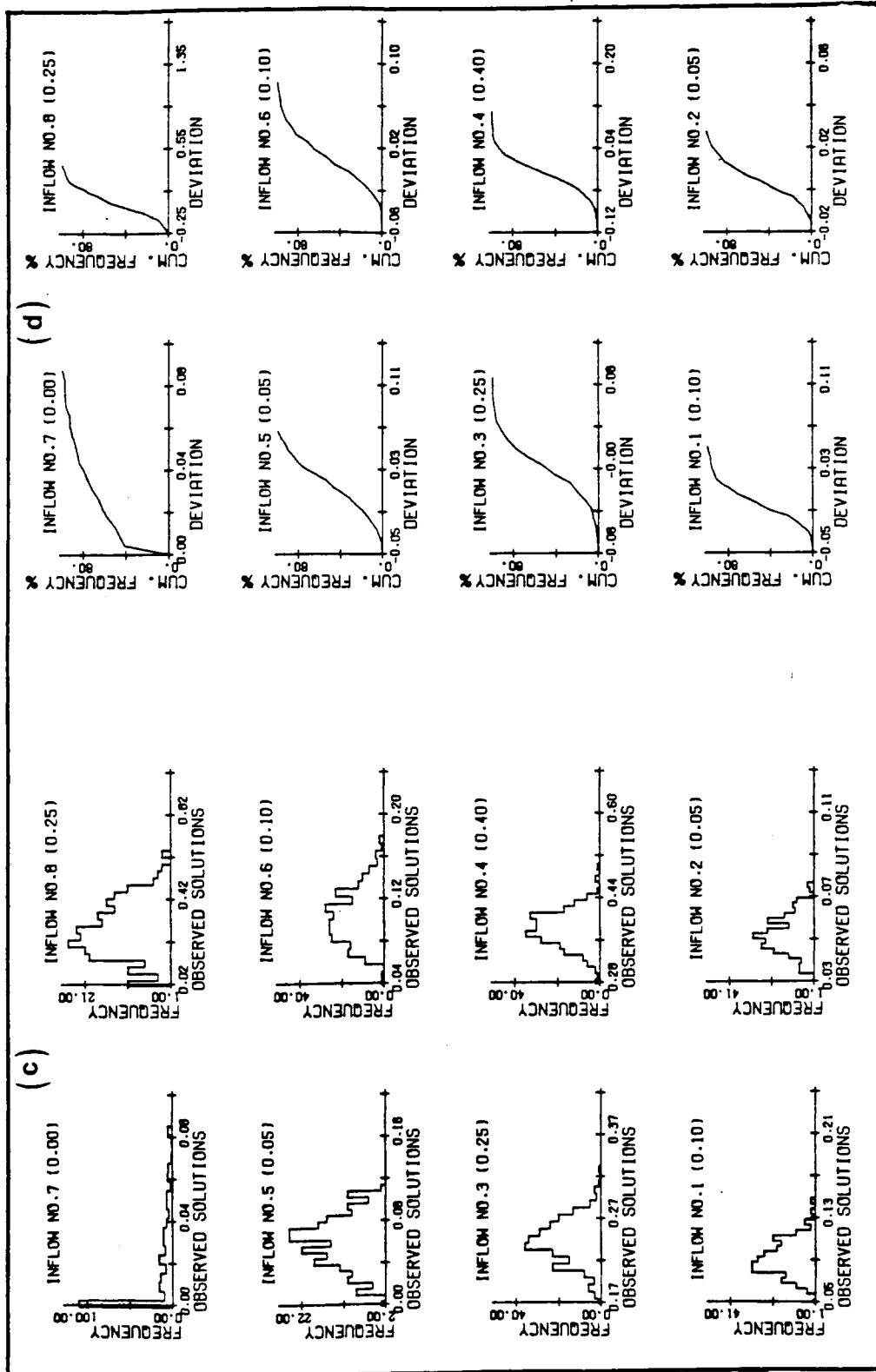


Figure 56--continued
 (C) frequency distributions of computed Q values
 (D) cumulative frequencies of Q estimation errors

Table 7. Average inflows and statistics from 250 realizations with chemical and isotopic constraints

	Constraints										
	Ionic Balance	E.C./TOC	D/O	Q1	Q2	Q3	Q4	Q5	Q6	Q7	Q8
Expected Inflows				0.1	0.05	0.25	0.40	0.05	0.10	0.00	0.25
Average Calculated Inflows	10.0	30-55	5-11	0.0875	0.0458	0.193	0.315	0.086	0.125	0.068	0.295
	10.0	35-55	6-10	0.0882	0.0462	0.185	0.320	0.075	0.120	0.060	0.285
	3.0	30-60	6-9	0.080	0.042	0.200	0.320	0.070	0.120	0.060	0.320
	3.0	35-60	6-9	0.087	0.044	0.218	0.350	0.063	0.109	0.039	0.320
	3.0	35-55	6.5-9	0.093	0.047	0.935	0.375	0.056	0.105	0.028	0.280
	2.0	35-55	6.5-8.5	0.095	0.048	0.240	0.383	0.056	0.102	0.016	0.260
Percentage Deviation from the Expected Inflows	10.0	30-55	5-11	12.5	8.4	22.8	21.3	70.0	25.0		18.0
	10.0	35-55	6-10	12.0	7.6	26.0	20.0	50.0	20.0		9.4
	3.0	30-60	6-9	20.0	16.0	20.0	20.0	40.0	20.0		28.0
	3.0	35-60	6-9	13.0	12.0	12.8	12.5	27.0	9.0		28.0
	3.0	35-55	6.5-9	7.0	6.0	6.0	7.5	12.0	5.0		12.0
	2.0	35-55	6.5-8.5	5.5	4.4	4.0	4.25	12.0	2.0		3.2
Standard Deviation	10.0	30-55	5-11	0.04	0.022	0.058	0.068	0.060	0.058	0.070	0.230
	10.0	35-55	6-10	0.04	0.021	0.056	0.070	0.058	0.0575	0.055	0.240
	3.0	30-60	6-9	0.0385	0.021	0.0575	0.070	0.058	0.057	0.070	0.260
	3.0	35-60	6-9	0.038	0.019	0.042	0.045	0.040	0.043	0.050	0.170
	3.0	35-55	6.5-9	0.028	0.015	0.032	0.039	0.032	0.037	0.037	0.130
	2.0	35-55	6.5-8.5	0.017	0.009	0.025	0.034	0.024	0.0281	0.0215	0.130
Coefficient of Variation	10.0	30-55	5-11	0.457	0.480	0.301	0.216	0.698	0.464	1.029	0.780
	10.0	35-55	6-10	0.454	0.455	0.303	0.219	0.773	0.460	0.917	0.842
	3.0	30-60	6-9	0.481	0.500	0.288	0.219	0.829	0.475	1.167	0.813
	3.0	35-60	6-9	0.437	0.443	0.193	0.129	0.630	0.390	1.282	0.513
	3.0	35-55	6.5-9	0.308	0.330	0.136	0.105	0.554	0.357	1.339	0.464
	2.0	35-55	6.5-8.5	0.185	0.188	0.104	0.089	0.430	0.235	1.295	0.504

CHAPTER 7

APPLICATION OF MODEL TO LOWER ARAVAIPA VALLEY

Sufficient information is available to allow applying our proposed model to the unconfined aquifer in the lower Aravaipa basin. A qualitative description of the inputs and outputs into the water table aquifer was given in Chapter 5 (Figure 19). Quantitative estimates of annual pumpage rates were listed in Table 1, and an estimate of the net annual discharge from the aquifer (concentrated near Aravaipa Spring) was given at the end of Chapter 4. Discharge due to evapotranspiration is considered to be negligible. We now wish to use our model to obtain quantitative estimates of the various recharge components in Figure 19 which contribute to the downstream portion of the water table aquifer.

An outline of the modeled portion is shown in Figure 57. The lateral boundaries of the model correspond to the contact (on the surface) between the young alluvium (comprising the modeled aquifer) and older deposits such as the Hell Hole conglomerate and the old alluvium. The upstream boundary of the model passes through Haby Spring, the downstream boundary through Aravaipa Spring. The Sharizona section (Figure 19) is excluded from the model because the precise location of the upstream aquifer boundary, which passes through this section, is uncertain.

The modeling area is subdivided into 5 mixing cells. The chemical concentrations assigned to each cell are taken to be the averages of

Figure 57. Outline of the modeled portion of the water table aquifer

LEGEND

-  Lateral inflow from Rattlesnake alluvial fan
-  Inflow from Sharizona section
-  Lateral inflow from the eastern Old Alluvium
-  Lateral inflow from the western Old Alluvium
-  Lateral inflow from the Stowe-Gulch basin
-  Lateral inflow from Fourmile Canyon
-  Outflow by means of pumpage
-  Streambed infiltration during floods
-  Upward leakage from the deep aquifer
-  Flow between cells
-  Well

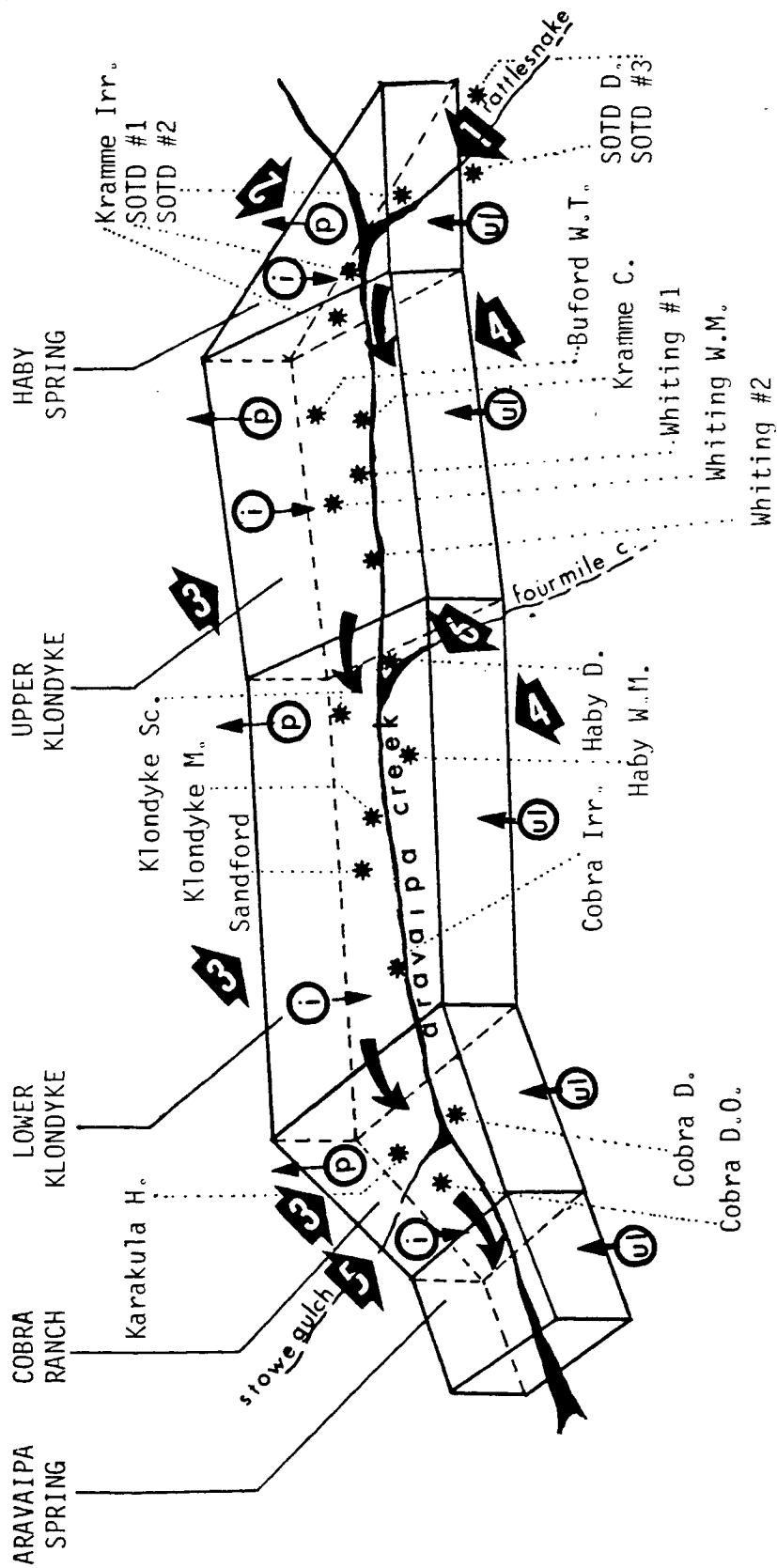


Figure 57. Outline of the modeled portion of the water table aquifer

values determined in wells tapping the unconfined aquifer within the confines of the cell (see Figure 57). The division into cells is done so as to minimize variations in the chemical compositions of the waters sampled in each cell. Wells and springs, the waters of which are used to assign chemical concentrations to the various input and output components are listed in Table 8. Table 9 lists also the cell and input/output concentrations used in the model (as computed by averaging the concentrations in the corresponding wells and springs), together with the standard deviations of these values. These standard deviations represent not only spatial variation in chemical concentrations between adjacent wells, but also (and probably more so) errors in the laboratory determination of the concentrations (refer to Table 5 in Appendix C).

As an added check on the manner in which the water samples are grouped into cell and input/output values, we used the computer program WATEQF (Truesdell and Jones, 1973, 1974; Plummer et al., 1976) to investigate the chemical relationships between the sampled waters and selected minerals with which these waters might interact. WATEQF uses the Debye-Huckel equation to transform concentrations into activities on the basis of ionic strength. These activities are then substituted into mass action equilibrium equations (for selected mineral-solute reactions) to compute equilibrium solubility constants, K , and activity products, AP . The ratio between AP and K is related to the Gibbs free energy, ΔG_R , of each reaction by means of the equation

$$\Delta G_R = 2.303 RT \log (AP/K)$$

where R is the universal gas constant and T is absolute temperature in degrees Kelvin. If ΔG_R is negative for a given reaction, the water is

Table 8. Type of inflow and the representative water sample associated with each cell in the modeled area

Cell 1. Haby Spring

Estimated annual pumpage: 100 acre ft./yr.

<u>Inflows</u>	<u>Water Sample</u>
1. Lateral Inflow from Upper Valley	Sharizona Section
2. Lateral Inflow through Alluvial Fan	Rattlesnake
3. Upward Leakage	S.O.T.D. #3
4. Streambed Infiltration	Winter and Summer Floods

Cell 2. Upper Klondyke

Estimated Annual Pumpage: 900 acre ft./yr.

<u>Inflows</u>	<u>Water Sample</u>
1. Lateral Inflow from Upstream	Cell 1
2. Lateral Inflow through Western Pediment	Squaw Sp. (T), Squaw Cave sp.
3. Lateral Inflow through Eastern Pediment	Lamb Camp, Whiting Hill
4. Upward Leakage	Whiting Deep, Long Hollow, Squaw Deep
5. Streambed Infiltration	Winter and Summer Floods

Table 8--continued

Cell 3. Lower Klondyke

Estimated Annual Pumpage: 800 acre ft./yr.

<u>Inflows</u>	<u>Water Sample</u>
1. Lateral Inflow from Upstream	Cell 2
2. Lateral Inflow through Alluvial Fan	Fourmile (camp-ground)
3. Lateral Inflow through Eastern Pediment	3667 WM, Laurel Canyon
4. Upward Leakage	Klondyke Deep #2
5. Streambed Infiltration	Winter and Summer Floods

Cell 4. Cobra Ranch

Estimated Annual Pumpage: 250 acre ft./yr.

<u>Inflows</u>	<u>Water Sample</u>
1. Lateral Inflow from Upstream	Cell 3
2. Lateral Inflow through Alluvial Fan	Stowe Gulch
3. Lateral Inflow through Eastern Pediment	3667 W.M.
4. Upward Leakage from Deep Aquifer	Cobra N. Irrig.
5. Streambed Infiltration	Winter and Summer Floods

Cell 5. Aravaipa Spring

Estimated Annual Discharge: 10,000 acre ft./yr.

<u>Inflows</u>	<u>Water Sample</u>
1. Lateral Inflow from Upstream	Cell 4
2. Upward Leakage	Karakula Adobe

Table 9. Average concentrations for each cell and inflow whose dissolved constituents were obtained from several water samples

(Data in meq/l except for: E.C [μmH0]; Si [ppm]; D and 0-18 [0/00])

<u>Cell #1. Haby Spring</u>														
Wells: Song of the Desert #1, Song of the Desert #2, and Kramme Irrigation														
	<u>E.C</u>	<u>Mg</u>	<u>Ca</u>	<u>Na</u>	<u>K</u>	<u>HCO3</u>	<u>Cl</u>	<u>NO3</u>	<u>SO4</u>	<u>F</u>	<u>Li</u>	<u>Si</u>	<u>D</u>	<u>0-18</u>
Average Values	334.1	0.67	1.98	0.87	0.055	2.47	0.29	0.097	0.69	0.02	0.002	18.6	- 72.4	- 9.53
Standard Deviation	48.0	0.11	0.34	0.13	0.004	0.47	0.14	0.004	0.02	0.001	0.0001	2.3	0.6	0.13
<u>Cell #2. Upper Klondyke</u>														
Wells: Kramme Corral, Bufford W.T., Whiting #1, Whiting W.M. and Whiting #2														
	<u>E.C</u>	<u>Mg</u>	<u>Ca</u>	<u>Na</u>	<u>K</u>	<u>HCO3</u>	<u>Cl</u>	<u>NO3</u>	<u>SO4</u>	<u>F</u>	<u>Li</u>	<u>Si</u>	<u>D</u>	<u>0-18</u>
Average Values	353.8	0.71	1.93	0.86	0.052	2.78	0.205	0.038	0.49	0.018	0.003	17.0	- 71.8	- 9.65
Standard Deviation	41.1	0.07	0.28	0.08	0.017	0.55	0.071	0.019	0.19	0.004	0.001	1.75	0.0	0.18

Table 9---continued

Cell #3. Lower Klondyke

Wells: Haby Dom, Haby W.M., Klondyke M., Klondyke School, Sanford and Cobra Irrigation

	<u>E.C</u>	<u>Mg</u>	<u>Ca</u>	<u>Na</u>	<u>K</u>	<u>HCO3</u>	<u>Cl</u>	<u>NO3</u>	<u>SO4</u>	<u>F</u>	<u>Li</u>	<u>Si</u>	<u>D</u>	<u>0-18</u>
Average Values	349.9	0.73	1.93	0.89	0.05	2.61	0.29	0.09	0.54	0.023	0.002	17.9	- 68.9	- 9.49
Standard Deviation	30.3	0.03	0.25	0.05	0.004	0.46	0.10	0.03	0.15	0.01	0.000	2.4	1.9	0.24

Cell #4. Cobra Ranch

Wells: Cobra Ranch Dom, Cobra Ranch (Old) and Karakula New House

	<u>E.C</u>	<u>Mg</u>	<u>Ca</u>	<u>Na</u>	<u>K</u>	<u>HCO3</u>	<u>Cl</u>	<u>NO3</u>	<u>SO4</u>	<u>F</u>	<u>Li</u>	<u>Si</u>	<u>D</u>	<u>0-18</u>
Average Values	421.1	0.97	3.02	0.80	0.030	3.27	0.32	0.070	1.10	0.033	0.002	15.6	- 74.0	- 9.54
Standard Deviation	66.5	0.15	0.60	0.11	0.008	0.60	0.04	0.017	0.31	0.010	0.001	1.3	0.1	0.14

Table 9---continued

<u>Inflow from the Sharizona Section Wells: Sharizona, H. Cl. WM, H. Cl. Irrig. and 3699</u>														
	<u>E.C</u>	<u>Mg</u>	<u>Ca</u>	<u>Na</u>	<u>K</u>	<u>HCO3</u>	<u>Cl</u>	<u>NO3</u>	<u>S04</u>	<u>F</u>	<u>Li</u>	<u>Si</u>	<u>D</u>	<u>0-18</u>
Average Values	353.7	0.74	1.97	0.97	0.06	3.07	0.21	0.08	0.42	0.023	0.003	18.01	- 73.8	- 9.74
Standard Deviation	33.9	0.05	0.27	0.07	0.025	0.34	0.03	0.01	0.078	0.002	0.001	2.29	3.96	0.16
<u>Inflow from the Rattlesnake Alluvial Fan Wells: S.O.T.D. #3, S.O.T.D. D.</u>														
	<u>E.C</u>	<u>Mg</u>	<u>Ca</u>	<u>Na</u>	<u>K</u>	<u>HCO3</u>	<u>Cl</u>	<u>NO3</u>	<u>S04</u>	<u>F</u>	<u>Li</u>	<u>Si</u>	<u>D</u>	<u>0-18</u>
Average Values	187.0	0.36	0.81	0.39	0.035	0.89	0.093	0.001	0.795	0.00	0.00	18.2	- 66.3	- 8.56
Standard Deviation	3.05	0.01	0.045	0.02	0.005	0.04	0.013	0.000	0.035	0.00	0.00	0.63	0.0	0.00
<u>Inflow from the Stowe-Gulch Basin Wells and Spring: W. Claridge D., Karakula N.H., and Stowe Gulch Spring</u>														
	<u>E.C</u>	<u>Mg</u>	<u>Ca</u>	<u>Na</u>	<u>K</u>	<u>HCO3</u>	<u>Cl</u>	<u>NO3</u>	<u>S04</u>	<u>F</u>	<u>Li</u>	<u>Si</u>	<u>D</u>	<u>0-18</u>
Average Values	523.9	1.23	3.66	0.77	0.027	3.92	0.307	.022	1.33	0.058	0.002	13.8	-69.0	- 9.54
Standard Deviation	47.4	0.16	0.17	0.05	0.006	0.33	0.036	0.013	0.12	0.012	0.001	1.29	1.8	0.29

undersaturated with respect to the corresponding mineral; if ΔG_R is positive, the water is supersaturated; otherwise, it is saturated.

Application of WATEQF to all the cell water samples used in our model has shown that these are well below saturation with respect to most minerals. Near saturated conditions exist with respect to calcite, chalcedony, cristobalite and quartz. The latter fact suggests that Ca^{++} and Mg^{++} should behave essentially as conservative tracers. Spatial variations between the computed ΔG_R values for given reactions are small, implying that there are no major differences between the water types within the region of the cell model. This is illustrated in Figures 58 A and B which show log-activity diagrams for $\text{Ca}^{+2} / (\text{H}^+)^2$ versus H_4SiO_4 , and $\text{Mg}^{+2} / (\text{H}^+)^2$ versus $\text{Ca}^{+2} / (\text{H}^+)^2$, respectively. In both diagrams, the water samples are seen to be clustered within narrow regions. Samples from given cells show a further clustering into still narrower regions suggesting that, despite the similarity between the samples, there is some difference between the waters of the various model cells.

Figures 59 A and B show the same log-activity diagrams for water samples representing recharge inputs into the model. Most sample points fall within narrow clusters, with the exception of samples from the deep aquifer and the Rattlesnake alluvial fan.

In the model, recharge due to direct infiltration of rainfall is disregarded. Due to the semiarid climate of the region and the fact that depth to water table exceeds 40 feet along much of the valley, this recharge component is deemed to be insignificant. To include it formally in our model would require sampling of infiltrating rain water

* Haby Spring * Lower Klondyke * Cobra ● Upper Klondyke

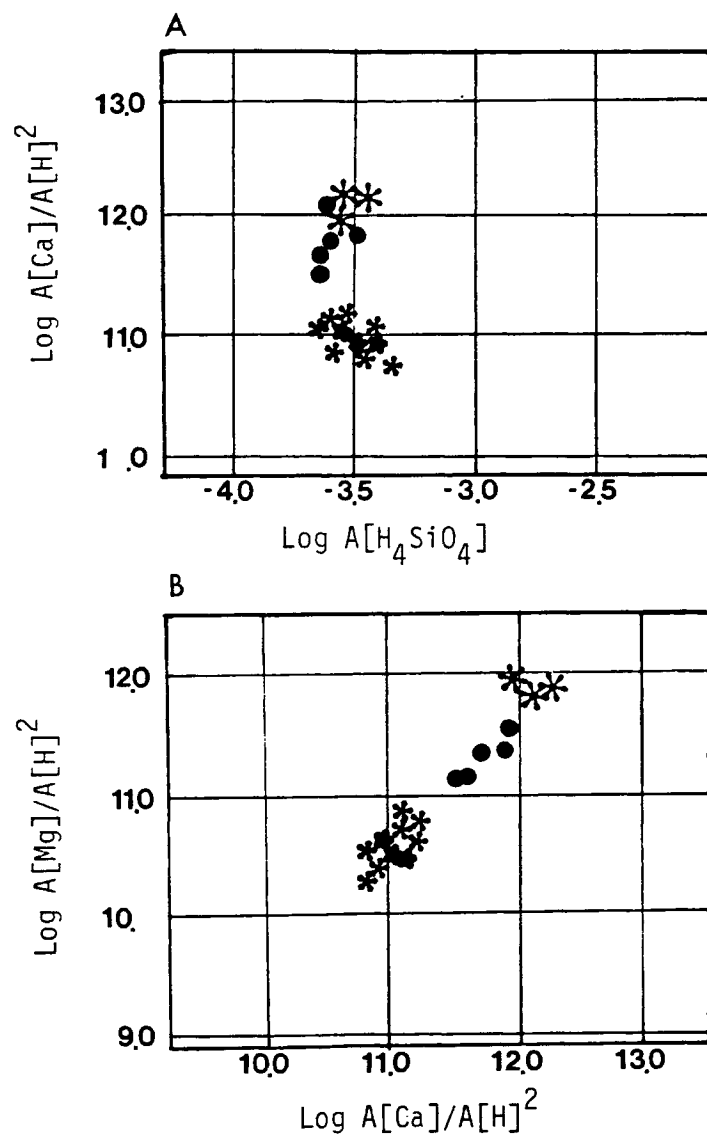


Figure 58. Activity diagrams for waters in the mixing cells

Rattlesnake
 Stowe Gulch
 Sharizona

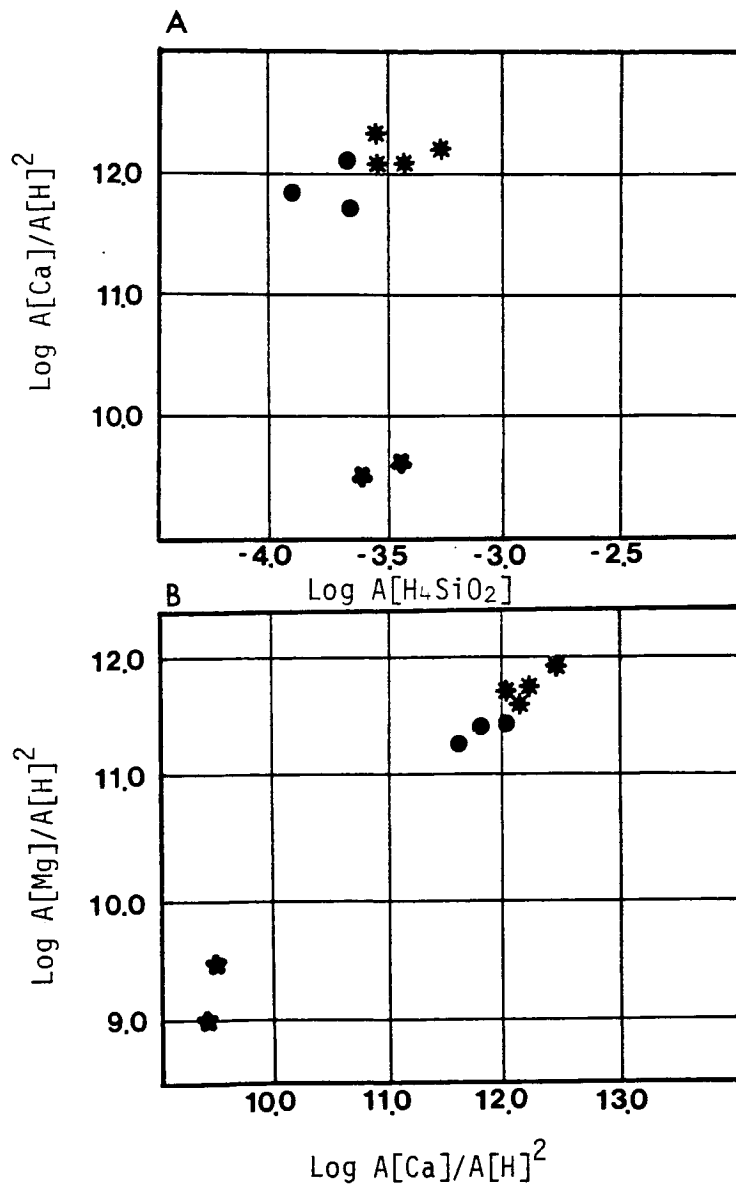


Figure 59. Activity diagrams for waters among selected inflows

from the unsaturated zone below the root zone, within which major chemical changes are expected to occur. This was beyond the scope of our research. We did attempt to run the model by considering such recharge by assigning rainfall concentrations to the corresponding model inputs. The algorithm failed to converge, which we found is generally an indication that the input data are incorrect.

As in Chapter 6, the weight matrix \underline{W} is taken to be diagonal. However, the nonzero terms are assigned in a somewhat different manner:

$$W_{11} = Q_{out}^{-2}; W_{ll} = w_k (C_{ok} \beta_k)^{-2} \quad (1)$$

$$l = k + 1; k = 1, 2, 3, \dots, K$$

Here Q_{out} is the known rate of outflow from the downstream cell at Aravaipa Spring, C_{ok} is the concentration of the k th species at the outlet (i.e., associated with Q_{out}), β_k is the coefficient of variation of errors in determining the laboratory standards as defined in equation (18) in Chapter 6, w_k is a positive coefficient that is equal to unity if the k th species is conservative and less than 1.0 otherwise, and K is the number of species (in our case, $K = 14$). As in Chapter 6, the effect of dividing by Q_{out}^{-2} and C_{ok}^2 is to normalize the balance equations so they are all expressed on a scale relative to the downstream outflow equations. The effect of dividing by β_k^2 is to reduce this weight in proportion to the variance of the laboratory error. The effect of w_k^2 is to decrease the weight of any nonconservative species by an arbitrary amount determined subjectively by the modeler.

The total number of unknown flow rates in the model, including flow rates from one cell to another, is 23. For each of the five cells we write one water balance and 14 chemical balance equations, resulting in a total of 75 mass balance expressions. In assigning values of w_k and β_k , it is important to remember that, if the resulting weight w_{l1} (where $l = k + 1$) in (1) is very small relative to other weights, the mass balance equations for the k^{th} species have little influence on the solution. The effect of making w_{l1} very small is to virtually eliminate five equations (one for each cell) from the model. To maintain a number of equalities in excess of the number of unknowns, not more than ten species should be assigned very low weights; otherwise, the solution will be meaningless.

Table 10 lists the three \underline{w} , and two $\underline{\beta}$, vectors for which results are reported in this chapter. The vector \underline{w}_1 corresponds to the case where all the constituents are treated as if they were conservative. The vector \underline{w}_2 treats Cl, D, and O-18 as conservative species, and EC as a parameter which is almost conservative. As mentioned earlier in this chapter, Ca and Mg were found by WATEQF to be near their saturation levels within each cell and in most inflows. This means that they are not likely to dissolve or precipitate; \underline{w}_2 treats them as being moderately conservative. Na, K, and F were found to be far below saturation. However, they do not appear as major constituents among the local minerals and, therefore, they are probably not generated in significant quantities by mineral dissolution; \underline{w}_2 treats these three constituents as being somewhat less conservative than Ca and Mg. HCO_3

Table 10. Examples of weight vectors used in the model

Type of Weight Vector	E.C.	Mg	Ca	Na	K	HCO ₃	Cl	NO ₃	SO ₄	F	Li	Si	D	0-18
\underline{w}_1	1.0	1.0	1.0	1.0	1.0	1.0	1.0	1.0	1.0	1.0	1.0	1.0	1.0	1.0
\underline{w}_2	0.9	0.7	0.6	0.6	0.45	0.3	1.0	0.2	0.3	0.5	0.3	0.2	1.0	1.0
\underline{w}_3	0.9	0.7	0.6	0.6	0.45	0.3	0.75	0.1	0.3	0.2	0.2	0.2	1.0	1.0
$\underline{\beta}_1$	1.0	1.0	1.0	1.0	1.0	1.0	1.0	1.0	1.0	1.0	1.0	1.0	1.0	1.0
$\underline{\beta}_2$	0.032	0.054	0.103	0.103	0.010	0.031	0.165	0.133	0.062	0.090	.06	0.15	0.064	0.023

is highly sensitive to CO_2 and carbonate content as well as to sampling conditions; NO_3 and SO_4 are highly variable; and little is known about the behavior of Li. These four constituents are therefore weighted low. SiO_2 is in a state of oversaturation and its concentration is known to decrease after sampling due to precipitation on the walls of the container; its weight in \underline{W}_2 is therefore equally low. The numerical values assigned to the components of \underline{W}_2 in Table 10 are based on such considerations as well as on numerical experiments which showed that these weights lead to relatively low mass balance errors in each cell. \underline{W}_3 is a slightly modified version of \underline{W}_2 .

The vector $\underline{\beta}_1$ corresponds to the case where laboratory errors are disregarded. $\underline{\beta}_2$ represents actual coefficients of variation of the laboratory standards.

Sensitivity of Computed Inflow Rates
to Weights, Pumping Rates and Source Distribution

Table 11 lists the computed inflow rates, water balance errors, and salt balance errors for $\underline{\beta}_2$ and the three weight vectors \underline{W}_1 , \underline{W}_2 , \underline{W}_3 . The results are clearly sensitive to variations in the weights. Water balance errors in individual cells are quite small in all three cases as are the total water balance errors. The latter do not exceed 4%. The total salt balance error is smallest when \underline{W}_2 is used (the weight vector we consider to be the most "reasonable"). It is larger when all the constituents are regarded as conservative ($\underline{W} = \underline{W}_1$), and larger still when some of the assigned weights are very low ($\underline{W} = \underline{W}_3$). The total salt balance does not exceed 5%.

Table 11. Computed inflows, water balance, and salt balance for β_2 with W_1 , W_2 , and W_3

Cell Source	W_1		W_2		W_3	
	Rate of Inflow (o/o)	Water Balance (o/o)	Rate of Inflow (o/o)	Water Balance (o/o)	Rate of Inflow (o/o)	Water Balance (o/o)
Sharizona	0.034	-1.74	3.604	-0.56	5.216	+1.25
1 Rattlesnake	0.000		0.213		0.000	
Winter flows	0.007		0.000		0.000	
Lamb Camp	0.000		0.893		1.803	
Upward leakage (Whiting Deep)	0.444		3.908		3.819	
2 Squaw Sp.	0.595	-2.48	7.738	-1.38	8.025	-1.11
Whiting Hill	0.705		4.362		3.641	
Winter floods	0.000		0.0003		0.0003	
Summer floods	0.264		2.131		1.855	
Fourmile	0.000		0.000		0.000	
3667 W.M.	4.099		7.526		6.159	
3 Upward leakage (Klondyke D#2)	29.950	+1.68	5.764	-1.69	1.283	-1.93
Winter floods	0.000		0.000		0.000	
Summer floods	0.474		0.748		0.675	
Upward leakage (Cobra N. Irr.)	23.770		21.230		15.888	
4 Stowe Gulch	48.749	-0.67	48.339	-0.17	57.670	+1.85
Winter floods	0.000		0.000		0.000	
Summer floods	0.000		0.000		0.000	
5 Upward leakage (Karakula Adobe)	0.000	-0.30	2.333	-0.01	4.372	+0.25
Water balance:		-3.506		-3.808		+2.192
Salt balance:		+1.72		+0.31		4.84

Table 12 lists the computed inflow rates, water balance errors, and salt balance errors for \underline{W}_2 and the two vectors $\underline{\beta}_1$ and $\underline{\beta}_2$. The results are essentially identical. Sensitivity to $\underline{\beta}$ was found to be more pronounced in the less realistic case where $\underline{W} = \underline{W}_1$.

The sensitivity of the model to changes in pumping rate, when $\underline{W} = \underline{W}_2$ and $\underline{\beta} = \underline{\beta}_2$, is indicated in Table 13. In general, the effect is small, though an increase in pumpage tends to be compensated for by an increase in inflow rates. Our best estimate of pumping rates is represented by case (1). The results are only slightly different from those of case (5) where pumpage is completely eliminated from consideration.

Until now, we assumed that the recharge components into each cell, and the wells or springs which represent them, had been correctly identified. However, some ambiguity in the distribution of the sources and their representative water samples is unavoidable. To investigate the degree to which the model is sensitive to variations in this distribution, we considered a variety of possibilities, seven of which are summarized in Table 14. Case (A) represents the source distribution with which we have been working thus far, and which we regard as being the most "reasonable." Case (B) is similar except that the Lamb Camp well samples have been replaced by water samples from summer floods, the Squaw Spring samples have been replaced by samples from the Long Hollow well, and those from 3667 W. M. have been replaced by samples from the Laurel Canyon well. Since cell 1 has a very small surface area, the contribution of floods to recharge into this cell should be very small. Indeed, the computed recharge from summer floods is zero. Similarly,

Table 12. Computed inflows, water balance, and salt balance for W_2 with β_1 and β_2

Cell	Source	β_1		β_2	
		Rate of Inflow (o/o)	Water Balance (o/o)	Rate of Inflow (o/o)	Water Balance (o/o)
1	Sharizona	3.608		3.606	
	Rattlesnake	0.210	-0.56	0.213	-0.56
	Winter flows	0.000		0.000	
	Lamb Camp	0.892		0.893	
2	Upward leakage (Whiting Deep)	3.907		3.908	
	Squaw Sp.	7.738		7.738	
	Whiting Hill	4.359	-1.37	4.362	-1.38
	Winter floods	0.0003		0.0003	
	Summer floods	2.130		2.131	
3	Fourmile C.	0.000		0.000	
	3667 W.M.	7.526		7.526	
	Upward leakage (Klondyke D#2)	5.760	-1.68	5.764	-1.69
	Winter floods	0.000		0.000	
	Summer floods	0.747		0.748	
4	Upward leakage (Cobra N. Irr.)	21.23		21.23	
	Stowe Gulch	48.42	-0.18	48.34	-0.17
	Winter floods	0.000		0.000	
	Summer floods	0.000		0.000	
5	Upward leakage (Karakula Ad.)	2.332	0.01	2.333	-0.01
Water balance:			-3.808	Water balance:	-3.808
Salt balance:			0.31	Salt balance:	+0.31

Table 13. Computed inflows, water balance, and salt balance for β_2 and W_2 with variable pumping rates

Cell Source	(1)			(2)			(3)		
	Rate of Pumpage (o/o)	Rate of Inflow (o/o)	Water Balance (o/o)	Rate of Pumpage (o/o)	Rate of Inflow (o/o)	Water Balance (o/o)	Rate of Pumpage (o/o)	Rate of Inflow (o/o)	Water Balance (o/o)
Sharizona		3.606			3.924			3.523	
1 Rattlesnake	0.3	0.213	-0.56	0.5	0.232	-0.61	0.1	0.208	-0.59
Winter flow		0.000			0.000			0.000	
Lamb Camp		0.893			0.971			0.872	
Upward leakage (Whiting Deep)		3.908			4.210			3.864	
Squaw Sp.		7.738			8.324			7.665	
2 Whiting Hill	6.0	4.362	-1.38	8.0	4.715	-1.39	4.0	4.297	-1.37
Winter floods		0.0003			0.003			0.0003	
Summer floods		2.131			2.296			2.106	
Fourmile C.		0.000			0.000			0.000	
3667 W.M.		7.526			7.834			7.782	
Upward leakage	3.1	5.764	-1.69	5.0	6.871	-1.71	4.0	4.869	-1.70
3 (Klondyke D#2)		0.000			0.000			0.000	
Winter floods		0.748			0.789			0.759	
Summer floods		21.23			22.691			21.70	
Upward leakage (Cobra N. Irr.)		48.34			49.368			49.19	
4 Stowe Gulch	3.1	0.000	-0.17	4.0	0.000	-0.17	3.0	0.000	-0.17
Winter floods		0.000			0.000			0.000	
Summer floods		2.333			2.399			2.377	
5 Upward leakage (Karakula Ad.)	0.1		-0.01	1.0		0.00	2.0		-0.05
Total water balance			-3.808			-3.874			-3.88
Total salt balance			+0.31			+0.43			0.24

Table 13--continued

Cell Source	Rate of Pumpage (o/o)	Rate of Inflow (o/o)	Water Balance (o/o)	Rate of Pumpage (o/o)	Rate of Inflow (o/o)	Water Balance (o/o)
Sharizona		3.437			2.928	
1 Rattlesnake	0.0	0.203	-0.58	0.0	0.173	-0.57
Winter flow		0.000			0.000	
Lamb Camp		0.851			0.725	
Upward leakage (Whiting Deep)		3.793			3.207	
Squaw Sp.		7.527			6.401	
2 Whiting Hill	3.0	4.209	-1.37	0.0	3.601	-1.35
Winter floods		0.0002			0.0002	
Summer floods		2.068			1.768	
Fourmille C.		0.000			0.000	
3667 M.M.		7.804			7.039	
Upward leakage	6.0	4.381	-1.70	0.0	3.639	-1.70
(Klondyke D#2)						
Winter floods		0.000			0.000	
Summer floods		0.755			0.565	
Upward leakage (Cobra N. Irr.)		21.84			18.37	
4 Stowe Gulch	2.0	47.92	-0.18	0.0	46.39	-0.18
Winter floods		0.000			0.000	
Summer floods		0.000			0.000	
5 Upward leakage (Karakula Ad.)	0.0	2.336	-0.04	0.0	2.220	-0.04
Total water balance			-3.87			-3.840
Total salt balance			+0.21			-0.17

Table 14. Computed inflow rates into the water table aquifer for different source distributions

Cell	(A) Source	Rate of Inflow (o/o)	(B) Source	Rate of Inflow (o/o)	(C) Source	Rate of Inflow (o/o)	(D) Source	Rate of Inflow (o/o)
1	Sharizona	3.606		3.214		5.670		3.540
	Rattlesnake	0.213		0.065		0.115		0.250
	Winter flows	0.000		0.000		0.000		0.000
	Lamb Camp	0.893	Summer floods	0.000	Summer floods	0.000	No Source	
2	Upward leakage (Whiting Deep)	3.908		2.451		3.870	Lamb Camp	0.710
	Squaw Sp.	7.738	Long Hollow	0.000		7.780		7.910
	Whiting Hill	4.362		7.300		3.980		4.580
	Winter floods	0.0003		10.05		0.000		0.003
	Summer floods	2.131		0.586		1.969		2.100
3	Fourmile C.	0.000		0.640		0.000		0.000
	3667 W. M.	7.526	Laurel Canyon	0.564		7.540		7.520
	Upward leakage (Klondyke D#2)	5.764		4.976		5.520		5.860
	Winter floods	0.000		0.000		0.000		0.000
	Summer floods	0.748		0.286		0.750		0.750
4	Upward leakage (Cobra N. Irr.)	21.23		4.428		21.18		21.26
	Stowe Gulch	48.34		63.56		48.38		48.34
	Winter floods	0.000		0.000		0.000		0.000
	Summer floods	0.000		0.000		0.000		0.000
5	Upward leakage (Karakula Ad.)	2.333		5.593		2.330		2.333
	Water balance	-3.808		-8.878		-3.810		-3.61
	Salt balance	+0.31		-9.14		+0.64		+0.46

Table 14--continued

Cell	(A) Source	(E) Source	Rate of Inflow (o/o)	(F) Source	Rate of Inflow (o/o)	(G) Source	Rate of Inflow (o/o)
1	Sharizona		1.854		1.801		1.146
	Rattlesnake		0.109		0.106		0.068
	Winter flows		0.000		0.000		0.000
	Lamb Camp		0.459		0.446		0.284
2	Upward leakage (Whiting Deep)		0.686		0.666		0.417
	Squaw Sp.		0.000		0.000		0.000
	Whiting Hill		3.090		2.999		1.867
	Winter floods	Upward leakage (Klondyke D#2)	15.153	Upward leakage (Klondyke D#2)	14.701	Upward leakage (Klondyke D#2)	9.063
3	Summer floods		0.728		0.707		0.441
	Fourmile C.		0.684		0.666		0.447
	3667 W. M.		4.652		4.483		2.363
	Upward leakage (Klondyke D#2)	Upward leakage (Whiting Deep)	0.000	Upward leakage (Whiting Deep)	0.000	Upward leakage (Whiting Deep)	0.000
4	Winter floods	Upward leakage (Klondyke D#2)	3.089	Upward leakage (Klondyke D#2)	2.982	Upward leakage (Klondyke D#2)	1.639
	Summer floods		0.354		0.344		0.227
	Upward leakage (Cobra N. Irr.)		12.156		22.198		6.486
	Stowe Gulch		33.459		31.594		15.838
5	Winter floods		0.000	Haby Corral	21.844	No Source	
	Summer floods		0.000		0.000	No Source	
	Upward leakage (Karakula Ad.)	Upward leakage (Cobra N. Irr.)	35.86		1.517	Haby Corral	29.361
						Upward leakage (Cobra N. Irr.)	35.030
	Water balance		+2.03		-3.24		-3.170
	Salt balance		-0.18		+5.76		+3.75

Long Hollow is a deep well located far from the stream and its waters are not expected to be recharging cell 2; again, the model confirms this by computing a zero recharge value for this "source." Laurel Canyon is a shallow well representing waters in a local alluvial fan which contributes a small amount of recharge to cell 3; on the other hand, 3667 W. M. is representative of the vaster recharge source in the eastern pediments. This also is reflected in the results in Table 14. The relatively large water and salt balance errors in case (B) suggest that the source distribution in this case is less reliable than in case (A).

In case (D), the recharge source represented by Lamb Camp has been assigned to cell 2, instead of cell 1 as in the standard case (A). This has had only a minor effect on the magnitude of this source.

In the standard case (A), upward leakage into cell 2 is represented by the deep Whiting Deep well, and upward leakage into cell 5 by the deep Karakula Adobe well. The waters of these two wells have similar compositions. Upward leakage into cell 3 is represented by the shallower Klondyke D#2 well, and into cell 4 by the relatively shallow Cobra N. Irrigation well. The waters of these two shallow wells have identical compositions, but are very different from the waters from the above two deep wells. It is highly likely that to properly represent upward leakage into cells 2 and 5, we should have used samples from shallower depths than Whiting Deep and Karakula Adobe, respectively. Unfortunately, such shallow wells are not available within the lower aquifer in cells 2 and 5. Therefore, in case (E), we added the possibility of Klondyke D#2 type waters leaking upward into cell 2, and Cobra

N. Irrigation type waters leaking upward into cell 5. In cell 3, we added the possibility of Whiting Deep type waters also contributing to such leakage. This latter contribution was found to be zero. On the other hand, the rates of upward leakage into cells 2 and 5 have increased significantly, suggesting that it is the waters in the upper portion of the deep aquifer which contribute recharge to the unconfined aquifer; direct contribution from the deeper portions of the lower aquifer is not evidenced by the available data.

To investigate this point further, the shallow part of the confined aquifer in the valley was represented by a single cell receiving recharge from the deeper portion below, deep flow from the upper reaches of the valley, deep flows from the eastern and western pediments, and floods (both summer and winter). The only outflow from this cell was due to upward leakage to the unconfined aquifer. 41% of the contribution was found to come from below, 32% from the upper reaches, 27% from the eastern pediments, and zero from the western pediments and floods. The lack of contribution from the western pediments may be due to an impermeable fault zone which separates them from the lower aquifer at depth.

Cases (F) and (G) consider the possibility of an additional source into cell 4 from the west, represented by the Haby Corral well. Previous investigations by Ellingson (1979) suggest that the area in which this well is located lies west of a fault zone which isolates it from the valley. Indeed, the waters of this well are very different in composition from those inside cell 4. Table 14 shows that when the area

represented by Haby Corral is considered to be a recharge source, its contribution is significant and comes largely at the expense of recharge from Stowe Gulch. However, the relatively large salt balance errors associated with cases (F) and (G) cast some doubt about the reliability of this finding. Overall, Table 14 indicates the sensitivity of the computed flow rates to the ambiguity in the distribution of the sources and their representative water samples.

To assess the validity of the computed inflow rates into the lower Aravaipa Valley, we used the transmissivity value obtained for Whiting #1 (Figure 57) in Darcy's equation:

$$Q = -bT\nabla h \quad (2)$$

where Q is the flow rate in acre-feet per day, b is the width of the aquifer normal to the flow direction, T is the transmissivity in ft^2/day and ∇h is the hydraulic head gradient.

The transmissivity in Whiting #1 was estimated to be 81,000 ft^2/day (Appendix B). The width of the water table aquifer across Whiting Ranch is approximately 850 ft., and the water table gradient was estimated from the longitudinal water table profile to be 6.8⁰/₁₀₀ (Figure 13B). The use of the latter values in equation (1) yields a Q of 10.13 acre-feet/day or 3,699.00 acre-feet/year.

Summation of computed inflow rates up to Whiting Ranch (in the upper Klondyke section) indicates that the annual recharge is around 25% of the total annual recharge. Assuming a steady state (Chapter 4), the average annual recharge is equal to the average annual discharge at the Aravaipa Spring. The average annual outflow plus irrigation was

estimated to be 13,000 acre-foot/year. This brings the average annual recharge above Klondyke to 3,250 acre-feet/year, which is close to what was obtained from Darcy's law.

Stowe Gulch basin was found to contribute about 48% or 4,800 acre-foot/year of the total discharge at Aravaipa Spring. The amount of pumpage within the basin is limited to one domestic well and three wind-mills for livestock support. There is no irrigation in Stowe Gulch basin and extraction by pumping can be neglected. Assuming steady hydraulic conditions and that Aravaipa Spring is the only outlet of the Stowe Gulch aquifer, 4,800 acre-feet/year should be equal to the average annual recharge over approximately 43 square miles. In other words, the average annual recharge over Stowe Gulch is 2.09 inches/year or between 7% and 9% of the annual rainfall as measured in the Horse Mountain rain gauge. This makes us believe that the computed inflow rates into the lower Aravaipa Valley are reasonable.

CHAPTER 8

CONCLUSIONS

This study leads to a number of important general conclusions about the use of hydrochemical and isotopic data in hydrogeology, and to a series of specific findings concerning the subsurface flow regime in the Aravaipa Valley of southern Arizona:

(1) Regional hydrochemistry and environmental isotope data have traditionally been used by hydrogeologists as an important qualitative tool to help in the postulation, support, or rejection of hypotheses about flow regimes in subsurface environments. However, only on rare occasions have such data been used in a quantitative manner to compute the magnitudes of physical quantities characterizing these flow regimes. By excluding hydrochemical and stable isotope data from the domain of quantitative hydrogeology, much valuable information may be lost. This is especially true in situations, such as that existing in the Aravaipa basin of southern Arizona, where information about hydraulic gradients and aquifer parameters is relatively limited. For such situations, it is useful to have a mathematical model which can extract information about basin hydrology from the spatial distribution of chemicals and stable isotopes dissolved in surface and subsurface waters.

(2) In this work, a mathematical model has been postulated for the computations of recharge into, discharge from, and flow through an aquifer system. The model has been developed specifically for basins in

which information about environmental hydrochemistry and the spatial distribution of stable isotopes is more easily accessible than information about groundwater levels and aquifer parameters (such as transmissivity). Its development has been prompted by actual conditions encountered in the semiarid Aravaipa basin. Here, water level data are limited largely to the immediate vicinity of Aravaipa Creek along the axis of the valley, and transmissivity is available from only one pumping test. These data are insufficient to compute flows into, through, and out of the local aquifers, especially in directions transverse to the valley axis. In other words, the hydraulic data do not allow one to compute vertical recharge from above, vertical leakage from one aquifer to another, lateral recharge from tributaries and alluvial fans, recharge of the alluvial valley sediments from the surrounding mountain-forming bedrock, and subsurface flow rates along the valley. The proposed model computes these quantities on the basis of the (known) total outflow from the basin at Aravaipa Spring, and hydrochemical as well as isotopic data obtained from samples of rain water, floods, springs, and waters pumped from wells. Had the total rate of discharge from the basin been unknown, the model could still compute the magnitudes of the above quantities relative to each other.

(3) The proposed model assumes that the basin can be subdivided into a number of mixing cells arranged in a one, two, or three-dimensional pattern. All waters entering the cell mix instantaneously with the water in the cell, so that the concentrations of the constituents within each cell are uniform (this modeling approach has been originally

promulgated by Simpson et al., 1975; see also Campana, 1975, and Rasmussen, 1982. The concentration of dissolved constituents within a cell is computed by averaging the concentrations in water samples obtained from wells which have been completed in the same cell. The concentrations of constituents dissolved in recharge waters are computed on the basis of water samples that characterize each recharge source. The model works with average annual flow rates and treats the system as being at steady state on an average annual basis. The assumption of steady state, while justified under the conditions in Aravaipa Valley, may have to be relaxed for other basins.

A system of water and chemical balance equations is written for each cell. The resulting system of coupled equations is solved for the unknown annual flow rates by quadratic programming (this approach is patterned after the work of Woolhiser et al., 1982, who used it in connection with a single cell representing a river reach). The algorithm minimizes the sum of squared errors in the mass balance expressions, normalized with respect to the total (known) outflow from the basin and associated concentrations. These errors are further weighted so as to account for uncertainties in the results of chemical laboratory analyses, and to minimize the adverse effect of nonconservative constituents on the mass balance calculations (as chemical reactions are ignored in the current version of the model).

(4) The spatial distribution of recharge sources is determined qualitatively on the basis of all the available geologic, geophysical, hydrologic, and hydrochemical information. Here, stable isotopes play a very important role. In the unconfined aquifer that underlies Aravaipa

Creek, the spatial distribution of stable isotopes is easily demonstrated to be caused by the mixing of waters from relatively well-defined sources, including floods and contributions from alluvial fans. The identification of recharge sources to the underlying confined aquifer is greatly facilitated by demonstrating that stable isotope concentrations in this aquifer are the result of the mixing of its waters with those originating in precipitation on the mountain slopes and with the waters of certain tributaries. Hydrochemical data are also useful in this context, especially where there are distinct spatial variations in the mineral composition of the rocks surrounding the valley. The hydrologist's ability to differentiate between sources in this manner hinges on their waters having distinct isotopic or chemical signatures.

(5) The sensitivity of the proposed model to errors in the data was investigated by means of a Monte Carlo approach. A set of "exact" data was generated synthetically by the mixing cell model and then corrupted by Gaussian noise. The noisy data were then fed into the quadratic programming algorithm to yield corresponding estimates of the "unknown" flow rates. A comparison of these computed flow rates with their known true values showed that the model works reasonably well (leads to estimates characterized by a small bias and a near-Gaussian estimation error having a small variance) as long as the sources are properly identified, ionic balance is maintained between the dissolved constituents (a condition laboratory analyses will generally satisfy), the relation between O-10 and D is such that $D/O-18$ varies between 6.5 to 8.5 analytical errors are small, and the chemicals are conservative. Clearly, for

the solution to be meaningful, the number of constituents must be sufficiently large so that the number of mass balance expressions one can write for each cell exceeds the number of unknown flow rates by a substantial margin.

(6) The model was applied to a portion of the unconfined aquifer underlying Aravaipa Creek. The modeled portion of the aquifer was divided into five cells, for each of which we were able to write 15 water and chemical balance expressions. The weights assigned to these expressions were based on known errors in the analyses of laboratory standards and on our subjective assessment of the degree to which each constituent might satisfy the assumption that it is conservative. Some degree of objectivity was injected into this assessment process by using the computer program WATEQF (Plummer et al., 1976) to investigate the extent to which the dissolved chemicals might be in equilibrium with selected minerals. This led to a set of weights which we considered to be "reasonable." By varying the weights about their "most reasonable" values, we found that the computed flow rates are quite sensitive to these values. Particularly large variations in the computed flow rates occur when too many of the weights are made small compared to the remaining weights. In this case, the number of water and chemical balance equations influencing the solution is reduced, as equations assigned small weights have only a marginal effect on the computed flow rates. While this may lead to small errors in the water and chemical balance in each cell, the results may nevertheless be meaningless.

By varying the cells into which given sources contribute their recharge waters, we found that the quality of the computed flow rates will depend quite heavily on the hydrologist's ability to properly identify the spatial distribution of these sources.

(7) Using what we consider to be a "reasonable" range of weights, the algorithm has yielded the following recharge rates into the modeled portion of the unconfined aquifer in Aravaipa Valley (numbers in brackets show the maximum range obtained with all the weights used):

- (a) inflow from upper Aravaipa Valley--from 3.5% to 5.5%
[2% - 6%];
- (b) direct inflows through alluvial fans--around 0.3%
[0.01% - 0.95%];
- (c) direct lateral inflow from western pediments--from 4.4% to 6.0% [3.5% - 8.0%];
- (d) direct lateral inflow from eastern pediments--from 13.3% to 14.0% [12% - 15%];
- (e) upward leakage from lower confined aquifer in upper and lower Klondyke sections--from 8.5% to 10.5%
[7.8% - 14.5%];
- (f) upward leakage in Cobra section--from 22% to 25%
[19.8% - 26.5%];
- (g) lateral inflow from Stowe Gulch basin--from 46% to 49% [45% - 63%];
- (h) total annual streambed infiltration--from 2.0% to 2.8% [0.0% - 3.5%].

The maximum error in water balance for each cell was below 1.75%, and the maximum error in salt balance below 1%. The maximum error in water balance over the entire modeled area was less than 3.6%.

The computed recharge from streambed infiltration is surprisingly low. The model has consistently assigned this entire recharge rate to summer floods, whereas the computed contribution of winter floods is always zero. We suspect that, since these floods have almost identical chemical signatures and differ only by their stable isotope ratios (see Table 2 in Appendix C), the model has been unable to distinguish between them in a satisfactory manner.

Additional comments which can be made about the model results for Aravaipa Valley include the following:

- (a) Most of the lateral recharge into the water table aquifer derives from the eastern pediments. Recharge from the western pediments is diverted mainly into the underlying confined aquifer.
- (b) The Aravaipa Valley upstream of the modeled area, which accounts for almost 55% of the entire valley, provides less than 6% of the total inflow into the modeled aquifer. This is most probably due to heavy pumping for irrigation in the Eureka section.
- (c) Direct recharge from streambed infiltration is limited to 4% of the total recharge per year. This is reasonable in light of the short length of the

stream. While streambed infiltration is the major contributor of water to storage in alluvial fans, these fans were also found to contribute only minute amounts of recharge to the water table aquifer. On the other hand, streambed infiltration along the major western tributaries was found to be an important source of recharge to the lower aquifer (see Chapter 7).

- (d) In the absence of significant pumping from the confined aquifer, the only major avenue of discharge from the deep aquifer is provided by upward leakage to the overlying water table aquifer. This leakage is found to be quite significant. Its existence is supported by hydraulic and radioisotopic data.
- (e) Stowe Gulch seems to support almost 48% of the annual discharge through Aravaipa Spring. This means an average recharge of 4,500 acre-foot/year, or 2.09 inches of deep percolation per year over approximately 43 square miles of the Stowe Gulch basin. Pumping from Stowe Gulch is limited to domestic use (one family) and cattle support. The Stowe Gulch component of recharge is critically important during dry seasons when the water table aquifer in the lower Valley is heavily used for irrigation by the Whiting and Cobra ranches.

(8) We see that the model provides much useful information about the hydrologic regime of Aravaipa Valley which could not be obtained from the available data by other existing methods of analysis. The reader must be aware, however, that the results are tentative because independent means to verify them are currently lacking. We are encouraged by the fact that the computed flow rate along the axis of the valley could be verified independently by means of Darcy's law on the basis of measured hydraulic gradients and the single transmissivity value available for the unconfined aquifer (see the end of Chapter 7). Nevertheless, the demonstrated sensitivity of the model to errors in the data, to the magnitudes of the weights, and to the distribution of sources, means that the model results must be interpreted with caution. While the model appears to be a useful tool, it must be recognized as being merely a first step toward the development of more sophisticated models which describe the relationships between hydrochemical, isotopic, and hydrologic data in a more complex and accurate manner. Our work along these lines continues.

APPENDIX A

ARAVAIPA WELL LOGS

Driller logs have been used to elaborate on lithology, aquifer units, and water bearing layers. Fourteen well logs were obtained from the United States Department of the Interior, Geological Survey, (U.S.G.S.) Water Resources Division. An additional 14 were obtained from State of Arizona, Water Resources Department, Water Rights Division. All well logs, except for two, are based on drillers' reports, and one should be aware of potential inaccuracies in the identification of geological units and in the use of lithological terminology. Three wells (Holt #1, Eureka #11, and Eureka #6) have comprehensive and accurate logs. The well log from Whiting Deep well has been confirmed by a photographic survey by means of a submersible camera (Arad and Adar, 1981).

The location of wells is given in two ways, using standard U.S.G.S. location as well as a system of local working coordinates (L.C.S.). The U.S.G.S. method of well location is best explained in the following paragraph from Davis (1967).

The well numbers used by the U.S. Geological Survey in Arizona accord with the Bureau of Land Management system of land subdivision. The land survey in Arizona is based on the Gila and Salt River meridian and base line, which divides the state into four quadrants. These quadrants are designated counterclockwise by the capital letters A, B, C, and D. All land north and east of the point of origin is in A quadrant, and that south and east in D quadrant. The first digit of a well number indicates the township, the second the range, and

the third the section in which the well is situated. The lowercase letters a, b, c, and d after the section number indicate the well location within the section. The first letter denotes a particular 160-acre tract, the second the 40-acre tract, and the third the 10-acre tract. These letters also are assigned in a counterclockwise direction, beginning in the northeast quarter. If the location is known within a 10-acre tract, three lowercase letters are shown in the well number. In the example shown (Figure A-1), well number (D-4-5) 19caa designates the well as being in the NE 1/4 NE 1/4 SW 1/4 sec. 19, TRS, R5E. Where there is more than one well within a 10-acre tract, consecutive numbers beginning with 1 are added as suffixes.

Our own local coordinate system (L.C.S. is shown in Figure A-2.

Details of the well logs follow.

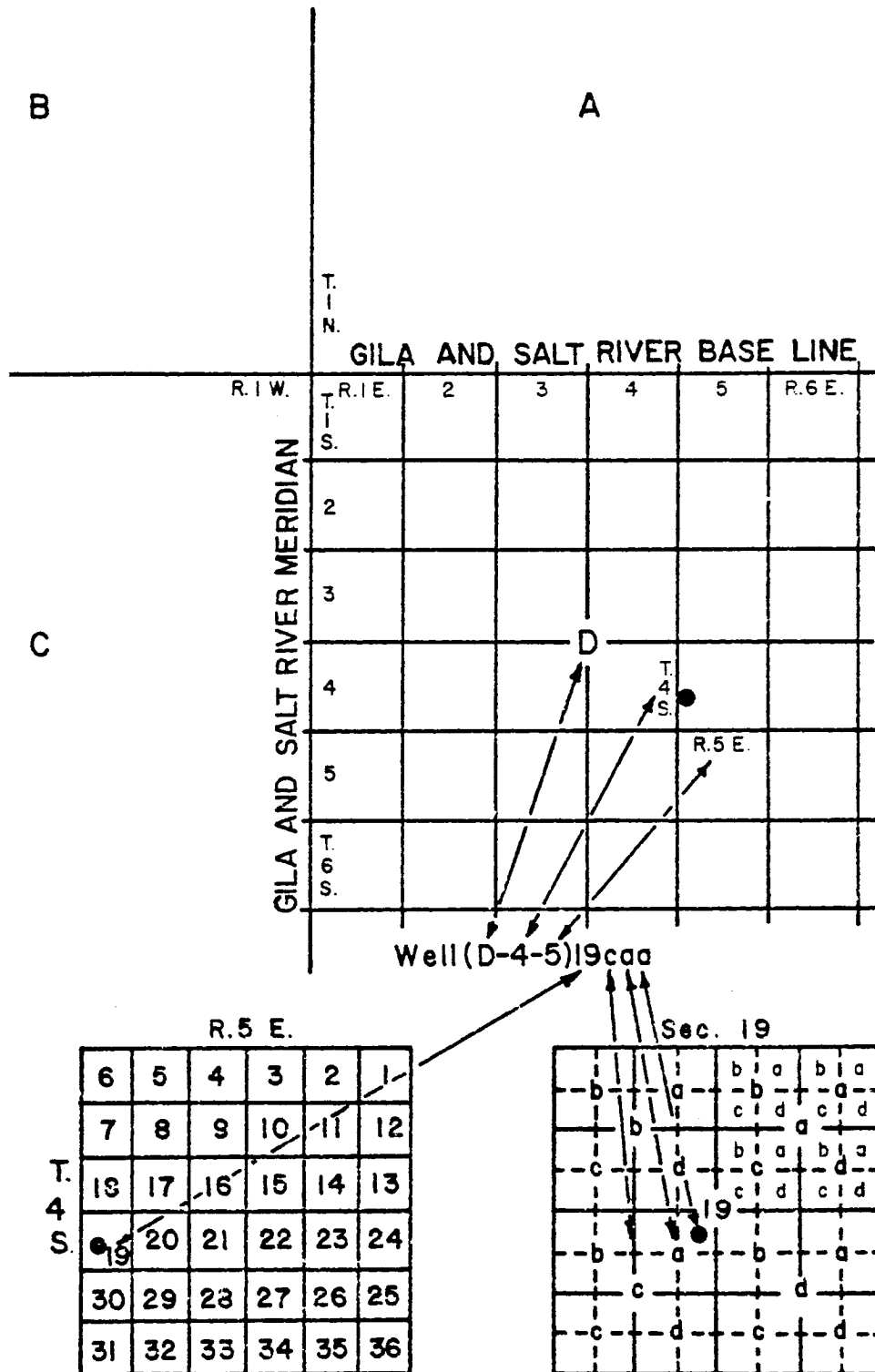


Figure A-1. USGS method of well location

WELL: Turnbull Irrigation
 LOCATION: U.S.G.S. (D-6-19)35bbb
 L.C.S. 18.93 / 7.19
 ALTITUDE: 3,300
 DEPTH TO WATER: 8.5 Year 7.19.1983

Log Interval	
(Feet)	Description
0-5	Top soil
5-24	Sand
24-27	Sand, rocks
27-29	Rocks, boulders
29-31	Gravel
31-33	Boulders
33-49	Gravel, rocks

WELL: Cobra Ranch Domestic (Old)
 LOCATION: U.S.G.S. (D-6-19)35ada
 L.C.S. 18.76 / 7.97
 ALTITUDE: 3,360
 DEPTH TO WATER: 24 Year 07.22.1983

Log Interval	
(Feet)	Description
0-5	Sand
15-35	Red clay
35	Conglomerate

COMMENT: The red clay starts at 32 feet and water appears above the clay in humid seasons.

WELL: Cobra Ranch Domestic (New)
 LOCATION: U.S.G.S. (D-6-19)36bcc
 L.C.S. 18.67 / 8.05
 ALTITUDE: 3351
 DEPTH TO WATER: 16 Year 7.19.1983

Log Interval	
(Feet)	Description
0-19	Sandy clay
19-47	Sand, gravel (water)

WELL: Cobra Ranch Irrigation (New)

LOCATION: U.S.G.S. (D-6-1936cab

L.C.S. 18.4 / 8.29

ALTITUDE: 3,375

DEPTH TO WATER: 11 Year 2.01.1982

7 7.19.1983

Log Interval	
(Feet)	Description
0-2	Top soil
2-19	Sand, gravel, boulders
19-21	Clean sand, gravel (water)
21-27	Clay, sand, gravel
27-31	Sand, gravel (water)
31-52	Conglomerate (warm water)
52-116	Conglomerate (water)

WELL: Karakula New House (Domestic)

LOCATION: U.S.G.S. (D-6-19)25cca

L.C.S. 19.31 / 8.26

ALTITUDE: ~ 3,445

DEPTH TO WATER: 45 Year 1979

41 1983

Log Interval	
(Feet)	Description
0-4	Top soil (fill)
4-6	Gravel
6-45	Sandy clay
45-86	Sand, gravel (water)
86-88	Clay, sand, gravel
88-92	Red clay

WELL: Hilliard (Delta Bryce)
 LOCATION: U.S.G.S. (D-6-19)34abb
 L.C.S. 18.90 / 6.07
 ALTITUDE: ~ 3,280/90
 DEPTH TO WATER: - * Year -

Log Interval	
(Feet)	Description
0-18	Sand, river rocks
18-28	Sand, gravel (water)
28-30	River rock

*No Access

WELL: W. Claridge/Imperial Mtn.
 LOCATION: U.S.G.S. (D-6-20)5cbb
 L.C.S. 23.4 / 10.2
 ALTITUDE: ~ 4,760
 DEPTH TO WATER: 10 Year 1966

Log Interval	
(Feet)	Description
1-8	Sand, gravel
8-12	Rock, clay (hard formation)
12-22	Rock (water bearing formation)
22-25	Hard clay and rock

WELL: Dowdle (ASLD - W. Mill)
 LOCATION: U.S.G.S. (D-6-20)18dcc
 L.C.S. 21.42 / 9.52
 ALTITUDE: 3,865
 DEPTH TO WATER: 35 Year 10.12.1967
 95 7.19.1983

Log Interval	
(Feet)	Description
0-35	Fill
35-89	Rock, clay
89-97	Sand (water)
97-100	Rocks, clay

COMMENT: The well has been destroyed.

WELL: Sanford
 LOCATION: U.S.G.S. (D-7-19)Iddd
 L.C.S. 17.50 / 8.98
 ALTITUDE: 3,380
 DEPTH TO WATER: 60 Year 1960

Log Interval	
(Feet)	Description
0-30	Fill
30-100	Gravel, sand
100-110	Red clay
110-150	Gravel (water)

WELL: Long Hollow
 LOCATION: U.S.G.S. (D-7-19)25ddd
 L.C.S. 13.07 / 8.94
 ALTITUDE: 4,260
 DEPTH TO WATER: 470 Year 1974

Log Interval	
(Feet)	Description
0-165	Sandstone, conglomerate
165-168	Sandstone (water)
168-490	Conglomerate
490-495	Sandstone (water)
495-525	Conglomerate
525-527	Sandstone (water)
527-540	Sandstone, conglomerate
540-546	Sandstone (water)
546-560	Conglomerate

WELL: Whiting Irrigation #1
 LOCATION: U.S.G.S. (D-7-20)21bda
 L.C.S. 14.67 / 11.36
 ALTITUDE: 3,536
 DEPTH TO WATER: 39 Year 7.22.1983

Log Interval	
(Feet)	Description
0-51	Fill
51-54	Gravel (water)
54-77	Clay rock
77-87	Sand (water)
87-95	Clay rock
95-96	Sand (water)
96-115	Conglomerate
115-116	Sand (water)
116-152	Conglomerate

WELL: Whiting Irrigation #2
 LOCATION: U.S.G.S. (D-7-20)21bbc
 L.C.S. 14.86 / 11.14
 ALTITUDE: 3,528
 DEPTH TO WATER: 43 Year 7.22.1983

Log Interval	
(Feet)	Description
0-64	Fill
64-69	Gravel (dry)
69-84	Rocks, dirt
84-96	Gravel (water)
96-122	Rocks, dirt
122-136	Gravel (water)
136-150	Clay

WELL: Song of the Desert Irrigation #1 (S.O.T.D. #1)
 LOCATION: U.S.G.S. (D-7-20)27ada
 L.C.S. 13.62 / 12.93
 ALTITUDE: 3,620
 DEPTH TO WATER: 13.5 Year 7.21.1983

Log Interval	
(Feet)	Description
0-12	Soil fill
12-18	Gravel
18-38	Gravel, red clay (water)
38-61	Rock, red clay (water)
61-65	Gravel (water)
65-68	Red clay
68-72	Gravel (water)
78-83	Rock (water)
83-90	Red clay

WELL: Whiting Ranch Deep Well
 LOCATION: U.S.G.S. (D-7-20)21bdb
 L.C.S. 14.76 / 11.26
 ALTITUDE: 3,535
 DEPTH TO WATER: 23 Year 7.22.1983

Log Interval	
(Feet)	Description
0-78	Fill
78-99	Gravel (water)
99-124	Conglomerate
124-127	Gravel (water)
127-253	Conglomerate
253-256	Gravel (water)
256-277	Conglomerate
277-281	Gravel (water)
281-324	Conglomerate
324-328	Gravel (water)
328-478	Conglomerate
478-481	Gravel (water)
481-541	Conglomerate
541-545	Gravel (water)
545-594	Conglomerate
594-596	Gravel (water)
596-698	Conglomerate
698-700	Gravel (water)
700-711	Conglomerate
711-716	Gravel (water)
716-734	Conglomerate
734-736	Gravel (water)
736-762	Conglomerate

COMMENT: The submersible camera photo shows a very hard rock starting at \approx 720 feet, suggesting transformation of lithology into the Hell Hole Conglomerate (Arad and Adar, 1981).

WELL: Holt #1
 LOCATION: U.S.G.S. (D-7-20)4dd
 L.C.S. 17.25 / 17.80
 ALTITUDE: 3,620
 DEPTH TO WATER: 13.5 Year 7.21.1983

Log Interval	
(Feet)	Description
0-20	Sand, gravel, clay streaks, red clay
20-65	Sand, cobbles
65-160	Clay (pink and brown)
160-196	Sand, clay
196-450	Red and brown clay with streaks of sand
450-455	Dry sandstone
455-497	Clay (blue and brown)
497-540	Blue, fine sand
540-580	Sand
580-620	Clay
620-715	Shale, clay, little sand and sandstone

COMMENT: This description is a generalization out of a very detailed log prepared by the U.S.G.S. The well has not been found.

WELL: Song of the Desert Irrigation #3 (S.O.T.D. #3)
 LOCATION: U.S.G.S. (D-7-20)27dbd
 L.C.S. 13.24 / 12.64
 ALTITUDE: 3,623
 DEPTH TO WATER: 12.2 Year 7.21.1983

Log Interval	
(Feet)	Description
0-1	Topsoil
1-15	Red clay, rock, sand
15-18	Gravel (water)
18-28	Red clay, rock, sand
28-40	Gravel
40-63	Red clay, rock, sand
63-73	Gravel
73-115	Red clay, rock
115-127	Gravel
127-180	Red clay, rock

WELL: - ? (H. Claridge)
 LOCATION: U.S.G.S. (D-7-20)8bbb
 L.C.S. 16.9 / 10.15
 ALTITUDE: ~ 3,520
 DEPTH TO WATER: 35 Year 1965

Log Interval	
(Feet)	Description
1-40	Fill, clay
40-70	Gravel (water)
70-92	Conglomerate

COMMENT: The well has not been found!

WELL: Mattice / Claridge
 LOCATION: U.S.G.S. (D-7-20)28bda
 L.C.S. 13.75 / 11.45
 ALTITUDE: ~ 3,620
 DEPTH TO WATER: 20 Year 8.30.1947

Log Interval	
(Feet)	Description
0-26	Rock, dirt
26-98	Sand, gravel (water)
98-102	Clay

COMMENT: The well has not been found!

WELL: H. Claridge (beside S.O.T.D. #3)

LOCATION: U.S.G.S. (D-7-20)27dcb

L.C.S. 13.19 / 12.62

ALTITUDE: 3,605

DEPTH TO WATER: 18 Year Nov. 1979

12 July 1983

Log Interval

(Feet)	Description
0-18	Sand, gravel, boulders (water)
18-58	Hilla conglomerate, boulders
58-76	Sand, gravel (water)
76-78	Hard red clay

WELL: Boyed Wilson #1

LOCATION: U.S.G.S. (D-8-21)dcd

L.C.S. 10.40 / 15.60

ALTITUDE: 3,845

DEPTH TO WATER: 27 Year 7.21.1983

Log Interval

(Feet)	Description
0-16	Topsoil
16-39	Sand, red clay, rock
39-53	Gravel (water)
53-58	Blue sand (water)
58-65	Sand, rock, red clay
65-76	Gravel (water)
76-86	Sand, rock
86-105	Gravel (water)
105-115	Red sand, clay
115-125	Gravel (water)
125-132	Red clay

WELL: Sheep Corral
 LOCATION: U.S.G.S. (D-8-21)22aca
 L.C.S. 8.69 / 18.76
 ALTITUDE: 4,125
 DEPTH TO WATER: 125 Year 7.22.1983

Log Interval		
(Feet)		Description
0-10		Fill
10-200		Conglomerate, sand, boulders

COMMENT: Water Between 100 Feet Through 200 Feet.

WELL: Eureka #4 (new irrigation well)
 LOCATION: U.S.G.S. (D-9-21)10dda
 L.C.S. 4.3 / 18.75
 ALTITUDE: 4,145
 DEPTH TO WATER: 60 Year 11.5.1982

Log Interval		
(Feet)		Description
0-5		Black sandy loam (topsoil)
5-15		Red sandy clay
15-60		Solid red clay
60-225		Red sandy clay
225-300		Fine sand, gravel (water)

WELL: 2 E Spring
 LOCATION: U.S.G.S. (D-8-22)29acb
 L.C.S. 7.71 / 22.83
 ALTITUDE:
 DEPTH TO WATER: 69 Year 1952

Log Interval		
(Feet)		Description
0-20		Fill
20-172		Loose conglomerate
172-300		Hard conglomerate

WELL: Cedar Springs (Eureka)
 LOCATION: U.S.G.S. (D-7-21)36da
 L.C.S. 12.13 / 20.75
 ALTITUDE: ~ 4,700
 DEPTH TO WATER: 31 Year 1951

Log Interval	
(Feet)	Description
0-81	Granite

WELL: Eureka Ranch (1,500 feet) #6
 LOCATION: U.S.G.S. (D-9-21)14caa
 L.C.S. 3.30 / 19.15
 ALTITUDE: 4,155
 DEPTH TO WATER: 27 Year 7.18.1983

Log Interval	
(Feet)	Description
0-27	Sand, gravel
27-244	Clay, gravel, sand
244-380	Red clay
380-852	Clay, gravel
852-1000	Cemented sand and gravel
1000-1085	Red clay
1085-1135	Lava, conglomerate
1135-1155	Clay
1155-1175	Lava, conglomerate
1175-1501	Clay (sticky and hard)

COMMENT: Pressurized water from the lava and conglomerate layers. Very low discharge.

WELL: Eureka - Bird Cage
 LOCATION: U.S.G.S. (D-9-22)19dcc
 L.C.S. 2.07 / 18.57
 ALTITUDE: 4,280
 DEPTH TO WATER: 105 Year 7.23.1983

Log Interval	
(Feet)	Description
0-2	Clay, fill
2-10	Clay, sand
10-12	Boulders
12-35	Hard sand
35-40	Dry sand
40-50	Hard sand
50-124	Clay
124-129	White clay (sand) (water)
129-184	Clay
184-189	Gravel (water)
189-218	Clay
218-224	Red sand (clay)
224-228	Clay with gravel streaks

WELL: Eureka #11 (6" windmill)
 LOCATION: U.S.G.S. (D-9-21)27daa
 L.C.S. 1.48 / 15.86
 ALTITUDE: 4,430
 DEPTH TO WATER: 259 Year 7.23.1983

Log Interval	
(Feet)	Description
0-80	Fill, broken rock, silt, clay
80-600	Hard blue malpais (water-235)
600-605	Soft red clay
605-1205	Volcanic rock, dacite, tuff

WELL: Eureka #11 (16" Irrigation Well)

LOCATION: U.S.G.S. (D-9-21)27daa

L.C.S. 1.47 / 15.86

ALTITUDE: 4,430

DEPTH TO WATER: 259 Year 7.23.1983

Log Interval	
(Feet)	Description
0-20	Silt
20-110	Clay
110-140	Clay, boulders
140-235	Hard broken rocks (water-235)
235-660	Broken rock
660-710	Brown malipi (very hard)
710-765	Orange malipi, streaks of clay
765-820	Hard malipi, small streaks
820-895	Hard black lava, tuff
895-1000	Hard lava
1000-1050	Hard shells, streaks of brown sand
1050-1110	Hard black lava, streaks of brown mud
1110-1160	Hard black lava

COMMENT: Water Between Lava Layers.

APPENDIX B

PUMPING TEST RESULTS FOR KLONDYKE SECTION

(From Arad and Adar [1981])

Whiting's Deep Well (Confined Aquifer)
Drawdown Stage, August 12, 1981

<u>t (min)</u>	<u>Drawdown, Ft.</u>	<u>t (min)</u>	<u>Drawdown, Ft.</u>
1.55	51.30	9.50	68.20
1.75	52.80	10.00	68.70
2.00	54.20	10.50	69.10
2.17	54.90	11.00	69.40
2.35	55.80	12.00	70.20
2.58	56.70	13.00	70.60
2.80	57.30	14.00	71.50
3.00	58.80	15.00	72.00
3.50	59.40	16.00	72.80
3.75	60.50	17.00	73.10
4.00	60.80	18.00	73.60
4.25	60.80	19.00	74.00
4.50	61.40	20.00	74.50
4.75	61.90	22.00	75.20
5.00	62.40	24.00	76.00
5.25	63.10	26.00	76.50
5.50	63.30	28.00	77.10
5.75	63.80	30.00	77.60
6.00	64.10	35.00	78.70
6.25	64.30	40.00	79.80
6.50	64.70	45.00	80.60
7.00	65.60	50.00	81.50
7.50	66.20	60.00	81.90
8.00	66.70	70.00	82.00
8.50	67.30	80.00	82.00
9.00	67.60		

Jacob's Semilog Method (Kruseman and DeRidder, 1976)

$$Q = 82.04 \text{ g.p.m.}$$

$$T = 2.3 Q / 4\pi s \text{ (for one log cycle of } t)$$

$$s = 19.5 \text{ ft.}$$

$$T = \frac{2.3 \times 820.4 \text{ g.p.m.} \times 1440 \text{ min}}{4 \pi \times 19.5 \text{ ft} \times \text{day}} = 11,098 \text{ g.p.d./ft} = 1,482 \text{ ft}^2/\text{day}$$

$$S = 2.25 T \times t_0 / r_w^2$$

$$= 2.25 \times 1,482 \frac{\text{ft}^2}{\text{day}} \times \frac{1.9676 \times 10^{-6} \text{ days}}{.25 \text{ ft}^2}$$

$$S = 2.62 \times 10^{-2}$$

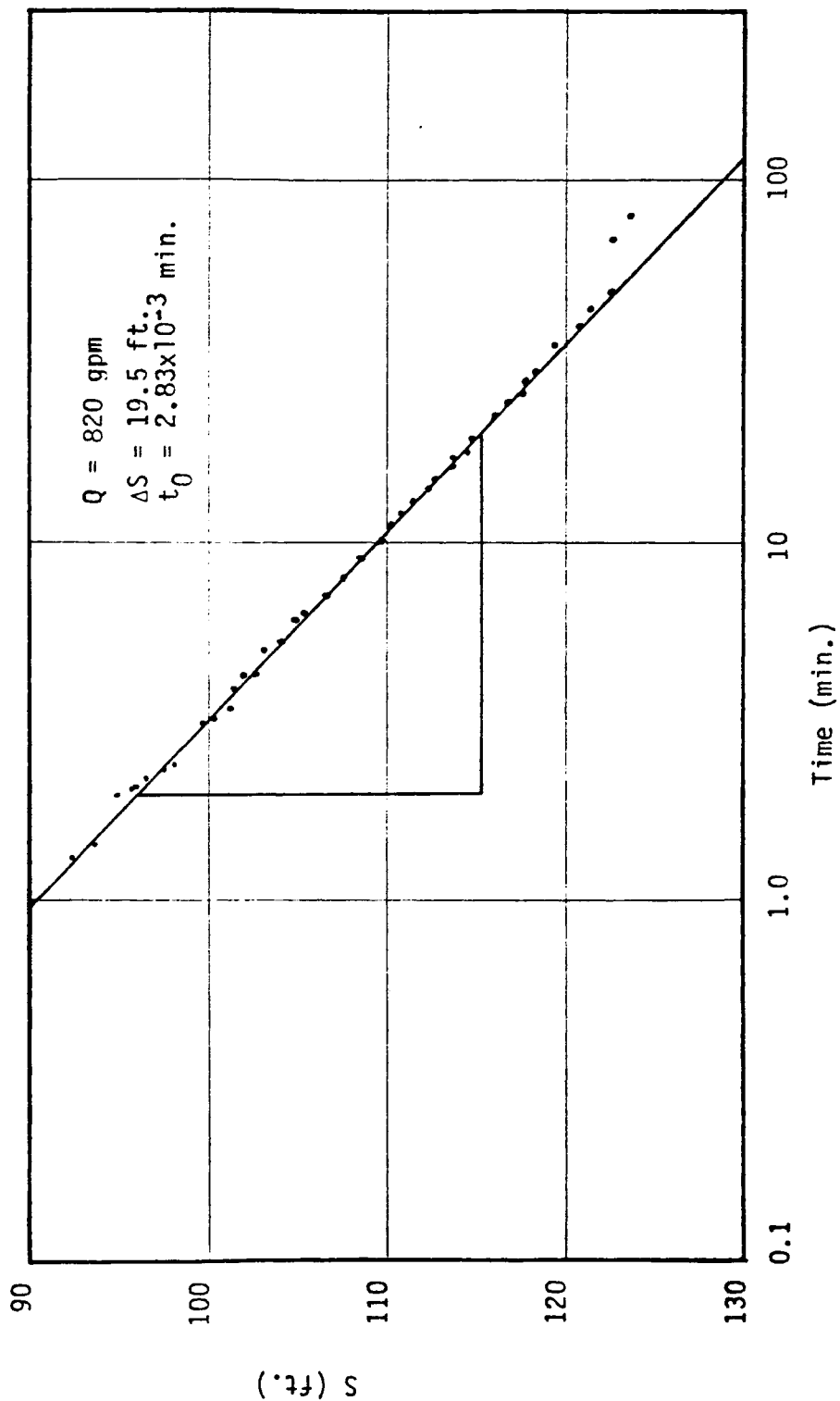


Figure B-1. Drawdown test results from Whiting's Deep well

Whiting's Deep Well (confined aquifer)
Recovery Stage, August 12, 1981

t'' (min)	t/t''	s'' (ft)	t'' (min)	t/t''	s'' (ft)
0	∞	204.3	12.00	36.0	50.6
1.15	366.22	107.1	12.50	34.6	49.7
1.25	337.00	103.3	13.00	33.3	49.0
1.38	305.30	100.1	13.50	32.1	48.4
1.53	275.50	97.1	14.00	31.0	47.5
2.00	211.00	91.8	15.00	29.0	46.8
2.25	187.70	90.3	16.00	27.3	45.5
2.50	169.00	86.6	17.00	25.7	44.5
2.75	153.70	84.5	18.00	24.3	43.5
3.00	141.00	83.5	19.00	23.1	42.2
3.25	130.20	81.6	20.00	22.0	41.5
3.50	121.00	79.1	21.00	21.0	40.7
3.75	113.00	77.3	22.00	20.1	39.9
4.00	106.00	75.9	23.00	19.3	39.1
4.25	99.80	74.8	24.00	18.5	38.4
4.50	94.30	73.6	25.00	17.8	37.7
4.75	89.40	72.5	30.00	15.0	34.8
5.00	85.00	71.0	35.00	13.0	32.6
5.25	81.00	69.9	40.00	11.5	30.7
5.50	77.40	68.8	45.00	10.3	29.6
6.00	71.00	66.8	50.00	9.4	28.9
6.50	65.60	65.0	55.00	8.6	28.2
7.00	61.00	63.2	60.00	8.0	27.8
7.50	57.00	61.7	65.00	7.5	27.2
8.00	53.50	60.3	70.00	7.0	26.7
8.50	50.40	58.9	75.00	6.6	26.3
9.00	47.70	57.4	80.00	6.3	25.8
9.50	45.20	55.9	90.00	5.7	25.1
10.00	43.00	54.8	100.00	5.2	24.4
10.50	41.00	53.8	150.00	3.8	24.0
11.00	39.20	52.6	180.00	3.3	23.2
11.50	37.50	51.6	770.00	1.5	16.9

Theis Recovery Method (Kruseman and DeRidder, 1976)

$Q = 1331$ g.p.m. $t =$ time in days since pumping started;
 $t = 420$ min. $t'' =$ time in days since
 $t_0 = .17$ sec. $s'' =$ residual drawdown in ft.

$$t = \frac{2.30}{4\pi\Delta s} Q = \frac{2.3 \times 1331 \text{ g.p.m.} \times 1440 \text{ min}}{4\pi \times 50 \text{ ft} \text{ day}} = 7,015.98 \text{ g.p.d./ft} = 937.9 \text{ ft}^2/\text{day}$$

Whiting's IR-1 - Recovery Stage
August 13, 1981

<u>t" (min)</u>	<u>t/t"</u>	<u>s" (ft)</u>	<u>t" (min)</u>	<u>t/t"</u>	<u>s" (ft)</u>
0	∞	1.81	30.00	9.0	0.45
4.47	54.7	0.90	35.00	7.9	0.38
5.35	45.9	0.85	40.00	7.0	0.35
6.80	36.3	0.70	45.00	6.3	0.32
8.42	29.5	0.68	50.00	5.8	0.28
9.65	25.9	0.65	55.00	5.4	0.26
10.55	23.7	0.63	60.00	5.0	0.24
12.00	21.0	0.62	70.00	4.4	0.24
14.00	18.7	0.58	80.00	4.0	0.23
17.00	15.7	0.53	90.00	3.7	0.22
20.00	13.0	0.50	105.00	3.3	0.20
23.00	11.4	0.50	120.00	3.0	0.17
28.00	9.6	0.47	150.00	2.6	0.10
			180.00	2.3	0.08

Theis Recovery Method (Kruseman and DeRidder, 1976)

$$T = \frac{2.3Q}{4\pi\Delta s}$$

$$Q = 1061.5 \text{ g.p.m.}$$

$$\Delta s = 0.46 \text{ ft.}$$

$$T = 608,194.7 \frac{\text{g.p.d.}}{\text{ft}} = 81,298.6 \frac{\text{ft}^2}{\text{day}}$$

t = time in days since pumping started

t" = time in days since pumping stopped

s" = residual drawdown in ft.

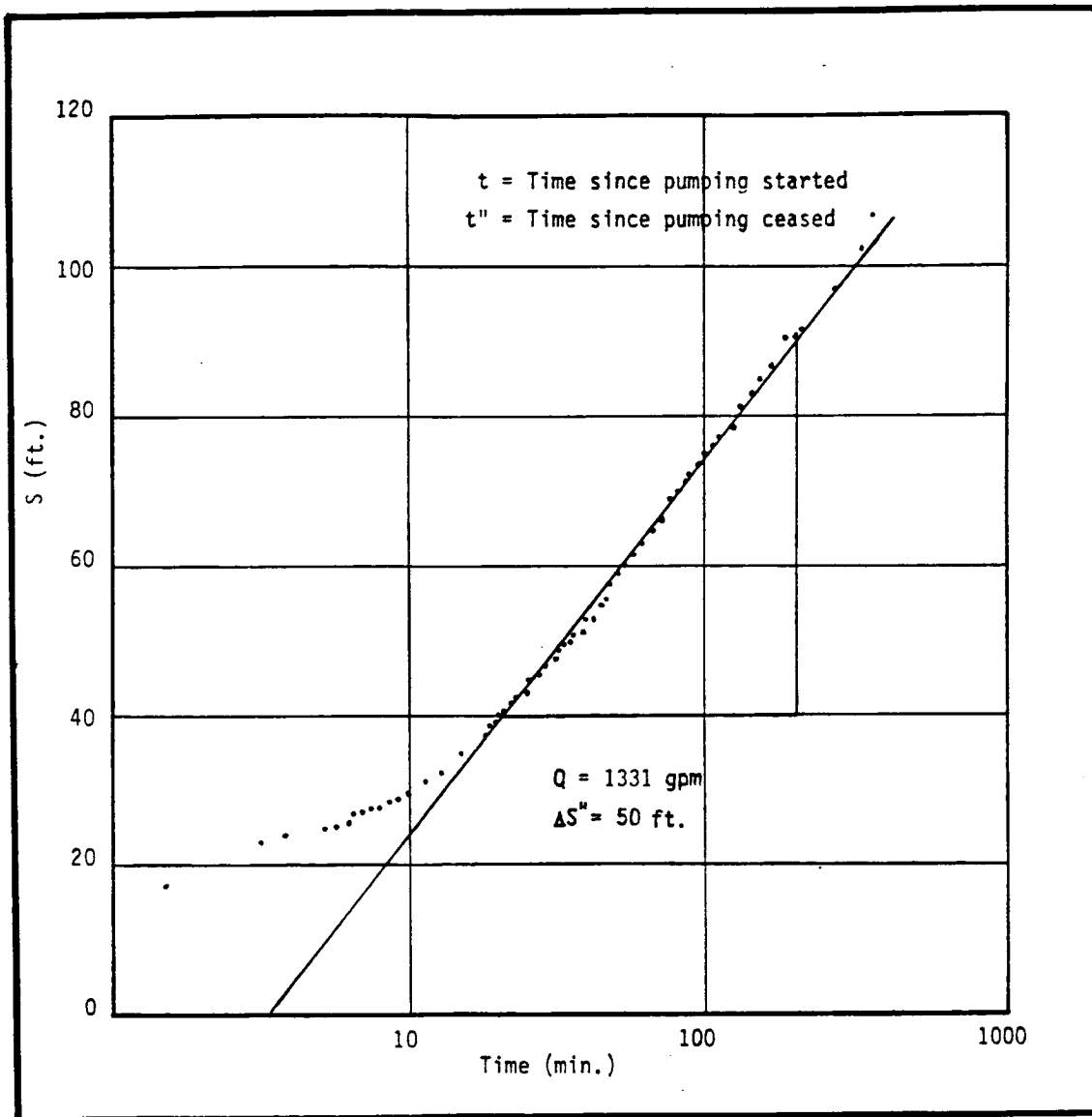


Figure B-2. Recovery test data from Whiting's Deep well

Whiting's Observation Well, Drawdown Stage
Interference Test, August 13, 1981

t'' (min)	t/r^2	s (ft)	$s' = 2 - s^2/2D$
2	1.05×10^{-4}	0	
4	2.10×10^{-4}	.370	.369
5	2.63×10^{-4}	.420	.419
7	3.68×10^{-4}	.470	.469
8	4.20×10^{-4}	.510	.508
9	4.73×10^{-4}	.520	.518
10	5.25×10^{-4}	.540	.538
11	5.78×10^{-4}	.550	.548
12	6.30×10^{-4}	.570	.568
13	6.85×10^{-4}	.600	.598
15	7.88×10^{-4}	.620	.618
17	8.93×10^{-4}	.690	.687
18	9.45×10^{-4}	.700	.697
21	1.10×10^{-3}	.720	.717
23	1.21×10^{-3}	.740	.736
26	1.37×10^{-3}	.750	.746
31	1.63×10^{-3}	.770	.766
38	2.00×10^{-3}	.820	.816
43	2.26×10^{-3}	.790	.786
47	2.47×10^{-3}	.870	.865
51	2.68×10^{-3}	.830	.826
53	2.78×10^{-3}	.870	.865
58	3.05×10^{-3}	.890	.885
63	3.31×10^{-3}	.890	.885
77	4.04×10^{-3}	.910	.905
87	4.57×10^{-3}	.920	.915
103	5.41×10^{-3}	.950	.944
118	6.20×10^{-3}	.990	.984
133	6.98×10^{-3}	1.070	1.063
165	8.66×10^{-3}	1.100	1.092
195	1.02×10^{-2}	1.120	1.112
221	1.16×10^{-2}	1.120	1.112
235	1.22×10^{-2}	1.130	1.122

Theis' curve matching method applied to interference test.
August 13, 1981

Whiting's Observation Well, Drawdown Stage
Interference Test, August 13, 1981
 (Continued)

Match	Point	Values
$W(u)$	$= 4\pi T s/Q$	$= 10$
s'	$= 1.9$	
$1/u$	$= 10^2$	
t/r^2	$= 1.9 \times 10^{-3}$	

$$T = QW(us)/4\pi s' = \frac{1061 \text{ gal} \times 10 \times 1440 \text{ min}}{\text{min} \cdot 4 \times \pi \times 1.9 \text{ ft} \cdot \text{day}} = 639,903 \frac{\text{gpd}}{\text{ft}} = 85,537.15 \frac{\text{ft}^2}{\text{day}}$$

$$S = 4T(t/r^2)U = 4 \times 85,537.15 \frac{\text{ft}^2}{\text{day}} \times 1.9 \times 10^{-3} \frac{\text{min}}{\text{ft}^2} \frac{1 \text{ day}}{1440 \text{ min}} \times 0.01$$

$$= 4.51 \times 10^{-3}$$

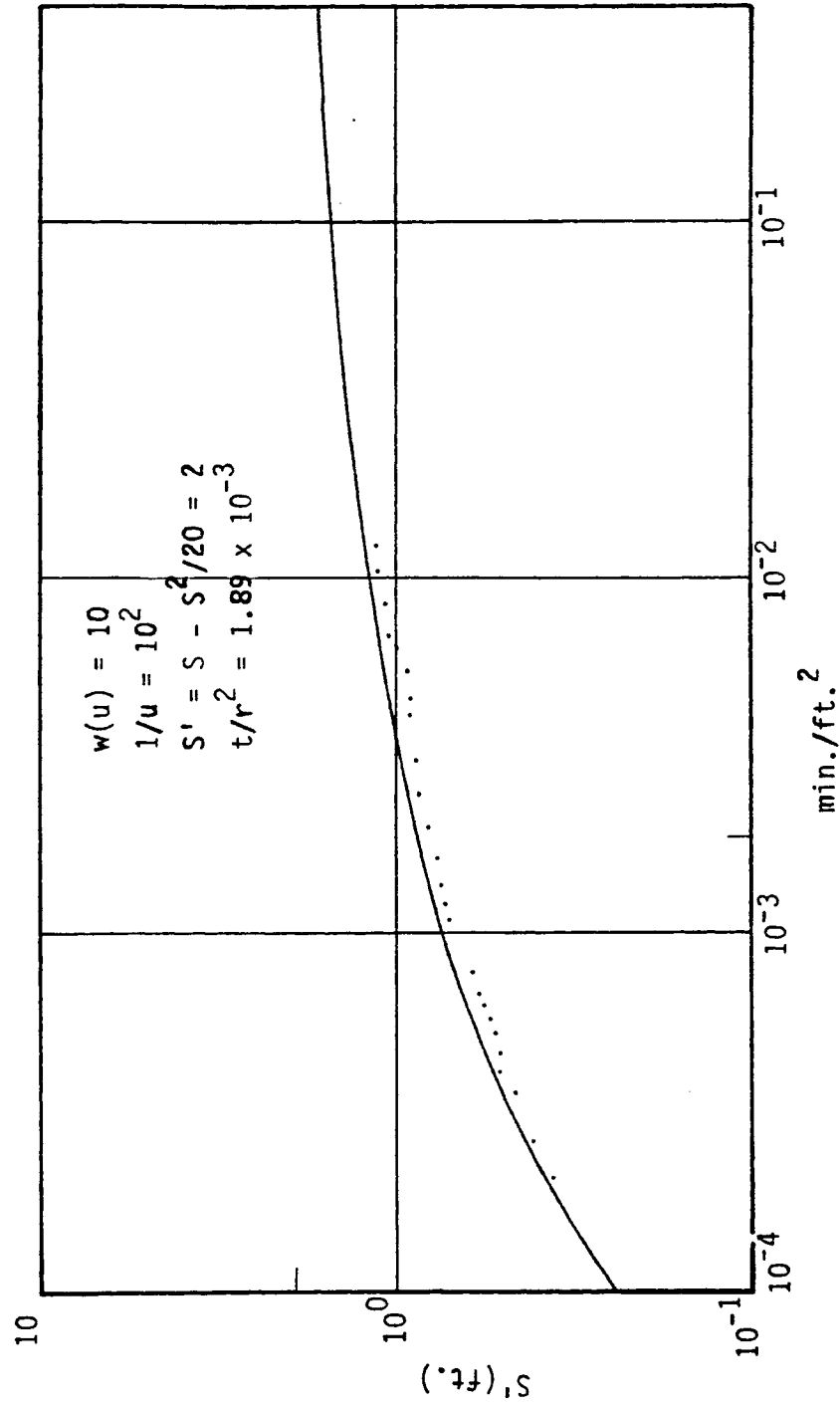


Figure B-3. Interference test in upper aquifer drawdown in the observation well

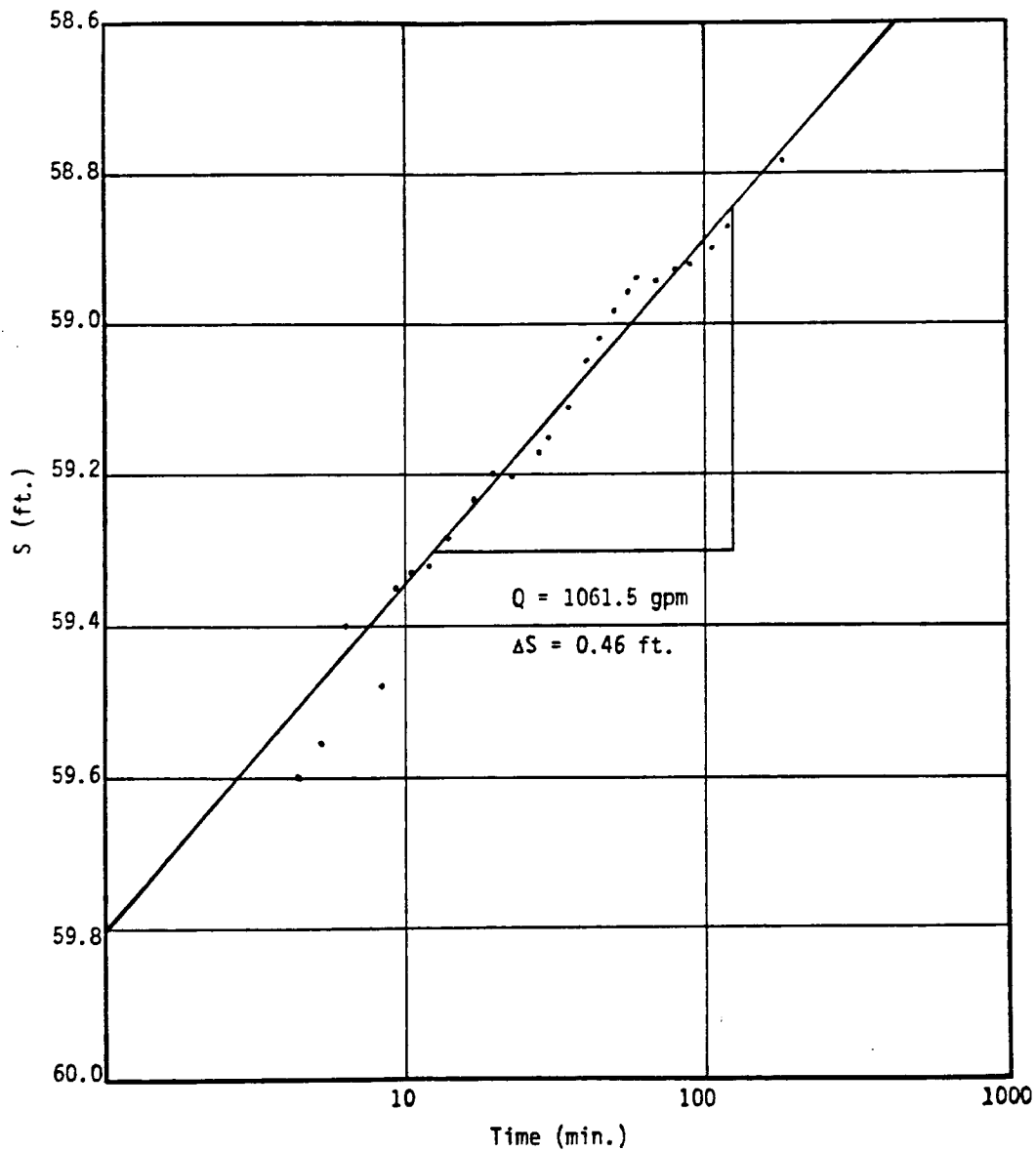


Figure B-4. Recovery test in Whiting's IR-1

APPENDIX C

LOCATION, CHEMICAL AND ISOTOPE SAMPLING
RESULTS FOR WELLS AND SPRINGS IN ARAVAIPA WATERSHEDC.1 Collection and Analyses of Water Samples

One hundred and eight wells and developed springs, to which an access has been obtained, were accurately located on a 1:62,400 topographical map. This was accomplished with basic information as the following: elevation, depth of well, depth to water table, type of pump, access and drillers' logs, if available. The altitude, depth of wells and depth to water are summarized in Table 2. The locations are given in terms of the local coordinate system as explained in the introduction to Appendix A. This is accomplished with a map (Figure A-2) showing the location of all the sampled wells and springs. The sites are presented with code names as found in parenthesis in Tables 1, 2 and 3.

Water samples were collected at least once during the last 24 months with a repeat on some key wells and springs taken each three to six months. Base flow in the canyon was sampled once a month and flood water was sampled whenever possible. The parameters measured during sampling generally included temperature, pH, electrical conductivity, and depth to water table. Water chemistry analyses of major cations and anions including fluorine, lithium and silicate, were performed at the University of Arizona, Analytical Center. The results are presented in the following tables: the average values are in Table 1 and detailed results, including the date of sampling, in Table 2.

Environmental isotopes of oxygen, hydrogen and carbon had been checked in groundwater, baseflow, and floods. The data of all environmental isotopes are presented in Table 3. The stable isotope analyses included 106 oxygen-18 and 59 deuterium samples. In addition, water dating analyses including 10 carbon-14 and 21-tritium samples were performed on key wells as listed in Table 4. The stable isotopes and the carbon-14 analyses have been conducted at the Isotope Laboratory, Department of Geoscience, University of Arizona. The tritium analyses have been completed in Weizmann Institute of Science, Rehovot, Israel.

The accuracy of the chemistry analyses has been checked in November of 1982 and in March of 1984. Laboratory standards were analyzed for Mg, Ca, Na, K, HCO_3 , Cl, NO_3 , and SO_4 , up to 30 times each. Electrical conductivity was repeated 150 times; H-2, 122; and O-18 78 times. Extensive data for F, Li, and Si could not be obtained, except for the coefficient of variations. The average, standard deviation and the coefficient of variation are given for each species in Table 5. Nitrate has been found to have the highest deviation of 13 percent, sulfate -10 percent, fluorine -9 percent and lithium -6 percent. The rest are below a 5 percent deviation from the mean.

The accuracy of oxygen-18 analysis is reported to be ± 0.02 percent and for deuterium the accuracy was 3 permil. However, recently the deuterium analysis has been improved to ± 1.0 percent due to the conversion of process from uranium line to zinc line (Long, 1983; personal communication).

The accuracy of carbon-14 and tritium measurements, as submitted by the laboratories for each separate analysis, is presented also in Table 4.

C.2. Tables of Chemical and Isotopic Data

Table 1. Yearly average concentrations in Aravaipa Watershed

(99.0--Missing Value)
 (*Abbreviations as seen in Figure 6)

NAME OF WELL OR SPRING	TMP. C	COND. MMHO	MG CA	NA MEQ	K MEQ	HCO ₃ MEQ	CL MEQ	NO ₃ MEQ	SO ₄ MEQ	F MEQ	LI MEQ	SI PPM	TDI MEQ	COORDINATES		
														LONG.	LAT.	
Aravaipa Spring	19.2	406.3	.88	2.76	.85	.048	3.14	.310	.079	1.03	.027	.0015	18.82	9.10	7.90	18.60
Cobra Ranch New Domes- tic Well	18.8	498.5	1.11	3.43	.96	.020	3.84	.382	.049	1.29	.046	.0024	13.62	11.13	8.05	18.67
Cobra Ranch Old Domes- tic Well	99.0	374.0	.72	1.80	1.57	.043	3.61	.230	.063	.27	.030	.0052	15.00	8.32	7.97	18.76
Valenzuela	19.4	428.5	1.04	3.46	.70	.030	3.53	.310	.090	1.36	.034	.0016	16.17	10.47	7.95	18.44
Cobra Ranch New Irriga- tion (Cobra N. Irr.*)	21.0	355.5	.69	2.10	.89	0.50	2.90	.175	.142	.56	.024	.0023	18.55	7.52	8.29	18.40
Cobra Ranch New Irriga- tion (Top Sample)	21.0	402.0	.82	2.59	.91	.050	2.77	.310	.103	1.10	.021	.0020	19.00	8.68	8.29	18.40
Song of the Desert (S.O.T.D.*) Domestic	16.9	190.1	.37	.85	.41	.030	.93	.080	.000	.83	.000	.0003	18.80	3.50	12.76	13.60

Table 1--continued

NAME OF WELL OR SPRING	TMP. C	COND. MMHO	MG MEQ	CA MEQ	NA MEQ	K MEQ	HCO ₃ MEQ	CL MEQ	NO ₃ MEQ	SO ₄ MEQ	F MEQ	LI MEQ	SI PPM	COORDINATES		
														LONG.	LAT.	
Song of the Desert (S.O.T.D.*) #1	19.0	363.9	.75	2.13	.97	.060	2.78	.250	.102	.71	.020	.0014	19.30	7.76	12.93	13.62
Song of the Desert (S.O.T.D.*) #2	19.4	266.3	.51	1.51	.68	.050	1.81	.135	.097	.66	.017	.0022	15.45	5.41	12.93	13.43
Whiting #1	19.7	404.0	.66	2.13	.97	.070	3.11	.265	.001	.2899	.000	99.0	16.90	7.42	11.36	14.67
Whiting #1 Windmill (W.M.*)	18.0	354.0	.76	2.00	.91	.074	3.11	.110	.055	.54	.015	.0023	19.00	7.56	11.45	14.43
Whiting #2	20.0	326.0	.81	1.60	.78	.031	2.79	.130	.044	.42	.018	.0026	15.30	6.90	11.14	14.86
Buford Wa- ter Tank (W.T.*)	19.0	392.0	.74	2.30	.89	.038	3.19	.280	.044	.37	.024	.0040	14.90	7.88	11.83	14.40
BLM-Camp- ground (C.G.*)	99.0	356.0	1.72	3.18	.73	.034	3.64	.140	.046	1.93	.015	.0016	14.80	11.43	9.36	15.90
Haby Domes- tic (D*)	19.8	294.4	.69	1.80	.94	.054	2.60	.375	.057	.48	.018	.0019	18.35	6.69	9.79	16.17
Haby Wind- mill (WM*)	18.0	346.0	.72	2.05	.83	.051	2.52	.250	.076	.63	.011	.0017	23.00	7.13	9.50	16.53

Table 1--continued

NAME OF WELL OR SPRING	TMP.	COND.	MG	CA	NA	K	HCO ₃	CL	NO ₃	SO ₄	F	LI		SI	TDI		COORDINATES	
												MEQ	MEQ		MEQ	MEQ	MEQ	MEQ
Haby Corral (CO.*)	18.0	578.0	1.20	4.11	.79	.037	3.60	.430	.192	1.69	.029	.0014	18.80	12.08	8.31	17.95		
Klondyke Mill	18.7	350.6	.75	1.90	.88	.050	2.66	.205	.065	.29	.020	.0022	15.70	7.04	9.35	17.30		
Cobra Irrigation Old Well (IRR.*)	18.4	336.2	.76	2.17	.75	.040	2.44	.263	.073	.66	.018	.0011	16.43	6.98	8.67	18.11		
Dowdle	19.0	374.0	.75	2.25	.96	.046	3.16	.200	.120	.56	.030	.0023	17.00	8.08	9.52	18.41		
Sandford Old Adobe	19.2	392.0	.78	1.47	.81	.042	1.69	.530	.160	.78	.042	.0010	17.70	6.31	9.46	17.50		
Klondyke School (SC.*)	19.8	342.6	.71	2.10	.91	.054	2.98	.200	.080	.52	.016	.0025	16.00	7.56	9.98	16.24		
Kramme Domestic (D.*)	99.0	386.2	.81	2.75	1.04	.059	3.29	.270	.019	.7799	.000	.0029	21.00	9.00	13.00	13.90		
Kramme Irrigation (IRR.*)	19.5	372.0	.75	2.30	.96	.056	2.82	.480	.092	.71	.019	.0028	21.00	8.17	12.77	13.70		
Kramme Corral (Co.*)	18.5	293.0	.60	1.60	.74	.046	1.70	.240	.045	.83	.013	.0016	19.00	5.82	11.25	14.01		

Table 1--continued

NAME OF WELL OR SPRING	TMP.	COND.	MG	CA	NA	K	HCO ₃	CL	NO ₃	SO ₄	F	LI		SI		TDI		COORDINATES		
												MEQ	MEQ	MEQ	MEQ	MEQ	MEQ	MEQ	MEQ	MEQ
Sharizona	19.3	412.0	.82	2.39	1.09	.064	3.65	.220	.095	.54	.024	.0030	17.00	8.89	13.45	12.71				
H. Claridge Windmill (H. Cl. W.M.*)	20.1	341.0	.67	1.93	.92	.072	2.88	.193	.070	.44	.022	.0025	18.85	7.18	13.12	12.83				
H. Claridge Irrigation (H. Cl. Irr.*)	20.7	335.0	.72	1.90	.96	.022	3.00	.164	.089	.35	.026	.0019	15.00	7.23	12.99	12.90				
3699 Windmill (W.M.*)	20.5	327.0	.75	1.64	.90	.089	2.77	.243	.074	.35	.021	.0030	21.20	6.84	14.19	11.81				
H. Claridge Domestic (H. Cl. D.*)	99.0	451.0	.91	2.65	1.09	.069	4.12	.172	.110	.50	.020	.0032	17.00	9.36	15.76	11.17				
Davis Old House (Davis*)	19.1	365.0	.78	2.10	1.04	.066	3.17	.240	.056	.46	.025	.0026	15.00	7.94	15.81	10.14				
Davis Old House New Well (Davis*)	99.0	99.0	99.0	99.0	99.0	99.0	99.0	99.0	99.0	99.0	99.0	99.0	99.0	99.0	99.0	15.81	10.10			
B. Wilson	99.0	99.0	.53	1.71	.58	.054	2.34	.110	.045	.46	.012	.0014	18.70	5.84	15.48	10.60				
Peyote	20.7	277.7	.83	1.70	1.60	.080	3.13	.353	.043	.17	.035	.0020	19.10	7.91	15.95	9.38				

Table 1--continued

NAME OF WELL OR SPRING	TMP.	COND.	MG	CA	NA	K	HCO ₃	CL	NO ₃	SO ₄	F	LI		SI		TDI		COORDINATES	
												MEQ	MEQ	MEQ	MEQ	MEQ	MEQ	MEQ	MEQ
Eureka #1	18.0	377.5	.75	2.13	1.24	.074	3.04	.270	.184	.63	.013	.0030	18.10	8.33	19.57	3.64			
Little Windmill (W.M.*)	19.0	357.0	1.56	2.65	1.01	.080	3.99	.209	.055	.98	.018	.0030	21.20	10.58	16.48	8.81			
Bull Pasture	16.0	258.0	.90	2.20	2.59	.024	5.00	.121	.089	.18	.018	.0030	11.40	11.26	19.33	4.76			
Puddy Lynch (Ly.*)	20.0	275.0	1.47	2.05	2.29	.059	5.36	.206	.092	.10	.008	.0030	13.60	11.74	18.40	5.81			
3867 Windmill (W.M.*)	18.2	362.0	.79	2.10	1.65	.066	3.91	.248	.052	.46	.011	.0030	21.90	9.38	16.31	9.19			
Eureka Ranch Old Flowing Well	20.2	250.0	.51	.89	1.14	.116	2.52	.121	.037	.09	.016	.0019	26.60	5.43	19.15	3.30			
Eureka Domestic	22.0	215.0	.58	.88	1.22	.117	2.31	.255	.040	.07	.024	.0022	23.45	5.45	18.67	2.83			
Eureka #11	99.0	278.0	.74	.87	1.06	.129	2.49	.019	.043	.09	.025	.0016	36.40	5.47	15.86	1.48			
Eureka Bird Cage	19.8	376.0	.86	.98	2.88	.880	4.12	.626	.071	.18	.016	.0040	15.60	9.62	21.57	2.07			
Eureka McGee	23.0	250.0	.55	1.02	1.09	.063	2.43	.169	.044	.13	.026	.0019	20.70	5.51	21.20	.40			

Table 1--continued

NAME OF WELL OR SPRING	TMP.	COND.	MG	CA	NA	K	HCO ₃	CL	NO ₃	SO ₄	F	LI	SI	COORDINATES		
														MEQ	MEQ	MEQ
Eureka Wilson Windmill (W.M.*)	99.0	309.0	1.66	1.06	1.98	.060	4.21	.155	.039	.08	.011	.0060	7.20	9.34	20.57	8.67
Eureka Big Tank	99.0	270.0	.81	1.54	.62	.076	2.33	.243	.294	.18	.019	.0023	10.80	6.12	22.75	.65
Eureka Sheep Cor- ral (Co.*)	19.0	106.7	1.51	1.79	1.25	.063	2.74	.948	.235	.79	.068	.0210	21.20	9.40	18.76	8.69
Eureka Apple Tree (A.T.*)	22.0	263.0	.71	.90	1.04	.120	2.25	.201	.062	.08	.023	.0019	20.80	5.46	17.76	4.21
Black Canyon	15.0	190.0	.33	1.03	.13	.089	.98	.079	.010	.52	.003	.0005	13.80	3.17	19.86	1.76
Deer Creek	12.0	357.0	.94	1.67	1.24	.047	3.59	.276	.039	.15	.023	.0040	34.50	7.98	12.75	4.45
Whiting Deep Well	25.3	304.5	.10	.24	2.01	.048	2.52	.263	.022	.05	.036	.0022	14.00	5.30	11.26	14.76
Klondyke Mill Deep #1 (K.D. #1*)	20.0	99.0	99.0	99.0	99.0	99.0	99.0	99.0	99.0	99.0	99.0	99.0	99.0	99.0	9.30	17.22
Klondyke Mill Deep #2 (K.D. #2*)	20.3	362.0	.66	2.06	0.87	0.05	2.93	.140	.080	.51	.022	.0020	17.10	7.32	9.29	17.21

Table 1--continued

NAME OF WELL OR SPRING	TMP.	COND.	MG	CA	NA	K	HCO ₃	CL	NO ₃	SO ₄	F	COORDINATES				
												C	MMHO	MEQ	MEQ	MEQ
Long Hollow	22.9	370.3	.77	1.67	1.70	.069	3.04	.690	.224	.14	.008	.0032	8.80	8.30	8.94	13.87
Squaw Deep Well	21.0	351.0	1.46	3.45	.81	.030	4.64	.340	.020	.88	.013	.0013	9.70	11.69	10.50	10.52
Whiting Hill Deep Well	20.5	454.0	1.28	2.52	.98	.028	3.71	.419	.059	.64	.012	.0016	16.35	9.64	11.79	16.55
Song of the Desert #3 (S.O.T.D. #3*)	14.9	184.0	.35	.76	.37	.040	.85	.105	.000	.76	.000	.0002	17.55	3.24	12.64	13.24
Haby Old House (O.H.*)	20.5	311.0	1.15	1.85	.61	.033	2.18	.270	.074	1.08	.010	.0012	10.00	7.26	9.35	16.30
Karakula Adobe (Ad.*)	24.0	302.8	.05	.30	2.89	.020	2.52	.320	.021	.19	.080	.0040	14.25	6.29	8.38	19.45
Karakula House Domes-tic (H.*)	18.2	526.8	1.07	3.59	.83	.025	4.29	.270	.031	1.17	.041	.0026	13.00	10.76	8.26	19.31
Aravaipa Town (T.*)	20.3	428.0	1.04	2.89	.60	.030	3.23	.200	.000	1.25	.040	99.0	11.20	9.35	8.25	24.90
Landsman Camp (C.*)	18.2	658.5	1.35	4.41	.40	.015	5.10	.295	.080	1.63	.020	.0001	21.75	12.57	10.10	25.40

Table 1--continued

NAME OF OF WELL OR SPRING	TMP.	COND.	MG	CA	NA	K	HCO ₃	CL	NO ₃	SO ₄	F	LI	SI	COORDINATES		
														C	MMHO	MEQ
Tule Spring Shaft (Sp.*)	16.3	549.3	.58	4.44	.46	.056	3.47	.278	.026	1.64	.115	.0020	9.79	11.05	9.71	24.30
Tule Spring Wash	17.9	827.0	2.59	4.62	1.10	.040	4.18	.450	.000	4.16	.050	.0001	16.20	17.19	9.65	24.38
Stowe Gulch Spring (G.Sp.*)	19.3	464.4	1.45	3.50	.78	.020	3.49	.355	.003	1.36	.069	.0017	12.90	10.53	8.75	23.15
W. Claridge Domestic	16.9	580.5	1.18	3.90	.71	.035	3.99	.295	.000	1.46	.063	.0010	15.70	11.45	8.40	22.10
Dowdle 3667 Windmill (3667 W.M.*)	17.0	205.0	.91	1.85	.73	.034	1.80	.180	.043	1.45	.033	.0009	15.70	7.02	9.05	20.05
Dog Water Mine (D.W. Mine*)	25.0	230.0	.37	.58	1.03	.050	1.47	.230	.000	.16	.300	99.0	99.0	4.20	11.17	18.80
Laurel Canyon	15.2	147.8	.84	.41	.33	.030	.07	.070	.008	.98	.120	99.0	7.80	2.86	10.17	18.14
Lamb Camp	23.8	190.0	.44	.65	.83	.069	1.23	.340	.000	.29	.024	.0038	10.00	3.85	14.52	16.60
Buford Hill (H.*)	18.0	680.0	99.0	99.0	99.0	99.0	99.0	99.0	99.0	99.0	99.0	99.0	99.0	99.0	17.60	17.25

Table 1--continued

NAME OF OF WELL OR SPRING	TMP.	COND.	MG	CA	NA	K	HCO ₃	CL	NO ₃	SO ₄	F	LI		SI		COORDINATES	
												MEQ	MEQ	MEQ	PPM	MEQ	MEQ
Fourmile Spring-Old (4Mile I*)	24.9	496.3	1.34	2.59	1.13	.030	4.73	.303	.020	.15	.013	.0040	.0040	29.50	10.26	6.14	13.10
Fourmile Spring-New (4Mile II*)	23.8	445.0	1.28	2.45	1.03	.020	4.25	.230	.024	.15	.012	.0040	.0040	26.10	9.44	5.25	13.10
Fourmile Old Mill	13.9	721.0	99.0	99.0	99.0	99.0	99.0	99.0	99.0	99.0	99.0	99.0	99.0	99.0	99.0	4.95	14.60
Squaw Cave Spring (#1*)	99.0	270.0	.50	1.93	.33	.048	2.19	.341	.253	.10	.012	.0010	.0010	14.20	5.71	11.60	13.50
Squaw Trail Spring (#2*)	99.0	385.0	.60	2.67	.32	.044	2.78	.155	.118	.66	.013	.0001	.0001	12.80	7.10	11.35	12.85
Jackson Spring	16.7	393.5	1.18	1.93	.78	.030	3.28	.140	.000	.33	.010	.0010	.0010	23.80	7.75	3.75	17.35
Bleak Spring	18.5	608.0	2.44	3.56	.62	.020	5.39	.280	.000	.93	.020	99.0	99.0	34.60	13.28	.70	15.70
Virgus Virg. Sp.*)	18.0	350.0	1.49	1.50	.73	.010	3.19	.130	.029	.19	.020	99.0	99.0	44.70	7.30	1.30	14.40
Parson (Pars. Sp.*)	14.5	470.0	2.25	2.16	.66	.030	3.98	.200	.000	.73	.020	99.0	99.0	33.50	10.02	1.43	15.42

Table 1--continued

NAME OF WELL OR SPRING	TMP. C	COND. MG C	CA MEQ	NA MEQ	K MEQ	HCO ₃ MEQ	CL MEQ	NO ₃ MEQ	SO ₄ MEQ	F MEQ	LI MEQ	SI PPM	COORDINATES			
													TDI MEQ	LONG. MEQ	LAT. MEQ	
Goat Hardes (Goat H. Sp.*)	18.0	569.0	3.71	4.56	.54	.030	7.28	.270	.010	1.08	.020	.0013	35.70	17.46	.10	15.60
Oak Spring	17.0	372.0	1.71	1.70	.54	.010	3.37	.140	.000	.16	.010	99.0	35.70	7.63	2.50	15.70
Dry Camp Spring	14.4	325.0	.87	2.14	.74	.040	3.16	.413	.145	.08	.015	.0013	22.60	8.35	3.95	22.95
Dry Camp Domestic Well	99.0	563.0	1.31	3.77	.55	.070	3.70	.210	.030	1.71	.020	.0001	20.00	11.35	4.05	22.93
Dry Camp Windmill (W.M.*)	16.4	495.0	1.38	3.04	.71	.042	2.67	.274	.055	1.96	.021	.0010	17.00	10.16	4.45	23.90
McNair Canyon	21.2	344.0	.77	2.01	.50	.061	2.29	.230	.005	1.31	.016	.0011	10.00	7.10	6.90	19.35
Bear Canyon	18.9	438.0	.82	2.62	1.12	.050	2.67	.230	.121	1.12	.040	99.0	30.20	8.80	6.27	22.95
Turnbull Irrigation	16.7	436.0	1.07	2.54	.71	.024	3.28	.150	.078	1.27	.016	.0018	11.50	9.07	7.19	18.93
McNair T.	19.2	416.7	.82	2.55	1.04	.046	3.11	.130	.153	.81	.031	.0022	21.00	8.69	6.85	19.05
McNair H.	19.1	407.8	.81	2.55	1.00	.051	3.23	.120	.126	.87	.026	.0023	21.00	8.76	6.74	19.05
Hilliard	18.1	432.0	.91	2.70	.87	.046	2.79	.240	.077	1.27	.012	.0017	23.00	9.00	6.67	18.85

Table 1--continued

NAME OF WELL OR SPRING	TMP.	COND.	MG	CA	NA	K	HCO ₃	CL	NO ₃	SO ₄	F	COORDINATES				
												LI	SI	TDI		
C	MMHO	MEQ	MEQ	MEQ	MEQ	MEQ	MEQ	MEQ	MEQ	MEQ	MEQ	PPM	MEQ	LONG.	LAT.	
Guest House (G.H.*)	18.5	430.0	.82	2.60	1.00	.059	3.00	.180	.114	.92	.022	.0022	21.00	9.70	6.33	19.12
Luepke	20.0	415.5	.34	1.70	2.22	.036	3.47	.080	.058	.60	.147	.0015	19.00	8.65	5.92	19.52
Schnell	17.5	388.5	.82	2.89	1.00	.059	3.24	.260	.073	1.12	.025	.0022	19.00	9.54	5.57	20.05
Tapia	19.5	484.6	.91	2.60	1.13	.051	2.74	.280	.040	1.17	.032	.0028	20.00	8.93	5.88	20.21
San Chez	18.5	482.0	.91	2.94	1.17	.049	3.08	.320	.040	1.31	.046	.0030	21.00	9.88	5.17	20.50
Goat Cave	18.7	391.5	.78	2.24	1.25	.035	3.05	.260	.080	1.01	.060	.0040	17.40	8.76	4.14	20.33
B. Salazar	20.5	484.8	.78	2.79	1.65	.072	3.21	.450	.052	1.19	.079	.0045	21.00	10.28	3.95	20.80
Tax Salazar	20.5	481.8	.80	2.70	1.65	.041	3.79	.260	.050	.79	.079	.0044	21.20	10.15	3.70	20.50
Buford (Stream*)	5.5	99.0	99.0	99.0	99.0	99.0	99.0	99.0	99.0	99.0	99.0	99.0	99.0	99.0	99.0	99.0
Fourmile at the Quarry (Stream)	13.6	445.7	1.18	1.99	.81	.030	3.04	.170	.025	.63	.012	.0030	21.75	7.87	99.0	99.0
Fourmile Last (Stream)	22.2	99.0	99.0	99.0	99.0	99.0	99.0	99.0	99.0	99.0	99.0	99.0	99.0	99.0	99.0	99.0
T. Creek (Stream)	22.0	280.0	.05	.25	4.26	99.0	3.28	.620	.030	.06	.060	99.0	25.50	9.05	99.0	99.0

Table 1--continued

NAME OF WELL OR SPRING	TMP.	COND.	MG	CA	NA	K	HCO ₃	CL	NO ₃	SO ₄	F		LI		SI		TDI		COORDINATES		
											MEQ	MEQ	MEQ	MEQ	MEQ	MEQ	MEQ	MEQ	MEQ	MEQ	LONG.
C	MMHO	MEQ	MEQ	MEQ	MEQ	MEQ	MEQ	MEQ	MEQ	MEQ	MEQ	MEQ	MEQ	MEQ	MEQ	MEQ	MEQ	MEQ	MEQ	MEQ	LAT.
Aravaipa Old School (Stream)	18.9	407.4	.87	2.52	.85	.055	2.99	.177	.092	1.01	.020	.0012	.0012	15.70	8.58	99.0	99.0				
Aravaipa G.H. (Stream)	19.6	407.5	.86	2.54	.85	.053	2.82	.240	.078	1.03	.030	.0016	.0016	21.23	8.52	99.0	99.0				
Aravaipa Hydrometric Station (Stream)	20.5	423.5	.85	2.60	1.71	.048	2.62	.263	.080	1.32	.043	.0041	.0041	18.70	8.67	99.0	99.0				
Summer Floods	19.5	332.3	.62	2.31	.69	.174	2.97	.151	.030	.38	.025	.0013	.0013	16.83	7.35	99.0	99.0				
Winter Floods	10.2	242.0	.39	1.51	.33	.064	1.20	.086	.044	.63	99.0	99.0	99.0	99.0	4.27	99.0	99.0				
Winter Runoff and Snow Melt in the Upper Valley	10.5	146.0	.52	1.13	.51	.048	1.40	.080	.036	.67	.007	.0003	.0003	17.70	4.41	99.0	99.0				

Table 2. Original data for wells, springs, baseflow and floods in Aravaipa Valley

(* - Abbreviations as seen only in Figure 6)
(** - The data of sampling is in a decimal form in terms of month and day only;
e.g. Sampling day of 10.50 means: month-Oct., day-30 x .50 = 15 - Oct. 15)

1	2	3	4	5	6	7	8	9	10	11	12	13	14	15	16	17	18	19	20	21	22	23	24	25
NAME OF WELL OR SPRING	IMP. COND. C°	MMHO	MG	CA	NA	K	HCO ₃	CL	NO ₃	SO ₄	F	LI	SI	TDI	COORDINATES	ALTTT	WELL DEPTH FEET	WATER LEVEL FEET	DATE **	H-2	O/00	H-3	O/00	PNC
Aravaipa Spring	22.0	300.	.91	2.70	.83	2.88	.46	.05	.69	.022	19.0	8.6	18.60	7.90	3335.	0	0	7.75						
			.74	3.30	.40	.04	3.93	.24	.96		16.0	9.6	18.60	7.90	3335.	0	0	11.47						
	18.3		1.01	2.81	1.09	.03	3.44	.28	.07	1.15	.035	.0007	10.0	9.9	18.60	7.90	3335.	0	4.99	-71.6	-9.51			
	20.3	375.	1.04	2.75	1.28	.03	3.28	.48	.05	1.19	.029	.0011	26.8	10.1	18.60	7.90	3335.	0	4.99	-73.5	-10.02			
	19.0	392.	1.01	3.17	.89	.06	3.84	.25	.04	1.04	.040	15.1	10.3	18.60	7.90	3335.	0	0	5.87	-74.5	-9.86			
	24.0	470.	.88	2.73	.89	.06	3.04	.28	.06	1.06	.030	30.7	9.0	18.60	7.90	3335.	0	0	7.67					
	21.2	438.	.91	2.89	.87	.06	3.28	.26	.04	.98	.017	.0017	20.0	9.3	18.60	7.90	3335.	0	10.47					
	14.5	472.	.85	2.45	.90	.05	2.66	.48	.10	1.09	.031	.0030	18.4	8.6	18.60	7.90	3335.	0	12.99	-71.0	-9.95			
	14.5	397.	.76	2.59	.65	.04	2.19	.22	.22	1.38	.017	.0010	20.8	8.1	18.60	7.90	3335.	0	2.60		-9.31			
			.64	2.50	.69	.06	2.87	.15	.09	0.71	.023	.0014	11.4	7.5	18.60	7.90	3335.	0	11.63		-10.07			
Cobra Ranch New Domestic Well	21.0	410.	1.16	4.40	.96	4.56	.45	.02	.88	.055	14.5	12.5	18.67	8.05	3351.	47.	33.	7.70						
	18.3	512.	1.20	3.88	1.09	.01	4.59	.28	.05	1.42	.048	.0039	10.0	12.6	18.67	8.05	3351.	47.	4.99		-9.54			
	18.1	548.	1.11	2.15	.74	.03	4.16	.28	.01	1.29	.040	.0001	13.0	9.8	18.67	8.05	3351.	47.	5.90					

Table 2--continued

NAME OF WELL OR SPRING	C°	1	2	3	4	5	6	7	8	9	10	11	12	13	14	15	16	17	18	19	20	21	22	23	24	25	
																											IMP. COND.
Song of the Desert (S.O.T.D.*) #1	18.9	351.	.72	1.86	.94	.06	2.79	.16	.10	.54	.020	.0001	21.6	7.2	13.62	12.93	3620.	90.	12.	5.90							
	19.0	377.	.77	2.40	1.00	.06	2.77	.34	.11	.87	.019	.0026	17.0	8.3	13.62	12.93	3620.	90.	12.	10.13							
Song of the Desert (S.O.T.D.*) #2	19.2	178.	.30	.73	.36	.04	.58	.10	.79					11.9	2.9	13.43	12.93	3620.	60.	14.	5.90	-72.4	-9.66				
	19.5	355.	.72	2.29	1.00	.06	3.03	.17	.10	.52	.017	.0022	19.0	7.9	13.43	12.93	3620.	60.	14.	10.43							
Whitting #1		402.	.65	2.12	.97		3.15	.22	.00	.29				7.4	14.67	11.36	3536.	152.	51.	6.57				13.3			
	19.7	406.	.66	2.13	.96	.07	3.06	.31	.00	.26				16.9	7.4	14.67	11.36	3536.	152.	51.	8.43	-71.8	-9.80	17.8	-13.4	87.	
Whitting #1 Windmill (W.M.*)	18.0	354.	.76	2.00	.91	.07	3.11	.11	.06	.54	.015	.0023	19.0	7.6	14.43	11.45	3539.	100.	27.	10.43							
Whitting #2	20.0	326.	.81	1.60	.78	.03	2.79	.13	.04	.42	.018	.0026	15.3	6.9	14.86	11.14	3528.	150.	84.	4.99							
Burford Water Tank (W.T.*)	19.0	392.	.74	2.30	.89	.04	3.19	.28	.04	.37	.024	.0040	14.9	7.9	14.40	11.83	3550.	100.	50.	12.97							
BLM-Campground (C.G.*)		356.	1.72	3.18	.73	.03	3.64	.14	.05	1.93	.015	.0016	14.8	11.4	15.90	9.36	3500.	139.	111.	7.73	-67.0	-8.43					
Haby Domestic (D*)	22.0	240.	.66	1.55	1.04		2.72	.47	.04	.23	.022			16.7	6.2	16.17	9.79	3445.		7.70							
	17.5	349.	.72	2.05	.83	.05	2.48	.28	.08	.73	.013	.0019	20.0	7.2	16.17	9.79	3445.		10.40								

Table 2--continued

1	2	3	4	5	6	7	8	9	10	11	12	13	14	15	16	17	18	19	20	21	22	23	24	25	
NAME OF WELL OR SPRING	IMP. COND. C°	MG	CA	NA	K	HCO ₃	CL	NO ₃	SO ₄	F	LI	SI	TDI	COORDINATES	ALTIT	WELL DEPTH	WATER LEVEL	DATE	H-2	H-3	O/00	O/00	O/00	PMC	
		MEQ	MEQ	MEQ	MEQ	MEQ	MEQ	MEQ	MEQ	MEQ	MEQ	PPM	MEQ	LAT.	LONG.	FEET	FEET	**	O/00	I.U.	O/00	O/00			
Kramme Corral (Co.★)	18.5	293.	.60	1.60	.74	.05	1.70	.24	.05	.83	.013	.0016	19.0	5.8	14.01	11.25	3551.	35.	10.43						
Sharizona	19.3	412.	.82	2.39	1.09	.06	3.65	.22	.10	.54	.024	.0030	17.0	8.9	12.71	13.45	3666.	30.	11.63	-74.1	-9.91				
H. Claridge Windmill (H. Cl. W.M.★)	20.9	352.	.69	2.10	.91	.07	3.08	.20	.07	.42	.026	.0022	27.0	7.6	12.83	13.12	3653.	35.	11.67	-78.5	-9.27				
	19.2	339.	.64	1.76	.92	.07	2.68	.19	.07	.45	.017	.0027	10.7	6.8	12.83	13.12	3653.	35.	2.60						
H. Claridge Windmill (H. Cl. Irr.★)	20.7	335.	.72	1.90	.96	.02	3.00	.16	.09	.35	.026	.0019	15.0	7.2	12.90	12.99	3650.	30.	11.67						
3699 Windmill (W.M.★)	20.5		.75	1.64	.90	.09	2.77	.24	.07	.35	.021	.0030	21.2	6.8	11.81	14.19	3694.	40.	12.99						
H. Claridge Domes- tic (H. Cl. D.★)	451		.91	2.65	1.09	.07	4.12	.17	.11	.50	.020	.0032	17.0	9.4	11.17	15.76	3780.	50.	11.67						
Davis Old House (Davis★)	19.1	365.	.78	2.10	1.04	.07	3.17	.24	.06	.46	.025	.0026	15.0	7.9	10.14	15.81	3825.	30.	11.63						
Davis Old House New Well (Davis★)														10.10	15.81	3825.	112.	30.	7.60						
B. Wilson			.53	1.71	.58	.05	2.34	.11	.05	.46	.012	.0014	18.7	5.8	10.60	15.48	3780.	110.	27.	7.70	-63.0	-7.84			
Peyote	22.5	270.	.91	1.90	1.91	3.69	.47	.04	.13	.029		22.7	9.2	9.38	15.95	3864.		7.70							
	290.		.83	1.85	1.19	3.20	.45	.04	.10	.055		19.5	8.4	9.38	15.95	3864.		7.70							

Table 2--continued

NAME OF WELL OR SPRING	1 IMP. COND. C°	2 MG	3 CA	4 NA	5 K	6 HCO ₃	7 CL	8 NO ₃	9 SO ₄	10 F	11 LI	12 SI	13 TDI	14 MEQ	15 LAT.	16 LONG.	17 ALTT FEET	18 WELL DEPTH FEET	19 WATER LEVEL FEET	20	21	22	23	24	25	
																				DATE	H-2	O-18	H-3	C-13	C-14	
Peyote (cont.)	18.9	273.	.74	1.34	.97	.08	2.49	.14	.05	.29	.020	.0020	15.1	6.1	9.38	15.95	3864.	58.	5.90							
Eureka #1	18.0	378.	.75	2.13	1.24	.07	3.04	.27	.18	.63	.013	.0030	18.1	8.3	3.64	19.57	4139.	58.	2.73							
Little Windmill (W.M.*)	19.0	357.	1.56	2.65	1.01	.08	3.99	.21	.06	.98	.018	.0030	21.2	10.6	8.81	16.48	3900.	56.	24.	12.90						
Bull Pasture	16.0	258.	.90	2.20	2.59	.02	5.00	.12	.09	.18	.018	.0030	11.4	11.3	4.76	19.33	4166.	150.	80.	12.90						
Puddy Lynch	20.0	275.	1.47	2.05	2.29	.06	5.36	.21	.09	.10	.008	.0030	13.6	11.7	5.81	18.40	4072.	83.	46.	12.90						
3867 Windmill (W.M.*)	18.2	362.	.79	2.10	1.65	.07	3.91	.25	.05	.46	.011	.0030	21.9	9.4	9.19	16.31	3867.	90.	26.	12.90						
Eureka Ranch Old Flowing Well	23.5	250.	.51	.89	1.14	.12	2.52	.12	.04	.09	.016	.0019	26.6	5.4	3.30	19.15	4155.	1500.	4.	7.60						
Eureka Domestic	180.		.58	.95	1.22		2.33	.34	.02	.04	.026		20.0	5.5	2.83	18.67	4310.	200.	140.	7.72						
Eureka #11	22.0	250.	.58	.81	1.21	.12	2.29	.17	.06	.10	.022	.0022	26.9	5.4	2.83	18.67	4310.	200.	140.	2.73						
Eureka Bird Cage	19.8	376.	.86	.98	2.88	.88	4.12	.63	.07	.18	.016	.0040	15.6	9.6	2.07	21.57	4280.	278.		12.90						
Eureka McGee	23.0	250.	.55	1.02	1.09	.06	2.43	.17	.04	.13	.026	.0019	20.7	5.5	.40	21.20	4350.		7.60							
Eureka Wilson Windmill (W.M.*)	30.3	309.	1.66	1.06	1.98	.06	4.21	.16	.04	.08	.011	.0060	7.2	9.3	3.67	20.57	4242.	126.	113.	12.90						

Table 2--continued

1	2	3	4	5	6	7	8	9	10	11	12	13	14	15	16	17	18	19	20	21	22	23	24	25
NAME OF WELL OR SPRING	IMP. COND.	MG	CA	NA	K	HCO ₃	CL	NO ₃	SO ₄	F	LI	SI	TDI	COORDINATES	ALTIT	WELL DEPTH FEET	WATER LEVEL FEET	DATE	H-2	H-3	H-3	C-13	C-14	PMC
C°	PHHO	MEQ	MEQ	MEQ	MEQ	MEQ	MEQ	MEQ	MEQ	MEQ	MEQ	PPM	MEQ	LAT.	LONG.	FEET	FEET	**	O/OO	O/OO	I.U.	O/OO	O/OO	
Eureka Big Tank	20.2	270.	.81	1.54	.62	.08	2.33	.24	.29	.18	.019	.0023	10.8	6.1	.65	22.75	4355.	270.	155.	7.65	-60.3	-8.57		
Eureka Sheep Corral (Co.*)	19.0	107.	1.51	1.79	1.25	.06	2.74	.95	.24	.79	.068	.0210	21.2	9.4	8.69	18.76	4145.	202.	120.	12.90		-7.67		
Eureka Apple Tree (A.T.*)	22.0	263.	.71	.90	1.04	.12	2.25	.20	.06	.08	.023	.0019	20.8	5.5	4.21	17.76	4258.	222.	2.73	-75.8	-10.01			
Black Canyon	15.0	190.	.33	1.03	.13	.09	.98	.08	.01	.52	.003	.0005	13.8	3.2	1.76	19.86	4272.	94.	7.60	-58.0	-7.83			
Deer Creek	12.0	357.	.94	1.67	1.24	.05	3.59	.28	.04	.15	.023	.0040	34.5	8.0	4.45	12.75	0	0	12.99					
Whiting Deep Well	26.6	306.	.08	.22	2.56	.04	2.34	.38	.01	.00			5.7	14.76	11.26	3535.	762.	27.	6.57		0.7			
	25.0	318.	.15	.37	1.43	.06	2.59	.30	.02	.00			4.9	14.76	11.26	3535.	762.	27.	8.40		-8.67	1.6	-12.6	32.
	25.5	320.	.09	.25	1.43	.06	2.63	.30	.01	.03		12.0	4.9	14.76	11.26	3535.	762.	27.	8.40					
	24.0	274.	.06	.13	2.61	.03	2.51	.07	.05	.16	.036	.0022	16.0	5.7	14.76	11.26	3535.	762.	27.	10.43	-70.2	-8.93		
Klondyke Mill Deep (M.D.#1*)	20.0														17.22	9.30	3405.	215.	11.	4.10	-68.0	-8.85	5.4	
	20.0														17.22	9.30	3405.	215.	11.	4.10	-68.0	-8.56		
Klondyke Mill Deep (M.D.#2*)	20.3	362.	.66	2.06	.87	.05	2.93	.14	.08	.51	.022	.0023	17.1	7.32	17.21	9.29	3400.	156.	15.	11.60	-69.3	-9.61		
Long Hollow	23.5	369.	.77	1.70	1.70	.05	2.95	.76	.18	.13	.000	.0032	8.8	8.2	13.07	8.94	4260.	560.	80.	10.40	-58.5	-6.61	1.2	38.1

Table 2--continued

1	2	3	4	5	6	7	8	9	10	11	12	13	14	15	16	17	18	19	20	21	22	23	24	25
IMP.	COND.	MG	CA	NA	K	HCO ₃	CL	NO ₃	SO ₄	F	LI	SI	TDI	COORDINATES	ALTT	WELL	WATER	DATE	H-2	0-18	H-3	C-13	C-14	
C°	MMHO	MEQ	MEQ	MEQ	MEQ	MEQ	MEQ	MEQ	MEQ	MEQ	MEQ	PPM	MEQ	LAT.	LONG.	FEET	DEPTH	**	0/00	0/00	I.U.	0/00	PHC	
Long Hollow (cont.)	22.2	372.	.77	1.63	1.69	.09	3.13	.62	.27	.15	.015	.0032	8.8	8.4	13.07	8.94	4260.	80.	2.73	-67.6	-6.43			
Squaw Deep Well	21.0	351.	1.46	3.45	.81	.03	4.64	.34	.02	.88	.013	.0013	9.7	11.7	10.52	10.50	4027.	100.	4.70	-7.30				
Whiting Hill Deep Well	20.5	439.	1.23	2.54	1.00	.03	3.80	.37	.05	.35	.008	.0016	19.0	9.4	16.55	11.79	3870.	200.	10.40	-76.7	-10.22	4.7		
	20.4	469.	1.32	2.49	.96	.03	3.62	.47	.07	.92	.015	.0016	13.7	9.9	16.55	11.79	3870.	200.	4.10	-75.9	-10.13	-11.9	89.0	
Song of the Desert (S.O.T.D. #3*)	16.0	184.	.38	.85	.39	.04	1.06	.11	.00	.73	.000	.0003	20.0	3.6	13.24	12.64	3623.	160.	5.90	-67.8	-8.81			
	14.6		.31	.67	.35	.04	.64	.10	.00	.79	.000	.0001	15.1	2.9	13.24	12.64	3623.	160.	10.43	-64.8	-8.31	23.0	-16.8	119.8
	14.0													13.24	12.64	3623.	180.	9.	9.10	-64.8	-8.31			
Heby Old House (O.H.*)	20.5	311.	1.15	1.85	.61	.03	2.18	.27	.07	1.08	.010	.0012	10.0	7.3	16.30	9.35	3445.	79.	10.40	-66.5	-8.94	22.0		
Karakula Adobe (Ad.*)	24.0	290.	.08	.40	3.00		2.48	.48	.03	.23	.090		11.4	6.6	19.45	8.38	3440.	44.	7.70	-77.2	-9.76	4.5		
	24.0	313.5	.02	.20	2.77	.017	2.56	.16	.03	.15	.072	.0037	17.1	6.0	19.45	8.38	3440.	44.	11.63		-9.12			
Karakula House Domestic (H.*)	18.2	527.	1.07	3.59	.83	.03	4.29	.27	.03	1.17	.041	.0026	13.0	10.8	19.31	8.26	3445.	91.	10.43		-9.71			

Table 2--continued

1	2	3	4	5	6	7	8	9	10	11	12	13	14	15	16	17	18	19	20	21	22	23	24	25	
IMP.	COND.	MG	CA	NA	K	HCO ₃	CL	NO ₃	SO ₄	F	LI	SI	TDI	COORDINATES	ALTIT	WELL	WATER	DATE	H-2	H-3	C-13	C-14			
C°	MMHO	MEQ	MEQ	MEQ	MEQ	MEQ	MEQ	MEQ	MEQ	MEQ	MEQ	PPM	MEQ	LAT.	LONG.	FEET	DEPTH	LEVEL	**	O/00	I.U.	O/00	O/00	PMC	
Aravaipa Town (T.*)	20.3	428.	1.04	2.89	.60	.03	3.23	.20	.00	1.25	.040	11.2	9.4	24.90	8.25	4560.	850.	750.	7.63		0-18	18.0	-20.0	78.0	
Landsman Camp (C.*)	17.4	644.	1.27	3.53	.37	.01	4.91	.25	.08	1.64	.020	.0001	17.3	10.8	25.40	10.10	5200.	0	0	5.87					
	18.9	673.	1.43	5.29	.43	.02	5.29	.34	1.62	.020		26.2	14.3	25.40	10.10	5200.	0	0	7.66						
Tule Spring Shaft (Sp.*)	15.4	530.	.63	4.19	.43	.05	3.47	.28	.03	1.64	.130	.0001	10.0	10.9	24.30	9.71	4620.	0	0	5.87					
	16.7	561.	.49	5.09	.46	.06	4.01	.32	.01	1.79	.122	.0023	9.7	12.4	24.30	9.71	4620.	0	0	7.67		-8.94			
	16.7	561.	.54	4.34	.42	.06	2.43	.31	.04	1.66	.153	.0029	9.7	9.9	24.30	9.71	4620.	0	0	7.67		-8.95	10.0		
		545.	.68	4.14	.52	.06	3.95	.20	.02	1.46	.053	.0025	11.1	24.30	9.71	4620.	0	0	10.40				-10.9	84.0	
Tule Spring Wash	17.9	827.	2.59	4.62	1.10	.04	4.18	.45	.00	4.16	.050	.0001	16.2	17.2	24.38	9.65	4620.	0	0	5.87					
Stowe Gulch Spring (G.Sp.*)	21.0	370.	1.32	3.45	.87		3.69	.45	.00	.88	.084	15.8	9.8	23.15	8.75	3990.	0	0	7.73						
	17.5	559.	1.57	3.54	.70	.02	3.28	.26	.01	1.83	.053	.0017	10.0	11.3	23.15	8.75	3990.	0	0	4.99		-70.8	-9.78	20.0	
M. Claridge Domestic	16.8	571.	1.12	4.06	.68	.03	4.16	.34	.03	1.39	.068	.0001	18.4	11.9	22.10	8.40	3835.	120.	90.	7.67					
	17.0	590.	1.23	3.74	.74	.04	3.82	.25	.03	1.52	.058	.0019	13.0	11.4	22.10	8.40	3835.	120.	90.	10.47		-9.13	13.4		

Table 2--continued

NAME OF WELL OR SPRING	1 IMP.	2 COND.	3 MG	4 CA	5 NA	6 K	7 HCO ₃	8 CL	9 NO ₃	10 SO ₄	11 F	12 LI	13 SI	14 TDI	15 COORDINATES	16 LAT.	17 LONG.	18 WELL DEPTH FEET	19 WATER LEVEL FEET	20 DATE **	21 H-2	22 0-18	23 H-3	24 C-13	25 C-14	
																										1 C°
Dowdle 3667 Windmill (3667 W.M.*)	17.0	205.	.91	1.85	.73	.03	1.80	.18	.04	1.45	.033	.0009	16.7	7.0	20.05	9.05	3667.	110.	89.	7.67	-67.7	-9.61				
Dog Water Mine (D.W. Mine*)	25.0	230.	.37	.58	1.03	.05	1.47	.23	.00	.16	.300			4.2	18.80	11.10	3840.	0	0	7.67						
Laurel Canyon	15.2	148.	.84	.41	.33	.03	.07	.07	.01	.98	.120			7.8	2.9	18.14	10.17	3540.	90.	25.	7.67	-68.9	-9.36			
Lamb Camp	23.8	190.	.44	.65	.83	.07	1.23	.34	.00	.29	.024	.0038	10.0	3.9	16.60	14.52	4480.	80.	20.	10.40	-69.2	-8.76				
Ruford Hill (H.*)	18.0	680.												17.25	17.60	5170.	55.	10.	12.99		-9.64					
Fourmile Spring - (Old (4 Mile 1*))	24.0	330.	1.40	2.80	1.17		4.92	.41	.01	.04	.016			29.2	10.8	13.10	6.14	4080.	0	7.70						
	490.		1.15	2.90	.93	.01	4.41	.18	.01					9.6	13.10	6.14	4080.	0	0							
	26.0	550.	1.19	2.63	1.12	.03	4.75	.28	.05					24.0	10.2	13.10	6.14	4080.	0	8.37			8.2			
	23.5	600.	1.52	2.55	1.33	.05	5.49	.37	.01					36.1	11.4	13.10	6.14	4080.	0	8.37						
	600.		1.50	2.50	1.34	.05	5.43	.39						36.1	11.4	13.10	6.16	4075.	0	8.37			4.3			
	26.0	452.	1.32	2.32	1.01	.02	3.99	.22	.02	.20	.011	.0040	26.8	9.1	13.10	6.14	4080.	0	0	12.97	-71.9	-9.05				
	24.5	452.	1.32	2.42	1.01	.02	4.09	.27	.03	.21	.011	.0040	24.8	9.4	13.10	6.14	4080.	0	0	12.97		-9.05				
	25.5													13.10	6.14	4080.	0	0	2.60		-9.11					

Table 2--continued

NAME OF WELL OR SPRING	1	2	3	4	5	6	7	8	9	10	11	12	13	14	15	16	17	18	19	20	21	22	23	24	25
	IMP. COND. OR C°	COND.	MG	CA	NA	K	HCO ₃	CL	NO ₃	SO ₄	F	LI	SI	TDI	COORDINATES	ALTIT	WELL DEPTH	FEET	FEET	DATE	H-2	H-3	H-3	C-13	C-14
Fourmile Spring - New (4 Mile II*)	24.5	445.	1.28	2.45	1.03	.02	4.25	.23	.02	.15	.012	.0040	26.1	9.4	13.10	6.25	4075.	0	0	12.97	-63.1	-7.92			
		23.0												13.10	6.25	4075.	0	0	2.60						
Fourmile Old Mill	13.9	721.												14.60	4.95	3564.	17.	0	2.73	-60.7	-9.25				
Squaw Cave Spring (#1*)	270.		.50	1.93	.33	.05	2.19	.34	.25	.10	.012	.0010	14.2	5.7	13.50	11.60	3660.	0	0	12.97					
Squaw Trail Spring (#2*)	385.		.60	2.67	.32	.04	2.78	.16	.12	.66	.013	.0001	12.8	7.1	12.85	11.35	3800.	0	0	12.97	-45.7	-7.22			
Jackson Spring	16.7	394.	1.18	1.93	.78	.03	3.28	.14	.00	.33	.010	.0010	23.8	7.8	17.35	3.75	3480.	0	0	5.63					
Bleak Spring	18.5	608.	2.44	3.56	.62	.02	5.39	.28	.00	.93	.020		34.6	13.3	15.70	.70	4510.	0	0	5.97					
Virgus (Virg. Sp.*)	18.0	350.	1.49	1.50	.73	.01	3.19	.13	.03	.19	.020		44.7	7.3	14.40	1.30	4680.	0	0	5.97					
Parson (Pars. Sp.*)	14.5	470.	2.25	2.16	.66	.03	3.98	.20	.00	.73	.020		33.5	10.0	15.42	1.43	4540.	0	0	5.99					
Goat Herdes (Goat H. Sp.*)	18.0	569.	3.71	4.56	.54	.03	7.28	.27	.01	1.08	.020	.0013	35.7	17.5	15.60	.10	4560.	0	0	5.97					
Oak Spring	17.0	372.	1.71	1.70	.54	.01	3.37	.14	.00	.16	.010		35.7	7.6	15.70	2.50	4400.	0	0	5.99					
Dry Camp Spring	19.3	289.	.91	1.95	.54	.02	2.95	.25	.13	.07	.020	.0020	10.0	9.1	22.95	3.95	3450.	0	0	4.99					

Table 2--continued

1	2	3	4	5	6	7	8	9	10	11	12	13	14	15	16	17	18	19	20	21	22	23	24	25
IMP.	COND.	MG	CA	NA	K	HCO ₃	CL	NO ₃	SO ₄	F	LI	SI	TDI	COORDINATES	ALTIT	WELL	WATER	DATE	H-2	H-2	H-3	C-13	C-14	
C°	MMHO	MEQ	MEQ	MEQ	MEQ	MEQ	MEQ	MEQ	MEQ	MEQ	MEQ	PPM	MEQ	LAT.	LONG.	FEET	DEPTH	LEVEL	**	0/00	0/00	T.U.	0/00	PMC
Schnell	17.5	389.	.82	2.89	1.00	.06	3.24	.26	.07	1.12	.025	.0022	19.0	9.5	20.05	5.57	3200.	10.47						
Tapia	19.5	485.	.91	2.60	1.13	.05	2.74	.28	.04	1.17	.032	.0028	20.0	8.9	20.21	5.38	3190.	10.37						
San Chez	18.5	482.	.91	2.94	1.17	.05	3.08	.32	.04	1.31	.046	.0030	21.0	9.9	20.50	5.17	3180.	10.37						
Goat Cave	18.5	377.	.80	2.24	1.20	.02	3.11	.25	.07	1.02	.060	.0040	15.3	8.8	20.33	4.14	3160.	0	4.99					-9.41
B. Salazar	18.9	406.	.75	2.23	1.29	.05	2.99	.27	.09	1.00	.060		19.5	8.7	20.33	4.14	3260.	0	5.90					
Tax Salazar	20.5	485.	.78	2.79	1.65	.07	3.21	.45	.05	1.19	.079	.0045	21.0	10.3	20.80	3.95	3100.	10.37						
Buford (Stream)	20.5	482.	.80	2.70	1.65	.04	3.79	.26	.05	.79	.079	.0044	21.2	10.2	20.50	3.70	3065.	10.37						
Fourmile at the Quarry (Stream)	17.0	438.	1.33	2.32	1.03	.02	4.05	.22	.02	.23	.011	.0040	25.4	9.2				12.97						-9.54
Fourmile Last (Stream)	22.2		1.03	1.65	.58	.04	2.03	.12	.03	1.02	.012	.0020	18.1	6.5				2.43						-8.63
T. Creek (Stream)	22.0	280.	.05	.25	4.26	3.28	.62	.03	.06	.060		25.5	9.1					2.43						-8.23
																		2.73						-8.01

Table 2--continued

1	2	3	4	5	6	7	8	9	10	11	12	13	14	15	16	17	18	19	20	21	22	23	24	25
NAME OF WELL OR SPRING	IMP. COND.	MG	CA	NA	K	HCO ₃	CL	NO ₃	SO ₄	F	LI	SI	TDI	COORDINATES	ALTTIT	MELL DEPTH	WATER LEVEL	DATE	H-2	H-3	C-13	C-14	PMc	
C°	MMHO	MEQ	MEQ	MEQ	MEQ	MEQ	MEQ	MEQ	MEQ	MEQ	MEQ	PPM	MEQ	LAT.	LONG.	FEET	FEET	**	0/00	0/00	I.U.	0/00	0/00	PMc
Aravaipa G.H. (Stream) (cont.)																								
18.3	412.																	11.30	-75.5					-9.42
13.9	420.																	1.80	-68.7					-10.59
15.6	415.	.86	2.67	.84	.07	2.85	.28	.12	1.17	.022	.0020	16.6	9.0					2.60	-70.2					-9.94
		.80	3.09	1.06	.08	3.83	.21	.06	.85	.036	.0023	19.4	10.2					11.63						
Aravaipa Hydro-metric Station (Stream)																								
20.6	444.	.88	2.52	1.00	.03	3.28	.19	.04	1.04	.050	.0030	10.0	9.0					4.99						
16.7	365.			3.75	.03	2.76	.23	.07	.48	.030	.0070	20.5	7.4					5.90						
27.9	446.	.82	2.56	1.03	.06	2.82	.27	.07	1.19	.050		26.2	8.9					7.66						
16.7	438.	.85	2.72	1.07	.07	1.62	.36	.14	2.55	.040	.0023	18.1	9.4					2.60	-70.2					-8.75
Summer Floods in Aravaipa Canyon																								
20.0		1.03	3.24	1.03	.18	4.43	.37	.15	.52	.040		39.7	11.0					7.57						
20.0	437.	.72	2.55	.74	.14	3.87	.09	.00	.04	.013	.0014	13.0	8.2					7.99						
19.0	398.	.54	2.35	.74	.13	2.69	.16	.00	.85	.017	.0014	15.0	7.5					8.37						
21.0	335.	.42	2.13	.90	.12	2.50	.10	.00	.41	.040	.0009	11.3	6.6					8.53						
19.5	300.	.55	2.34	.41	.22	2.33	.09	.04	.22	.036	.0009	11.3	6.2					9.33						

Table 2--continued

NAME OF WELL OR SPRING	1 C°	2 IMP. COND.	3 MG	4 CA	5 NA	6 K	7 HCO ₃	8 CL	9 NO ₃	10 SO ₄	11 F	12 LI	13 SI	14 TDI	15 COORDINATES	16 LAT.	17 LONG.	18 WELL DEPTH FEET	19 WATER LEVEL FEET	20	21	22	23	24	25
																				DATE	**	0/00	0/00	I,U.	0/00
Summer Floods in Aravaipa Canyon (cont.)	19.5	233.	.35	1.56	.47	.20	1.85	.10	.05	.20	.035	.0009	11.3	4.8						9.33					
	17.8		.54	2.89	.65	.19	3.75	.16	.00	.21	.009	.0015	16.0	8.4						9.37	-70.0	-8.93			
	16.4	290.	.78	1.45	.61	.20	2.34	.14	.00	.58	.009	.0019	17.0	6.1						9.40	-66.3	-7.96			
	21.0																			8.26	-44.3	-6.50			
	20.0																			8.30		-5.04			
	20.0																			9.20		-7.74			
Winter Floods in Aravaipa Canyon	10.6	254.	.19	1.52	.51	.07	1.65	.09	.05	.53				4.6						11.99	-71.0	-8.28			
	8.9	167.	.30	1.23	.29	.06	.59	.08	.00	.63				3.2						2.20	-64.5	-8.62			
	16.7	383.	.75	2.55	.59	.08	2.84	.14	.16	.66				7.8						2.40	-65.9	-9.02			
	7.8	164.																		1.99	-67.2	-9.16			
	6.5																			3.17		-10.39			
	12.0		.30	1.14	.28	.06	.49	.06	.00	.55				2.89						3.17		-9.93			
	7.5																			3.63		-8.50			
	12.0		.42	1.12	.35	.05	.45	.07	.00	.77				2.89						3.70		-8.69			

Table 2--continued

1	2	3	4	5	6	7	8	9	10	11	12	13	14	15	16	17	18	19	20	21	22	23	24	25	
NAME OF WELL OR SPRING	COND. MMHO	MG CA	NA	CL	CO ₃	SO ₄	NO ₃	MEQ	MEQ	MEQ	LI	SI	TDI	COORDINATES	ALTIT	MELL DEPTH	WATER LEVEL	DATE	H-2	H-3	I.U.	O/00	O/00	PMC	
Winter Floods in Aravaipa Canyon (cont.)	10.0																		3.83						
Winter Runoff and Snowmelt in the Upper Valley	10.0	150.	1.16	2.19	1.25	.07	3.85	.07	.06	.71	.005	.0003	21.2	9.4					12.90	-59.8	-7.89				
	7.0																		12.95		-8.22				
	8.0		.34	.96	.22	.07	.81	.10	.05	.60	.007	.0003	15.3	3.2					12.99	-59.3	-8.52				
	13.8	143.	.27	.64	.35	.04	.35	.11	.00	.82	.009	.0003	16.6	2.6					2.73		-8.25				
	10.4	145.	.31	.74	.22	.01	.59	.05	.03	.57	.006	.0003	17.7	2.5					2.73		-8.46				
	14.0																		4.20	-62.6	-9.33				
	10.5																		11.60		-9.18				
Summer Floods in the Upper Valley	24.0																		5.77	-67.7	-9.70				

Table 3. Average values of environmental isotopes and location, altitude and water level at each sampling location

NAME OF WELL OR SPRING	COORDINATES		ALTI- TUDE FEET	WELL DEPTH	WATER LEVEL	0-18 0/00	H-2 0/00	H-3 T.U.	C-13 0/00	C-14 PMC
	LONG.	LAT.								
Aravaipa Spring	7.90	18.60	3335.	0	0	-9.73	-72.7	23.7	-12.1	103.0
Cobra Ranch New Domestic Well	8.05	18.67	3351.	47.	33.	-9.74	99.0	99.0	99.0	99.0
Cobra Ranch Old Domestic Well	7.97	18.76	3360.	46.	29.	-9.37	99.0	99.0	99.0	99.0
Valenzuela	7.95	18.44	3350.	99.	17.	-9.43	-73.9	20.7	99.0	109.6
Cobra Ranch New Irrigation (Cobra N. Irr.*)	8.29	18.40	3375.	116.	11.	-9.85	-72.3	99.0	99.0	99.0
Cobra Ranch New Irrigation (Top Sample)	8.29	18.40	3375.	116.	11.	-9.32	99.0	99.0	99.0	99.0
Song of the Desert (S.O.T.D.*) Domestic	12.76	13.60	3615.	35.	8.	99.0	99.0	99.0	99.0	99.0
Song of the Desert (S.O.T.D.*) #1	12.93	13.62	3620.	90.	12.	-9.40	99.0	19.0	99.0	99.0
Song of the Desert (S.O.T.D.*) #2	12.93	13.43	3620.	60.	14.	-9.66	-72.4	99.0	99.0	99.0
Whiting #1	11.36	14.67	3536.	152.	51.	-9.80	-71.8	15.6	-13.4	87.1
Whiting #1 Windmill (W.M.*)	11.45	14.43	3539.	100.	27.	99.0	99.0	99.0	99.0	99.0
Whiting #2	11.14	14.86	3528.	150.	84.	99.0	99.0	99.0	99.0	99.0

*Average Values for 0-18 and H-2

Table 3--continued

NAME OF WELL OR SPRING	COORDINATES		ALTI- TUDE FEET	WELL DEPTH	WATER LEVEL	0-18 0/00	H-2 0/00	H-3 T.U.	C-13 0/00	C-14 PMC
	LONG.	LAT.								
Buford Water Tank (W.T.*)	11.83	14.40	3550.	100.	50.	-9.76	99.0	99.0	99.0	99.0
BLM-Campground (C.G.*)	9.36	15.90	3500.	139.	111.	-8.43	-67.0	99.0	-8.43	99.0
Haby Domestic (D*)	9.79	16.17	3445.	99.	99.	-9.34	99.0	99.0	99.0	99.0
Haby Windmill (W.M.*)	9.50	16.53	3430.	99.	99.	-9.36	99.0	99.0	99.0	99.0
Haby Corral (CO.*)	8.31	17.95	3354.	99.	99.	-10.38	99.0	99.0	99.0	99.0
Klondyke Mill	9.35	17.30	3410.	160.	25.	-9.91	-70.9	99.0	99.0	99.0
Cobra Irrigation Old Well (Irr.*)	8.67	18.11	3374.	125.	45.	-9.46	99.0	99.0	99.0	99.0
Dowdle	9.52	18.41	3392.	100.	35.	-9.36	99.0	99.0	99.0	99.0
Sandford Old Adobe	9.46	17.50	3427.	99.	49.	99.0	99.0	99.0	99.0	99.0
Klondyke School (Sc.*)	9.98	16.24	3455.	100.	60.	99.0	99.0	99.0	99.0	99.0
Kramme Domestic (D.*)	13.00	13.90	3598.	100.	35.	99.0	99.0	99.0	99.0	99.0
Kramme Irrigation (Irr.*)	12.77	13.70	3580.	110.	30.	99.0	99.0	99.0	99.0	99.0
Kramme Corral (Co.*)	11.25	14.01	3551.	75.	35.	-9.39	99.0	99.0	99.0	99.0
Sharizona	13.45	12.71	3666.	80.	30.	-9.91	-74.1	99.0	99.0	99.0
H. Claridge Windmill (H.C1.W.M.*)	13.12	12.83	3653.	65.	35.	-9.53	-78.5	99.0	99.0	99.0

Table 3--continued

NAME OF WELL OR SPRING	COORDINATES		ALTI- TUDE FEET	WELL DEPTH	WATER LEVEL	0-18 0/00	H-2 0/00	H-3 T.U.	C-13 0/00	C-14 PMC
	LONG.	LAT.								
H. Claridge Irrig. (H.Clk.Irr.*)	12.99	12.90	3650.	90.	30.	99.0	99.0	99.0	99.0	99.0
3699 Windmill (W.M.*)	14.19	11.81	3694.	70.	40.	-9.75	99.0	99.0	99.0	99.0
H. Claridge Domestic (H.Cl.D.*)	15.76	11.17	3780.	84.	50.	-9.76	99.0	0	99.0	99.0
Davis Old House (Davis*)	15.81	10.14	3825.	112.	30.	99.0	99.0	99.0	99.0	99.0
Davis Old House New Well (Davis*)	15.81	10.10	3825.	112.	30.	99.0	99.0	99.0	99.0	99.0
B. Wilson	15.48	10.60	3780.	110.	27.	-7.84	-63.0	99.0	99.0	99.0
Peyote	15.95	9.38	3864.	99.	99.	-9.29	99.0	99.0	99.0	99.0
Eureka #1	19.57	3.64	4139.	552.	58.	-8.94	-56.6	99.0	99.0	99.0
Little Windmill (W.M.*)	16.48	8.81	3900.	56.	24.	-9.82	-66.1	99.0	99.0	99.0
Bull Pasture	19.33	4.76	4166.	150.	80.	-11.02	-73.1	99.0	99.0	99.0
Puddy Lynch (Ly.*)	18.40	5.81	4072.	83.	46.	-8.55	-59.1	99.0	99.0	99.0
3867 Windmill (W.M.*)	16.31	9.19	3867.	90.	26.	-9.39	99.0	99.0	99.0	99.0
Eureka Ranch Old Flowing Well	19.15	3.30	4155.	1500.	4.	-9.55	-68.0	99.0	99.0	99.0
Eureka Domestic	18.67	2.83	4310.	200.	140.	-10.22	-69.5	99.0	99.0	99.0
Eureka #11	15.86	1.48	4430.	1206.	259.	-9.45	-68.4	99.0	99.0	99.0

Table 3--continued

NAME OF WELL OR SPRING	COORDINATES		ALTI- TUDE FEET	WELL DEPTH	WATER LEVEL	0-18 0/00	H-2 0/00	H-3 T.U.	C-13 0/00	C-14 PMC
	LONG.	LAT.								
Eureka Bird Cage	21.57	2.07	4280.	278.	99.	-9.69	-67.5	99.0	99.0	99.0
Eureka McGee	21.20	.40	4350.	99.	99.	-8.67	99.0	99.0	99.0	99.0
Eureka Wilson Windmill (W.M.*)	20.57	3.67	4242.	126.	113.	-10.11	99.0	99.0	99.0	99.0
Eureka Big Tank	22.75	.65	4355	270.	155.	-8.57	-60.3	99.0	99.0	99.0
Eureka Sheep Corral (Co.*)	18.76	8.69	4145.	202.	120.	-7.67	-59.0	99.0	99.0	99.0
Eureka Apple Tree (A.T.*)	17.76	4.21	4258.	242.	222.	-10.01	-68.9	99.0	99.0	99.0
Black Canyon	19.86	1.76	4272.	99.	94.	-7.83	-58.0	99.0	99.0	99.0
Deer Creek	12.75	4.45	99.0	99.	99.	99.0	99.0	99.0	99.0	99.0
Whiting Deep Well	11.26	14.76	3535.	762.	27.	-8.80	-70.2	1.2	-12.6	32.4
Klondyke Mill Deep #1 (M.D.#1*)	9.30	17.22	3405.	215.	11.	-8.71	-68.0	5.4	99.0	99.0
Klondyke Mill Deep #2 (M.D.#2*)	9.29	17.21	3400.	156.	11.6	-9.61	-69.3	99.0	99.0	99.0
Long Hollow	8.94	13.07	4260.	560.	80.	-6.52	-63.1	1.2	99.0	38.1
Squaw Deep Well	10.50	10.52	4027.	270.	100.	-7.30	99.0	99.0	99.0	99.0
Whiting Hill Deep Well	11.79	16.55	3870.	360.	200.	-10.18	-76.3	4.7	-11.9	89.0
Song of the Desert #3 (S.O.T.D.#3*)	12.64	13.24	3623.	180.	9.	-8.56	-66.3	23.0	-16.8	119.8

Table 3--continued

NAME OF WELL OR SPRING	COORDINATES		ALTI- TUDE FEET	WELL DEPTH	WATER LEVEL	0-18 0/00	H-2 0/00	H-3 T.U.	C-13 0/00	C-14 PMC
	LONG.	LAT.								
Haby Old House (O.H.*)	9.35	16.30	3445.	99.	79.	-8.94	-66.5	22.0	99.0	99.0
Karakula Adobe (Ad.*)	8.38	19.45	3440.	132.	44.	-9.76	-77.2	4.5	99.0	99.0
Karakula House Domestic (H.*)	8.26	19.31	3445.	91.	45.	-9.71	99.0	99.0	99.0	99.0
Aravaipa Town (T.*)	8.25	24.90	4560.	850.	750.	-9.11	99.0	18.0	-20.0	77.8
Landsman Camp (C.*)	10.10	25.40	5200.	0	0	99.0	99.0	99.0	99.0	99.0
Tule Spring Shaft (Sp.*)	9.71	24.30	4620.	0	0	-8.95	99.0	10.0	-10.9	84.4
Tule Spring Wash	9.65	24.38	4620.	0	0	99.0	99.0	99.0	99.0	99.0
Stowe Gulch Spring (G.Sp.*)	8.75	23.15	3990.	0	0	-9.78	-70.8	20.0	99.0	99.0
W. Claridge Domestic	8.40	22.10	3835.	120.	90.	-9.13	99.0	13.4	99.0	99.0
Dowdle 3667 Windmill (3667 W.M.*)	9.05	20.05	3667.	110.	89.	-9.61	-67.7	99.0	99.0	99.0
Dog Water Mine (D.W. Mine*)	11.10	18.80	3840.	0	0	99.0	99.0	99.0	99.0	99.0
Laurel Canyon	10.17	18.14	3540.	90.	25.	-9.36	-68.9	99.0	99.0	99.0
Lamb Camp	14.52	16.60	4480.	80.	20.	-8.76	69.2	99.0	99.0	99.0
Buford Hill (H.*)	17.60	17.25	5170.	55.	10.	-9.64	99.0	99.0	99.0	99.0
Fourmile Spring-01d (4 Mile I*)	6.14	13.10	4079.	0	0	-9.07	-71.9	6.3	99.0	99.0

Table 3--continued

NAME OF WELL OR SPRING	COORDINATES		ALTI- TUDE FEET	WELL DEPTH	WATER LEVEL	0-18 0/00	H-2 0/00	H-3 I.U.	C-13 0/00	C-14 PMC
	LONG.	LAT.								
Fourmile Spring-New (4 Mile II*)	6.25	13.10	4075.	0	0	-8.44	-63.1	99.0	99.0	99.0
Fourmile Old Mill	4.95	14.60	3564.	17.	0	-9.25	-60.7	99.0	99.0	99.0
Squaw Cave Spring (#1*)	11.60	13.50	3660.	0	0	-7.85	99.0	99.0	99.0	99.0
Squaw Trail Spring (#2*)	11.35	12.85	3800.	0	0	-7.22	-45.7	99.0	99.0	99.0
Jackson Spring	3.75	17.35	3480.	0	0	99.0	99.0	99.0	99.0	99.0
Bleak Spring	.70	15.70	4510.	0	0	99.0	99.0	99.0	99.0	99.0
Virgus (Virg. Sp.*)	1.30	14.40	4680.	0	0	99.0	99.0	99.0	99.0	99.0
Parson (Pars. Sp.*)	1.43	15.42	4540.	0	0	99.0	99.0	99.0	99.0	99.0
Goat Harde (Goat H. Sp.*)	.10	15.60	4560.	0	0	99.0	99.0	99.0	99.0	99.0
Oak Spring	2.50	15.70	4400.	0	0	99.0	99.0	99.0	99.0	99.0
Dry Camp Spring	3.95	22.95	3450.	0	0	-7.95	-65.0	99.0	99.0	99.0
Dry Camp Domestic Well	4.05	22.93	3435.	223.	110.	99.0	99.0	99.0	99.0	99.0
Dry Camp Windmill (W.M.*)	4.45	23.90	3584.	99.	99.	-9.75	-71.7	99.0	99.0	99.0
McNair Canyon	6.90	19.35	3400.	0	0	99.0	99.0	99.0	99.0	99.0
Bear Canyon	6.27	22.95	3980.	0	0	99.0	99.0	99.0	99.0	99.0

Table 3--continued

NAME OF WELL OR SPRING	COORDINATES		ALTI- TUDE FEET	WELL DEPTH	WATER LEVEL	0-18 0/00	H-2 0/00	H-3 T.U.	C-13 0/00	C-14 PMC
	LONG.	LAT.								
Turnbull Irrigation	7.19	18.93	3300.	49.	6.	99.0	99.0	99.0	99.0	99.0
McNair T.	6.85	19.05	3285.	99.	99.	99.0	99.0	99.0	99.0	99.0
McNair H.	6.74	19.05	3280.	99.	99.	99.0	99.0	99.0	99.0	99.0
Hilliard	6.67	18.85	3270.	99.	99.	99.0	99.0	99.0	99.0	99.0
Guest House (G.H.*)	6.33	19.12	3250.	99.	99.	99.0	99.0	99.0	99.0	99.0
Luepke	5.92	19.52	3220.	99.	99.	99.0	99.0	99.0	99.0	99.0
Schnell	5.57	20.05	3200.	99.	99.	99.0	99.0	99.0	99.0	99.0
Topia	5.38	20.21	3190.	17.	10.	99.0	99.0	99.0	99.0	99.0
San Chez	5.17	20.50	3180.	99.	99.	99.0	99.0	99.0	99.0	99.0
Goat Cave	4.14	20.33	3210.	0	0	-9.41	99.0	99.0	99.0	99.0
B. Salazar	3.95	20.80	3100.	99.	99.	99.0	99.0	99.0	99.0	99.0
Tax Salazar	3.70	20.50	3065.	99.	99.	99.0	99.0	99.0	99.0	99.0
Buford (Stream*)	99.0	99.0	99.0	99.	99.	-9.76	99.0	99.0	99.0	99.0
Fourmile at the Quarry (Stream)	99.0	99.0	99.0	99.	99.	-8.80	-62.9	99.0	99.0	99.0
Fourmile Last (Flow)	99.0	99.0	99.0	99.	99.	-8.01	99.0	99.0	99.0	99.0

Table 3--continued

NAME OF WELL OR SPRING	COORDINATES		ALTI- TUDE FEET	WELL DEPTH	WATER LEVEL	0-18 0/00	H-2 0/00	H-3 T.U.	C-13 0/00	C-14 PMC
	LONG.	LAT.								
T. Creek (Stream)	99.0	99.0	99.0	99.	99.	99.0	99.0	99.0	99.0	99.0
Aravaipa G. H. (Stream)	99.0	99.0	99.0	99.	99.	-10.40	-71.5	24.6	-12.5	104.0
Aravaipa Hydrometric Station (Stream*)	99.0	99.0	99.0	99.	99.	-8.75	-70.2	99.0	99.0	99.0
Summer Floods in the Canyon	99.0	99.0	99.0	99.	99.	-7.41	-58.7	99.0	99.0	99.0
Winter Floods in the Upper Valley	99.0	99.0	99.0	99.	99.	-8.97	-67.2	99.0	99.0	99.0
Winter Runoff and Snow Melt in the Upper Valley	99.0	99.0	99.0	99.	99.	-8.55	-60.6	99.0	99.0	99.0
Summer Floods in the Upper Valley	99.0	99.0	99.0	99.	99.	-9.70	-67.7	99.0	99.0	99.0

TABLE 4. Radioisotope Values from Aravaipa Valley

SAMPLING POINT	DATE	TRITIUM* (T.U.)	CARBON-14** (PMC)
1) Aravaipa Spring	11.14.81	23.7 ± 0.5	103.3 ± 0.8
	10.14.82	19.0 ± 4.0	-
2) Aravaipa Canyon (base flow)		24.6 ± 1.06	104.0 ± 1.0
3) Valenzuela	11.15.81	20.77	109.5 ± 1.0
4) Whiting #1	8.13.81	17.8 ± 0.4	87.0 ± 0.75
	6.17.81	13.3 ± 0.9	-
5) Whiting Deep Well	8.12.81	1.6	32.36 ± 0.84
	6.17.81	0.7 ± 0.3	-
6) Whiting Hill	20.3.83	4.7 ± 0.4	89.0 ± 0.6
7) Aravaipa Town	7.19.83	18.0 ± 0.4	77.8
8) Long Hollow	2.22.83	1.2 ± 0.7	38.1 ± 0.4
9) Tule Spring	7.20.82	10.0 ± 0.4	84.4 ± 0.8
10) Stowe Gulch	4.30.82	20.0 ± 0.4	-
11) Haby Old House	10.12.82	22.0 ± 0.4	-
12) S.O.T.D. #3	10.13.82	23.0 ± 0.4	119.8
13) S.O.T.D. #1	5.27.82	19.0 ± 0.3	-
14) Klondyke Mill Deep	12.29.82	5.4 ± 0.4	-
15) Karakula Adobe	10.12.82	4.5 ± 0.3	-
16) W. Claridge Dom.	10.14.82	13.4 ± 0.4	-
17) Fourmile Spring (Main)	8.11.81	8.2 ± 0.3	-
18) Fourmile Spring (Small)	8.11.81	4.3 ± 0.2	-

* Tritium analyses were conducted in the Weizmann Institute of Science, Rehovot, Israel, 76100.

**Carbon-14 analyses have been completed in the Laboratory of Isotope Geochemistry, Department of Geoscience, University of Arizona, Tucson Arizona 85721

Table 5. Statistics obtained for 14 ionic and isotopic species from repeated laboratory standards*

	Expected Value	No. of Repeated Analyses	Average	Standard Deviation	Variance-1	Coefficient of Variation	Percentage (1) Error		Coefficient of Variation(2)
							\bar{X}	σ	
E.C**	420.0	150	422.0	13.99	0.0051	0.0316	0.0132	0.0320	
Mg	56.5	17	57.6	3.13	0.1020	0.0543	-0.0189	0.0537	0.052
Ca	141.0	20	136.3	14.09	0.0050	0.1030	-0.0333	0.0999	0.041
Na	207.0	27	202.7	20.84	0.0023	0.1030	0.0205	0.1007	0.085
K							0.0220xxx	0.1000	0.054
HCO ₃	724.0	27	761.5	87.53	1.31x10 ⁻⁴	0.1150	0.0498	0.1237	0.031
Cl	251.0	30	229.9	37.86	0.0007	0.1650	0.0840	0.1510	0.490
NO ₃	558.0	30	573.3	76.32	0.0002	0.1330	-0.0390	0.1370	2.090
SO ₄	223.0	29	232.2	14.23	0.0049	0.0613	-0.0410	0.0620	0.068
F						0.0900xxx			
Li						0.0600xxx			
Si						0.1500xxx			
² H(3)	-58.0	122	-58.1	3.71	0.0727	0.0639	0.0115	0.0420	
¹⁸ O(3)	-8.6	78	-8.56	0.198	25.6	0.0230	-0.0047	0.0250	

Table 5--continued

*Unless marked differently, analyses were conducted by the University of Arizona Analytical Center, Department of Chemistry, University of Arizona, Tucson, AZ 85721.

**Electrical Conductivity.

xxxEstimated values.

- (1) Percentage error of the i^{th} species and for the j^{th} analysis E_{ij} is defined as:

$$E_{ij} = (S_{di} - M_{ij}) / S_{di} ;$$

$$i = 1, 2, \dots, I$$

$$j = 1, 2, \dots, J$$

where S_{di} is the laboratory standard of the i^{th} species;

and M_{ij} is the measured value of S_{di} in the j^{th} analysis.

- (2) 25 repeated water analyses conducted at the USDA Southwest Rangeland Watershed Research Center Laboratory, Tucson, AZ 85719.
- (3) Analyses were conducted by the Laboratory of Isotope Geochemistry, Department of Geosciences, University of Arizona, Tucson, AZ 85721.

APPENDIX D

RAIN SAMPLER FOR STABLE ISOTOPES

Evaporation from an ordinary rain collector enriches the rain sample in heavy isotopes, and precludes the use of such samples for isotopic analysis. This causes difficulties with remote stations in arid zones that are sampled infrequently.

For a stable isotope analysis, the rain sample must be isolated from the atmosphere immediately after collection. Adar et al. (1980) designed and tested a multi-stage rain sampler which was built specifically for arid rain storms. However, with that device, the samples had to be removed after each rain event, which made it impractical for remote areas such as Aravaipa Valley.

A simple and reliable rain sampler was designed to permit up to ten inches of rain to accumulate; an amount sufficient for a four-week sampling cycle. A general picture of the sampler is given in Figure D-1.

Rain waters are accumulated in a glass beaker which has a valved outlet at the bottom. The beaker is equipped with a conical float constructed from thin glass and surrounded by a clean (vacuum) oil. The float is used to minimize the amount of oil which provides a complete isolation for the rain water from the atmosphere. The conical shape of the float prevents raindrops from adhering to its surface and provides a rapid path for the raindrops to the margins and underneath the oil.

The sampler was tested during three summer months with a laboratory standard for isotopic analysis ($\delta^{18}\text{O} = -8.6 \text{ ‰}$ and $\delta\text{D} = -58.0 \text{ ‰}$, (SMOW). The isotopic ratio of the tested sample did not undergo thorough fractionation due to evaporation; $\delta^{18}\text{O}$ was found to be -8.58 ‰ and δD was -57.3 ‰ which is well within the analytical accuracy (Table 5 of Appendix C). Almost two years of data were used to investigate the spatial distribution of O-18 and D in rainfalls over Aravaipa Valley.

RAINFALL ISOTOPE SAMPLER

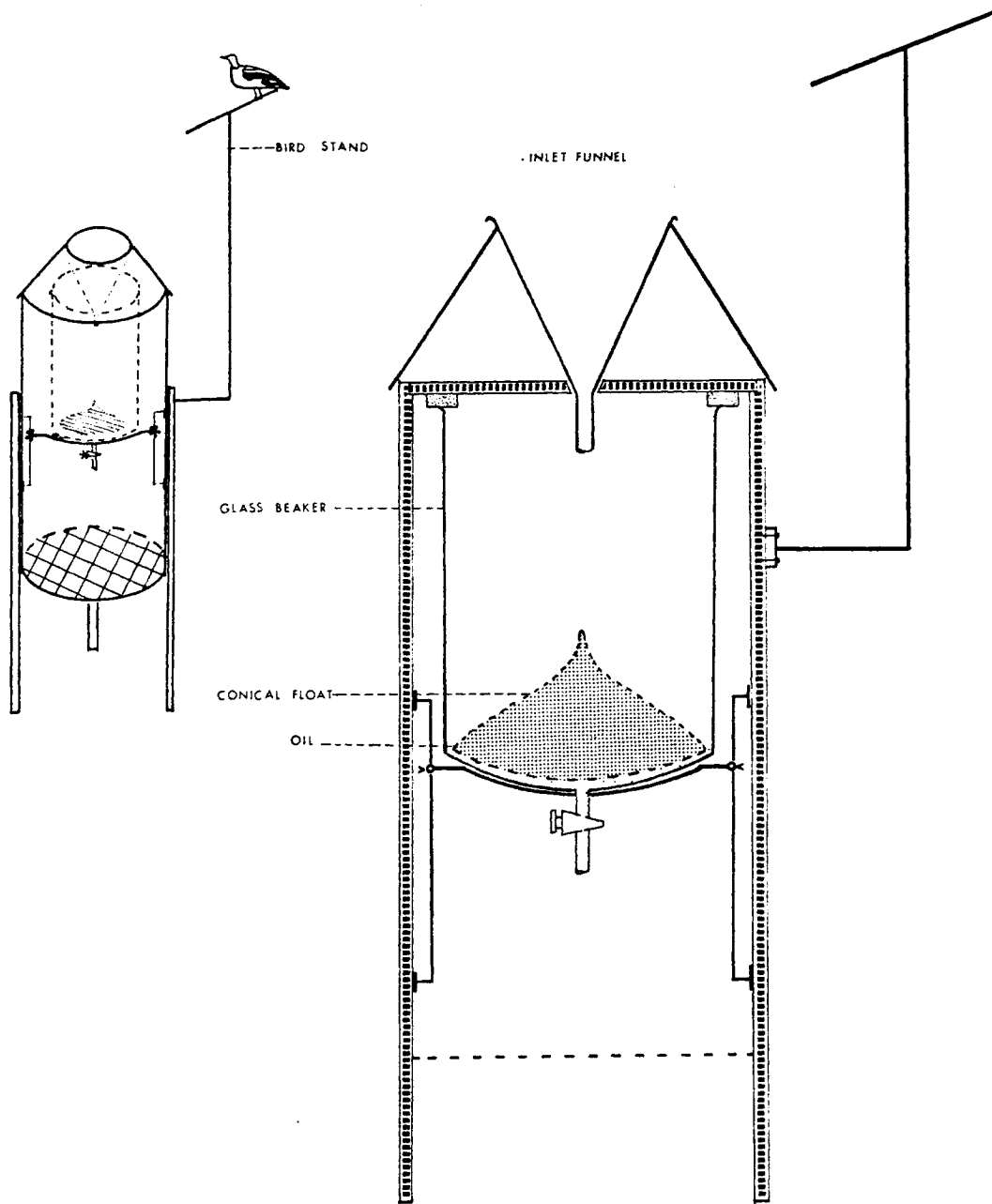


Figure D-1. Rain sampler for oxygen-18 and deuterium

APPENDIX E

SYNTHETIC DATA USED FOR TESTING
THE MULTI-CELL MATHEMATICAL ALGORITHM

Table 1. Synthetic data used in test no. 1⁽¹⁾

(4 cells, 14 dissolved species and 8 unknown inflows)

Inflow	EC(2)	Mg	Ca	Na	K	HCO ₃	Cl	NO ₃	SO ₄	F	Li	Si	D(3)	O-18(4)
1	353.8	.74	1.97	.97	.062	3.08	.205	.082	.42	.023	.0030	18.01	-73.8	-9.73
2	147.8	.84	.41	.33	.030	1.97	.070	.008	.98	.120	.0010	7.80	-68.9	-9.36
3	303.7	.08	.27	2.45	.034	2.52	.292	.019	.12	.058	.0030	14.13	-71.0	-9.12
4	356.0	1.72	3.18	.73	.340	3.64	.140	.046	1.93	.015	.0020	14.80	-67.0	-8.43
5	531.6	1.22	3.66	.66	.025	4.02	.283	.027	1.37	.047	.0030	14.91	-69.0	-9.43
6	184.0	.35	.76	.37	.040	.85	.105	.001	.76	.001	.0010	17.55	-66.3	-8.56
7	407.5	.86	2.59	.87	.056	2.91	.240	.077	1.01	.031	.0020	21.07	-71.5	-10.40
8	184.0	.35	.76	.37	.040	.85	.105	.001	.76	.001	.0010	17.55	-63.3	-8.56
Cell #1	285.1	.77	1.45	.76	.051	2.71	.160	.057	.61	.055	.0023	14.61	-72.2	-9.61
Cell #2	329.1	1.05	1.98	1.31	.199	3.14	.193	.038	1.15	.035	.0024	14.55	-69.0	-8.82
Cell #3	323.9	.98	1.94	1.16	.170	2.92	.188	.033	1.12	.032	.0023	14.92	-68.7	-8.83
Cell #4	292.1	.84	1.67	.98	.140	2.45	.169	.026	1.04	.025	.0020	15.52	-67.5	-8.77

(1) Concentrations are in meq/l unless otherwise indicated.

(2) Electrical conductivity (μ MHO/cm).

(3) Deuterium (0/00)

(4) Oxygen-18 (0/00)

Table 2. Synthetic data used in test no. 2⁽¹⁾

(4 cells, 14 dissolved species and 19 unknown inflows)

<u>Inflow</u>	<u>EC(2)</u>	<u>Mg</u>	<u>Ca</u>	<u>Na</u>	<u>K</u>	<u>HCO₃</u>	<u>Cl</u>	<u>NO₃</u>	<u>SO₄</u>	<u>F</u>	<u>Li</u>	<u>SI</u>	<u>D(3)</u>	<u>0-18(4)</u>
1	353.8	.74	1.97	.97	.062	3.08	.205	.082	.42	.023	.0026	18.01	-73.8	-9.73
2	187.1	.36	.81	.39	.035	.89	.093	.001	.80	.001	.0003	18.18	-66.3	-8.56
3	146.0	.52	1.13	.51	.048	1.40	.080	.036	.67	.007	.0003	17.70	-60.6	-8.55
4	332.3	.62	2.31	.69	.174	2.97	.151	.030	.38	.025	.0013	16.83	-58.7	-7.41
5	304.5	.10	.24	2.01	.048	2.52	.263	.022	.05	.036	.0022	14.00	-67.2	-8.70
6	370.3	.77	1.67	1.70	.069	3.04	.690	.224	.14	.008	.0032	8.80	-63.1	-6.52
7	454.0	1.28	2.52	.98	.028	3.71	.419	.059	.64	.012	.0016	16.35	-76.3	-10.18
8	242.0	.39	1.51	.33	.063	1.20	.086	.044	.63	.030	.0020	17.70	-67.1	-8.98
9	332.3	.62	2.31	.69	.174	2.97	.151	.030	.38	.025	.0013	16.83	-58.7	-7.41
10	356.0	1.72	3.18	.73	.034	3.64	.140	.046	1.93	.015	.0016	14.80	-67.0	-8.43
11	147.8	.84	.41	.33	.030	.07	.070	.008	.98	.120	.002	7.80	-68.9	-9.36
12	362.0	.66	2.06	.87	.050	2.93	.140	.080	.51	.022	.0023	17.10	-69.3	-9.66
13	242.0	.39	1.51	.33	.063	1.20	.086	.044	.63	.030	.0020	17.70	-67.1	-8.98
14	332.3	.62	2.31	.69	.174	2.97	.151	.030	.38	.025	.0013	16.83	-58.7	-7.41
15	355.5	.70	2.10	.89	.050	2.90	.175	.142	.56	.024	.0023	18.55	-72.3	-9.68

Table 2--continued

<u>Inflow</u>	<u>EC(2)</u>	<u>Mg</u>	<u>Ca</u>	<u>Na</u>	<u>K</u>	<u>HCO3</u>	<u>Cl</u>	<u>NO3</u>	<u>SO4</u>	<u>F</u>	<u>Li</u>	<u>SI</u>	<u>D(3)</u>	<u>O-18(4)</u>
16	444.2	1.15	3.21	.76	.029	3.39	.275	.027	1.36	.052	.0016	14.58	-68.6	-9.56
17	242.0	.39	1.51	.33	.063	1.20	.086	.044	.63	.030	.0020	17.70	-67.1	-8.98
18	332.3	.62	2.31	.69	.174	2.97	.151	.030	.38	.025	.0013	16.83	-67.7	-9.70
19	302.8	.05	.30	2.89	.020	2.52	.320	.021	.19	.080	.0037	14.25	-74.8	-9.44
Cell #1	321.9	.6771	.788	.865	.0608	2.712	.1832	.0678	.480	.0194	.0022	17.98	-71.82	-9.461
Cell #2	322.9	.6551	.733	.902	.0671	2.646	.2019	.065	.468	.0207	.0021	17.44	-70.89	-9.303
Cell #3	314.4	.7341	.807	.818	.060	2.538	.1793	.0594	.623	.0254	.0020	16.78	-69.885	-9.186
Cell #4	324.20	.7441	.895	.844	.0583	2.593	.1871	.0575	.667	.0286	.0020	16.62	-69.856	-9.235

(1) Concentrations are in meq/l unless otherwise indicated
(2) Electrical conductivity (μ MHO/cm)
(3) Deuterium (0/00)
(4) Oxygen-18 (0/00)

REFERENCES

- Adar, E., M. Levin, and A. Barzilay, 1980, Development of self-sealing sampler for Wadi floods, Water Resources Research, Vol. 16, No. 3, pp. 592-596.
- Advisory Committee on Irrigation Efficiency - Wellton-Mohawk Irrigation and Drainage District, 1979, Special report on measures for reducing return flows from the Wellton-Mohawk Irrigation and Drainage District, 109 p.
- Arad A. and E. Adar, 1981, Water balance study in the Aravaipa watershed, Arizona, Final Report to the George Whittell Wildlife Preserve, Tucson, Arizona, University of Arizona, Water Resources Center, 19 p.
- Bard, Yonathan, 1974, Nonlinear Parameter Estimation (Appendix D), Academic Press, p. 332.
- Belan, R. A., 1972, Hydrogeology of a portion of the Santa Catalina mountains, M.S. thesis, University of Arizona, 68 pp.
- Ben-Asher, J., 1978, Evaluation of evapotranspiration from climatological data and its relation to a basin water balance; Israel Meteorological Research Papers Vol. II, Meteorology of semi-arid zones, selected papers from joint conference American Meteorological Society-Israel Meteorological Society, pp. 297-314.
- Besbes, M., 1978, L'Estimation des Apports aux Nappes Souterraines; Un modèle Régional d'Infiltration Efficace, Docteur es Sciences dissertation, Université Pierre et Marie Curie (Paris VI), France.
- Besbes, M., J. P. Delhomme, and G. DeMarsily, 1978, Estimating recharge from ephemeral streams in arid regions: A case study at Kariouan, Tunisia, Water Resources Research, 14(2), pp. 281-290.
- Blake, G., E. Schlichting, and M. Zimmermann, 1973, Water recharge in a soil with shrinkage cracks, Soil Science Society of America Proceedings, Vol. 37, pp. 669-672.
- Bos, M. G., and J. Nugteren, 1974, On irrigation efficiencies, International Institute for Land Reclamation and Improvement, Publication 19, Wageningen, The Netherlands, p. 89.

- Boulton, N. S., 1963, Analysis of data from non-equilibrium pumping tests allowing for delayed yield from storage, Proc. Inst. Civ. Eng., Vol. 26, pp. 469-482.
- _____, 1964, Analysis of data from non-equilibrium pumping tests allowing for delayed yield from storage, Discussion, Proc. Inst. Civ. Eng., Vol. 28, pp. 604-610.
- Box, G.E.P., and E. Muller, 1958, "A Note on the Generation of Random Normal Deviates," Ann. Math. Statist., Vol. 29, pp. 610-611.
- Bredenkamp, D. B., J. M. Schulte and G. J. Du Toit, 1974, Recharge of a dolomite aquifer as determined from tritium profiles, International Atomic Energy Agency, Proceedings, Vienna, pp. 73-94.
- Briggs, P. C. and L. L. Werho, 1966, Infiltration and recharge from the flow of April 1965 in the Salt River near Phoenix, Arizona, Arizona State Land Department, Water Resources Report No. 29, p. 12.
- Burkham, D. E., 1970, Depletion of streamflow by infiltration in the main channels of the Tucson Basin, Southeastern Arizona, U.S. Geological Survey Water Supply Paper 1939-B, p. 36.
- Campana, M. E., 1975, Finite state models of transport phenomena in hydrologic studies. Ph.D. dissertation, Department of Hydrology and Water Resources, University of Arizona, Tucson, Arizona, 252 p.
- Carrera-Ramirez, J., 1984, Estimation of aquifer parameters under transient and steady-state conditions, Ph.D. dissertation, University of Arizona, Tucson, Arizona, 258 p.
- Craig, H., 1961, Isotopic variations in meteoric water, Science, Vol. 133, No. 26, pp. 1702-1703.
- Craig, H., L. I. Gordon, and Y. Horibe, 1963, Isotopic effects in the evaporation of water, Journal of Geophysical Research, Vol. 68, No. 17, pp. 5079-5087.
- Dansgaard, W., 1964, Stable isotopes in precipitations, Tellus, Vol. 16, pp. 436-468.
- Davis, R. W., 1967, A geophysical investigation of hydraulic boundaries in Tucson Basin, Pima County, Arizona, Ph.D. dissertation, Tucson, Arizona, University of Arizona.
- Davis, S. N., and H. Bentley, 1982, Dating groundwater in nuclear and chemical dating techniques: interpreting the environmental records, ACS Symposium Series, No. 176, pp. 187-222.
- Degallier, R., 1972, Un modèle de simulation des écoulements superficiels et souterrains: Le modèle SIMERO, Bull. BRGM, p. 2, III (3).

- Dincer, T., A. Al-Mugrin, and M. Zimmermann, 1974, Study of the infiltration and recharge through the sand dunes in arid zones with special reference to the stable isotopes and thermonuclear tritium, Journal of Hydrology, Vol. 23, pp. 79-109.
- Dincer, T., et al, 1974, Study of groundwater recharge and movement in shallow and deep aquifers in Saudi Arabia with stable isotopes and salinity data, Isotope Techniques in Groundwater Hydrology, Vol. 1, pp. 363-378, Vienna.
- Duffy, C. J., L. W. Gelhar, and G. W. Gross, 1978, Recharge and groundwater conditions in the Western Region of the Roswell Basin, Partial technical completion report, Proj. No. A-055-NMEX, New Mexico Water Resources Research Institute, Las Cruces, New Mexico.
- Durbin, T. J., G. W. Kapple, and J. R. Freckleton, 1978, Two-dimensional and three-dimensional digital flow models for the Salinas Valley groundwater basin, California, U.S. Geological Survey Water Resources Investigations 78-113, Open File Report, Menlo Park, Calif., p. 134.
- Eakin, T. E., 1966, A regional interbasin ground-water system in the White River area, southeastern Nevada, Water Resources Research, 2(2), pp. 251-272.
- Ellingson, C. T., 1979, Hydrology of the Aravaipa watershed, Final Report to the Defenders of Wildlife, Tucson, Arizona, University of Arizona, Water Resources Center, 85 p.
- _____, 1980, The hydrology of Aravaipa Creek, Southern Arizona, M.S. thesis, University of Arizona, Tucson, Arizona.
- Fauer, G., 1977, Principles of Isotope Geology, John Wiley and Sons, New York, 464 p.
- Fontes, J. C., and Garnier, 1979, Water Resources Research, Vol. 15, pp. 399-413.
- Flug, M., G. V. Abi-Ghanem, and Duckstein, 1980, An event-based model of recharge from an ephemeral stream, Water Resources Research, Vol. 16, No. 4, pp. 685-690.
- Feth, J. H., D. A. Barker, L. G. Morre, R. J. Brown, and C. E. Veirs, 1966, Lake Bonneville: Geology and hydrology of the Weber Delta District, including Ogden, Utah, U.S. Geological Survey, Professional Paper 518, p. 76.
- Gat, J. R., and Y. Tzur, 1967, Modification of the isotopic composition of rainwater by processes which occur before groundwater recharge, Isotopes in Hydrology, IAEA, Vienna, pp. 49-60.

- Gat, J. R. and W. Dansgaard, 1972, Stable isotope survey of the fresh water occurrence in Israel and the Jordan rift valley, Journal of Hydrology, Vol. 16, pp. 177-211.
- Gat, J. R., 1980, The isotopes of hydrogen and oxygen in precipitation, in Handbook of Environmental Isotope Geochemistry, P. Fritz and J. Ch. Fontes, editors, Elsevier, Amsterdam, 282 p.
- Gelhar, L. W., 1974, Stochastic analysis of phreatic aquifers, Water Resources Research, 10(3), pp. 539-545.
- Gorelick, S. M., B. Evans, and I. Remson, 1983, Identifying sources of groundwater pollution: an optimization approach, Water Resources Research, Vol. 19, No. 3, pp. 779-790.
- Gould, J. A., and R. P. Wilson, 1975, Map showing ground-water conditions in the Aravaipa area, Graham and Pinal Counties, Arizona - 1975, U.S. Geological Survey Investigations 76-107, Open-file Rep. (sheet 1 of 1).
- Hadley, G., 1970, Nonlinear and Dynamic Programming, Addison-Wesley Publishing Company, 484 p.
- Heerman, D. F., and D. C. Kincaid, 1974, Scheduling irrigations with a programmable calculator, Agricultural Research Service, ARS-NC-12.
- Hillel, D., 1974, Computer simulation of soil water dynamics, International Research Centre, Ottawa, Canada, 214 p.
- Hoefs, J., 1980, Stable Isotope Geochemistry, Springer-Verlag, Berlin, 208 p.
- Howard, K. W. F., and J. W. Lloyd, 1979, The sensitivity of parameters in the Penman evaporation equations and direct recharge balance, Journal of Hydrology, 41, pp. 329-344.
- International Association of Scientific Hydrology, Proceedings of the Reading Symposium, July 1970, World Water Balance.
- Issar, A., 1983, On the source of water from the thermomineral springs of lake Kinneret (Israel), Journal of Hydrology, Vol. 60, pp. 175-183.
- Issar, A., and Joel Gat, 1981, Environmental Isotopes as a tool in hydrogeological research in arid basin, Ground Water, Vol. 19, No. 5, pp. 490-494.
- Issar, A., and Dror Gilad, 1982, Groundwater flow systems in the arid crystalline line province of southern Sinai, Hydrological Sciences-Journal, Vol. 27, pp. 309-325.

- Jacob, C. E., 1943, Correlation of groundwater levels and precipitation on Long Island, New York, I, Trans. Amer. Geophys. Union, 24, pp. 564-573.
- _____, 1944, Correlation of groundwater levels and precipitation on Long Island, New York, II, Trans. Amer. Geophys. Union, 25, pp. 928-939.
- Kafri, U., and J. Ben Asher, 1978, Computer estimates of natural recharge through soils in southern Arizona, U.S.A., Journal of Hydrology, 38, pp. 125-138.
- Karmeli, D., L. J. Salazar, and W. Walker, 1978, Assessing the spatial variability of irrigation water applications, U. S. Environmental Protection Agency, EPA-600/2-78-041, p. 201.
- Keith, S. J., 1981, Stream channel recharge in the Tucson Basin and its implications for ground water management, M.S. thesis, Tucson, Arizona, University of Arizona.
- King, T. G., and J. R. Lambert, 1976, Simulation of deep seepage to a water table, Trans. Amer. Soc. Agr. Eng., 19, pp. 50-54.
- Krausman, G. P., and N. A. DeRidder, 1976, Analysis and evaluation of pumping test data, Bull. 11 Inter. Institute for Land Reclamation and Improvement, Wageningen, The Netherlands, 200 p.
- Lawrence, F. W., and S. B. Upchurch, 1982, Identification of recharge areas using geochemical factor analysis, Ground Water, Vol. 20, No. 6, Nov.-Dec.
- Levin, M., J. R. Gat, and A. Issar, 1980, Precipitation, flood - and groundwaters of the Negev highlands: an isotopic study of desert hydrology, International Atomic Energy Agency, Proceedings, Vienna, pp. 3-22.
- Leggette, R. M., 1936, Note in Trans. Amer. Geophys. Union, 17, pp. 341-344.
- Marsh, J. A., 1968, The effect of suspended sediment and discharge on natural infiltration of ephemeral streams, M.S. thesis, Tucson, Arizona, University of Arizona, 42 p.
- Matlock, W. G., 1965, The effect of silt-laden water on infiltration in alluvial channels, Ph.D. dissertation, Tucson, Arizona, University of Arizona, 102 p.
- _____, 1970, Mathematical analysis of ground water recharge, Transactions of the American Society of Civil Engineers, Vol. 13, No. 6, pp. 785-791.

- Matlock, W. G., and P. R. Davis, 1972, Groundwater in the Santa Cruz Valley, Arizona, Tucson, Arizona, Technical Bulletin 194, University of Arizona Agricultural Experiment Station, 37 pp.
- Mazor, E., 1982, Rain recharge in the Kalahari - a note on some approaches to the problem, Journal of Hydrology, Vol. 55, pp. 137-144.
- Mazor, E., B. T. Verhagen, J. P. F. Senschop, N. S. Robins and L. G. Hutton, 1974, Kalahari groundwaters: Their hydrogen, carbon and oxygen isotopes, in Isotope Techniques in Groundwater Hydrology 1974, Vol. I, Proceedings of a Symposium, Vienna, 11-15 March, 1974, International Atomic Energy Agency, Vienna, pp. 203-223.
- Mero, F., 1963, Application of the groundwater depletion curves in analyzing and forecasting spring discharges influenced by well fields, Intern. Association Sci. Hydrology Publication, No. 63, pp. 107-117.
- _____, 1969, An approach to daily hydrometeorological water balance computation of surface and groundwater basins, Proc. UNESCO Seminar on Integrated River Basin Development, Delft, The Netherlands.
- _____, 1978, The MM08 hydrometeorological simulation system: Basic concepts and operators guide, Rep. T/78/02, Tahal, Tel Aviv, Israel.
- Moench, A. F. and C. C. Kisiel, 1970, Application of the convolution relation to estimating recharge from an ephemeral stream, Water Resources Research, 6(4), pp. 1087-1094.
- Mook, W. G., 1980, Carbon-14 in hydrological studies, in Handbook of Environmental Isotope Geochemistry, P. Fritz, and J. Ch. Fontes, editors, Elsevier, Amsterdam, 282 p.
- Moore, R. T., 1962, Geologic cross-sections of Arizona, section 7: Tucson, Arizona Bureau of Mines.
- Neuman, S. P., R. A. Feddes, and E. Bresler, 1975, Finite element analysis of two-dimensional flow in soils considering water uptake by roots: I. Theory, Soil Sci. Soc. Am. Proc., 39(2), pp. 224-230.
- Neuman, S. P., and S. Dasberg, 1977, Peat Hydrology in the Hula Basin, Israel: II. Subsurface Flow Regime, Journal of Hydrology, Vol. 32, pp. 241-256.
- Neuman, S. P., 1975, Analysis of pumping test data from anisotropic unconfined aquifers considering delayed gravity response, Water Resources Research, Vol. 11, No. 2, pp. 329-342.

- Neuman, S. P., 1980, A statistical approach to the inverse problem of aquifer hydrology; 3. Improved solution method and added perspective. Water Resources Research, Vol. 16, No. 2, pp. 331-346.
- Nydal, R., and K. Lovseth, 1983, Tracing bomb C-14 in the atmosphere, 1962-1980, Journal of Geophysical Research, Vol. 88, No. C6, pp. 3621-3642.
- Olmstead, F. H., D. J. Loeltz, and B. Irelan, 1973, Water Resources of Lower Colorado River-Salton Sea Area, U.S. Geological Survey Prof. Paper 486-H.
- Plummer, L.N., B.F. Jones, and A.H. Truesdell, 1976. WATEQF - A fortran IV version of WATEQ, a computer program for calculating chemical equilibrium of natural waters. Natl. Tech. Info. Serv. PB 261027, 61 p.
- Preller, C., 1978, Trend und Spektralanalysen von Grundwasserstahdsganglinien und Klimatologischen Reihen zur Ermittlung der Grundwasserneubildung in Drei Gebieten von Berlin (West), Verlag von Dietrich Reimer in Berlin.
- Rantz, S. E., and T. E. Eakin, 1971, A summary of methods for the collection and analysis of basis hydrologic data for arid regions, Open File Report, U.S. Geological Survey Water Resources Division, Menlo Park, California, 125 p.
- Rasmussen, T. C., 1982, Solute transport in saturated fractured media, M.S. thesis, University of Arizona, Tucson, Arizona.
- Robinson, J. R., 1976, Interpretation of gravity anomaly data from the Aravaipa Valley area, Graham and Pinal Counties, Arizona, M.S. thesis, University of Arizona, Tucson, Arizona.
- Ross, C. P., 1925, Geology and ore deposits of the Aravaipa and Stanley mining districts, Graham County, Arizona, U.S. Geological Survey Bulletin 763.
- Sampson, R. J., 1978, Surface II graphic system, Kansas Geological Survey, Lawrence, Kansas, 240 p.
- Schick, A., 1977, A tentative sediment budget for an extremely arid watershed in the Southern Negev, Geomorphology Symposium, 8th, Bingham, New York, Geomorphology in Arid Regions, pp. 139-163.
- Shampine, W. J., T. Dincer and M. Noory, 1979, An evaluation of isotope concentrations in the groundwater of Saudi Arabia, Proc. Isotope Hydrology, 1978, IAEA, Vienna, Vol. 2, pp. 443-463.

- Simons, F. S., 1964, Geology of the Klondyke quadrangle, Graham and Pinal Counties, Arizona, U.S. Geological Survey Prof. Paper 461.
- Simpson, E. S., D. B. Thorud, and I. Friedman, 1970, Distinguishing seasonal recharge to groundwater by deuterium analysis in southern Arizona.
- Simpson, E. S., and L. Duckstein, 1975, Finite state mixing-cell models, paper presented at Bilateral United States-Yugoslavian Seminar in Karst Hydrology and Water Resources, Dubrovnik, Yugoslavia, June, 1975.
- Simpson, E. S., M. E. Campana, and L. Duckstein, 1982, Discret-State Compartment Model: Part I, Computational Procedure, unpublished, University of Arizona, Tucson, Arizona.
- Tanji, K., 1977, A conceptual hydrosalinity model for predicting salt load in irrigation return flows, in Dregne, H. E., Managing saline water for irrigation, Proceedings of the International Conference on Managing Saline Water for Irrigation, Planning for the future, Center for Arid and Semi-arid Land Studies, Texas Tech. University, pp. 49-72.
- Thorntwaite, C. W. and J. R. Mather, 1957, Instructions and tables for computing potential evapotranspiration and the water balance, in Publications in climatology, Laboratory of Climatology. 10(3), p. 311.
- Truesdell, A. H., and B. F. Jones, 1973, WATEQ, a computer program for calculating chemical equilibria of natural waters. Nat. Tech. Info. Serv. PB 220464, 73 p.
- _____, 1974, WATEQ, a computer program for calculating chemical equilibria of natural waters, U.S. Geological Survey Jour. Research, Vol. 2, pp. 233-248.
- Venetis, C., 1971, Estimating infiltration and/or the parameters of unconfined aquifers from ground water level observations, Journal of Hydrology, 12(2), pp. 161-169.
- Verhagen, B. Th., Z. Dziembowski, and J. H. Oosthuizen, 1978, An environmental isotope study of a major dewatering operation at Sishen mine, Northern Cape province, International Atomic Energy, Proceedings, pp. 65-81.
- Verhagen, B. Th., J. P. F. Sellschop, and C. M. H. Jennings, 1970, Contribution of environmental tritium measurements to some geohydrological problems in Southern Africa, International Atomic Energy Proceedings, Vienna, pp. 289-313.